VILNIUS UNIVERSITY

Giedrė Balčiūnaitė

Structural myocardial changes in patients with severe aortic valve stenosis and their clinical implications

DOCTORAL DISSERTATION

Medical and Health Sciences,
Medicine (M 001)

VILNIUS 2022

Academic supervisor – Prof. Dr. Sigita Glaveckaitė (Vilnius University, Medical and Health Sciences, Medicine – M 001).

Academic consultant – Prof. Dr. Nomeda Valevičienė (Vilnius University, Medical and Health Sciences, Medicine – M 001).

This doctoral dissertation will be defended in a public meeting of the Dissertation Defence Panel:

Chairman – **Prof. Dr. Janina Tutkuvienė** (Vilnius University, Medical and Health Sciences, Medicine – M 001).

Members:
Prof. **Dr. Gintaras Kalinauskas** (Vilnius University, Medical and Health Sciences, Medicine – M 001),
Assoc. Prof. Dr. Tomas Lapinskas (Lithuanian University of Health Sciences, Lithuania, Medical and Health Sciences, Medicine – M 001),
Prof. Dr. Grzegorz Smolka (Silesian University, Katowice, Poland, Medical and Health Sciences, Medicine – M 001),
Prof. Dr. Diana Zakarkaitė (Vilnius University, Medical and Health Sciences, Medicine – M 001).

The dissertation shall be defended at a public meeting of the Dissertation Defence Panel at 10 a.m. on the 1st of December 2022 in Red auditorium (A122) at Santaros clinics.
Address: Santariškių st. 2, Vilnius, Lithuania.

The text of this dissertation can be accessed at the library of Vilnius University, as well as on the website of Vilnius University: *www.vu.lt/lt/naujienos/ivykiu-kalendorius*

https://orcid.org/0000-0001-7447-3001

VILNIAUS UNIVERSITETAS

Giedrė Balčiūnaitė

Miokardo struktūrinių pokyčių nustatymas ir jų klinikinės reikšmės įvertinimas pacientams, sergantiems didelio laipsnio aortos vožtuvo angos stenoze

DAKTARO DISERTACIJA

Medicinos ir sveikatos mokslai,
Medicina (M 001)

VILNIUS 2022

Disertacija rengta 2017 – 2021 metais Vilniaus universitete.

Mokslinė vadovė:
Prof. dr. Sigita Glaveckaitė (Vilniaus universitetas, medicinos ir sveikatos mokslai, medicina – M 001).

Mokslinė konsultantė:
Prof. dr. Nomeda Valevičienė (Vilniaus universitetas, medicinos ir sveikatos mokslai, medicina – M 001).

Gynimo taryba:
Pirmininkė: **Prof. dr. Janina Tutkuvienė** (Vilniaus universitetas, medicinos ir sveikatos mokslai, medicina – M 001).

Nariai:
Prof. dr. Gintaras Kalinauskas (Vilniaus universitetas, medicinos ir sveikatos mokslai, medicina – M 001);
Doc. dr. Tomas Lapinskas (Lietuvos sveikatos mokslų universitetas, medicinos ir sveikatos mokslai, medicina – M 001);
Prof. dr. Grzegorz Smolka (Silezijos medicinos universitetas, Katowice, Lenkija, medicinos ir sveikatos mokslai, medicina – M 001);
Prof. dr. Diana Zakarkaitė (Vilniaus universitetas, medicinos ir sveikatos mokslai, medicina – M 001).

Disertacija ginama viešame Gynimo tarybos posėdyje 2022 m. gruodžio 1 d. 10:00 val. Vilniaus universiteto ligoninėje Santaros klinikose, Raudonojoje auditorijoje, (A122). Adresas: Santariškių g. 2, Vilnius, Lietuva.

Disertaciją galima peržiūrėti Vilniaus universiteto bibliotekoje ir VU interneto svetainėje adresu: www.vu.lt/lt/naujienos/ivykiu-kalendorius

TABLE OF CONTENTS

ABBREVIATIONS

6MWT – 6-minute walking test
AS – aortic stenosis
ATTR – transthyretin
ATTR-CA – transthyretin cardiac amyloidosis
AV – aortic valve
AVA – aortic valve area
AVR – aortic valve replacement
BNP – brain natriuretic peptide
CAD – coronary artery disease
CMR – cardiovascular magnetic resonance
ECG – electrocardiography
ECV – extracellular volume
eGFR – estimated glomerular filtration rate
EuroScore-II – European System for Cardiac Operative Risk Evaluation II score
GLS – global longitudinal strain
Hs-Tn-I – high-sensitivity troponin I
LA – left atrium
LGE – late gadolinium enhancement
LV – left ventricle
LVEF – left ventricular ejection fraction
MLHFQ – Minnesota living with heart failure questionnaire
MOLLI – Modified Look-Locker inversion recovery pulse sequence
NT-proBNP – N-terminal pro-brain natriuretic peptide
NYHA – New York Heart Association
RAS – relative apical sparing
STE – speckle tracking echocardiography
STS – Society of Thoracic Surgeons' risk model score
T – Tesla
T1 – T1 myocardial relaxation
TAVI – transcatheter aortic valve implantation
VUH – Vilnius University Hospital

LIST OF PUBLICATIONS

This thesis is based on the following papers, which are referred to in the text by their numerals.

No.	Reference with DOI	Quartile	IF
1.	**Balciunaite G**, Skorniakov V, Rimkus A, Zaremba T, Palionis D, Valeviciene N, Aidietis A, Serpytis P, Rucinskas K, Sogaard P, Glaveckaite S. Prevalence and prognostic value of late gadolinium enhancement on CMR in aortic stenosis: meta-analysis. Eur Radiol. 2020 Jan;30(1):640-651. DOI: <u>10.1007/s00330-019-06386-3</u>	Q1	5.3
2.	**Balciunaite G**, Rimkus A, Zurauskas E, Zaremba T, Palionis D, Valeviciene N, Aidietis A, Serpytis P, Rucinskas K, Sogaard P, Glaveckaite S, Zorinas A, Janusauskas V. Transthyretin cardiac amyloidosis in aortic stenosis: Prevalence, diagnostic challenges, and clinical implications. Hellenic J Cardiol. 2020 Mar-Apr;61(2):92-98. DOI: <u>10.1016/j.hjc.2019.10.004</u>	Q3	1.9
`3.	**Balčiūnaitė G**, Palionis D, Žurauskas E, Skorniakov V, Janušauskas V, Zorinas A, Zaremba T, Valevičienė N, Aidietis A, Šerpytis P, Ručinskas K, Sogaard P, Glaveckaitė S. Prognostic value of myocardial fibrosis in severe aortic stenosis: study protocol for a prospective observational multi-center study (FIB-AS). BMC Cardiovasc Disord. 2020 Jun 8;20(1):275. DOI: <u>10.1186/s12872-020-01552-8</u>	Q2	2.0
4.	**Balčiūnaitė G**, Besusparis J, Palionis D, Žurauskas E, Skorniakov V, Janušauskas V, Zorinas A, Zaremba T, Valevičienė N, Šerpytis P, Aidietis A, Ručinskas K, Sogaard P, Glaveckaitė S. Exploring myocardial	Q2	2.2

	fibrosis in severe aortic stenosis: echo, CMR and histology data from FIB-AS study. Int J Cardiovasc Imaging. 2022 Mar 3:1–14. DOI: 10.1007/s10554-022-02543-w			
5.	Sigita Glaveckaitė, Darius Palionis, Tomas Zaremba, **Giedrė Balčiūnaitė**, Nomeda Rima Valevičienė, Audrius Aidietis, Kęstutis Ručinskas, Pranas Depretis, Peter Sogaard. Cardiovascular magnetic resonance parametric mapping. Methodological recommendations. Vilnius University, 2020.	-	-

A study protocol article (No.3) is licensed under an open access Creative Commons license (CC BY 4.0), therefore no separate permission from the publisher was required. A review article (No.2) is also an open access article under the CC BY-NC-ND license. For the other two articles (No.1 and No.4) licenses to reprint both printed and electronic versions were obtained from the Springer Nature Copyright Clearance Center.

FOREWORD

Valvular heart diseases have been of particular interest to me since the start of my sub-specialization in the field of cardiovascular imaging. The managing of patients with a valvular heart disease, including patients with aortic valve stenosis, makes up a significant proportion of my everyday clinical practice. Therefore, the opportunity to investigate these patients in the frame of this current doctoral study came as a natural consequence. This doctoral dissertation is a result of five years of continuous work. It has given me valuable knowledge and insights and hopefully will benefit my patients. I am very grateful to prof. S. Glaveckaitė for this opportunity and guidance throughout these years.

1. INTRODUCTION

1.1 Relevance of the research issue

Over the past two decades there has been a significant increase in the number of adults with severe valvular aortic stenosis (AS) undergoing surgical aortic valve replacement (AVR) or transcatheter aortic valve implantation (TAVI). This accounts for the increasing prevalence of AS in the aging population, as well as the development and introduction of a less invasive transcatheter treatment modality. According to the data provided by the Lithuanian Institute of Hygiene, the number of patients with valvular heart diseases (code I34-I39) has increased 3.9 times in absolute numbers and 4.9 times per 100,000 population between 2001 and 2020 (1) (**Figures 1 and 2**).
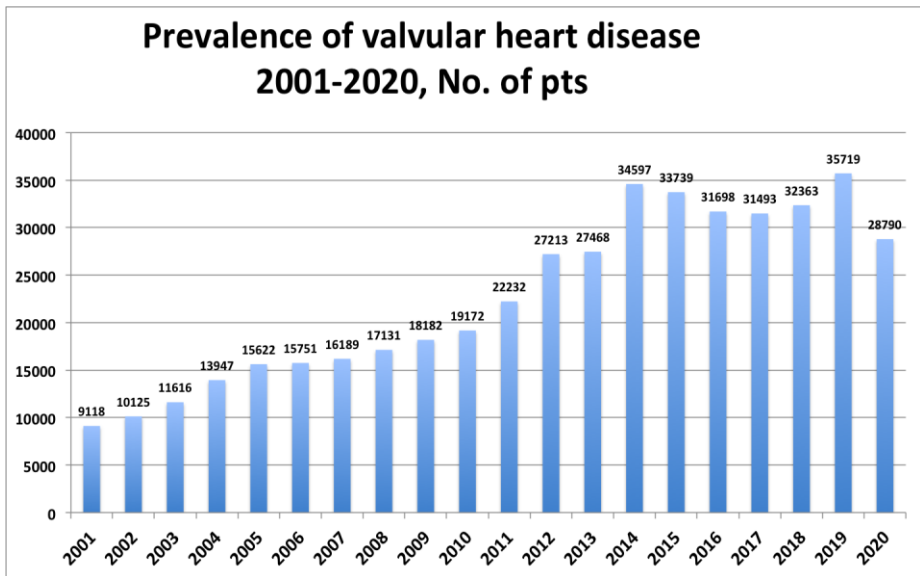
Fig. 1. Trend in the prevalence of valvular heart disease (code I34-I39) in Lithuania between 2001-2020 in absolute numbers (Data from the Lithuanian Institute of Hygiene).
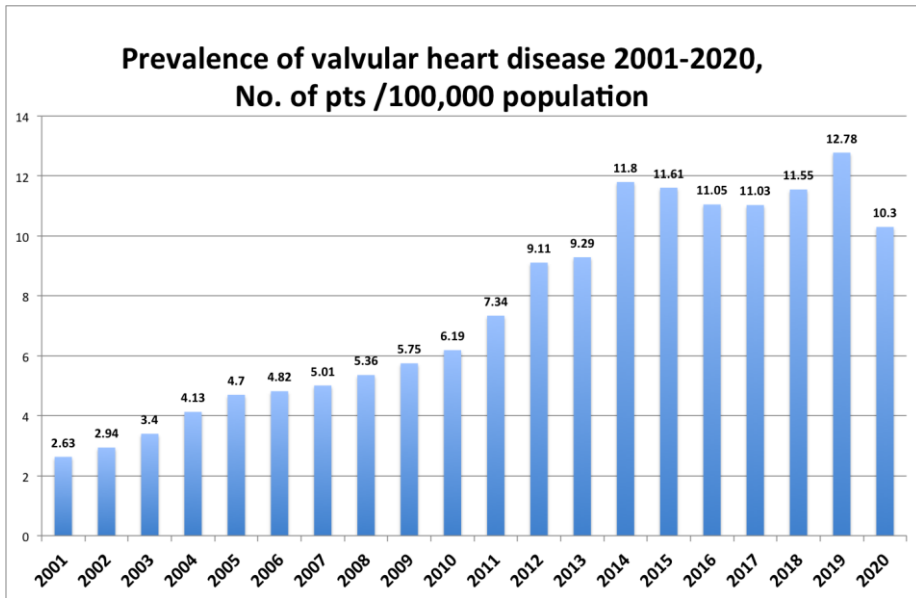
Fig. 2. Trend in the prevalence of valvular heart disease (code I34-I39) in Lithuania between 2001-2020, number of patients per 100,000 population (Data from the Lithuanian Institute of Hygiene).

These rising number of patients with valvular heart disease is not only due to the increasing prevalence of pathology, but also probably to the higher magnitude of referrals to cardiac centers. For patients who were previously considered too high risk and unsuitable for surgical intervention, new transcatheter therapies can now be offered. A significant increase in the number of aortic valve interventions was also observed not only in Western countries, but also across Lithuanian cardiac centers. Based on the data from the Lithuanian Institute of Hygiene, the number of aortic valve interventions, both surgical and transcatheter, increased by 28% in all Lithuanian cardiac centers, and by 31% in Vilnius University Hospital (VUH) Santaros clinics between 2011 and 2020 (1) (**Fig. 3**). The number of aortic valve interventions performed has been maintained irrespective of the unfavorable circumstances of the COVID-19 epidemiologic situation.
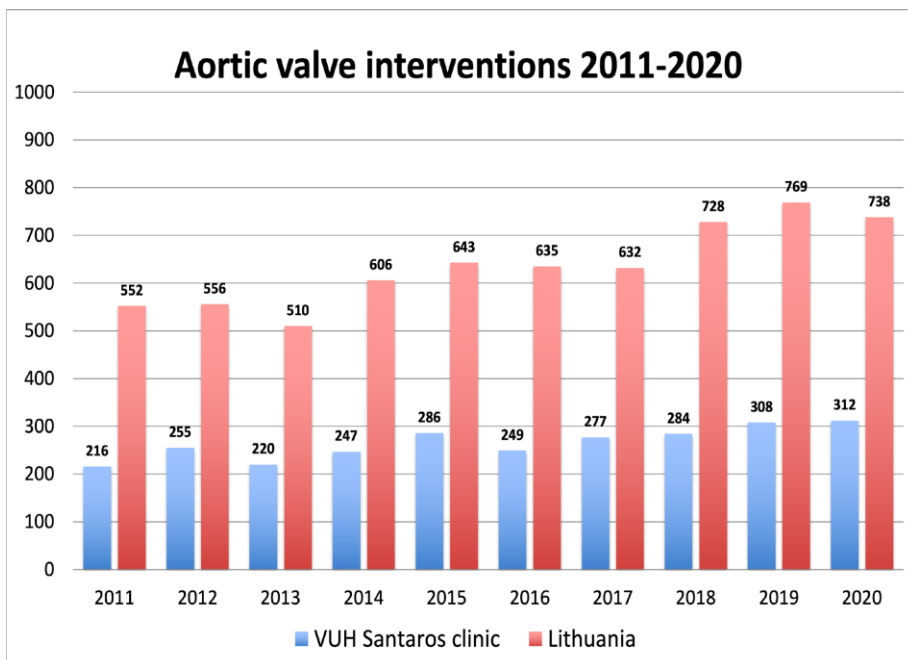
Fig. 3. Trend in aortic valve interventions, both surgical and transcatheter, between 2011-2020 in Lithuania (red bars) and in VUH Santaros clinic (blue bars) (Data from the Lithuanian Institute of Hygiene).

Therefore, timely diagnosis of severe AS and patient risk stratification has become increasingly relevant. It has been widely accepted that AS is not only a disease of the valve, but also a disease of the left ventricle (LV) and ultimately a disease of the whole heart. A growing body of evidence shows that the extent of LV damage in AS is an important determinant of post-interventional outcomes in both surgical and transcatheter AS patient cohorts (2,3). However, the currently recommended and used criteria for LV damage in AS patients lacks sensitivity. The only reference to AS consequences on LV myocardium mentioned in the current European Society of Cardiology guidelines on valvular heart disease is reduced LV ejection fraction (LVEF), defined as a reduction of LVEF <50% (4). Cardiac damage assessed by LVEF has numerous shortcomings: it is load dependent, may be compensated by concentric LV hypertrophy, and begins to decline only late in the course of the disease progression (5). Identification of new and more sensitive imaging biomarkers of LV injury and incorporating them into currently used diagnostic algorithms may help to avoid an irreversible negative effect of pressure overload on LV myocardium and challenge current recommendations. Several

new imaging biomarkers have been considered for this purpose, namely LV global longitudinal strain (GLS), measured by speckle tracking echocardiography (STE) and myocardial fibrosis, measured by cardiovascular magnetic resonance (CMR).

Myocardial fibrosis is fundamental in the pathogenesis of heart failure in the spectrum of cardiovascular diseases (6-8). Accurate detection and quantification of myocardial fibrosis, both regional and diffuse, is therefore critical to understanding pathophysiology, investigating possible therapies and predicting prognosis. Myocardial fibrosis is an early marker of LV decompensation which develops even before the LVEF deteriorates or overt symptoms develop (9). Myocardial fibrosis in AS patients has been linked to impaired LV function and adverse clinical outcomes (10,11). As a possible surrogate marker of myocardial fibrosis, LV myocardial GLS has been shown to be an independent predictor of adverse events in patients with severe AS, both with preserved and impaired LV systolic function (12,13). To date, there are limited data on the simultaneous assessment of diffuse myocardial fibrosis by noninvasive multimodality imaging and histological confirmation in severe AS.

Transthyretin cardiac amyloidosis (ATTR-CA) is a challenging and underdiagnosed cause of heart failure (14). Until recently, ATTR-CA was considered a rare type of infiltrative cardiomyopathy, and the traditional gold standard for diagnosis was a positive endomyocardial biopsy in the context of characteristic clinical and imaging features. Advances in diagnostic imaging, including CMR with T1 mapping and nuclear imaging with technetium-labeled bone-seeking tracers, have enabled noninvasive, non-histological diagnosis of ATTR-CA, which has significantly increased disease awareness and recognition in the last decade (14-16). ATTR-CA has been increasingly recognized in patients with degenerative AS (17,18). With the growing number of elderly patients undergoing TAVI, the identification of ATTR-CA in this group of patients is of high clinical importance. Excessive remodeling of LV myocardium and restrictive physiology with preserved LVEF are both features of ATTR-CA and AS (19). The prevalence of both ATTR-CA and AS increases with age, and a growing number of studies have investigated their coexistence (20-25). As both diseases share similar clinical and echocardiographic characteristics, the recognition of superimposed ATTR-CA in patients with AS can be very challenging. However, accurate diagnosis is critical for the management of both pathologies, guiding amyloid-directed therapies, as well as deciding on an AS treatment strategy. It has been demonstrated that the presence of cardiac amyloidosis in elderly AS patients

was associated with an increased risk for all-cause mortality and heart failure compared to lone AS patients (24,25). The prevalence of ATTR-CA has never been systematically investigated in a Lithuanian cohort of patients, making it a new and important research subject.

1.2 Value and novelty of the research

CMR imaging is an established tool for the quantification of myocardial mass, volumes, and function (26). Late gadolinium enhancement (LGE) imaging has become the gold standard technique for imaging focal myocardial fibrosis in the spectrum of cardiovascular diseases: coronary artery disease (CAD) and non-ischemic cardiomyopathies (27-29). However, cardiac pathologies characterized by diffuse myocardial fibrosis cannot be evaluated adequately only by LGE, as LGE images may not show any enhancement despite the presence of significant interstitial fibrosis, as exemplified by the CMR and histological images from one of our patients with severe AS (**Fig. 4**).
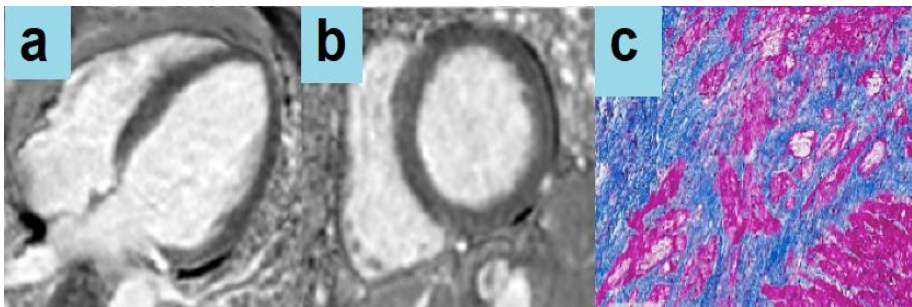
Fig. 4. Long axis (a) and short axis (b) LGE images of the left ventricle from a patient with severe AS and decompensated heart failure do not demonstrate any focal LGE. However, histological evaluation demonstrates dense interstitial fibrosis on haematoxylin & eosin stained myocardium (c).

While CMR has been used for tissue characterization for many years, it is only recent improvements in magnetic resonance imaging scanner technology and imaging reconstruction techniques that have allowed parametric mapping to become clinically feasible (30). After cine, LGE, and perfusion imaging, parametric mapping is widely regarded as the 4th era of myocardial CMR development. The European Society of Cardiology has named T1 and T2-mapping as one of six most innovative imaging methods in the evaluation of heart failure patients (31). In contrast to conventional CMR tissue characterization techniques, which rely on relative variations in image

intensities to highlight abnormal tissues, parametric mapping provides direct visualization of tissue magnetic resonance properties. T1 mapping techniques, following gadolinium contrast media injection, have demonstrated potential for the evaluation of diffuse pathological processes within myocardium, including myocardial fibrosis (32,33). Since the introduction of a CMR parametric mapping technique in 2010, the interest and research in myocardial fibrosis have surged, as evidence by the continually rising numbers of publications on the topic (34) **(Fig. 5).**
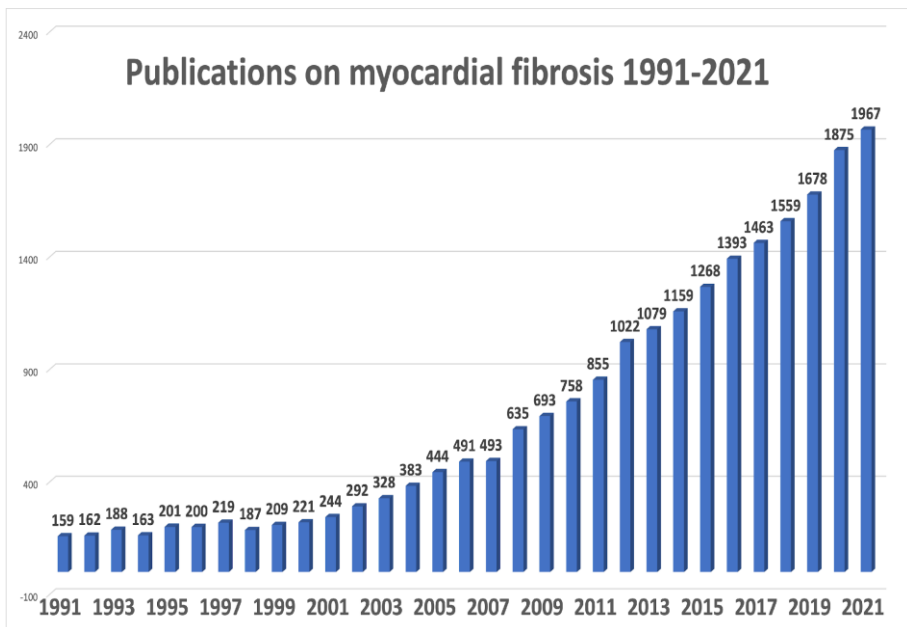
Fig. 5. Trend in publications on the topic of myocardial fibrosis between 1991-2021.

T1 relaxation time is a parameter that expresses the behavior of hydrogen nuclei in a magnetic environment. These protons release energy as they realign after exposure to an external field, with the time taken to realign being dependent on the nature of the tissue. T1 reflects the relaxation time in each pixel measured from its intensity in sequential images, often shown in a parametric display. T1 values obtained before and after contrast injection, together with hematocrit measurement, can be used to estimate the extracellular volume fraction (ECV) of a tissue (35).

A number of T1 mapping techniques have been shown to correlate with the degree of histological interstitial fibrosis in AS patients, suggesting a maladaptive response to pressure overload (36,37). The notion that

pathological LV remodeling in AS is, at least in part, driven by increasing levels of interstitial fibrosis suggests that T1 mapping may play a role in predicting future cardiovascular outcomes in AS or even help to time intervention. This makes assessment of myocardial fibrosis in AS a relevant and important issue.

The definition of normal ranges is essential for the interpretation of measured myocardial native T1 and ECV values. Myocardial T1 and ECV normal ranges depend on the magnetic field strength, the mapping sequence, protocol parameters and the regional evaluation strategy (38). Consequently, local reference values should be generated from datasets that have been acquired, processed, and analyzed in the same way as the intended application with the dedicated scanner and sequences. Local reference values should be compared with the published reported ranges; nevertheless, a local reference range should be primarily used. If local reference ranges are not available for T1 mapping, quantitative results should not be reported in routine clinical practice. According to the European Association for Cardiovascular Imaging consensus statement on CMR parametric mapping (38), it is currently considered optimal to define site-specific native T1 and ECV normal ranges from a minimum of 15 to, ideally, 50 or more healthy volunteers. For scenarios with large-magnitude biological changes of T1 value (e.g., in suspected amyloid or Anderson-Fabry disease), lower precision is acceptable (e.g., native T1 reference ranges may be calculated by obtaining values in 15-20 healthy subjects). For small-magnitude biological changes (e.g., diffuse myocardial fibrosis), high precision is required for native T1 mapping (e.g., native T1 reference ranges may be calculated by obtaining values in 50+ healthy subjects). Once a reference range is established, the major scan parameters, contrast agent/dose and systolic/diastolic phase should not be changed, and regularly repeated phantom-based quality control is recommended. In 2019, T1 mapping software was installed for the first time on a 1.5T Magnetom Aera (Siemens, Erlangen, Germany) scanner at VUH Santaros clinic, therefore local reference ranges of parametric mapping have to be established.

Novelty of the current research:

- We have performed the first large scale meta-analysis consolidating data on the topic of focal fibrosis in patients with AS and its clinical significance;
- Our prospective study is one of only a few worldwide studies investigating myocardial fibrosis in an AS population, integrating

data from multimodality cardiovascular imaging and a significant number of myocardial biopsies;

- The present work provides important new data on cardiovascular imaging biomarkers of subclinical LV myocardial injury in an AS population;
- This is the first study implementing CMR parametric imaging and providing T1 mapping data at VUH Santaros clinic;
- This is one of only a few research studies worldwide that has systematically screened AS patients for ATTR cardiac amyloidosis by implementing multimodality imaging and histological analysis.

1.3 Aim of the research

The aim of the research is to invasively and non-invasively explore LV myocardial structural changes in patients with severe AS and relate them to markers of cardiac decompensation.

1.4 Hypothesis of the research

- Primary – Myocardial fibrosis in patients with severe AS is associated with markers of LV decompensation and worse clinical outcomes: all-cause and cardiovascular mortality.
- Secondary – ATTR cardiac amyloidosis can be detected in patients with severe AS and is associated with more advanced cardiac remodeling.

1.5 Objectives of the research

1. To establish the prevalence and type of focal fibrosis in AS patients and determine its effect on post-operative clinical outcomes by performing a meta-analysis of published studies.
2. nvasively and non-invasively assess LV myocardial fibrosis in patients with severe AS undergoing surgical AVR and relate them to serum and imaging biomarkers of cardiac dysfunction.
3. To establish early biomarkers of LV myocardial injury in patients with severe AS.
4. To establish the prevalence of ATTR-CA in patients with severe AS undergoing surgical AVR.

1.6 Theses to be defended

1. Focal non-infarct type LV myocardial fibrosis is highly prevalent in severe AS patients and increases their all-cause and cardiovascular mortality.
2. CMR detected and histologically measured myocardial fibrosis is associated with more advanced LV remodeling, imaging and serum biomarkers of LV dysfunction.
3. Low GLS, elevated native T1 and elevated ECV can differentiate patients with more advanced LV remodeling and can serve as early biomarkers of LV damage.
4. ATTR cardiac amyloidosis can be detected in AS patients and is associated with more advanced LV remodeling and worse clinical outcomes.

2. LITERATURE REVIEW

2.1 Myocardial fibrosis in aortic stenosis

Degenerative AS is one of the most common valvular heart diseases, characterized by a progressive narrowing of the aortic valve (AV) and by compensatory hypertrophic remodeling of the LV myocardium (39). While LV hypertrophy maintains wall stress and cardiac output, it eventually decompensates, with cell death and myocardial fibrosis identified as key processes (5,40). Myocardial fibrosis is associated with the disruption of normal myocardial structure by excessive deposition of the extracellular matrix and creates a mechanistic base for adverse cardiac remodeling (41). Moreover, changes in cellular and extracellular matrix architecture, triggered by the greater afterload and wall stress in AS, increases tissue stiffness and impairs contraction (42). This complex interplay between components of cardiac remodeling can be evaluated by the histological analysis of myocardial biopsy samples or by the use of advanced imaging techniques with the ability of tissue characterization. CMR, strengthened by the development of T1 mapping, provides a non-invasive and global estimation of myocardial fibrosis. Two distinct types of myocardial fibrosis can be depicted by CMR: the LGE technique quantifies focal fibrosis (11,43), and diffuse interstitial expansion can be measured by T1 mapping (44).

2.1.1 LGE in aortic stenosis

Different trials have shown a variable prevalence of LGE in AS patient cohorts (43,45,46). The predominant location of myocardial fibrosis described was in the basal part of the LV. One possible explanation for this is the magnitude of hypertrophy at the base of the LV, this having the highest involvement of the basal septum (47). Treibel et al. (48), investigating 133 patients with severe AS undergoing surgical AVR, found that up to 60% of the LGE was located at the right ventricular insertion point. LGE, when isolated to the right ventricular insertion point, which is frequently observed in AS patients, may represent expanded extracellular volume rather than replacement fibrosis (49). It has been shown that in patients with hypertrophic cardiomyopathy, LGE that is isolated to right ventricular insertion points was not associated with increased risk (50). However, none of the studies investigated the association between the location of LGE and the risk for adverse events in AS populations.

Focal myocardial fibrosis has been shown to be irreversible following AVR, causing incomplete recovery of LV function and worse post-operative clinical outcomes, suggesting delayed timing of aortic valve intervention in some patients (51). Everett et al., in a cohort of 61 asymptomatic moderate and severe AS patients over a median follow-up of 2.1 years, demonstrated the rapid progression of mid-wall fibrosis (78% increase in LGE mass per year). None of the patients with LGE showed a resolution of established fibrosis post-AVR. In agreement with these findings, no change in LGE following AVR was reported in 5 other studies (11,43,52-54). It appears that once established, focal fibrosis is not reversible after valve intervention, leaving these patients with a residual risk of adverse events. These findings suggest that current management strategies do not completely identify high-risk patients with severe AS and that the scar that patients develop while waiting for intervention contributes to their poorer long-term prognosis.

2.1.2 T1 mapping in aortic stenosis

Several studies in AS patients have reported that native T1 and ECV values correlate with the degree of diffuse myocardial fibrosis assessed invasively. In a study investigating 31 patients with mixed valvular lesions, AS, aortic regurgitation and mitral regurgitation, a significant association between histologically measured myocardial fibrosis and ECV was found (r=0.78, p<0.001) (55). In a study by Lee et al. (37), investigating asymptomatic moderate to severe AS patients, native T1 values correlated well with the degree of diffuse myocardial fibrosis in intraoperative myocardial biopsy specimens (n=20) (r=0.777, p<0.001). In another study investigating 71 severe AS patients undergoing AVR, the ECV (r=0.465; p<0.0001), GLS (r=0.421; p=0.0003), and native T1 (r=0.429; p=0.0002) values were significantly correlated with the degree of myocardial fibrosis measured in myocardial biopsies (n=71) (56). However, there have been studies that failed to demonstrate this association (48), therefore the data is still conflicting.

Recently, several large studies have investigated the role of T1 mapping in the prognostic stratification of patients with AS, demonstrating its predictive value in terms of increased adverse events and prognosis following AVR (57-59). Everett et al. in a multicenter prospective study of severe AS patients (n=440) scheduled for surgical AVR or TAVI demonstrated that mortality from all causes progressively increases as the ECV increases, with a 10% increase in mortality for every 1% increase in ECV (57). It is thus stated that interstitial fibrosis quantified with the T1 mapping technique at CMR

constitutes an independent predictor of mortality, which overcomes age, sex and reduced LVEF. This study demonstrated another relevant finding in which the authors demonstrated a significant overlap between the T1 mapping measurements carried out in different centers using scanners of different brands, operating at variable magnetic fields (1.5T and 3T) and with diversified acquisition protocols, thus overcoming the major problem related to the lack of reproducibility of the T1 mapping values between different centers. However, this data was confirmed only for the ECV expressed as a percentage, while the native T1 values proved not to be reproducible between different centers. Kwak et al. in an international prospective multicenter study (n=799) aimed to identify prognostically important CMR markers in AS patients and their thresholds of mortality using machine learning (58). The authors demonstrated that CMR markers of fibrosis and their thresholds— ECV% >27% and LGE% >2%—provide significant prognostic information among patients with severe AS undergoing AVR. Importantly, among the subgroup of patients with no or minimal symptoms (NYHA functional class I to II: n=474), patients with higher levels of diffuse and replacement myocardial fibrosis on preoperative CMR had worse post-AVR survival rates compared with patients with lower levels of myocardial fibrosis. This raises the hypothesis that early detection of these markers of myocardial fibrosis could be taken as objective evidence that the LV is starting to fail and that AVR should be considered even in asymptomatic patients. In a single center prospective study by Hwang et al. severe AS patients (n=44) underwent CMR with T1 mapping prior to and one year following AVR (59). Patients were divided into three groups depending on their baseline native T1 values. The authors reported a significant decrease in native T1 values 1 year after the AVR (pre-AVR, 1233.8 ± 49.7ms; post-AVR, 1189.1 ± 58.4ms; p<0.001), which was associated with LV mass regression and systolic function improvement. This finding suggests that diffuse fibrosis measured by native T1 is reversible with afterload relief and demonstrates a potential to serve as an early marker of adverse LV remodeling.

2.2 ATTR cardiac amyloidosis in aortic stenosis

2.2.1 The prevalence of ATTR-CA in aortic stenosis

ATTR-CA is described as a progressive infiltrative cardiomyopathy with ventricular wall thickening and predominantly diastolic heart failure (14). ATTR-CA can be either hereditary due to >120 mutations in a transport

protein, TTR, or acquired based on wild-type ATTR-CA (20,60). Until recently, ATTR-CA was frequently overlooked in patients with AS or heart failure. Advances in diagnostic imaging techniques and the introduction of a new non-invasive diagnostic algorithm have significantly increased the capability of disease detection. According to Martinez-Naharro et al., it has resulted in a >30-fold higher rate of ATTR-CA diagnosis in the last decade (15). Data from postmortem studies in unselected subjects indicate a prevalence of cardiac amyloidosis of 22% to 25% in subjects older than 80 years of age (61). In an autopsy series of patients who had undergone TAVI, Nietlispach et al. found varying degrees of ventricular myocardium amyloid infiltration in approximately one-third of cases (62). In a recent series, the proportion of AS patients identified with ATTR-CA varied greatly and was between 4% and 16% (19,23,63,64). The large variability in the prevalence of ATTR-CA in AS patients could be explained by different study inclusion criteria and the diverse study populations that are investigated. A higher prevalence of ATTR-CA was found in TAVI cohorts. Scully et al. reported a 13.9% prevalence of ATTR-CA in severe AS patients referred for TAVI, with a mean age of 88 ± 6 years (63). In a study by Castano et al., occult ATTR-CA was identified in 16% of patients after TAVI (64). In that study, ATTR-CA patients were more frequently male (91.7%), with a mean age of 86.3 ± 5.7 years. A lower prevalence of ATTR-CA was described in a cohort of severe AS patients undergoing surgical AVR. Amyloid deposition was identified in the endomyocardial biopsies of 6 out of 146 (4%) patients at the time of surgical AVR (19). In a retrospective study by Cavalcante et al., out of 113 patients with severe and moderate AS, 9 patients (8%, all >80 years; 8/9 males) had cardiac amyloidosis confirmed by CMR with LGE (23). In that study, the average age for patients with cardiac amyloidosis was higher than those with isolated AS (88 ± 6 vs. 70 ± 14, p <0.0001). In a recent multi-center study (ATTRact-AS) out of 125 elderly (aged ≥ 75) patients with severe AS referred for TAVI, 13% were confirmed with occult cardiac amyloidosis (24).

In summary, it appears that approximately 1 in 7 patients currently undergoing TAVI have occult ATTR-CA—a higher prevalence than surgical AVR cohorts. Furthermore, ATTR-CA typically affects males more, and the prevalence increases progressively with age. It has important clinical implications, as with an aging population the number of patients with coexistent ATTR-CA and severe AS is likely to increase.

2.2.2. Diagnostic work-up of ATTR-CA in aortic stenosis

Given the high prevalence of calcific AS in the general population and the increasing frequency of aortic valve interventions, it is prudent to screen those in whom there is a suspicion of concomitant ATTR-CA. Echocardiography with deformation analysis may be an initial diagnostic step, followed by contrast enhanced CMR with T1 mapping. While endomyocardial biopsy with histological staining and tissue typing remain the gold standard for the diagnosis of ATTR-CA, it may not be appropriate in frail elderly patients. Nuclear imaging with technetium labeled bone-seeking tracers, coupled with serum and urine electrophoresis for the exclusion of monoclonal protein, may be a more suitable approach in this population. Bone scintigraphy carries the highest sensitivity for ATTR-CA detection; however, it would be a time and resource consuming strategy to scan all AS patients. Therefore, different diagnostic algorithms have been developed. Nietsche et al. proposed a score (RAISE score) that could help the clinician in identifying the subjects affected by both diseases (24). This score takes into account five main elements giving a different weight to each of them: (i) carpal tunnel syndrome (3 points), (ii) intra-ventricular electrical conduction disturbances (2 points for right bundle branch block, 1 point for low peripheral voltages, or a Sokolow–Lyon index <1.9 mV), (iii) restrictive myocardial remodeling (1 point for septal hypertrophy >18 mm, 1 point for altered E/A ratio), (iv) substrate of chronic myocardial damage (1 point for high sensitivity Troponin T >20 ng/L), (v) 1 point for age >85 years. In patients with two or more points, further investigation is warranted. However, due to disease heterogeneity and the wide spectrum of clinical presentation, the optimal diagnostic algorithm for cardiac amyloidosis screening in AS patients is still unclear and needs to be reviewed by further investigation. **Figure 6** summarizes the cardiovascular imaging modalities used for the diagnosis of ATTR-CA (65).
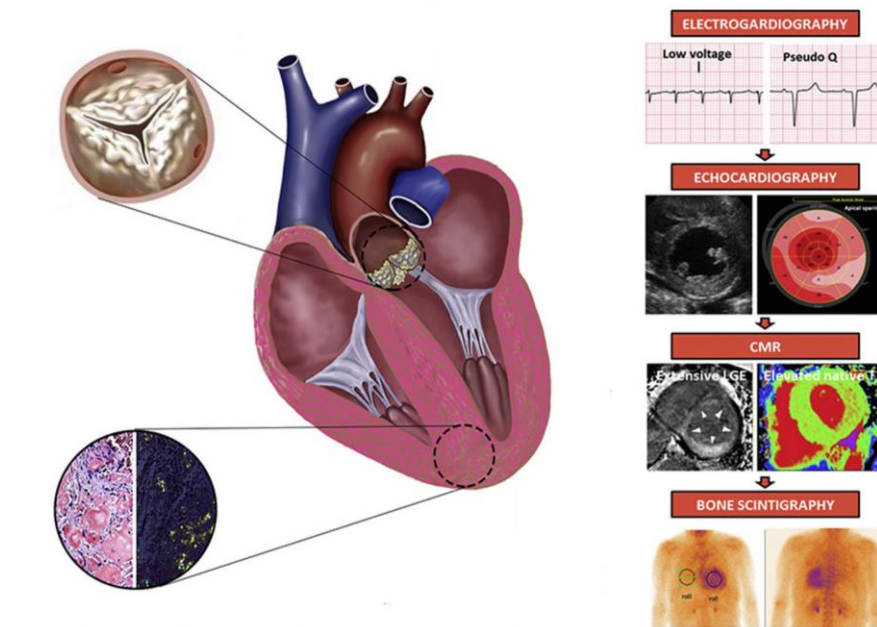
Fig. 6. Recognizing ATTR cardiac amyloidosis in aortic stenosis.

2.2.3 Management of patients with ATTR-CA and AS

The recognition of ATTR-CA is important before aortic valve intervention in order to provide better risk stratification and management choices. To date, there are no recommendations and no expert consensus on the management of patients with concomitant AS and ATTR-CA, which makes the treatment of these two diseases' coexistence challenging for clinicians. Until recently, either patients with ATTR-CA were considered too high a risk for aortic valve intervention and medical management or repeated aortic valve balloon valvuloplasties were preferred over the valve replacement strategies. Currently, an increasing body of new evidence from large prospective studies has brought changes to this disease's perception and reassurance to the patients. Several recent multicenter studies have investigated the clinical outcomes of severe AS patients who were screened for ATTR-CA by bone scintigraphy (24,25,66). It has been shown that aortic valve intervention, with TAVI being the most frequently used replacement strategy, has significantly improved survival rates in patients with AS and ATTR-CA compared to medical management, disproving the preconception

that TAVI may be futile in these patients. Importantly, periprocedural complications, namely vascular complications, kidney injury, and permanent pacemaker implantation of patients with ATTR-CA were the same as lone AS patients (25,66). Although this data comes from non-randomized clinical trials, it suggests that patients with concomitant AS and ATTR-CA should be offered TAVI as an effective and safe alternative. Most studies assessing patients following surgical AVR showed a high risk of mortality and modest improvement in functional class (19,21-23). Thus, it seems reasonable to prefer TAVI in patients with ATTR-CA, rather than open heart surgery as some small studies have suggested better outcomes with this approach.

The decision to intervene should depend on the severity of the cardiac involvement and the overall patient prognosis. In the reported series, compared to patients with lone AS, those with AS and ATTR-CA were older and had worse functional status, worse cardiac remodeling, higher circulating N-terminal pro-brain natriuretic peptide (NT-proBNP) and troponin levels plus they more frequently exhibited a low-flow, low-gradient AS pattern (24). Therefore, the risk and benefit of aortic valve intervention should be discussed by the heart team and with each patient individually. Cardiac biomarkers can be used to risk stratify cardiac amyloidosis patients. The staging system from the U.K. National Amyloidosis Center is applicable for both wild type and mutant type ATTR-CA, and discriminates patients into three prognostic categories depending on their NT-proBNP levels and estimated glomerular filtration rate (eGFR) (67). The risk and benefit of aortic valve intervention should be carefully reconsidered in patients at stage three cardiac amyloidosis.

Early diagnosis of ATTR-CA is also critical in order to gain the best efficacy of amyloid directed therapies. Contemporary treatment strategies that stabilize Transthyretin have been reported to improve survival in patients with ATTR-CA (68,69). Tafamidis treatment, compared to placebo, resulted in lower all-cause mortality, a 32% relative risk reduction in cardiovascular hospitalizations and a lower rate of decline in the 6-minute walk test (6MWT). The drug was approved by the U.S. Food and Drug Administration for ATTR-CA in 2019, and by the European Commission in 2020. Whether patients with AS and ATTR-CA after AVR will benefit from novel therapies that stabilize the ATTR tetramer (68) or reduce ATTR serum levels (70,71) is unclear, as patients with AS were excluded from previous randomized controlled trials in this area. Multicenter registries and larger studies of patients with cardiac amyloidosis following AVR are required to elucidate the benefit of ATTR therapy in this patient cohort.

3. METHODS

3.1 Meta-analysis

The meta-analysis was performed in accordance with the Preferred Reporting Items for Systematic Reviews and Meta-Analyses (PRISMA) statement (72). A systematic search of PubMed and EMBASE was performed from inception to October 2018. The indexing terms "aortic stenosis" and "late gadolinium enhancement", or "delayed gadolinium enhancement", or "LGE", or "cardiovascular magnetic resonance" were used to design the search strategy. The search was restricted to studies published in English and human studies. Reference lists of included articles were reviewed for relevant publications not identified in our initial search.

Prospective observational studies describing myocardial fibrosis detected by LGE-CMR in adult patients with AS were included in the meta-analysis. All included studies were pooled into 2 groups: 1) studies providing information about the presence or absence of LGE and 2) studies reporting adverse event rates between groups with and without LGE. All-cause mortality and cardiovascular mortality represent the main outcomes of this meta-analysis. Any pattern of LGE was accounted for to define the presence or absence of LGE. If several studies were performed within the same population, the studies with the largest number of patients were included. Data on the presence, pattern and extent of LGE were obtained. Data concerning the numbers of patients with and without adverse events, stratified by the presence or absence of LGE, were extracted from the original reports or estimated from the total number of patients and number of deaths in different groups. The review process is depicted in **Fig 7.**
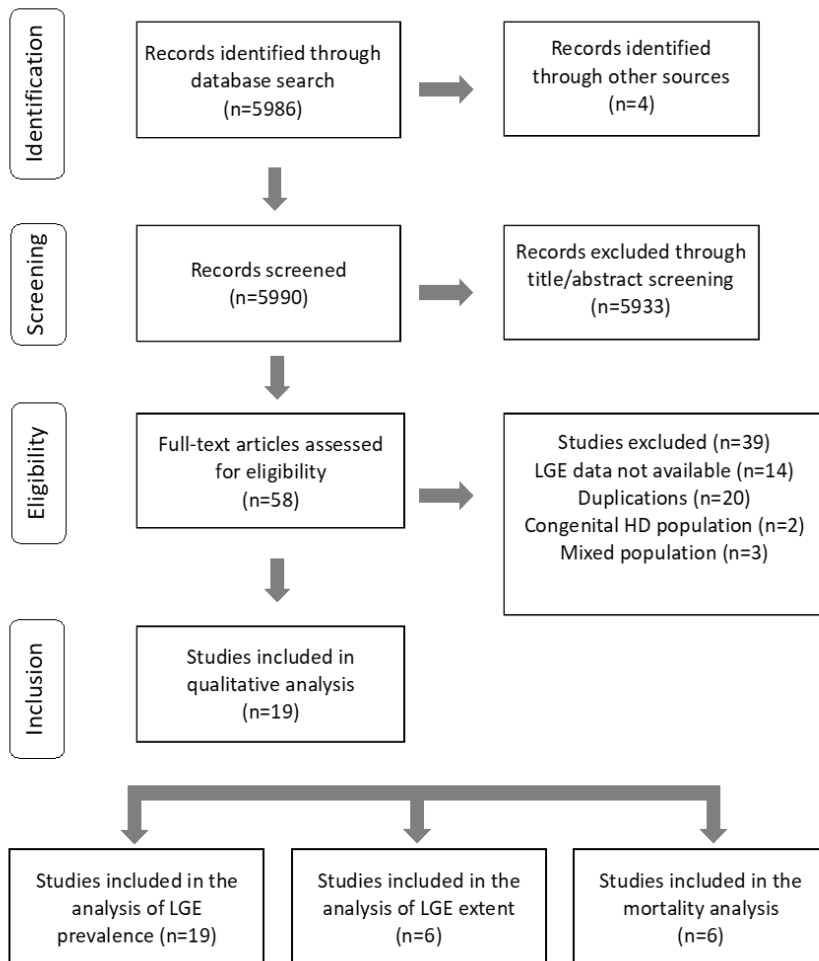
Fig. 7. PRISMA flow diagram.

3.2 FIB-AS study

3.2.1 Study design

In this prospective observational study at VUH Santaros clinics between November 2018 and March 2021, patients with severe symptomatic AS that were scheduled for AVR according to current treatment recommendations (4) were recruited. The study was approved by the Biomedical Research Ethics Committee of the Vilnius Region (Approval

Number: 158200-18/9-1014-558) and was performed as part of the FIB-AS study (NCT03585933). This study conformed to the principles of the Helsinki Declaration, and all subjects gave written consent to participate.

Patients were recruited prior to a pre-operative assessment and underwent a clinical assessment, comprising a clinical history, the Minnesota Living with Heart Failure Questionnaire (MLHFQ), the 6MWT, blood sampling [for hematocrit, renal function, brain natriuretic peptide (BNP) and high sensitivity troponin I (Hs-Tn-I)], a transthoracic echocardiogram, and CMR. The inclusion criteria were: patients who were undergoing AVR for severe AS, [defined as aortic valve area (AVA) $\leq$1cm^2 or AVA index $\leq$0.6cm^2/m^2, as determined by ultrasonography], age >18 years, ability to undergo a CMR scan, and consent to the study protocol. The exclusion criteria were: significant CAD (>50% lesion in an epicardial vessel), history of myocardial infarction, severe valve disease other than AS, eGFR <30mL/min/1.73m^2, CMR-incompatible devices, persistent atrial tachyarrhythmias, and previous cardiac surgery (**Table 1**; **Fig. 8**). Surgical AVR was performed by standard midline sternotomy or J mini sternotomy with cardiopulmonary bypass and mild hypothermia. The St. Jude Medical Trifecta aortic bioprosthesis (St. Jude Medical, Inc., St. Paul, MN, USA) or mechanical CarboMedics Standard Aortic Valve (CarboMedics, Inc.; Austin, Tex) prostheses of varying sizes were used according to the surgical team's or patient's preference. Patients were routinely followed and managed according to available guidelines (4). The study data were collected and stored in a dedicated online database, REDCap (Research Electronic Data Capture) (73).

Table 1. FIB-AS study inclusion and exclusion criteria.

Inclusion Criteria
- Severe AS (defined as AVA $\leq$1cm^2 or AVA index $\leq$0.6cm^2/m^2 as determined by echocardiography examination)   - Males and females of any ethnic group $\geq$18 years of age   - Signed an informed patient consent form
Exclusion Criteria
- Unable to provide informed consent   - Severe valvular heart disease other than AS   - Coronary artery disease (>50% lesion in an epicardial vessel)   - History of myocardial infarction   - Prior cardiac surgery   - Severe renal impairment – eGFR <30ml/min/1.73m^2 - Any absolute contraindication to CMR   - Permanent atrial fibrillation   - Patient with implanted cardiac devices (pacemaker, ICD)   - Inherited or acquired cardiomyopathy   - Other medical conditions that limit life expectancy or preclude AVR   - Pregnant or nursing women   - Mental condition rendering the patient unable to understand the nature, scope, and possible consequences of the study or to follow the protocol

AVA, aortic valve area; ICD, implantable cardioverter defibrillator; eGFR, estimated glomerular filtration rate.
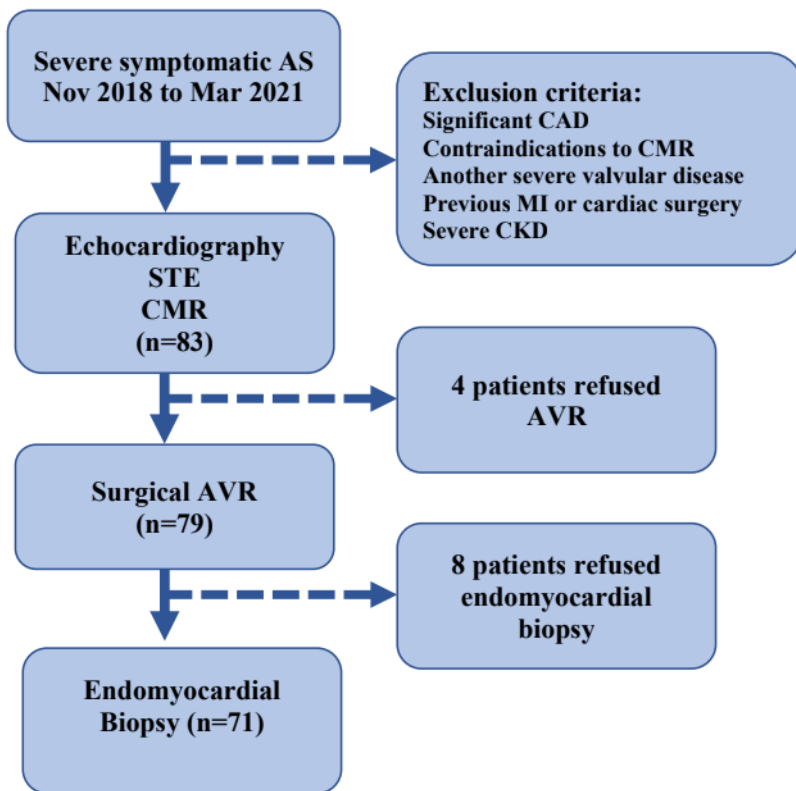
Fig. 8. FIB-AS study flow chart. CKD, chronic kidney disease; MI, myocardial infarction.

3.2.2 Investigations

3.2.2.1 Echocardiography with 2D strain analysis

Transthoracic 2D echocardiography was performed using the commercially available Vivid ultrasound system (S70, E9 or E95) (GE Healthcare, Horten, Norway), and the data were stored on a dedicated workstation for subsequent off-line analysis. AS severity and LV systolic and diastolic function were evaluated per the echocardiographic guidelines (74,75). AVA was calculated using the continuity equation.

From the 2D grey-scale images of the apical 2-, 3- and 4-chamber views, LV GLS was measured and processed off-line using commercially available software (EchoPac 112.0.1, GE Medical Systems, Horten, Norway) (76). The frame rate was adjusted from 50 to 80 FPS. End-systole was defined,

based on the closure click on the spectral tracing of the pulsed-wave Doppler of AV flow. GLS was acquired using the average regional strain curves (17-segment model for 2D STE). Segments with poor quality tracking or aberrant curves (despite manual adjustment) were removed from the analysis. The relative apical sparing (RAS) pattern of GLS was defined using the equation: (average apical longitudinal strain/ (average basal longitudinal strain + average midventricular longitudinal strain). Due to missing data or poor image quality, STE analysis was completed for 77 of 83 patients.

3.2.2.2 CMR with T1 mapping analysis

CMR scans were obtained using standard protocols on a 1.5T Siemens Aera scanner with surface coils and retrospective electrocardiography (ECG) triggering. LV end-systolic and end-diastolic diameters and maximum wall thickness were traced and recorded from the short-axis and long-axis views of the standard ECG-gated steady-state-free precession cine sequence. LV volumes, mass and ejection fraction were measured using commercial software (suiteHEART®) from a stack of sequential 8mm short-axis slices (0-2mm gap) from the atrio-ventricular ring to the apex. Measurements were indexed to the body surface area in m² (using the DuBois formula).

To detect late gadolinium enhancement images were acquired 10-15 minutes after the intravenous administration of gadobutrol (0.2 mmol/kg) (Gadovist, Bayer AG, Germany) using a breath-hold segmented inversion recovery fast-gradient echo sequence in the short-axis and long-axis planes of the LV, with an 8mm slice thickness and 0% distance factor. The region of myocardial fibrosis was defined as the sum of pixels with a signal intensity above 5 standard deviations of the normal remote myocardium in each short-axis slice. The presence of LGE was determined qualitatively by two independent readers, blinded to the clinical data.

Myocardial fibrosis was assessed using native and post contrast T1 mapping at a mid-ventricular short-axis section, acquired using a modified Look-Locker inversion recovery (MOLLI) sequence with motion correction (the '3-3-5' standard protocol) before and 15 minutes after contrast administration (77). Scanner-generated T1 maps were processed off-line using commercially available software (suiteHEART by NeoSoft). The region of interest was manually traced on the short-axis, native and post-contrast T1 maps in the septum at the mid-ventricular level. All T1-related measures were traced in the middle third of the myocardium to avoid partial volume effects. Segments containing LGE were excluded from the T1 mapping analysis (38).

To measure the T1 value of blood, circular regions of interest were positioned in the LV cavity, avoiding the papillary muscles. Native T1, ECV%, and indexed ECV values were then calculated. ECV was calculated using the formula: ECV% = ($\Delta R1m/\Delta R1b$) × (1 - hematocrit level) × 100, where R1 is 1/T1, R1m is R1 in the myocardium, R1b is R1 in the blood and $\Delta R1$ is the change in relaxation (**Table 2**) (78). Hematocrit was drawn on the day of CMR scanning. Due to incomplete datasets, T1 mapping parameters were measured in 67 of 83 patients. **Figure 9** shows the FIB-AS study CMR assessment protocol.

Table 2. Definitions of cardiac parametric mapping terms.

Term	Definition
T1 (ms)	Time constant representing the recovery of longitudinal magnetization (spin–lattice relaxation)
Native T1 (ms)	T1 in the absence of an exogenous contrast agent
ECV (%)	Extracellular volume fraction, calculated by $$ECV = \dfrac{\left(\dfrac{1}{T1\ myo\ post} - \dfrac{1}{T1\ myo\ nat}\right)}{\left(\dfrac{1}{T1blood\ post} - \dfrac{1}{T1blood\ nat}\right)} \times (100 - Ht)$$ where myo – myocardium; post – post contrast; nat – native; blood – intracavitary blood pool; Ht (hematocrit) – cellular volume fraction of blood (%).
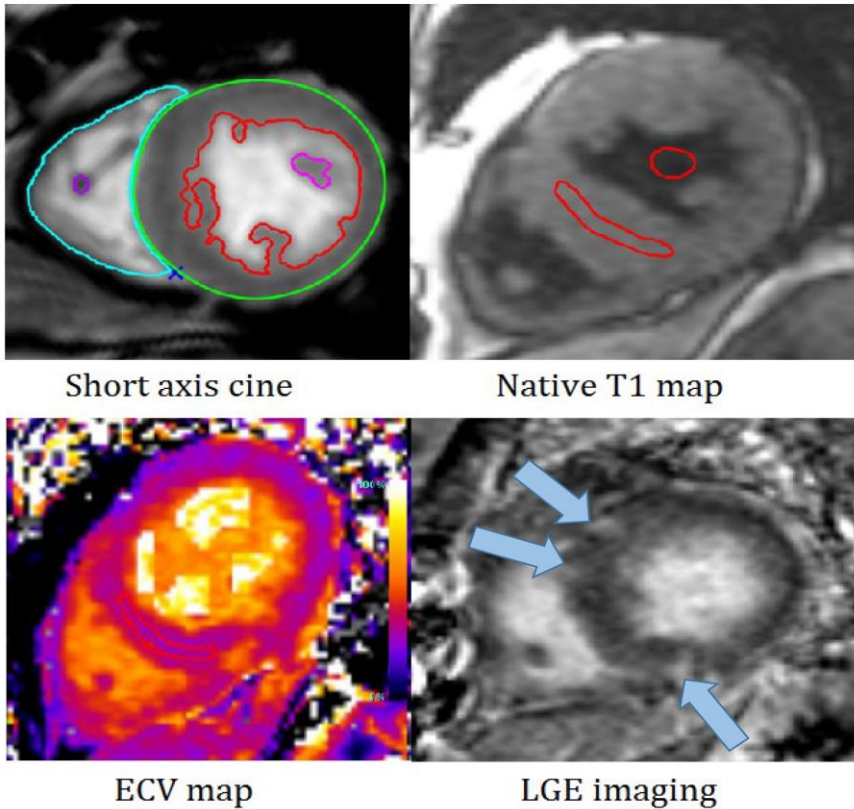
Fig. 9. Multiparametric CMR assessment protocol of FIB-AS study. Short axis images of patient with aortic stenosis: short axis cine, native T1 map, ECV map and LGE imaging showing areas of focal fibrosis (blue arrows).

3.2.2.3 Histological analysis

At the time of surgical AVR, biopsy specimens were obtained under direct vision by the surgical team using a surgical scalpel from the basal antero-septum just after removal of the diseased aortic valve. One intraoperative myocardial biopsy sample (mean area $22.5 \pm 12mm^2$) was taken from each patient. All myocardial tissue samples were fixed in 10% neutral buffered formalin and embedded in paraffin. Sections (3 µm thick) were sliced on a Leica RM2145 microtome and stained with hematoxylin and eosin, Masson's trichrome and Congo red. Digital images were captured on an Aperio Scan-Scope XT Slide Scanner (Aperio Technologies, Vista, CA, USA) under 20×objective magnification (0.5 µm resolution). Histologists, who were blinded to the clinical and CMR data, examined all biopsy specimens.

The fraction of myocardial volume that was occupied by collagen tissue (collagen volume fraction, CVF) was determined by quantitative morphometry on an automated image analysis system (HALO™). The area of myocardial fibrosis was calculated using the HALO™ Area Quantification v2.1.11 algorithm (IndicaLabs, NM, USA) (79). The subendocardial layer was defined as 1mm from the endocardial surface, whereas the rest of the tissue sample was defined as the midmyocardial layer. All study assessments are summarized in **Table 3.**

Table 3. Summary of study assessments.

Demographic data and comorbilities	• STS risk score • EuroSCORE II
Functional status and quality of life assessment	• New York Heart Association functional class • Minnesota Living with Heart Failure Questionnaire • 6-minute walking test
Serum biomarkers	• Brain natriuretic peptide • High sensitivity troponin I
Cardiovascular imaging	• 2D echocardiography with strain analysis • 1.5T contrast-enhanced CMR with T1 mapping
Myocardial histological analysis	• Quantitative myocardial fibrosis assessment • Myocardial amyloid deposition assessment

3.3 Statistical analysis

3.3.1 Meta-analysis

Statistical analysis was performed by making use of the R language and environment for statistical computing (version 3.5.1) (80), in particular the metafor package (version 2.1-0) (81) was used. To compute pooled estimators, a random effects model with restricted-likelihood estimator was applied (82). In order to present the results of the pooled analysis, forest plots were used. The effects' heterogeneity was assessed by use of the I^2 value, corresponding test and funnel plots. Publication bias was assessed by a linear Egger's test and was treated as significant at $p<0.10$. (83). Additionally, a 1-study removal analysis was performed to look for potentially influential studies and a cumulative meta-analysis to gain insight into the research dynamics in time. Differences were considered statistically significant at a 2-sided p value <0.05.

3.3.2 FIB-AS study

Variables were presented as mean ± standard deviation or median and interquartile ranges. Categorical variables were expressed as frequencies and percentages and were compared by a v2 test. An unpaired student's t-test and a Mann–Whitney U test were used to compare two groups of continuous variables. Pearson's and Spearman's correlation coefficients were calculated to assess the relationships between continuous variables. Intra- and inter-observer variation was analyzed by the Bland-Altman method and a calculation of the correlation coefficient. The statistical analysis was performed in R (version 4.1.2) (84). Differences were considered statistically significant at a 2-sided p value <0.05.

4. RESULTS

4.1 Meta-analysis results

In total, 19 studies, accounting for 2032 patients, were included in the meta-analysis (10,11,43,45,46,52,55,85-96). A significant number of single center studies (n=20) were excluded from the analysis due to possible data overlap. Six studies (10,11,43,45,85,86), combining 1,300 patients, were included in the calculations of the pooled ORs (Odds Ratios) of all-cause mortality. The data for cardiovascular mortality were not available in one study (85). Therefore, it was based on five studies comprising 1,246 patients. The characteristics of these studies and number of events stratified by the presence or absence of LGE are listed in **Table 4**. Finally, 6 studies (1,044 patients) were included for the calculations of the pooled ORs of quantitative LGE by the percentage of LV mass (43,45,55,85,88,90). All 19 studies were analyzed for the prevalence of LGE.

All studies were prospective cohort studies, and the majority were single-center, except for 2 studies, which were multicenter (45,96). The mean follow-up duration was 2.8 years. In the majority of studies, patients with severe AS underwent surgical AVR, and 6 studies also investigated patients undergoing TAVI (43,45,52,89,90,92).

The age of patients ranged from 47 to 83 years (mean 69.8), and male patients dominated in all of the studies. Hypertension was the most common comorbidity (61.4%). Also, 39.8% of all patients had significant CAD, and 7 studies excluded patients with CAD (46,55,85,87,93-95). The majority of patients had preserved LVEF (mean 57%) and high-gradient AS (mean AV pressure gradient 46mmHg) dominated in all of the studies. The patients' clinical characteristics are listed in **Table 5**.

The majority of investigators evaluated focal fibrosis by different signal intensity thresholds above the remote myocardium (43,55,85-90,94). 3 studies used a full width half maximum technique (11,45,95), and a small number of studies used visual assessment. The prevalence and extent of LGE are depicted in **Table 6**. LGE was present in a variable proportion of patients with AS (27% to 90%), and overall, 944 patients (49.6%) had LGE. Nine studies reported the type of LGE (10,11,43,45,46,55,86,87,89) and two thirds of AS patients (63.6%) exhibited a non-infarct LGE pattern.

Table 4. Description of studies included in the meta-analysis of clinical outcomes and number of outcomes by LGE status.

First author, study year	Study design	Number of patients	Population	Mean follow-up duration, yrs.	Valve intervention, n	All-cause mortality, n		CV mortality, n	
						LGE (-)	LGE (+)	LGE (-)	LGE (+)
Azevedo, 2010	Prospective longitudinal, single center	54	Severe AS (28), Severe AR (26)	4.3 ± 1.4	SAVR (54)	3	13	NR	NR
Dweck, 2011	Prospective longitudinal, single center	143	Moderate AS (57), Severe AS (86)	2 ± 1.4	SAVR (72)	2	25	2	21
Barone-Rochette, 2014	Prospective longitudinal, single center	154	Severe AS	2.9	SAVR (114), TAVI (40)	11	10	5	6
Chin, 2016	Prospective longitudinal, single center	166	Mild AS (34), Moderate AS (45), Severe AS (87)	2.9 ± 0.8	SAVR (37)	6	8	4	6
Rajesh, 2017	Prospective longitudinal, single center	109	Severe AS	0.96 ± 0.46	SAVR (38)	11	13	10	12
Musa, 2018	Prospective longitudinal, Multicenter	674	Severe AS	3.6	SAVR (399), TAVI (275)	45	100	16	54
Pooled, mean		1300		2.8		78	169	37	99

Values are presented as mean ± SD or n. AS, aortic stenosis; AR, aortic regurgitation; CV, cardiovascular; LGE (+), late gadolinium enhancement positive; LGE (-) late gadolinium enhancement negative; NR, not reported; SAVR, surgical aortic valve replacement; TAVI, transcatheter aortic valve implantation.

Table 5. Clinical and echocardiographic characteristics of patients included in the analysis of the prevalence of LGE.

First author, study year	No. of patients	Mean age, yrs.	Male gender, %	CAD, %	HTN, %	DM, %	AF, %	NYHA I/II/III/IV, %	LVEF, %	AV mean gradient, mm Hg
Debl, 2006	22	64	73	Excluded	NR	NR	NR	NR	52.7	>30
Azevedo, 2010	28	47.2 ± 13.5	64	Excluded	0	0	NR	4/43/53/0	53 ± 9	63 ± 20
Dweck, 2011	143	68 ± 14	67	57	54	25	19	NR	57.9	NR
Barone-Rochette, 2014	154	74 ± 9	62	29	62	23	9	27 (III-IV)	60 ± 15	49 ± 17
Mahmod, 2014	26	67.8 ± 9.73	73	Excluded	38	15	NR	NR	74.5 ± 5.8	NR
Chin, 2016	166	69	69	37	67	15	2	45/34/19/2	67 (63-71)	35±19
Rajesh, 2017	109	57.3 ± 12.5	57.8	34.8	50.4	10	NR	83.5 (I-II), 16.5 (III-IV)	56.5 ± 12.4	44.7 ± 13.6
Musa, 2018	674	74.6	63	29.2	53.1	21.7	12.5	13.3/42.3/40.7/3.6	61 ± 16.7	46 ± 18
Weidemann, 2009	46	69	60	Excluded	88	28	22	0/13/66/20	54.6	50.3
Nassenstein, 2009	40	76	57.5	Excluded	NR	NR	NR	NR	64.8 ± 13.3	NR
Kim, 2014	61	81.9 ± 5.3	52.5	68.9	95.1	27.9	36.1	NR	53.5 ± 13.8	43.4 ±17.3
Park, 2014	41	63.1 ± 8.7	58.5	Excluded	36.6	7.3	NR	57.9 (III-IV)	68 ± 8.2	55.6 ± 20.4
Hoffmann, 2014	30	78 ± 7	57	NR	NR	NR	Excluded	3/3/73/20	55 ± 10	53 ± 21
Ravenstein, 2015	31	70 ± 12	83	Excluded	75	17	33	48/52/0/0	NR	NR
Nucifora, 2016	43	83	51	17	89	40	27	NR	71	NR
Lee, 2017	127	68.8 ± 9.2	49.6	13.4	66.1	26.8	11.8	NR	61.8 ± 14.1	48 ± 19.3
Carter-Storch, 2017	87	70	62	32	59	18	NR	NR	62 ± 9	45.5
Singh, 2017	174	66.2 ± 13.34	76	NR	53.4	14.4	Excluded	NR	57	35.4
Buckert, 2018	30	78.8 ± 5.9	50	80	96.7	36.7	43.3	NR	56.7 ± 18.4	34 ± 14.6
Pooled, mean	2032	69.8	62.6	39.8	61.4	20.4	21.6		57.2	46.3

Values are mean ± SD, n (%), or median (interquartile range). AF, atrial fibrillation; AV, aortic valve; CAD, coronary artery disease; DM, diabetes mellitus; HTN, hypertension; LVEF, left ventricular ejection fraction; No., number; NR, not reported; NYHA, New York Heart Association.

Table 6. Studies included in analysis of the prevalence and extent of LGE.

First author, study year	Population	No. of patients	CMR field, T	Method for evaluation of LGE	LGE (+), n (%)	LGE non-infarct pattern, n (%)	LGE % of LV mass
Debl, 2006	Severe symptomatic AS	22	1.5	SI >2 SDs of remote myocardium	6 (27)	NR	4.3
Azevedo, 2010$	Severe AS (28), severe AR (26)	28	1.5	Mean SI of total myocardium ± 2 SDs of mean SI of remote area + 2 SDs of mean of air	17 (61)$	NR	3.15 ± 1.87$
Dweck, 2011	Moderate AS (57), severe AS (86)	143	1.5	FWHM	94 (66)	54 (38)	6.25
Barone-Rochette, 2014	Severe AS	154	1.5	SI >2.4 SDs of remote myocardium	44 (29)	30 (19)	3.5 ± 2.3
Mahmod, 2014	Severe AS	26	3	FWHM	21 (81)	NR	18.3 ± 9.4
Chin, 2016	Mild AS (34), moderate AS (45), severe AS (87)	166	3	Semiautomatic	44 (27)	44 (100)	NR
Rajesh, 2017	Severe AS	109	1.5	SI >2.4 SDs of remote myocardium	46 (42)	33 (30)	NR
Musa, 2018	Severe AS	674	1.5 and 3	FWHM	341 (50.6)	222 (65)	2.72 | 3.95
Weidemann, 2009	Severe AS	46	1.5	Visual	28 (60.8)	NR	NR
Nassenstein, 2009	Moderate AS (14), severe AS (26) with LVH ≥15mm	40	1.5	Visual	13 (32.5)	13 (100)	NR
Kim, 2014	Severe AS	61	1.5	Semiautomatic	42 (68.8)	NR	7.4
Park, 2014	Severe AS, preserved LVEF	41	1.5	Mean SI of total myocardium ± 2 SDs of mean SI of remote area + 2 SDs of mean of air	12 (29.3)	12 (100)	NR
Hoffmann, 2014	Severe AS	30	1.5	SI >6 SDs of remote myocardium	27 (90)	NR	7.7 ± 4.6

Ravenstein, 2015[$]	Severe AS (12), severe AR (9), severe MR (10)	31	3	SI >2.4 SDs of remote myocardium	17 (54.8)	17 (100)	1.4 ± 0.8[$]
Nucifora, 2016	Severe AS	43	1.5	SI >5 SDs of remote myocardium	29 (67.4)	NR	5.8
Lee, 2017	Moderate AS, severe AS	127	3	SI >5 SDs of remote myocardium	41 (32.3)	NR	5.2 ± 4.8
Carter-Storch, 2017	Severe AS	87	1.5	Visual	26 (30)	18 (20.6)	NR
Singh, 2017	Asymptomatic moderate-severe AS	174	3	NR	82 (47)	NR	4.3
Buckert, 2018	Severe AS	30	1.5	Visual	14 (46.7)	NR	NR
Pooled, mean		2032			944 (49.6)	443 (63.6)	5.8

Values are mean $\pm$ SD or n (%). ([$]) - Only the data of severe AS patients extracted; CMR, cardiovascular magnetic resonance; FWHM, full width half maximum; LVH, left ventricular hypertrophy; MR, mitral regurgitation; NR, not reported; SI, signal intensity; T, Tesla. Other abbreviations are as in Table 5.

An additional analysis of the type and prevalence of LGE depending on the CAD status was performed. Patients with concomitant coronary artery disease, compared to those with unobstructed coronary arteries, had a higher prevalence of LGE (62.8% vs. 44%, respectively). The vast majority of CAD-free patients exhibited non-infarct LGE pattern (93.6%), whilst infarct pattern LGE dominated in patients with coexistent CAD (54.6%) (**Table 7**).

Table 7. LGE prevalence by the presence of coronary artery disease and type of LGE.

Patients by CAD status	No. of patients	LGE (+) patients, n (%)	LGE non-infarct pattern, %
CAD (-)	976	430 (44.0)	93.6[$]
CAD (+)[&]	400	251 (62.8)	45.4

Values are n (%). Abbreviations are as in Tables 4 and 5. ([&]) Data from 5 studies reporting the presence of LGE by CAD status. ([$]) Data from 4 studies reporting LGE pattern in CAD free patients.

LGE is reported to be more prevalent in males and in those with systolic LV dysfunction and worse functional status. LGE was more frequently found in patients with higher indexed LV mass and higher indexed LV end-systolic and LV end-diastolic volumes. In addition, 12 studies reported the extent of LGE by percentage of LV mass, which ranged between 1.4% to 18.3% (11,43,45,52,55,85,88-90,94-96). The pooled extent of focal fibrosis as measured by LGE by percentage of LV mass was around 4% with precise point estimate and [95% CI] being equal to 3.83 and [2.14, 5.52], respectively (**Fig. 10**).
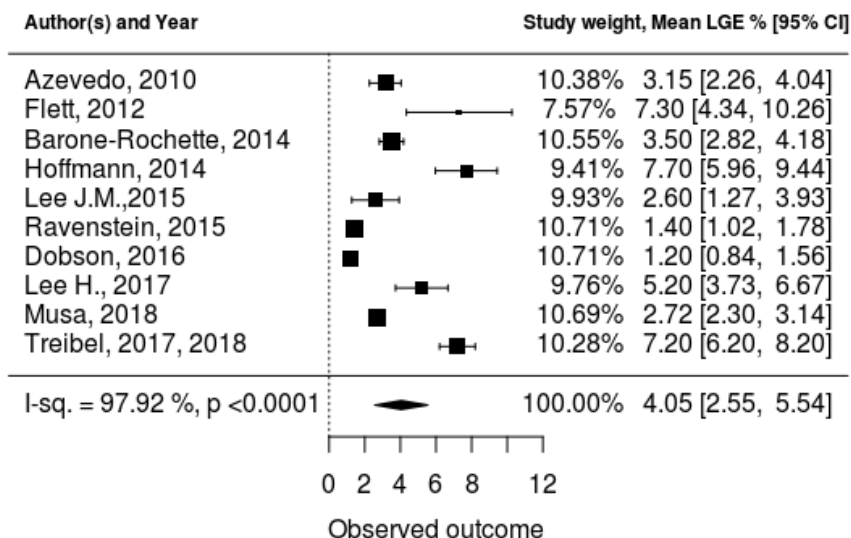
Fig. 10. Forest plot for quantitative LGE, expressed in percentage of LV mass. The pooled extent of focal fibrosis as measured by LGE by percentage of LV mass was 3.83%.

All-cause mortality occurred in 247 patients (19%), 169 of them with LGE (28% of LGE-positive patients) and 78 without LGE (11.2% of LGE-negative patients). The presence of LGE was associated with significantly higher all-cause mortality (pooled OR [95% CI]=3.26 [1.72, 6.18], p=0.0003) (**Fig. 11**).
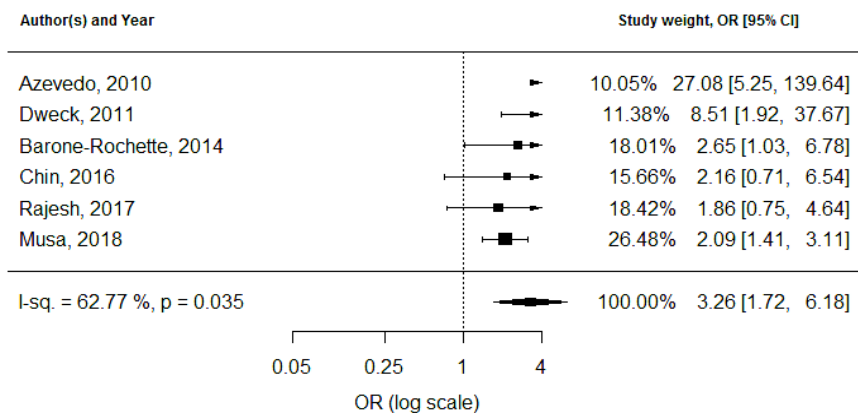
Fig. 11. Forest plot and pooled Odds Ratio (OR) for all-cause mortality. Calculated pooled OR=3.26.

Cardiovascular mortality occurred in 136 patients (10.9%), 99 of them with LGE (7.9% of LGE-positive patients) and 37 without LGE (3% of LGE-negative patients). The presence of LGE was associated with significantly higher cardiovascular mortality (pooled OR [95% CI] = 2.89 [1.90, 4.38], $p<0.0001$) (**Fig. 12**).

Fig. 12. Forest plot and pooled Odds Ratio (OR) for cardiovascular mortality. Calculated pooled OR=2.89.

2 studies analyzed the risk ratios expressed by quantitative LGE by percentage of LV mass (11,45). Dweck et al. (11) reported that with every 1% increase in the LGE mass, the risk of mortality increased by 5% (HR: 1.05; 95% CI: 1.01 to 1.09; p=0.005). Similarly, in a study by Musa et al. (45), a 1% increase in LV myocardial scar burden was associated with an 11% hig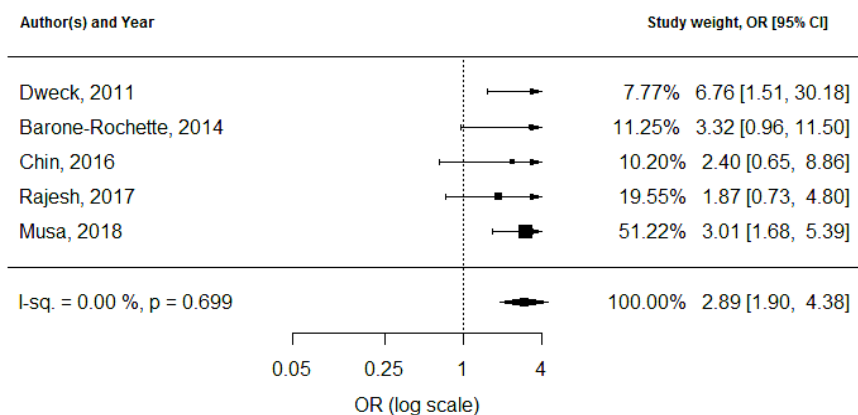her all-cause mortality hazard (HR 1.11; 95% CI: 1.05-1.17; p<0.001) and an 8% higher cardiovascular mortality hazard (HR 1.08; 95% CI: 1.01-1.17; p<0.001).

The data on predictors of all-cause mortality on multivariable analyses from individual studies were collected when available. In the studies, the factors independently associated with all-cause mortality were age, LVEF, NYHA functional class and LGE, both infarct and non-infarct type. Three studies found a significant association between poor functional status and all-cause mortality (43,45,86). A history of CAD, indexed LV mass and indexed LV end-diastolic volume did not predict adverse clinical outcomes (11,45).

In summary, our meta-analysis has demonstrated that LGE was present in a considerable proportion of patients with AS (49.7%) and had a significant association with the clinical outcomes- tripled all-cause and cardiovascular mortality (pooled ORs: 3.26 and 2.89, respectively).

4.2 Establishment of parametric mapping references values

In early 2019 the first T1 mapping software was installed in the 1.5T Magnetom Aera (Siemens, Erlangen, Germany) scanner at VUH Santaros clinics and on February 12th, 2019, the first parametric mapping exam was performed on a volunteer. Subsequently, through 2019-2021, magnetic resonance imaging scans in 30 healthy controls, free from any known cardiovascular diseases (43% males, mean age 35 ± 10 years) were performed and analyzed. The scanning parameters were as follows: flip angle of the readout sequence – 35; Gadolinium contrast dose – 0.2 mmol/kg; time between bolus contrast agent application and post-contrast T1 mapping – 10-12 minutes; region of interest – septal short axis, 1 slice. Exemplar parametric maps are presented in **Figure 13** and the local reference values of native T1 and ECV are presented in **Table 8.** The reference range for parametric CMR mapping established at VUH Santaros clinics is comparable with the values of myocardial T1 and ECV reported in cohorts of at least 30 healthy subjects using 1.5T magnetic resonance equipment. The methodological recommendations on CMR parametric mapping, aiming to provide a concise and comprehensive summary on the rationale, indications, and evidence of CMR parametric mapping, as well as presenting our initial clinical experience

while using this technique, have been published by the team led by prof. S. Glaveckaitė in 2020.
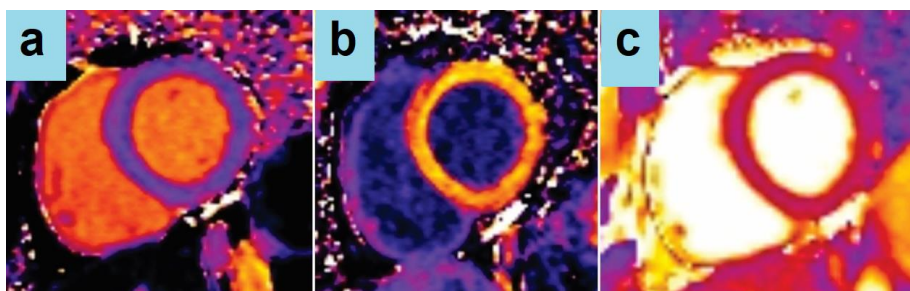
Fig. 13. Representation of obtained parametric maps in a healthy volunteer at VUH Santaros clinic. a) Native T1 map in basal short axis slice with a mean native T1 value of 948ms. b) Post-contrast T1 map corresponding as in a) basal short axis slice with a mean T1 of 372ms. c) T2 map the same as in a) and b) basal short axis slice with normal mean T2 value. Calculated ECV value – 25%.

Table 8. Normal values of myocardial native T1 and ECV, presented as mean ± standard deviation.

Variables	All subjects (n=30)	Females (n=17)	Males (n=13)
Native T1, ms	956 ± 59	931 ± 38	978 ± 67
ECV, %	24 ± 3	22 ± 1	26 ± 3

ECV, extracellular volume.

4.3 FIB-AS study results

4.3.1 Measurement of reproducibility

A measurement reproducibility analysis for GLS and CMR parametric mapping parameters was performed in twenty randomly selected patients. Both GLS and CMR parametric mapping measurements demonstrated excellent intra-observer and inter-observer reproducibility. The intraclass correlation coefficients for intra-observer and inter-observer variations are presented in **Table 9.**

Table 9. Results of inter-observer and intra-observer reproducibility analysis.

	ICC	95% CI	Bias
Inter-observer reproducibility			
Native-T1	0.958	0.91-0.98	9.1 ± 15.1
Post-contrast T1	0.973	0.94-0.99	0.8 ± 9.2
T2	0.968	0.93-0.99	0.2 ± 1.3
GLS	0.981	0.96-0.99	1.5 ± 1
Intra-observer reproducibility			
Native-T1	0.945	0.88-0.97	3.3 ± 11.0
Post-contrast T1	0.987	0.9-0.99	0.95 ± 7.53
T2	0.983	0.96-0.99	0.59 ± 0.84
GLS	0.969	0.93-0.98	0.51 ± 1.3

CI, confidence interval; ICC, intraclass correlation coefficient
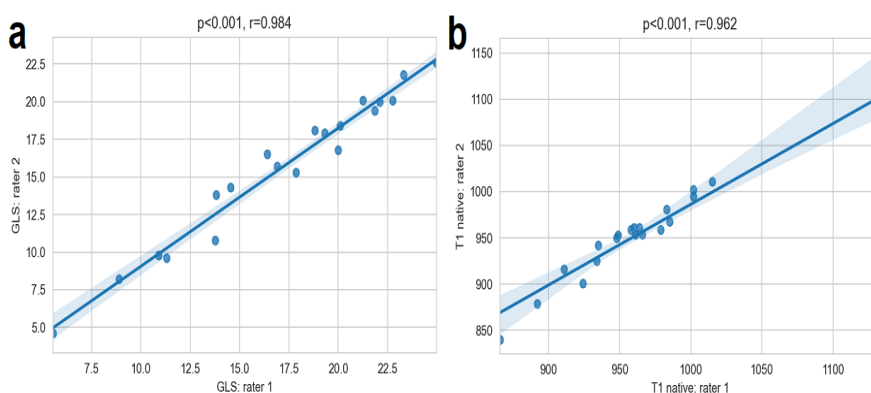

Fig. 14. Correlations between global longitudinal strain (GLS) (a) and native T1 (b) measurements performed by two different raters are shown.

4.3.2 Patients' cohort description

A total of 83 patients were included (age 66.4 ± 8.3 years, 58% female, AVA index 0.44 ± 0.1cm^2/m^2, peak AV velocity 4.8 ± 0.6m/s, mean gradient 57.8 ± 16mmHg). The main reasons for non-eligibility were significant CAD, renal dysfunction and other valvular abnormalities. The mean LVEF was 66.8 ± 13%, with 10% of patients having reduced LVEF (<50%). Overall, patients had low surgical risk, with STS-PROM and EuroScore II <2% (1.9% and 1.5%, respectively). Patients with congenital AS were more likely to be younger (p<0.001), were at lower surgical risk (p=0.004), and had better renal function (p=0.002). Of the 83 enrolees, 79 underwent surgical AVR and 4 declined surgery. In addition to AVR, 4% of

patients underwent aortic surgery. The patients' clinical and imaging characteristics are summarized in **Tables 10 and 11.**

Table 10. Clinical characteristics of all study cohort and patients stratified by the presence of focal fibrosis on CMR (LGE).

Variables	All patients (n=83)	LGE (+) patients (n=61)	LGE (-) patients (n=22)	P-value
Age, yrs	66.4 ± 8.3	65.8 ± 8.3	68.3 ± 8.3	0.235
Male gender	35 (42%)	29 (48%)	6 (27%)	0.162
BMI, kg/m^2	30 ± 5.8	30.4 ± 5.6	28.7 ± 6	0.245
BSA, m^2	1.9 ± 0.2	2.0 ± 0.2	1.8 ± 0.2	**0.011**
Systolic BP, mmHg	150 ± 25	148 ± 25	156 ± 23	0.223
Diastolic BP, mmHg	85 ± 11	84 ± 12	85 ± 11	0.842
Comorbidities				
Hypertension	73 (88%)	55 (90%)	19 (86%)	0.732
Dyslipidemia	66 (80%)	48 (79%)	19 (86%)	0.640
Unobstructive CAD	39 (47%)	30 (49%)	9 (41%)	0.677
Diabetes mellitus	14 (17%)	10 (16%)	5 (22%)	0.735
Atrial fibrillation	6 (7%)	5 (8%)	1 (5%)	0.931
History of PCI	1 (1%)	1 (2%)	-	1.000
Symptoms and functional status				
Dyspnea	61 (74%)	46 (75%)	15 (68%)	0.706
Chest pain	41 (49%)	30 (49%)	11 (50%)	1.000
Syncope	9 (11%)	9 (15%)	-	0.131
NYHA functional class				0.591*
I	16 (19%)	11 (18%)	5 (23%)	
II	24 (29%)	19 (31%)	5 (23%)	
III	40 (48%)	28 (46%)	12 (54%)	
IV	3 (4%)	3 (5%)	-	
6MWT, m	358 ± 106	352 ± 108	372 ± 101	0.459
MLHFQ score	35 ± 20	36 ± 20	31 ± 22	0.277
Drug history				
ACE-I/ARB	61 (74%)	43 (71%)	18 (82%)	0.453
Betablocker	57 (69%)	42 (69%)	15 (68%)	1.000
Statin	54 (65%)	40 (66%)	14 (64%)	1.000

Loop diuretic	15 (18%)	11 (18%)	4 (18%)	1.000
Spironolactone	22 (27%)	14 (23%)	8 (36%)	0.347
Risk scores				
STS-PROM, %	1.9 (1.2-2.3)	1.6 (1-2.2)	1.75 (1.4-2.4)	0.415
EuroSCORE II, %	1.5 (0.7-1.6)	1 (0.7-1.7)	1.2 (0.8-1.5)	0.415
Surgery (n=79)				
Tissue valve	70 (89%)	55 (90%)	15 (83%)	**0.037**
Mechanical valve	9 (11%)	6 (10%)	3 (17%)	0.927
Aortic intervention	3 (4%)	1 (2%)	2 (11%)	0.348
Valve morphology				
Tricuspid	54 (65%)	41 (67%)	13 (59%)	0.671
Bicuspid	28 (34%)	19 (31%)	9 (41%)	0.429
Unicuspid	1 (1%)	1 (2%)	-	1.000
Blood tests				
Creatinine μmol/l	76.2 ± 16.3	77 ± 17	73.9 ± 16	0.447
eGFR, ml/min/1.73m^2	78.6 (69-90)	85 (69-90)	86 (69-90)	0.996
Hs-Tn-I, pg/l	10 (5-19)	13.5 (6-29)	5.3 (5-9)	**0.003**
BNP, pg/l	122 (65-340)	167 (77-511)	74 (43-145)	**0.004**
ECG parameters				
Heart rate, b/min	77 ± 12.4	78 ± 12	76 ± 13	0.519
S-L voltage index (mm)	30.8 ± 10	31.7 ± 10	28.4 ± 10	0.189
QRS duration, ms	96.8 (88-102)	94 (88-102)	92 (85-101)	0.449

Continuous variables are presented as mean ± SD or median (interquartile range). Categorical variables are expressed as n (%). 6MWT, 6 minutes walking test; BMI, body mass index; BNP, brain natriuretic peptide; BP, blood pressure; BSA, body surface area; CAD, coronary artery disease; ECG, electrocardiography; LGE, late gadolinium enhancement; MLHFQ, Minnesota living with heart failure questionnaire; NYHA, New York Heart Association; PCI, percutaneous coronary intervention; S-L, Sokolow Lyon; STS, Society of Thoracic Surgeons' risk model score; EuroScore II, European System for Cardiac Operative Risk Evaluation II score; ACE-I, angiotensin-converting-enzyme inhibitor; ARB, angiotensin-receptor blocker; Hs-Tn-I, high sensitivity troponin I; eGFR, estimated glomerular filtration rate. *P-value for comparison among NYHA I and II vs. III and IV.

Table 11. Cardiovascular imaging and histology data of all study cohort and patients stratified by the presence of focal fibrosis on CMR (LGE).

Variables	All patients (n=83)	LGE (+) patients (n=61)	LGE (-) patients (n=22)	P-value
Echocardiography data (n=83)				
Peak AV velocity, m/s	4.8 ± 0.6	4.9 ± 0.6	4.6 ± 0.5	0.074
Mean AV gradient, mmHg	57.8 ± 16	59.8 ± 17	52.4 ± 14	0.071
Low gradient AS	10 (12%)	6 (10%)	4 (18%)	0.422
AV area, cm^2	0.84 ± 0.2	0.83 ± 0.2	0.88 ± 0.2	0.364
AV area index, cm^2/m^2	0.44 ± 0.1	0.43 ± 0.1	0.49 ± 0.1	**0.018**
IVSd, mm	12.7 ± 1.7	13.1 ± 1.5	11.5 ± 1.5	**<0.001**
Posterior wall diameter, mm	11.5 ± 1.4	11.9 ± 1.3	10.3 ± 1.2	**<0.001**
LVdd, mm	51.4 ± 5.4	52.1 ± 5.4	49.3 ± 4.9	**0.034**
LVsd, mm	32.7 ± 5.9	33.1 ± 6.1	31.7 ± 5.6	0.362
E/A	1.1 ± 0.5	1.1 ± 0.5	1.2 ± 0.3	0.615
E deceleration time, ms	259 ± 70	257 ± 69	262 ± 74	0.813
E/e' septal	17.6 ± 7	17.9 ± 6.3	16.8 ± 9.5	0.619
E/e' lateral	14.5 ± 6	15 ± 6.5	13.2 ± 5.8	0.276
E/e' mean	15.6 ± 6	16 ± 5.9	14.3 ± 5.7	0.254
LA volume index, ml/m^2	47.9 ± 12	49.2 ± 12	44.7 ± 12	0.129
PASP, mmHg	38 ± 15	40.5 ± 15	33.6 ± 12	0.175
RV S', cm/s	11.6 ± 3	11.4 ± 3	12 ± 2	0.377
TAPSE	21.7 ± 3	21.7 ± 4	21.8 ± 3	0.924
GLS, %*	-18 ± 5	-17.5 ± 4.8	-19.4 ± 5.3	0.147
CMR data (n=83)				
IVSd, mm	13.3 ± 2	13.6 ± 2	12.6 ± 2	0.062
LVdd, mm	50.6 ± 6	51 ± 6	49.3 ± 6	0.264
LVsd, mm	33.8 ± 8	34.2 ± 8	33 ± 9	0.561
LVEDV, ml	144.3 ± 44	149.7 ± 44	130 ± 44	0.079
LVESV, ml	51 (28-61)	46 (31-69)	29 (24-45)	0.106
LV stroke volume index, ml/m^2	48 ± 11	48.3 ± 10	48.4 ± 11	0.982
LVEF, %	66.8 ± 13	65.3 ± 13	70.8 ± 12	0.088
LVEF <50%	9 (11%)	8 (13%)	1 (5%)	0.427
LV mass index, g/m^2	97.6 ± 32	103.4 ± 32	82.6 ± 29	**0.009**
RVEDV, ml	125.3 ± 31	129.5 ± 31	114.2 ± 31	0.052
RVESV, ml	49.3 ± 18	49.7 ± 19	48.3 ± 17	0.747

RVEF, %	60.8 ± 10	61.9 ± 10	58 ± 8	0.111
Native T1, ms[#]	959.7 ± 34	961.8 ± 31	952.5 ± 43	0.359
Post-contrast T1, ms[#]	351 (326-362)	361 (325-376)	350 (326-358)	0.415
ECV, %[#]	22.7 ± 3.6	23.4 ± 3.7	22.2 ± 3.5	0.541
ECV index, %/m^2	11.8 ± 2	12.3 ± 2	11.3 ± 2	0.271
Histology data (n=71)				
CVF, %[&]	15.1 (9-21)	15.9 (9-19)	12.4 (9-24)	0.887
CVF subendocardial, %[&]	21.1 (12-29)	28.7 (19-33)	20.7 (15-30)	**0.040**

Continuous variables are presented as mean ± SD or median [interquartile range]. Categorical variables are expressed as n (%). AV, aortic valve; E, peak early velocity of the trans-mitral flow; CMR, cardiovascular magnetic resonance; CVF, collagen volume fraction; e', peak early diastolic velocity of the mitral annulus displacement; GLS, global longitudinal strain; ECV, extracellular volume; IVSd, interventricular septum diastolic diameter; LVEDV, left ventricular end-diastolic volume; LVESV, left ventricular end-systolic volume; LVEF, left ventricular ejection fraction; LA, left atrium; LGE, late gadolinium enhancement; LGE(+), patients with late gadolinium enhancement; LGE(-), patients without late gadolinium enhancement; PASP, pulmonary artery systolic pressure measured by echocardiography; RVEDV, right ventricular end-diastolic volume; RVEF, right ventricular ejection fraction; RVESV, right ventricular end-systolic volume; RV S', peak systolic velocity of the tricuspid annulus displacement; TAPSE, tricuspid annulus plane systolic excursion; * - value based on the data analysis of 77 patients; # - values based on the data analysis of 67 patients; & - values based on the data analysis of 71 patients.

4.3.3 Myocardial fibrosis by histology

Of 71 myocardial biopsies, 2 were epicardial. The data of one patient was excluded from the analysis due to an incidental finding of toxoplasmic myocarditis. CVF ranged from 2.06% to 41.30% and the median CVF was 15.1% (8.6-21). The distribution of CVF is shown in **Fig. 15**.
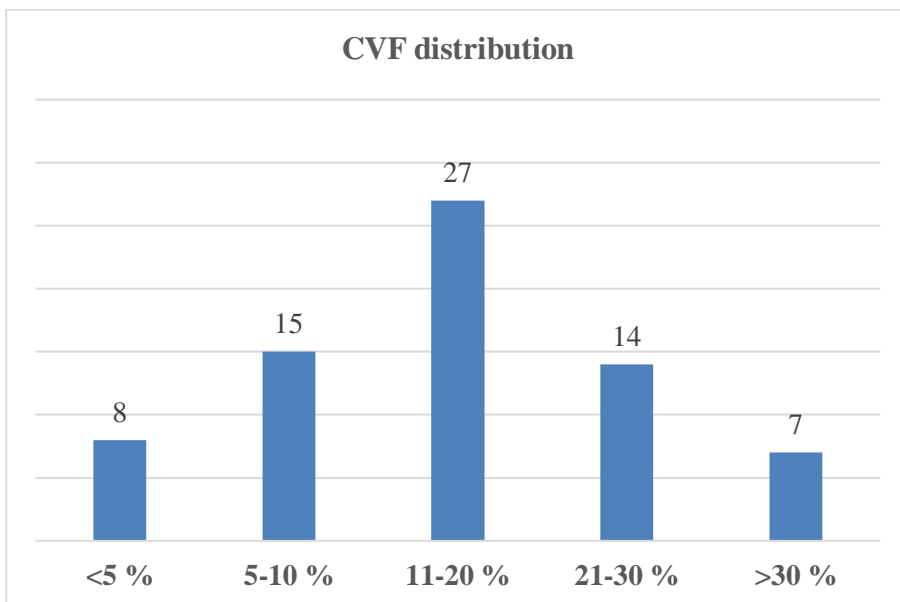
Fig. 15. The diagram shows the distribution of collagen volume fraction (CVF) in the myocardial biopsies of 71 patients. The majority of patients (38%) had moderate histological myocardial fibrosis (CVF 11-20%). 11% of patients had low (<5%) and 10% of patients had extensive (>30%) histological myocardial fibrosis.

Patients with higher CVF had a greater prevalence of hypertension (p=0.024) and dyslipidemia (p=0.036). Higher values of CVF were observed in LGE-positive versus LGE-negative patients—28.7% (19-33) vs. 20.7% (15-30), respectively (p=0.040). No significant differences in the median CVF value were noted between patients with and without unobstructed CAD [17.2% (10-23) vs. 13.4% (9-19), respectively; p=0.094]. Segmental analysis of myocardial biopsies revealed more fibrosis in the subendocardial layer compared with a midmyocardial layer [21.1% (12-29) vs. 8% (5-12); p<0.001; **Fig. 16**). Therefore, the amount of fibrosis in the myocardial biopsies varied substantially, from 2% to 41% (median 15%) with a higher amount of fibrosis detected in the subendocardial region and the LGE-positive patients.
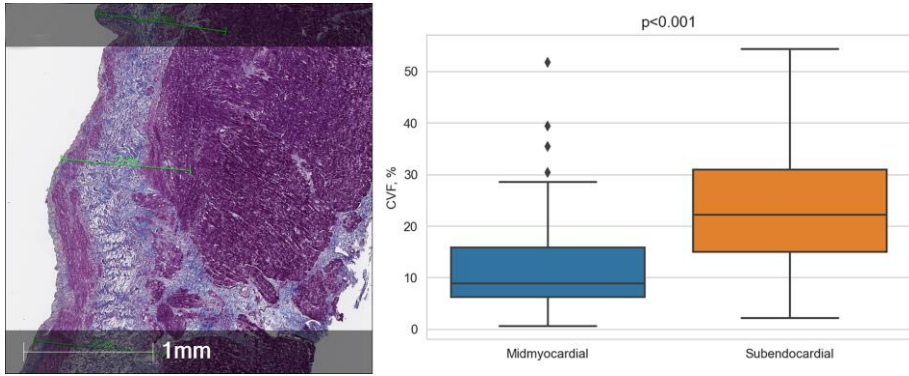
Fig. 16. The image on the left shows a myocardial biopsy sample stained with Masson's trichrome. The graph on the right shows a comparison of collagen volume fraction (CVF) in different layers of myocardium. A higher proportion of collagen was detected in subendocardium compared to midmyocardium (p<0.001).

4.3.4 Myocardial fibrosis by CMR

The median delay between CMR and surgery was 53.3 days (17-78). The mean native T1 was 959.7 ± 34ms (range: 897–1044ms), and the mean ECV was $22.7 \pm 3.6\%$ (range: 15.7%-34.4%). No significant difference in mean native T1 and ECV values was observed between men and women (962 ± 29ms vs. 957 ± 37ms, p=0.391 and $22.9 \pm 3\%$ vs. $22.6 \pm 4\%$, p=0.821, respectively).

To compare native T1 with clinical and structural parameters, we divided the variables (above and below the median: 957ms, **Table 12**). Patients with elevated native T1 had lower systolic blood pressure (p=0.006), higher QRS voltage on the ECG (p=0.036), greater systolic (p=0.009) and diastolic LV dimensions (p=0.049) and higher LV mass index (p=0.021). Among those with elevated native T1, a higher proportion of patients had reduced GLS (18% vs. 6%, respectively; p=0.049).

Table 12. Patients' clinical and imaging characteristics stratified by median native T1 values.

Variables	Native T1 ≥957 ms (n=34)	Native T1 <957 ms (n=33)	P-value
Age, yrs	65.8 ± 9	66 ± 9	0.917
Male gender	15 (44%)	11 (33%)	0.446
BSA, m^2	1.96 ± 0.16	1.93 ± 0.19	0.607
Systolic BP, mmHg	139 ± 21	156 ± 26	**0.006**
Diastolic BP, mmHg	82 ± 10	86 ± 13	0.203
Unobstructive CAD	20 (59%)	14 (42%)	0.893
Hypertension	27 (79%)	33 (100%)	0.109
Diabetes mellitus	6 (18%)	7 (21%)	1.0
NYHA f.cl. ≥ 3	16 (47%)	15 (46%)	0.749
MLHFQ score	37 ± 21	36 ± 20	0.839
6MWT, m	367 ± 106	352 ± 94	0.558
ECG			
Heart rate, b/min	78 ± 4	77 ± 12	0.742
QRS, ms	94 (89-102)	90 (84-101)	0.313
S-L voltage index, mm	34 ± 10	29 ± 9	**0.036**
Echocardiography data			
AV area index, cm^2/m^2	0.4 ± 0.1	0.45 ± 0.1	0.075
Peak AV velocity, m/s	5.0 ± 0.6	4.8 ± 0.6	0.105
Mean AV gradient, mmHg	64 ± 16	57 ± 15	0.052
IVSd, mm	13 ± 1.9	12.6 ± 1.6	0.368
LVdd, mm	53 ± 5	50 ± 5	**0.049**
LVsd, mm	35 ± 6	32 ± 6	0.057
E deceleration time, ms	252 ± 68	266 ± 75	0.759
E/e' septal	16.5 (12.8-18)	16 (12-20)	0.845
E/e' mean	15 ± 5	16 ± 7	0.909
LA volume index, ml/m^2	48 ± 9	48 ± 15	0.473
PASP, mmHg	41 ± 17	37 ± 12	0.947
GLS, %	-16.7 ± 5.6	-18.2 ± 4	0.120
GLS >-15%	10 (29%)	4 (12%)	**0.049**
CMR data			
IVSd, mm	14 ± 1.6	13 ± 2.3	0.364
LVdd, mm	52 ± 6	50 ± 5	0.074
LVsd, mm	36.5 ± 7	32 ± 6	**0.009**
LVEDV, ml	153 ± 40	143 ± 44	0.201
LVESV, ml	52 (37-72)	41 (28-53)	0.083

LVEF, %	62.4 ± 14	68 ± 12	0.053
LVEF <50%	6 (18%)	2 (6%)	0.541
LV mass index, g/m^2	109 ± 31	91 ± 30	**0.021**
LGE prevalence	27 (79%)	25 (76%)	0.802
Native T1, ms	987 ± 26	936 ± 18	**<0.001**
Post-contrast T1, ms	352 (328-362)	348 (318-362)	0.445
ECV, %	23 ± 3.2	22 ± 3.9	0.243
Histology data			
CVF, %	18.1 (8-24)	13.4 (10-21)	0.564
CVF subendocardial, %	22.3 (9-28)	18.8 (12-26)	0.855
Serum biomarkers			
BNP, pg/l	163 (73-581)	120 (62-260)	0.413
Hs-Tn-I, pg/l	14 (7-27)	7.5 (5-16)	0.089

Continuous variables are presented as mean ± SD or median (interquartile range). Categorical variables are expressed as n (%). The boldface values indicate statistical significance. Abbreviations are as in Tables 10 and 11.

Focal fibrosis, measured by LGE, was common, affecting 74% of all patients (83% of men and 67% of women). Although LGE was frequently found, the extent of focal fibrosis was mostly limited to 1 or 2 LV segments, 2.5 segments per patient on average (**Fig. 17**).
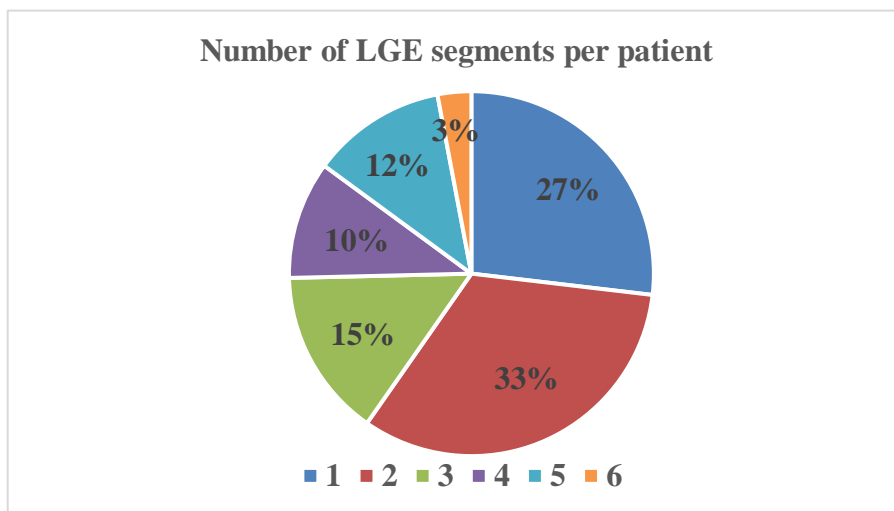

Fig. 17. The chart indicates the number of LGE segments per patient. More than half of all LGE positive patients had only 1 or 2 left ventricular segments with focal fibrosis. However, 10 patients were found to have as many as 5 or 6 left ventricular segments affected by focal fibrosis.

Furthermore, 92% of focal fibrosis were of non-infarct type (89% mid-myocardial, 3% subepicardial). Despite having unobstructed coronary arteries, 8% of patients had infarct-type focal fibrosis (**Fig. 18** and **Fig. 19**).
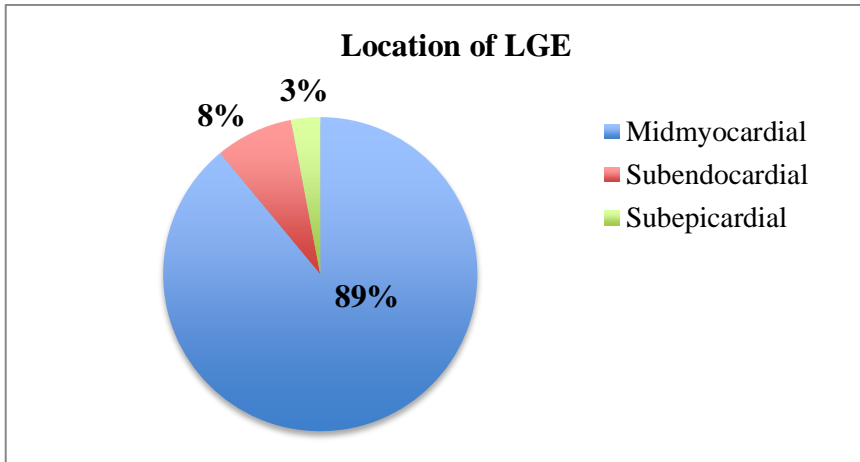

Fig. 18. The chart demonstrates the location of LGE within the left ventricular wall. The vast majority of patients (92%) presented with non-infarct type of LGE - midmyocardial and subepicardial location. 8% of patients were found to have ischemic type of LGE - subendocardial location.
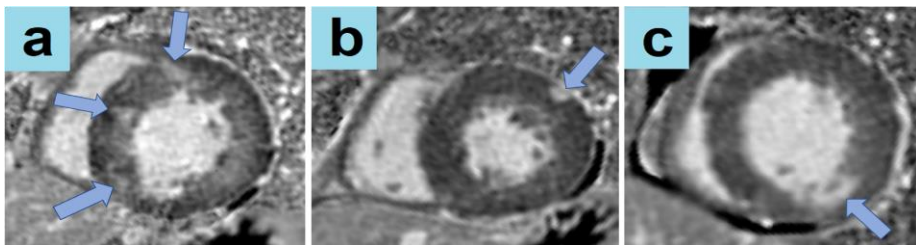

Fig. 19. Representative LGE images of 3 different patients with severe AS from our cohort, demonstrating the different locations of delayed focal enhancement: midmyocardial and subepicardial (a and b) and subendocardial (c) focal fibrosis (blue arrows).

The most common location of LGE was the right-left ventricular insertion points (68%). LGE was also detected in the anterolateral (11%), septal (8%), posterolateral (6%), inferior (6%) and apical (1%) segments (**Fig. 20**). No significant difference was found in the prevalence of LGE between patients with and without unobstructed CAD (77% and 70%, respectively; p=0.67) (**Fig. 20**).
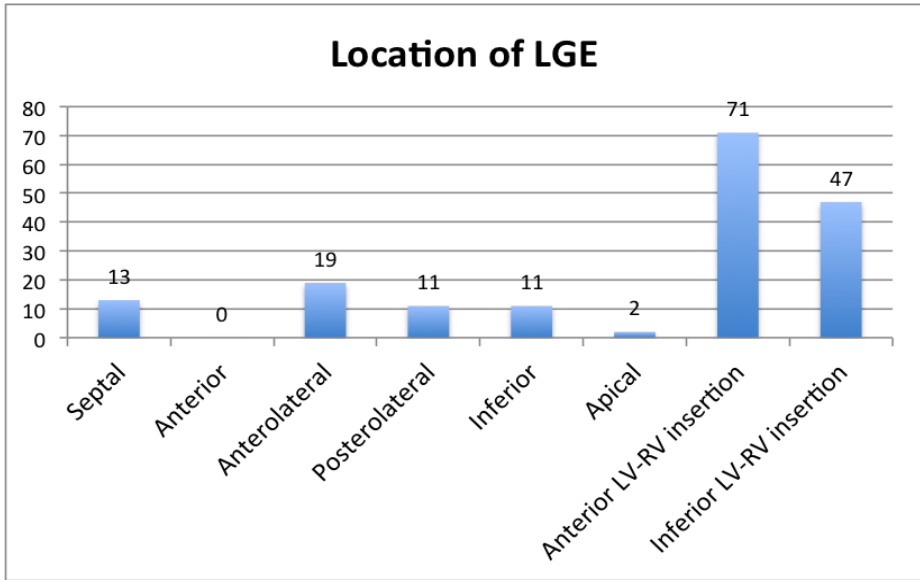
Fig. 20. Bar chart showing the number of LGE segments in different left ventricular locations. The most frequent locations of focal fibrosis were anterior and inferior left ventricular-right ventricular insertion points, constituting 68% of all LGE locations.

Fig. 21. The bar chart indicates the prevalence of LGE in patients with and without unobstructed coronary artery disease (CAD). Patients with unobstructive CAD had a similar prevalence of focal fibrosis as CAD free patients.

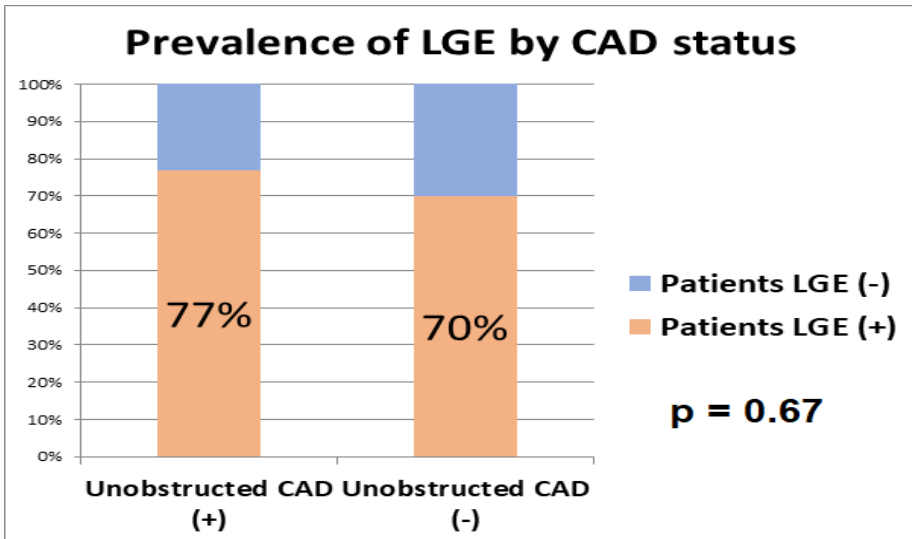Compared to patients without focal fibrosis, LGE-positive patients had more severe AS, as evidenced by a smaller AVA index (p=0.018). Patients with focal fibrosis also had more advanced LV remodeling as they presented with thicker LV walls (p<0.001), a larger LV diastolic diameter (p=0.034) and a higher LV mass index (p=0.009). Patients with LGE also had higher levels of BNP (p=0.004) and Hs-Tn-I (p=0.003).

In summary, our results demonstrate, that focal non-infarct type focal fibrosis is highly prevalent in severe AS patients. Patients with higher native T1 and focal fibrosis on CMR had more advanced LV remodeling, evidence of diastolic and systolic LV impairment and higher levels of serum biomarkers, indicative of heart failure and myocardial injury. The patients' clinical and imaging characteristics, stratified by the presence of LGE, are summarized in **Tables 10 and 11.**

4.3.5 GLS analysis

The mean GLS was -18 ± 5% (range: -3% to -31%), and a reduction in GLS >-20% was observed in 61% of patients (**Fig. 22**).
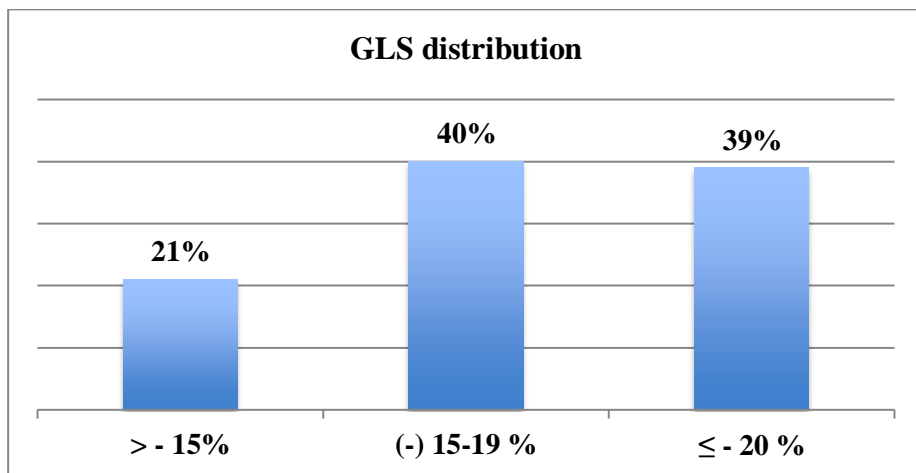
Fig. 22. The bar chart demonstrates the distribution of GLS. More than half of all patients (61%) had impaired longitudinal deformation (≥-19%).

To analyze GLS with regard to clinical and structural parameters, we dichotomized the variables (above and below median: -18.5%; **Table 13**). Patients with lower GLS had more severe AS, based on a smaller AVA index (p=0.018), a higher mean transvalvular gradient (p=0.004), a lower systolic blood pressure (p=0.005) and a greater QRS voltage on the ECG (p=0.011).

The low-GLS group also had thicker LV walls (p=0.009), higher LV volumes (p<0.001), a greater LV mass index (p<0.001) and a lower LVEF (p<0.001). This group showed signs of elevated LV filling pressures, as evidence by higher E/e' ratios (p=0.011), with consequently higher left atrial (LA) volume index (p=0.002) and pulmonary artery systolic pressure (p=0.031). Higher levels of BNP (p=0.001) and Hs-Tn-I (p=0.002) were detected in these patients.

Table 13. Patients' clinical and imaging characteristics stratified by median GLS values.

Variables	GLS ≥-18.5% (n=40)	GLS <-18.5% (n=37)	P-value
Age, yrs	66 ± 8	68 ± 8	0.256
Male gender	18 (45%)	14 (38%)	0.548
BSA, m^2	1.98 ± 0.2	1.86 ± 0.2	**0.004**
Systolic BP, mmHg	143 ± 23	158 ± 23	**0.005**
Diastolic BP, mmHg	83 ± 11	85 ± 11	0.485
Unobstructive CAD	20 (50%)	18 (49%)	1.0
Hypertension	36 (90%)	33 (89%)	0.447
Diabetes mellitus	8 (20%)	4 (11%)	0.768
NYHA f.cl. ≥3	26 (65%)	14 (38%)	0.085
MLHFQ score	37 ± 20	32 ± 20	0.257
6MWT, m	351 ± 105	358 ± 104	0.767
ECG			
Heart rate, b/min	80 ± 14	75 ± 11	0.100
QRS, ms	95 (90-102)	90 (86-98)	0.105
S-L voltage index, mm	34 ± 11	28 ± 8.5	**0.011**
Echocardiography data			
AV area index, cm^2/m^2	0.42 ± 0.1	0.47 ± 0.08	**0.018**
Peak AV velocity, m/s	5.0 ± 0.7	4.7 ± 0.5	0.055
Mean AV gradient, mmHg	63 ± 17.7	53 ± 13.2	**0.004**
IVSd, mm	13.3 ± 1.8	12.2 ± 1.4	**0.009**
LVdd, mm	53.7 ± 12	48.8 ± 4.7	**0.002**
LVsd, mm	35.4 ± 6	29.6 ± 4	**<0.001**
E deceleration time, ms	254 ± 76	264 ± 67	0.542
E/e' septal	17.1 (14-22)	14 (11.7-18)	**0.011**
E/e' mean	17.4 ± 6.9	14.2 ± 4.4	**0.021**
LA volume index, ml/m^2	53 ± 12	44 ± 11	**0.002**
PASP, mmHg	43.5 ± 18	32.9 ± 7	**0.031**

GLS, %	-14.3 ± 3.9	-21.7 ± 2.7	**<0.001**
GLS >-15%	16 (40%)	0	**<0.001**
CMR data			
IVSd, mm	14 ± 2	12.6 ± 2	**0.005**
LVdd, mm	53 ± 7	48.3 ± 5	**<0.001**
LVsd, mm	37 ± 9	30.6 ± 6	**<0.001**
LVEDV, ml	160.7 ± 48	126 ± 35	**<0.001**
LVESV, ml	56.9 (41-77)	29 (24-41)	**<0.001**
LVEF, %	59 ± 14	74 ± 7	**<0.001**
LVEF <50%	8 (20%)	0	**0.009**
LV mass index, g/m^2	113 ± 33	80.6 ± 24	**<0.001**
LGE prevalence	34 (85%)	23 (62%)	0.058
Native T1, ms	967 ± 31	950 ± 37	0.066
Post-contrast T1, ms	349 (326-354)	355 (332-366)	0.201
ECV, %	22.3 ± 4	22.9 ± 2.4	0.456
Histology data			
CVF, %	17.2 (10-22)	13.5 (8-20)	0.279
CVF subendocardial, %	23.4 (13-33)	18.4 (11-27)	0.199
Serum biomarkers			
BNP, pg/l	252 (98-813)	79 (59-173)	**0.001**
Hs-Tn-I, pg/l	15 (7.5-29)	6.9 (5-12.9)	**0.002**

Continuous variables are presented as mean ± SD or median [interquartile range]. Categorical variables are expressed as n (%). The boldface values indicate statistical significance. Abbreviations are as in Tables 10 and 11.

A ROC analysis was performed in order to investigate the ability of GLS to predict histological myocardial fibrosis and to determine the optimal cut-off value. GLS >-14% (sensitivity 33%, specificity 94%) can predict increased myocardial fibrosis: area under curve - 0.65, 95% CI [0.51-0.78], p= 0.034 (**Fig. 23**).
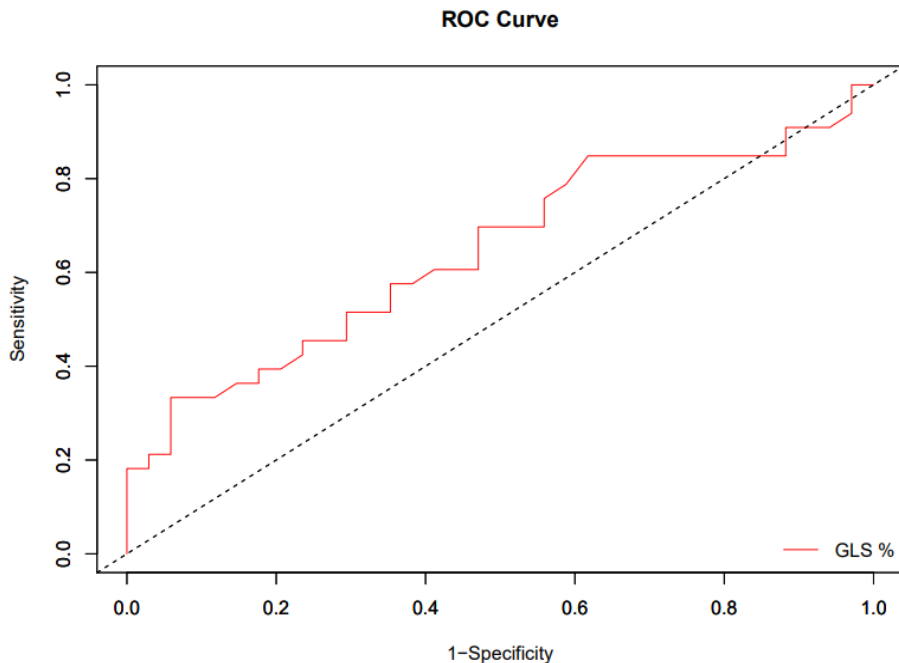
Fig. 23. Plot showing the ability of global longitudinal strain (GLS) to predict increased histologically measured myocardial fibrosis (more than median collagen volume fraction).

Additionally, a comparison of the imaging characteristics of patients was undertaken, with and without the relative apical sparing pattern of GLS. Patients with this GLS pattern had a higher AV peak velocity (p=0.005), a higher mean AV gradient (p=0.013) and evidence of more advanced LV remodeling: thicker LV walls (p<0.001), a larger LV diastolic diameter (p=0.006) and a larger LV mass index (p=0.001) as assessed by CMR. These patients also presented with worse LV systolic function, as they had a lower GLS (p=0.006) and a lower LVEF (p=0.040). RAS positive patients also had evidence of myocardial injury and heart failure, as they presented with higher serum levels of BNP (p=0.032) and Hs-Tn-I (p=0.026) (**Table 14**). Representative images of patients with various degrees of LV remodeling by echocardiography, CMR and histology are shown in **Fig. 24**.

Table 14. Patients' imaging characteristics stratified by the presence of relative apical sparing (RAS) pattern on GLS analysis.

Variables	RAS (+) (n=14)	RAS (-) (n=63)	P-value
Echocardiography data			
AV area index, cm^2/m^2	0.4 ± 0.1	0.5 ± 0.1	0.163
Peak AV velocity, m/s	5.3 ± 0.7	4.8 ± 0.6	**0.005**
Mean AV gradient, mmHg	70 ± 20	56 ± 14	**0.013**
IVSd, mm	14.6 ± 1.1	12.4 ± 1.5	**<0.001**
LVdd, mm	51.8 ± 4.4	51.2 ± 5.6	0.384
LVsd, mm	34.5 ± 6	32 ± 6	0.124
E/e' septal	17.1 (16-18)	16 (13-20)	0.238
E/e' mean	16 ± 7	16 ± 6	0.717
LA volume index, ml/m^2	52 ± 14	48 ± 12	0.253
PASP, mmHg	39 ± 18	38 ± 14	0.826
GLS, %	-14.9 ± 3	-18.7 ± 5	**0.002**
GLS >-15%	7 (50%)	9 (14%)	**0.006**
CMR data			
IVSd, mm	14.8 ± 1	12.9 ± 2	**0.004**
LVdd, mm	54 ± 4	50 ± 6	**0.006**
LVsd, mm	37 ± 7	33 ± 8	0.140
LVEDV, ml	149 ± 30	143 ± 348	0.265
LVESV, ml	56 (46-73)	36 (26-56)	0.062
LVEF, %	62 ± 12	68 ± 13	**0.040**
LVEF <50%	8 (20%)	0	0.089
LV mass index, g/m^2	125 ± 28	91 ± 32	**0.001**
LGE prevalence	34 (85%)	23 (62%)	0.175
Native T1, ms	973 ± 36	955 ± 33	0.094
Post-contrast T1, ms	351 (329-363)	352 (327-362)	0.739
ECV, %	23.4 ± 3	22.3 ± 3	0.292
Histology data			
CVF, %	22 (18-25)	22 (15-28)	0.729
CVF subendocardial, %	30 (23-32)	33 (22-40)	0.168
Serum biomarkers			
BNP, pg/l	409 (161-961)	119 (66-245)	**0.032**
Hs-Tn-I, pg/l	15 (13-29)	9 (5-18)	**0.026**

Continuous variables are presented as mean ± SD or median (interquartile range). Categorical variables are expressed as n (%). The boldface values indicate statistical significance. Abbreviations are as in Tables 10 and 11.
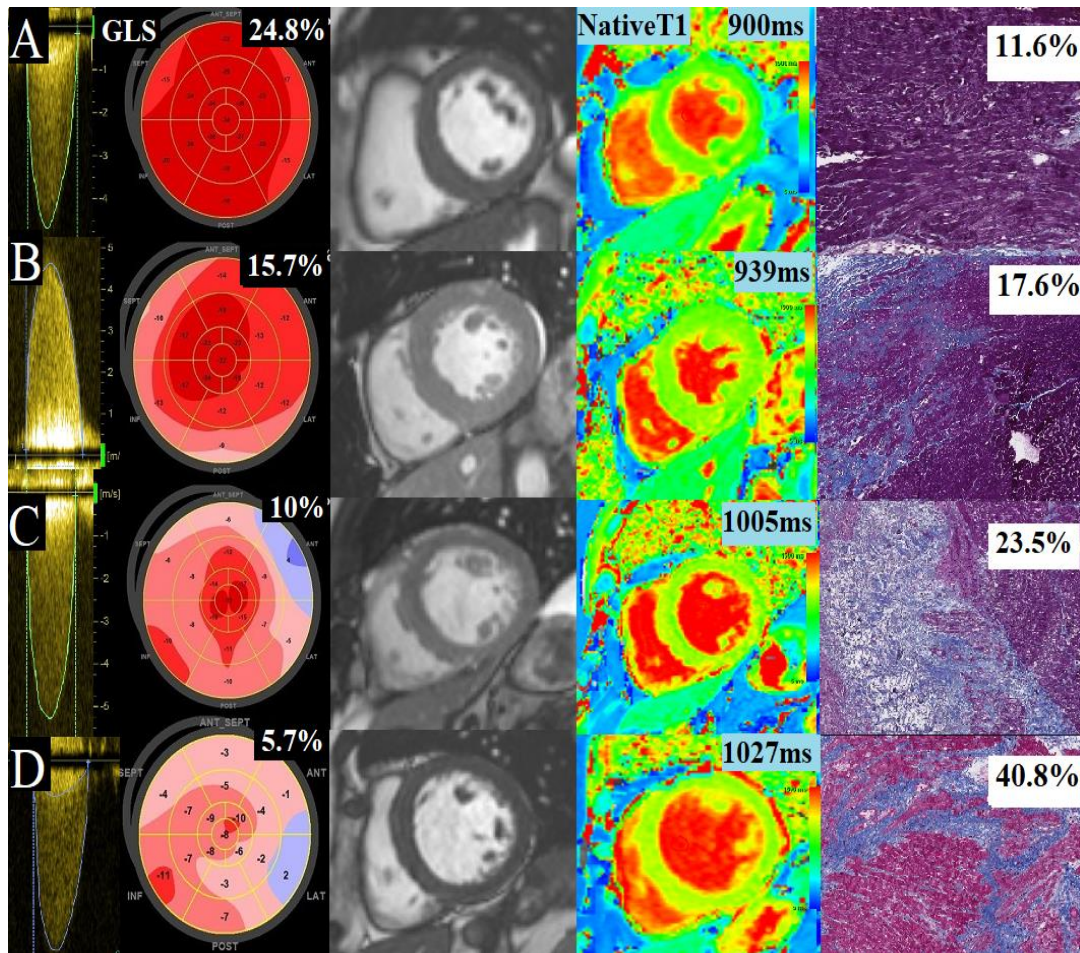
Fig. 24. Four exemplar patients showing progressive cardiac remodeling: continuous-wave Doppler (maximum velocities >4m/s; Column 1), global longitudinal strain (GLS; Column 2), short axis cine stills at end-diastole demonstrating degrees of left ventricular (LV) remodeling (Column 3), matching native T1 (Column 4) and collagen volume fraction (CVF) in myocardial biopsies stained with Masson's trichrome (Column 5). Patient A has preserved GLS, minimal LV hypertrophy, low native T1 and CVF of 11.6%. Patient B has reduced GLS, concentric LV hypertrophy, higher native T1 and moderate histological fibrosis (CVF – 17.6%). Patient C has a relative apical sparing pattern of GLS, evidence of LV hypertrophy, high native T1 and significant histological fibrosis (CVF – 23.5%). Patient D, with decompensated heart failure, has low GLS, LV cavity dilatation, high native T1 and extensive histological fibrosis (CVF – 40.8%).

4.3.6 Analysis of associations

CVF correlated with LV end-diastolic diameter (r=0.242, p=0.043), LV end-systolic volume (r=0.265, p=0.028), LVEF (r=-0.246, p=0.04) and LA volume index (r=0.314, p=0.009). When subendocardium was excluded from the analysis, CVF correlated with LV mass (r=0.247, p=0.041), LVEF (r=-0.354, p=0.003), GLS (r=-0.303, p=0.013) and BNP (r=0.242, p=0.045) (**Fig. 25**).
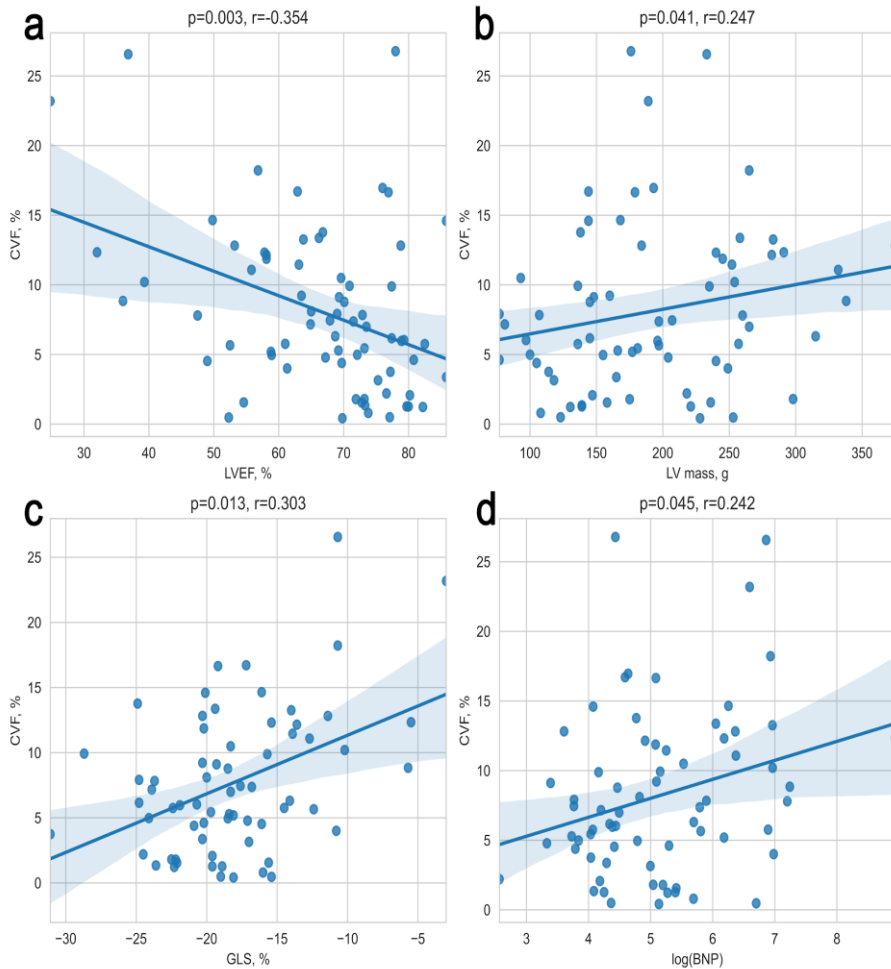

Fig. 25. Correlation between histological myocardial fibrosis (CVF) and LV ejection fraction (a), LV mass (b), GLS (c) and brain natriuretic peptide (BNP) (d) are shown. Abbreviations are as in **Fig. 24.**

With regards to LV structure and function, GLS correlated with LV end-diastolic volume (r=-0.485, p<0.001), LV end-systolic volume (r=-0.636, p<0.001), LV mass index (r=-0.615, p<0.001) and LVEF (r=0.7, p<001).
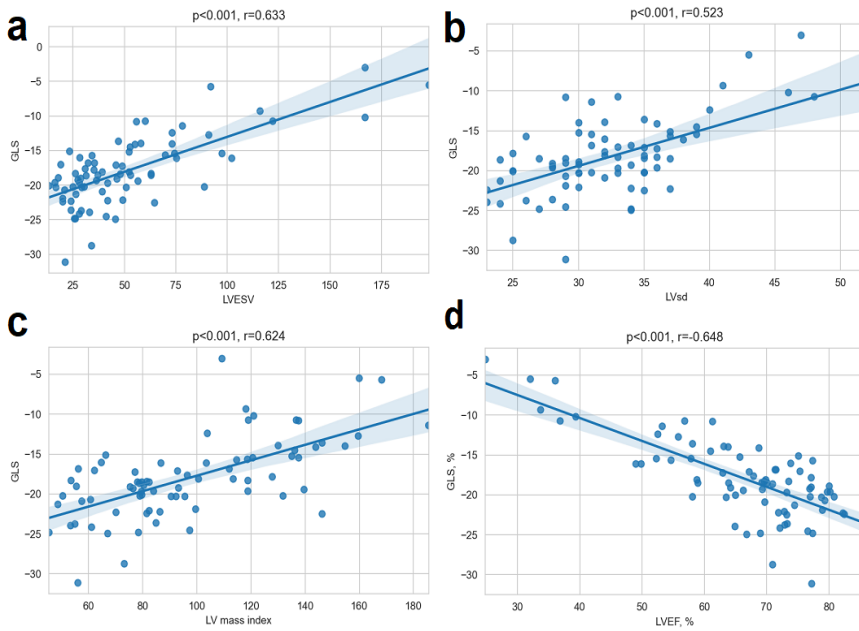

Fig. 26. Correlation between GLS and LV end-systolic volume (a), LV systolic diameter (b), LV mass index (c) and LV ejection fraction (d) are shown. Abbreviations are as in **Fig. 24.**

GLS was also linked to parameters that were associated with elevated LV filling pressures: mean E/e' (r=-0.4, p=0.002), LA volume index (r=-0.405, p<0.001) and estimated pulmonary artery systolic pressure (r=-0.376, p<0.05). Native T1 correlated with LV end-systolic volume (r=0.349, p=0.003), LV end-diastolic volume (r=0.269, p=0.03), LV mass index (r=0.414, p<0.001) and LVEF (r=-0.317, p<0.05). GLS and native T1 were associated with the degree of AS severity: AV mean gradient (r=-0.387, p<0.001 and r=0.408, p<0.001, respectively) and AVA (r=0.30, p<0.05 and r=-0.3, p=0.02, respectively).

With regard to serum biomarkers, GLS and native T1 correlated with BNP (r=-0.653, p<0.001 and r=0.371, p<0.05, respectively) and Hs-Tn-I (r=-0.486, p<0.001 and r=0.333, p<0.05, respectively) and with each other (r=-0.321, p<0.05) (**Fig 27**).

Our results therefore demonstrate, that invasively and non-invasively measured myocardial fibrosis is linked to adverse cardiac remodeling and markers of heart failure. GLS showed the best discriminatory ability to detect patient with unfavorable LV remodeling and can also serve as a surrogate marker of myocardial fibrosis, as it correlated with both invasively and non-invasively measured myocardial fibrosis. Our data also show, that RAS pattern of GLS in the AS population could be a sign of more advanced LV remodeling.
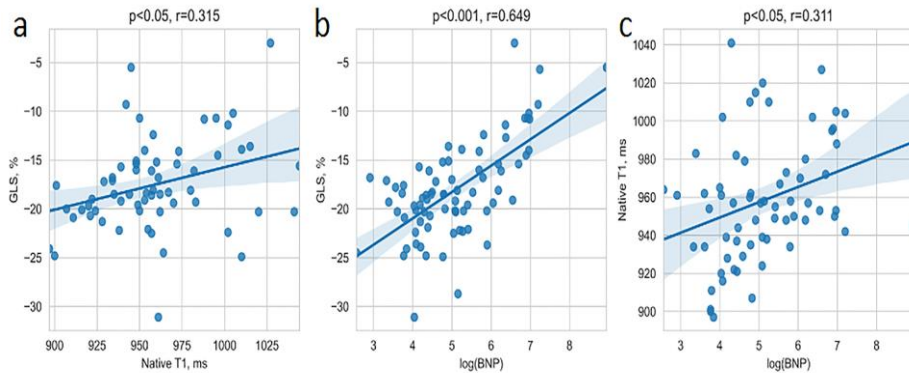
Fig. 27. Correlation between GLS and native T1 (a), GLS and BNP (b), native T1 and BNP (c) are shown. Abbreviations are as in **Figure 24**.

4.3.7 ATTR cardiac amyloidosis

Out of the 79 patients who underwent surgical AVR, 71 myocardial biopsy specimens from the basal antero-septum were sampled. Histological analysis was performed by Congo red staining on formalin-fixed and paraffin-embedded sections and viewed in brightfield and cross-polarized light. Histological analysis revealed no evidence of cardiac amyloidosis in any of the myocardial biopsies.

5. DISCUSSION

5.1 Meta-analysis

Our meta-analysis is the first large-scale analysis consolidating the data from single-center and multicenter studies on the prevalence, extent, as well as prognostic value of LGE in AS. From the data of 19 studies with 2,032 patients, we have demonstrated that LGE was present in a considerable proportion of patients with AS (49.7%) and had a strong and significant association with the clinical outcomes. This association was consistently observed across all studies and was independent of potential confounders on multivariable analysis. LGE remained an independent risk factor after adjusting for age, NYHA functional class, LV ejection fraction and other variables.

In the present meta-analysis, including 6 studies with 1,300 patients over a mean follow-up of 2.8 years, we have demonstrated that LGE tripled all-cause and cardiovascular mortality (pooled ORs: 3.26 and 2.89, respectively). Focal fibrosis was associated with increased mortality irrespective of scar aetiology, and both infarct and non-infarct pattern predicted worse outcome (11,45). Two studies (43,45), incorporating 315 patients, with severe AS patients undergoing TAVI, have demonstrated that the prognostic value of LGE also applies to this population. This is of great importance due to the fact that TAVI candidates represent a much higher risk population.

Our study extends the results of previous reports. Chen et al. (97) performed a meta-analysis evaluating 626 patients over a mean follow-up of 2.5 years, and significant associations between LGE and mortality were found.

The results of our meta-analysis were reproduced by another group performing meta-analysis on the same topic (98). Although there were minor differences in these studies, the results were very similar. Papanastasiou et al. in analyzing the data of six studies comprising of 1,151 patients with AS found the prevalence of LGE to be 49.1%. LGE was also found to be a strong univariate predictor of all-cause mortality (pooled unadjusted OR [95% CI] = 2.56 [1.83, 3.57], p<0.001). The fact that two separate groups of research have obtained very similar results by performing analysis on the same topic increases the validity and precision of the final result.

Although the presence of LGE clearly portends a higher risk for adverse events, it should not be used as a binary tool, as it is not only the presence, but also the amount of LGE that counts. Two studies (11,45)

reported that the extent of LGE was a strong independent predictor of adverse events, and a higher burden of scar was associated with higher all-cause and cardiovascular mortality. The reported extent of LGE was variable across different studies, and the pooled extent of focal fibrosis as measured by the percentage of LV mass was around 4%. These differences are probably due not only to the heterogeneity of the included populations, but also to the different methods used for myocardial fibrosis quantification. As there is no consensus for how to quantify LGE, different methods have been used. The majority of investigators used different signal intensity thresholds above remote myocardium, while the full width half maximum method was used by a few. In AS, LGE is frequently less well defined than in infarction, and the delineation of the myocardium with a normal signal may prove to be challenging. Previous reports have shown that the full width half maximum technique was the most reproducible for LGE quantification across the spectrum of cardiac diseases (99).

5.2 FIB-AS study

The presented prospective study presents a comprehensive assessment of the consequences of AS on LV myocardium by integrating CMR and STE data with a large number of myocardial biopsies.

The main study findings are as follows:

1. The non-infarct type of focal fibrosis is highly prevalent in severe low-risk AS patients and determines more advanced LV remodeling.
2. Histologically measured myocardial fibrosis is associated with imaging and serum biomarkers of LV dysfunction and left side chamber enlargement. The subendocardium is affected by myocardial fibrosis to a greater extent and determines longitudinal dysfunction.
3. GLS is associated with invasively and non-invasively measured myocardial fibrosis; low GLS and elevated native T1 differentiated patients with more advanced LV remodeling. GLS >-14% predicts increased myocardial fibrosis.
4. No evidence of amyloid deposition was found in the LV myocardium of severe AS patients undergoing surgical AVR in neither CMR studies, nor in the histological analysis.

Compared with previous studies in severe AS patients, our cohort was younger and free from significant CAD, thus representing low-risk isolated AS patients. Although 90% of our study population had preserved LVEF, a more detailed assessment of the myocardial structure and function, through

cardiac imaging and histological analysis, revealed evidence of varying degrees of myocardial injury.

The amount of fibrosis in the myocardial biopsies varied substantially, from 2% to 41%. Collagen tissue, which is present in a healthy myocardium, constituted less than 2% based on the autopsy results of subjects who died of non-cardiovascular causes (48,100). Whether the amount of myocardial fibrosis increases with age is less clear. We found that histological myocardial fibrosis was associated with LV and LA enlargement and worse LV systolic function, underscoring the role of myocardial fibrosis in alterations of LV morphology and function as well as the pathophysiological progression to heart failure in AS. Consistent with earlier studies, it was found that the subendocardial layer contained more fibrosis compared with a midmyocardium. Gradients of myocardial fibrosis in the LV wall have been described in patients with severe AS and those with hypertrophic cardiomyopathy and hypertensive heart disease—conditions that are both associated with chronic pressure overload and an increase in LV mass (48,100). These findings can be explained by a transmural gradient of wall stress and ischemia in the subendocardial layer due to the relative decrease in capillary density, with subsequent cell loss and reparative fibrosis (101).

GLS and native T1 median values differentiated patients with more advanced LV remodeling, wherein patients with lower GLS and higher native T1 had evidence of altered LV structure, diastolic and systolic impairments, and higher levels of serum biomarkers, which are indicative of heart failure and myocardial injury. Notably, patients with reduced GLS and elevated native T1 still had preserved LVEF, and only 20% of patients with adverse structural and functional cardiac remodeling had LVEF below 50%. Thus, only 1 in 5 patients with advanced cardiac remodeling would be detected if this echocardiographic criteriaon of cardiac decompensation was solely used, and thereby overlooking a substantial number of patients who would benefit from early AV intervention. Our results are consistent with previous studies showing that fibrotic changes that are induced by AS begin in the subendocardium and initially affect longitudinal function, which is not well represented by LVEF as it can be compensated by global radial function (5,93).

Notably, patient groups did not differ by symptom status, functional capacity or quality of life assessment. This finding suggests that symptom assessments can be challenging and misleading and do not always reflect the true cardiac condition, thus indicating that the decision to intervene should be

supported by objective markers of cardiac injury rather than based on a subjective assessment of symptom status.

Imaging biomarkers, or the integration of several parameters, may be particularly useful in patients with no or minimal symptoms or when ascertaining valve-related symptoms is challenging. Our data implicates GLS and native T1 as early markers of cardiac decompensation. Additionally, GLS can also be used as a surrogate marker of myocardial fibrosis as it is associated with both invasively and non-invasively measured myocardial fibrosis. Our data have shown that a GLS reduction below 14% can predict increased myocardial fibrosis – even if test sensitivity was low, specificity was high. This GLS cut-off value is in accordance with the results of a recent meta-analysis. Magne et al. demonstrated that in patients with severe asymptomatic AS and preserved LV ejection fraction, a GLS reduction below 14.7% was associated with a >2.5-fold increase in the risk of death (102).

Seventy-four percent of our patients had areas of focal fibrosis, 92% of which were the non-infarct type and which were independent of the presence of unobstructive CAD. Although only 1 or 2 segments were affected by LGE in most patients, data from a recent large multi-center study show that >2% of LGE in patients with severe AS who undergo AVR are associated with worse postoperative survival (57). We found that the myocardium of patients who have progressed to more advanced myocardial injury and have developed areas of irreversible replacement fibrosis on CMR also contain a higher degree of diffuse fibrosis measured histologically. Against our expectations, we found no association between CVF and CMR markers of diffuse fibrosis, for which there are several explanations: there was a possible sampling error, because only 1 biopsy sample per patient was analyzed. Further, the histological and T1 mapping analyses were performed at different levels and layers of the interventricular septum. The myocardial biopsies were endocardial and taken from the basal antero-septum, possibly containing higher amounts of fibrotic tissue, and the region of interest for the T1 mapping measurements was drawn in the middle of the septum at the midventricular level, avoiding the endocardial and epicardial borders. The data in this field are inconsistent, with some studies reporting significant associations between invasively and non-invasively measured myocardial fibrosis in AS cohorts (55,56) and others failing to demonstrate this association (48).

Although our patients presented with an increased LV mass and myocardial fibrosis in histological analysis, ECV values were not elevated in our cohort compared with our local reference range. This finding can be explained by the greater increase in cellular mass (adaptive hypertrophy), as

opposed to the expansion of extracellular space, owing to the fact that ECV per se represents the percentage of space that is occupied by the extracellular compartment of the total LV mass. The average native T1 and ECV values in our cohort were lower in comparison to the AS populations in other studies (56,57). Large T1 mapping data variability across different centers has been previously reported, in which it was influenced by differences in field strength, vendor-specific set-up and variations in sequences (103,104). Disparities in ECV values can also be expected with the non-uniformity of contrast agents and their doses (105). Another explanation for such variability relates to differences in the study cohorts. When interpreting our results, it should be considered that relatively young, low-risk patients, who were free from significant CAD, were examined, whereas other studies, especially those that included transcatheter treatment cohorts, enrolled patients who were in their 80s and had a higher rate of comorbidities (106).

Interestingly, 17% of our patients had a relative apical sparing type of GLS impairment (**Fig. 24**, patient C), however, all myocardial biopsies tested negative for amyloid deposition at histopathology and no evidence of amyloid deposition was found in the CMR images. These findings are of particular importance as wild type ATTR-CA has been increasingly recognized in patients with degenerative AS undergoing TAVI (65). A relative apical sparing pattern of GLS is considered a classic and early echocardiographic feature of cardiac amyloidosis (107). However, our data suggests that isolated AS patients may also exhibit this GLS pattern without evidence of infiltrative disorder. These patients had neither a low voltage, nor a pseudoinfarct pattern on the ECG, as well as no suspicion of infiltration on the CMR. We found that patients with a relative apical sparing pattern of GLS had a larger LV mass and higher levels of serum biomarkers of myocardial injury and heart failure. Therefore, the data suggests that a relative apical sparing pattern in the AS population could be a sign of unfavorable LV remodeling. The data from a recent study supports our findings. Abecasis et al. found a prevalence of relative apical sparing in 30.8% of patients with severe symptomatic AS undergoing AVR (108). Cardiac amyloidosis was excluded by histological and CMR analysis. In that study, patients with relative apical sparing had a larger LV mass, a lower LV ejection fraction and a higher amount of focal fibrosis.

5.3 ATTR-CA in aortic stenosis

Multiple studies have shown that wild type ATTR-CA is more prevalent in the elderly population (18-23). According to the published data, the mean age of AS patients who tested positive for ATTR-CA was between 75-88 years. Currently, it is not known why the disease effects the elderly population more frequently. In the case of ATTR-CA, the genetic sequence of transthyretin is normal, and it is believed that the aging process causes protein instability and altered aggregation. Currently, the causative link between AS and ATTR-CA has not been demonstrated. Some authors have postulated that amyloid deposits could be induced or accelerated in AS, because of the pressure overload (109). In contrast, Kristen et al. reported a high prevalence of amyloid deposits in surgically removed heart valves, mainly in AS (74% of aortic valves) (110), suggesting that amyloid deposits could induce or worsen AS. Concerns have been raised that amyloid proteins may also infiltrate and accumulate within the bioprosthetic valve leaflets and contribute to an accelerated structural deterioration of the prosthetic valve. Further studies are needed to determine whether ATTR-CA patients will have shorter valve durability following AVR.

In the only other study that systematically screened severe AS patients undergoing surgical AVR, out of the 146 biopsies taken at the time of surgery, 6 contained amyloid (a prevalence of 4.1%) (19). Typing by immunohistochemistry, supported by laser microdissection and mass spectroscopy, confirmed ATTR amyloid type in all 6 cases. The prevalence increased to 5.6% if only calcific AS patients >65 years of age were considered. There are several possible explanations as to why cardiac amyloidosis was not detected in the current study cohort. Firstly, the study patients were relatively young (mean age 66 years), with 36% of them having congenital aortic valve disease. Secondly, the tested sample size could be inadequately small to detect the disease with a proven low prevalence in surgical cohorts. The number of patients tested in our study cohort was twice as low as in the study by Treibel et al. (71 vs. 146 biopsy samples). A higher likelihood of detecting ATTR-CA would be in the AS patients evaluated for TAVI, as the reported prevalence in this group of patients is 2 to 3 times as big, ranging between 9-16%. Screening patients scheduled for TAVI could be a topic for future research studies at our center.

6. STUDY LIMITATIONS

6.1 Meta-analysis limitations

The main limitation of the present meta-analysis is the inclusion of observational studies, which all share an intrinsic risk of selection bias. As in many cardiac centers, CMR is not a routine workup test before AV intervention; some patients may have been referred for investigation on clinical grounds, which may have introduced a referral bias. This could have led to an overestimation of the LGE prevalence. The meta-analysis was also limited by the inconsistent characteristics of the study populations, cohorts with mixed valvular pathologies and variability in the degree of AV disease severity included. A significant number of single center studies were excluded from the analysis due to the risk of data overlap. This particularly applied to the studies from UK centers that have participated in the BSCMR Valve Consortium (45). Without access to individual patient data, we had to use estimated event rates in several studies which could have had an effect on the final result of the pooled analysis. Limited data and the inability to use raw datasets precluded subgroup analysis.

6.2 FIB-AS study limitations

The study was composed of a small number of AS patients, however it did include a substantial number of myocardial biopsies. Due to the COVID-19 pandemic there were delays in patient examinations and surgeries causing uneven time frames between the preoperative patient assessment (echocardiographic and CMR) and surgery with myocardial biopsy sampling, potentially affecting the final result. The proportion of histologically measured myocardial fibrosis could have been affected by the size and depth of biopsy samples, as more superficially sampled and smaller biopsies may contain a higher proportion of fibrotic tissue in comparison to larger biopsy samples. Although measuring T1 values only in the septum is a validated and common method, it might not represent the entire LV myocardium as the myocardial structure may not be homogenous. Moreover, while T1 mapping has clearly shown its potential for quantitative tissue characterization, it still requires further validation and standardization before full integration into clinical practice. Because we excluded patients with comorbidities, such as obstructive CAD, a history of myocardial infarction, renal failure and persistent atrial arrhythmias, our results should not be overgeneralized to the broader AS patient population.

7. CONCLUSIONS

1. According to our meta-analysis, LGE is present in up to the half of the studied AS populations (49.6%) and on average takes up to 4% of LV mass. The most frequent type of focal fibrosis is non-infarct type, present in 63.6% of AS patients. A meta-analysis of clinical outcomes showed that the presence of LGE triples an AS patient's all-cause (pooled OR [95% CI] = 3.26 [1.72, 6.18], p=0.0003) and cardiovascular mortality (pooled OR [95% CI] = 2.89 [1.90, 4.38], p<0.0001).

2. CMR and histological analysis of the FIB-AS study population revealed that focal non-infarct type and diffuse myocardial fibrosis was highly prevalent in severe AS patients undergoing surgical AVR. The presence of LGE indicated a more advanced LV remodeling. Histologically measured myocardial fibrosis was associated with imaging and serum biomarkers of LV dysfunction and left side chamber enlargement. The subendocardium was affected by myocardial fibrosis to a greater extent.

3. Low GLS and elevated native T1 differentiated patients with more advanced LV remodeling can therefore be used as early markers of LV damage. GLS can be used as a surrogate marker of myocardial fibrosis as it was associated with both invasively and non-invasively measured myocardial fibrosis. GLS >-14% predicted increased myocardial fibrosis.

4. Due to low disease prevalence in surgical AS cohorts, no evidence of ATTR cardiac amyloidosis was found in the LV myocardium of severe AS patients undergoing surgical AVR in neither CMR studies, nor in histological analysis.

8. PRACTICAL RECOMMENDATIONS

8.1 Myocardial fibrosis in aortic stenosis

The results of our meta-analysis and FIB-AS study have revealed that severe AS patients may develop LV injury which may not be apparent in conventional imaging studies. A significant proportion of AS patients were found to have various degrees of myocardial fibrosis, both focal and diffuse. This LV damage should not be ignored as it has important clinical implications. Therefore, it is important to include an extended assessment of AS consequences on LV myocardium to pre-interventional investigation protocols. Calculation of LVEF is a common clinical method to measure LV systolic function and will remain an important clinical tool. However, it lacks sensitivity, especially in patients with concentric LV hypertrophy. We should aim to identify early, subclinical markers of LV damage when conventional markers of systolic dysfunction may remain unchanged. Our data suggests that GLS, assessed by STE, and native T1, assessed by CMR, can be used as early biomarkers of LV adverse remodeling in severe AS patients, and may aid in AS patients risk stratification (**Fig. 28**). GLS can also be used as a surrogate marker of diffuse myocardial fibrosis and a cut off value of -14% can be applied. As GLS assessment is cheaper and widely available, it could be an initial step followed by CMR in selected patients when the symptom's status is equivocal or a decision to proceed to AVR is under consideration. Early detection of LV structural and functional alterations would allow an earlier referral to AV intervention and could possibly help to protect LV myocardium from irreversible changes and help to improve a patient's clinical outcomes. Current knowledge of the cardiology community is based on evidence from prospective multicenter studies; however, there is still a lack of randomized trials to update currently used clinical practice guidelines. A prospective multicenter randomized controlled trial, the EVOLVED (Early Valve Replacement Guided by Biomarkers of LV Decompensation in Asymptomatic Patients with Severe AS) trial is currently underway, aiming to assess the role of myocardial fibrosis measurements in the selection of patients for AVR (111). The decision for AVR versus observation in the EVOLVED trial will be driven by CMR identification of replacement fibrosis (mid-wall LGE). This trial should provide additional insights into this area and may further improve our knowledge and everyday clinical practice.

Imaging biomarkers of subclinical LV injury
Reduced GLS
Elevated native T1
Presence of LGE

Fig. 28 Imaging biomarkers of subclinical LV injury.

8.2 ATTR-CA in aortic stenosis

Due to the substantial prevalence of ATTR-CA in elderly populations of severe AS undergoing TAVI, it is necessary to follow a systematic approach for the care of such patients. As the first step, it is important to recognize clinical and imaging red flags for ATTR-CA. It should be remembered that an RAS pattern of GLS can be found in up to 17-30% of patients with isolated AS, therefore this cannot be used as a confirmatory sign of cardiac amyloidosis in AS populations. The second step is to confirm the diagnosis by performing additional tests, including bone scintigraphy, monoclonal light-chain analysis in blood and urine, and/or a myocardial biopsy to confirm the diagnosis and type of cardiac amyloidosis. The third step should enable the selection of the type of treatment; patients with confirmed severe AS should promptly undergo AVR, and TAVI should be preferred as it is usually associated with better outcomes than surgical AVR. Finally, if available, treatment with tafamidis should be considered in patients with confirmed ATTR-CA, regardless of the AS severity or the decision to perform AVR. Due to the low disease prevalence in relatively young and low risk AS patients, routine screening for ATTR-CA in surgical cohorts is not recommended.

CONTINUITY OF THE RESEARCH

Due to the unfavorable circumstances of the COVID-19 epidemiologic situation, there were delays in patient enrolment and hospitalization for surgery. In order to include a sufficient number of patients we had to extend the patient enrolment period up to the March of 2021, meaning the post-operative follow-up period was inadequately short to investigate the effect of myocardial fibrosis on patients' clinical outcomes before the end of the doctoral studies. The data from the patients' 12 months follow-up visits and clinical outcomes are continuously being collected. This will create a new package of data for future research on post-operative LV reverse remodeling and the effects of structural LV remodeling on patients' post-operative clinical outcomes. The FIB-AS study is being performed in collaboration with the cardiology center of Aalborg University Hospital in Denmark. Clinical and imaging data of severe AS patients undergoing TAVI are continuously being collected by our Danish colleagues and will be analyzed in conjunction with the data from VUH Santaros clinic in the future.

STUDY FUNDING

2014-2020 Operational Programme for the European Union Funds Investments in Lithuania

SANTRAUKA

SANTRUMPOS

AS – aortos stenozė,

AV – aortos vožtuvas,

AVA – aortos vožtuvo anga,

AVP – aortos vožtuvo protezavimas,

BID – bendra išilginė deformacija,

BNP – B tipo natriuretinis peptidas,

Dj-trop I – didelio jautrumo troponinas I,

ET – ekstraląstelinis tūris,

EuroScoreII – II Europos operacinės rizikos vertinimo skaičiuoklė,

GFR – glomerulų filtracijos greitis,

KS – kairysis skilvelis,

KSIF – kairiojo skilvelio išstūmimo frakcija,

KŠL – koronarinė širdies liga,

MLHFQ – Minesotos gyvenimo, sergant širdies nepakankamumu, klausimynas,

MRT – magnetinio rezonanso tomografija,

NYHA – Niujorko širdies asociacija,

SIVD – santykinai išsaugota viršūnės deformacija,

STS – Krūtinės ląstos chirurgų draugijos rizikos skaičiuoklė,

ŠMRT – širdies magnetinio rezonanso tomografija,

TAVI – transkateterinis aortos vožtuvo implantavimas,

TTR-ŠA – transtiretino širdies amiloidozė,

VKMK – vėlyvasis kontrastinės medžiagos kaupimas,

VUL – Vilniaus universitetinė ligoninė.

ĮŽANGINIS ŽODIS

Širdies vožtuvų ydomis domiuosi nuo pat pasirinktos subspecializacijos, susijusios su širdies ir kraujagyslių vaizdinimo sritimi, pradžios. Pacientų, sergančių širdies vožtuvų ligomis, įskaitant aortos vožtuvo stenozę, gydymas yra tapęs neatsiejama mano kasdienės klinikinės praktikos dalimi. Taigi doktorantūros studijų metu pasirinkta tirti širdies vožtuvų ligomis sergančius pacientus.

Daktaro disertacija yra penkerių metų nuoseklaus darbo rezultatas. Doktorantūros studijų metu įgijau vertingų žinių ir įgūdžių. Tvirtai tikiu, kad ši neįkainojama patirtis bus naudinga mano tolimesniame klinikiniame darbe ir mokslinėje veikloje. Esu labai dėkinga prof. dr. Sigitai Glaveckaitei už suteiktą galimybę studijuoti doktorantūroje, taip pat už vertingas mokslines konsultacijas, nuoseklų vadovavimą, įvairiapusišką pagalbą ir lyderystės pavyzdį.

1. ĮVADAS

1.1 Tyrimo aktualumas

Pastaraisiais dešimtmečiais itin padaugėjo pacientų, kuriems dėl didelio laipsnio aortos vožtuvo angos stenozės (AS) atliekamas chirurginis aortos vožtuvo protezavimas (AVP) arba perkateterinis aortos vožtuvo implantavimas (TAVI). Aortos vožtuvo (AV) intervencijų skaičiaus augimas gali būti siejamas tiek su didėjančiu AS paplitimu senėjančioje populiacijoje, tiek su mažiau invazinio perkateterinio gydomojo metodo pažanga ir plačiu jo pritaikymu klinikinėje praktikoje. Lietuvos higienos instituto duomenimis, nuo 2001 m. iki 2020 m. pacientų, sergančių širdies vožtuvų ligomis (ligos kodas I34-I39), skaičius padidėjo 3,9 karto, vertinant absoliučiaisiais skaičiais, ir 4,9 karto, skaičiuojant 100 000 gyventojų [1] (1 ir 2 pav.).
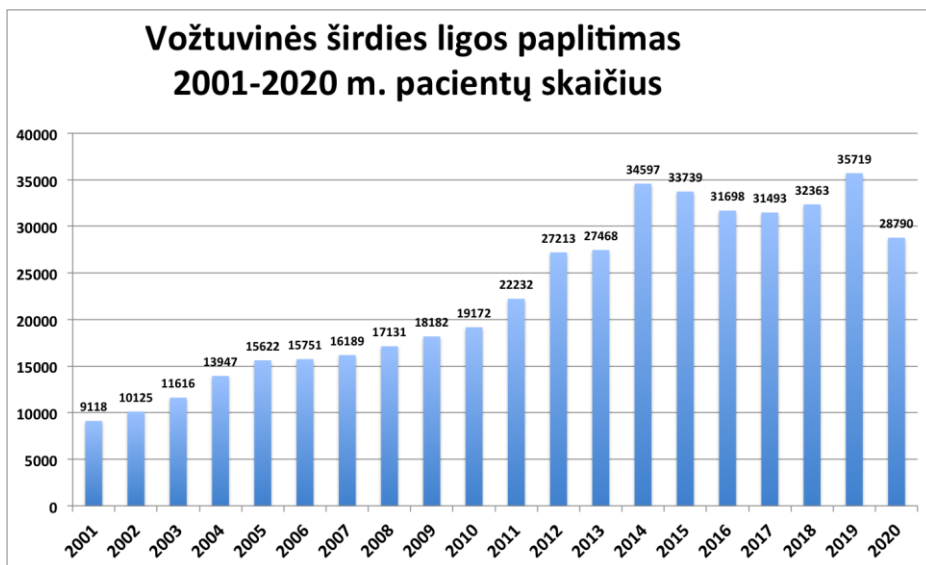

1 pav. Sergamumo širdies vožtuvų ligomis (ligos kodas I34-I39) tendencijos Lietuvoje 2001–2020 m., vertinant absoliučiaisiais skaičiais (Lietuvos higienos instituto duomenys)
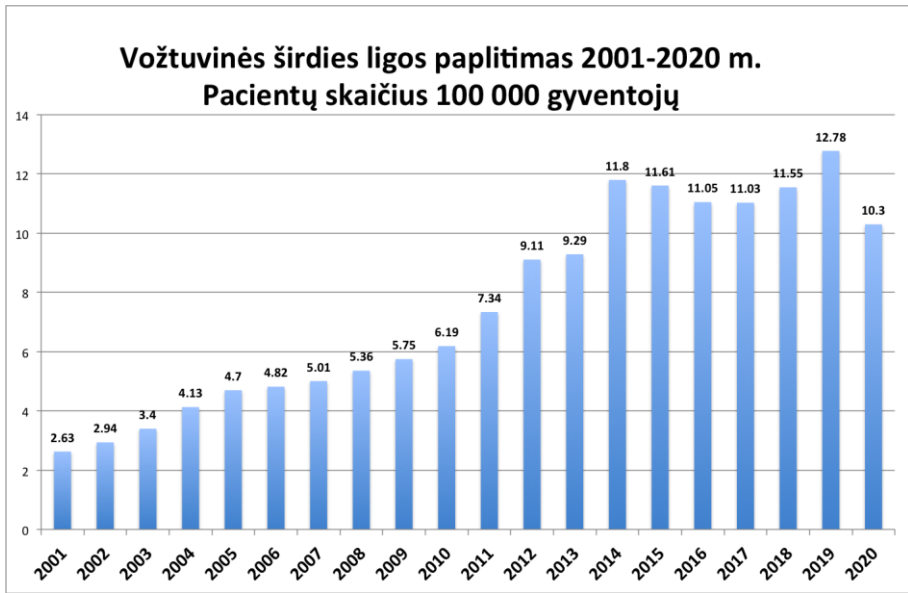
2 pav. Sergamumo širdies vožtuvų ligomis (ligos kodas I34-I39) tendencijos Lietuvoje 2001–2020 m., skaičiuojant 100 000 gyventojų (Lietuvos higienos instituto duomenys)

Didėjantį pacientų, sergančių širdies vožtuvų ligomis, skaičių lemia ne tik didėjantis patologijos paplitimas, bet ir, tikėtina, išaugusios gydytojų siuntimų į kardiologijos centrus apimtys. Pacientams, kurie anksčiau buvo priskirti didelės rizikos grupei, o jų būklė buvo netinkama chirurginei intervencijai, dabar galima taikyti naujus perkateterinius gydymo būdus. Akivaizdus aortos vožtuvo intervencijų skaičiaus augimas pastebimas visose Vakarų Europos šalyse. Šis skaičius išaugęs ir Lietuvos kardiologijos centruose. Remiantis Lietuvos higienos instituto duomenimis, aortos vožtuvo chirurginių ir perkateterinių intervencijų skaičius 2011–2020 m. visuose Lietuvos kardiologijos centruose padidėjo 28 proc. Minėtina, kad Vilniaus universiteto ligoninės (VUL) Santaros klinikose šis skaičius išaugo 31 proc. [1] (3 pav.). Svarbu atkreipti dėmesį, kad, nepaisant nepalankių COVID-19 epidemiologinės situacijos aplinkybių, atliktų aortos vožtuvo intervencijų skaičius išliko nepakitęs.
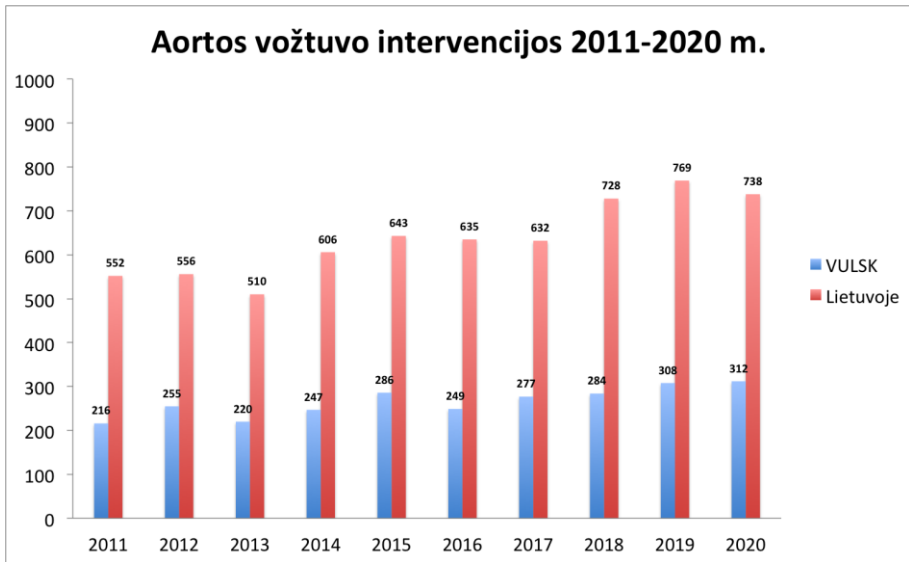
3 pav. Chirurginių ir perkateterinių aortos vožtuvo intervencijų tendencijos 2011–2020 m. Lietuvoje (raudona spalva) ir VUL Santaros klinikose (mėlyna spalva) (Lietuvos higienos instituto duomenys)

Atsižvelgiant į minėtas tendencijas, vis aktualesni tampa didelio laipsnio AS diagnostikos ir pacientų rizikos stratifikavimo klausimai. Plačiai pripažįstama, kad AS yra ne tik vožtuvo, bet ir kairiojo skilvelio (KS), o ilgainiui ir visos širdies liga. Mokslinėje literatūroje nemažai duomenų, jog tiek chirurginio, tiek perkateterinio AS gydymo atvejais KS pažeidimo laipsnis yra svarbus veiksnys, lemiantis periprocedūrines komplikacijas ir pacientų prognozę [2, 3]. Vis dėlto šiandien rekomenduojami ir taikomi AS sergančių pacientų KS pažeidimo vertinimo kriterijai yra nepakankamai jautrūs. Vienintelis rodiklis, nusakantis AS pasekmes KS miokardui, minimas dabartinėse Europos kardiologų draugijos išleistose širdies vožtuvų ligų rekomendacijose, yra sumažėjusi KS išstūmimo frakcija (KSIF), apibrėžiama kaip KSIF sumažėjimas <50 % [4]. KS miokardo pažeidimo vertinimas, vadovaujantis KSIF rodikliu, pasižymi daugybe trūkumų: jis priklauso nuo apkrovos sąlygų, gali būti kompensuotas koncentrinės KS remodeliacijos ir pradeda mažėti tik esant vėlyvai ligos stadijai [5]. Naujų jautresnių vaizdinių KS pažeidimo biožymenų nustatymas ir jų įtraukimas į šiuo metu naudojamus diagnostikos algoritmus gali padėti išvengti negrįžtamų, ilgalaikės perkrovos slėgiu sąlygotų KS miokardo pokyčių ir mesti iššūkį dabartinėms rekomendacijoms.

Kaip galimi naujieji KS pažaidos biožymenys vertinami šie širdies vaizdinimo tyrimų parametrai: bendra išilginė deformacija (BID), matuojama

taškelių žymėjimo echokardiografijos metodu, ir miokardo fibrozė, diagnozuojama širdies magnetinio rezonanso tomografijos (ŠMRT) metodu.

Pagrindinis širdies nepakankamumo priežastinis veiksnys yra miokardo fibrozė [6–8]. Taigi, siekiant geriau suvokti patofiziologiją, įvertinti galimus gydymo būdus ir tiksliau numatyti pacientų prognozę, labai svarbūs tampa tiek židininės, tiek difuzinės miokardo fibrozės ankstyvosios diagnostikos ir kiekybinio įvertinimo klausimai. Miokardo fibrozė yra ankstyvasis KS dekompensacijos žymuo, ji išsivysto dar prieš sumažėjant KSIF ar pasireiškiant pirmiesiems ligos simptomams [9]. Nustatyta, kad miokardo fibrozė pacientams, sergantiems AS, susijusi su sutrikusia KS funkcija ir nepalankiomis klinikinėmis baigtimis [10, 11]. Įrodyta, kad KS BID, kaip galimas miokardo fibrozės pakaitinis žymuo, yra nepriklausomas nepageidaujamų reiškinių prognostinis rodiklis pacientams, sergantiems didelio laipsnio AS, esant tiek išsaugotai, tiek sutrikusiai KS sistolinei funkcijai [12, 13]. Šiuo metu duomenų apie miokardo fibrozės įvertinimą pacientams, sergantiems didelio laipsnio AS, taikant neinvazinius širdies vaizdinimo metodus kartu su histologiniu patvirtinimu, mokslinėje literatūroje randama nedaug.

Transtiretino širdies amiloidozė (TTR-ŠA) – sudėtinga ir nepakankamai ištirta širdies nepakankamumo priežastis [14]. Dar neseniai TTR-ŠA buvo laikoma reta infiltracinės kardiomiopatijos rūšimi, o tradiciniu vadinamuoju „auksiniu diagnostikos standartu" buvo laikoma endomiokardo biopsija, kartu pasireiškiant būdingiems klinikiniams ligos požymiams ir esant širdies vaizdinimo tyrimų pakitimų. Diagnostinio vaizdinimo technologijų pažanga, įskaitant ŠMRT su T1 žemėlapiu ir scintigrafija su techneciu žymėtais radioaktyviais izotopais, suteikė galimybę neinvaziniu būdu diagnozuoti TTR-ŠA, o tai per pastarąjį dešimtmetį smarkiai išplėtė žinias apie šią ligą ir jos diagnozavimo galimybes [14–16].

TTR-ŠA vis dažniau diagnozuojama pacientams, sergantiems degeneracine AS [17, 18]. Daugėjant vyresnio amžiaus pacientų, kuriems taikoma TAVI, TTR-ŠA nustatymas šioje pacientų grupėje turi didelę klinikinę reikšmę. Išreikšta KS miokardo remodeliacija ir pažengusi KS diastolinė disfunkcija, esant išsaugotai KSIF, laikomos tiek TTR-ŠA, tiek AS požymiais [19]. Kadangi tiek TTR-ŠA, tiek AS dažniau diagnozuojamos vyresnio amžiaus pacientams, atlikta nemažai mokslinių tyrimų, skirtų bendro šių dviejų ligų egzistavimo ypatumams įvertinti [20–25]. Abiem minėtoms ligoms būdingos panašios klinikinės ir echokardiografinės charakteristikos, todėl pacientams, sergantiems AS, gali būti labai sudėtinga diagnozuoti TTR-ŠA. Nepaisant to, tiksli diagnozė labai svarbi abiem patologijoms gydyti: tiek

skiriant širdies amiloidozės specifinį gydymą, tiek priimant sprendimus dėl AS gydymo taktikos. Įrodyta, kad širdies amiloidozė pacientams, sergantiems AS, susijusi su didesne mirtingumo nuo įvairių priežasčių ir širdies nepakankamumo rizika, negu pacientams, sergantiems vien tik AS [24, 25]. Svarbu paminėti, kad TTR-ŠA paplitimas tarp Lietuvos pacientų niekada nebuvo sistemingai tirtas, todėl tai nauja ir svarbi tyrimo tema.

1.2 Mokslinio tyrimo reikšmė ir naujumas

ŠMRT suteikia galimybę tiksliai įvertinti širdies miokardo masę, tūrius ir funkciją [26]. Vėlyvojo kontrastinės medžiagos kaupimo (VKMK) vaizdai tapo vadinamuoju „auksiniu standartu" vaizdinimo tyrimais diagnozuoti židininę miokardo fibrozę, sergant širdies ir kraujagyslių ligomis: koronarine širdies liga (KŠL) ir neišeminės kilmės kardiomiopatija [27–29]. Vis dėlto širdies patologijų, kurioms būdinga difuzinė miokardo fibrozė, negalima tinkamai įvertinti taikant tik VKMK, nes tyrimo metu gali nebūti vėlyvo kaupimo vaizdo, nepaisant reikšmingos intersticinės fibrozės.

ŠMRT jau daugelį metų naudojama miokardui vaizdinti, tačiau tik naujausi magnetinio rezonanso tomografijos technologijos ir vaizdo atkūrimo metodų patobulinimai leido į klinikinę praktiką įdiegti parametrinį vaizdinimą [30]. Kitaip negu įprasti ŠMRT metodai, kurie remiasi santykiniais vaizdo intensyvumo skirtumais, siekiant išryškinti miokardo pakitimus, parametrinis vaizdinimas suteikia galimybę miokardo struktūrą vertinti tiesiogiai ir kiekybiškai. Tyrimai parodė, kad T1 žemėlapis, kartu panaudojant gadolinio turinčias kontrastines medžiagas, gali būti naudingas diagnozuojant miokardo difuzinius patologinius procesus, įskaitant miokardo fibrozę [32, 33]. T1 vertės, gautos prieš ir po kontrastinės medžiagos suleidimo, kartu su hematokrito matavimo rezultatais gali būti naudojamos audinio ekstraląstelinio tūrio frakcijai (ET) nustatyti [35]. Patologinę KS remodeliaciją, sergant AS, iš dalies lemia didėjantis intersticinės fibrozės laipsnis [36, 37], todėl T1 žemėlapis gali būti naudingas prognozuojant būsimas kardiovaskulines baigtis.

Išmatuotoms miokardo T1 ir ET vertėms interpretuoti būtina nustatyti norminių reikšmių intervalus. Miokardo T1 ir ET norminių reikšmių intervalai priklauso nuo MRT aparato magnetinio lauko stiprumo, parametrinio vaizdinimo sekos ir konkretaus centro tyrimo protokolų [38]. Taigi konkretaus centro norminės minėtų rodiklių reikšmės turi būti nustatomos remiantis duomenų rinkiniais, gautais, apdorotais ir išanalizuotais tokiu pat būdu, kaip ir numatyta taikyti būsiemiems pacientams. Gautos norminės reikšmės turi

būti lyginamos su mokslinėje literatūroje paskelbtais duomenimis. Remiantis Europos širdies ir kraujagyslių vaizdinimo tyrimų asociacijos konsensuso dokumentu dėl ŠMRT parametrinio vaizdinimo [38], rekomenduojama natyvinio T1 ir ET norminių reikšmių intervalus nustatyti ištyrus nuo mažiausiai 15 iki (idealiu atveju) 50 ar daugiau sveikų savanorių. Tiriant ligas, kurioms būdingas ryškus T1 vertės pokytis (pavyzdžiui, įtariama amiloidozė arba Andersono ir Fabry liga), priimtinas mažesnis tiriamųjų skaičius normalių verčių nustatymui (pavyzdžiui, pakanka įvertinti 15–20 sveikų asmenų duomenis). Tačiau tiriant ligas, kurioms būdingas nedidelis šių rodiklių pokytis (pavyzdžiui, difuzinės miokardo fibrozės atveju), būtina ištirti daugiau asmenų (pavyzdžiui, įvertinti 50 ir daugiau sveikų asmenų duomenis). Nustačius norminių reikšmių intervalą, pagrindiniai skenavimo protokolo parametrai, kontrastinė medžiaga (dozė) ir sistolinė ar diastolinė fazė neturėtų būti keičiama, todėl rekomenduojama reguliariai kartoti fantominę kokybės kontrolę. 2019 m. VUL Santaros klinikose 1,5 T „Magnetom Aera"(„Siemens", Erlangen, Vokietija) magnetinio rezonanso įrenginyje pirmą kartą įdiegta parametrinio vaizdinimo programinė įranga, todėl reikėjo nustatyti parametrinio vaizdinimo norminių reikšmių intervalus.

Disertacijoje pristatomo mokslinio tyrimo naujumas:

- Atlikta pirmoji didelės apimties metaanalizė, tiriant židininės miokardo fibrozės paplitimą, tipus ir klinikinę reikšmę AS sergantiems pacientams.

- Atliktas perspektyvusis tyrimas yra vienas iš nedaugelio pasaulyje atliktų tyrimų, kuriame, analizuojant širdies vaizdinimo tyrimų ir didelio kiekio miokardo biopsijų histologinės analizės duomenis, apibendrinami AS sergančių pacientų miokardo fibrozės ypatumai.

- Darbe pateikiami svarbūs nauji rezultatai apie širdies vaizdinimo biožymenis, kurie gali būti sėkmingai naudojami AS sergantiems pacientams diagnozuojant subklinikinį KS miokardo pažeidimą.

- Tai pirmasis tyrimas, kurio metu VUL Santaros klinikose pritaikytas ŠMRT parametrinis vaizdinimas ir gauti pirmieji T1 žemėlapio duomenys.

- Tai vienas iš nedaugelio tyrimų visame pasaulyje, kurio metu AS sergantys pacientai buvo sistemingai tirti dėl TTR širdies amiloidozės, pritaikant širdies vaizdinimo tyrimus ir miokardo histologinę analizę.

1.3 Tyrimo tikslas

Tyrimo tikslas – ištirti struktūrinius KS miokardo pokyčius, taikant invazinius ir neinvazinius tyrimo metodus pacientams, sergantiems didelio laipsnio AS, ir susieti šiuos pokyčius su KS disfunkcijos rodikliais.

1.4 Tyrimo hipotezė

- *Pirminė hipotezė.* Pacientams, sergantiems didelio laipsnio AS, miokardo fibrozė yra susijusi su KS disfunkcijos žymenimis ir blogesnėmis klinikinėmis baigtimis: mirtingumu dėl įvairių priežasčių ir kardiovaskuliniu mirtingumu.

- *Antrinė hipotezė.* Pacientams, sergantiems didelio laipsnio AS, gali būti diagnozuota TTR širdies amiloidozė. Ji susijusi su pažengusia KS remodeliacija.

1.5 Tyrimo uždaviniai

1. Atlikus publikuotų mokslinių tyrimų metaanalizę, nustatyti židininės miokardo fibrozės tipą ir jos paplitimą tarp pacientų, sergančių AS, įvertinti jos poveikį pooperacinėms klinikinėms išeitims.

2. Taikant invazinius ir neinvazinius tyrimo metodus, pacientams, sergantiems didelio laipsnio AS, kuriems taikomas chirurginis aortos vožtuvo protezavimas, įvertinti KS miokardo fibrozės ypatumus ir susieti juos su serumo ir širdies vaizdinimo tyrimų rodikliais.

3. Nustatyti ankstyvuosius KS miokardo pažeidimo biožymenis pacientams, sergantiems didelio laipsnio AS.

4. Įvertinti TTR širdies amiloidozės paplitimą pacientams, sergantiems didelio laipsnio AS, kuriems taikomas chirurginis aortos vožtuvo protezavimas.

1.6 Ginamieji teiginiai

1. Židininė neinfarktinio tipo KS miokardo fibrozė yra plačiai paplitusi tarp pacientų, sergančių didelio laipsnio AS, ir padidina jų mirtingumo dėl įvairių priežasčių bei kardiovaskulinio mirtingumo riziką.

2. ŠMRT metodu nustatyta ir histologiškai įvertinta miokardo fibrozė yra susijusi su pažengusia KS remodeliacija ir KS disfunkciją atspindinčiais širdies vaizdinimo ir serumo biožymenimis.

3. Sumažėjusi BID, padidėję natyvinio T1 ir ET rodikliai leidžia atpažinti

pacientus, kuriems būdinga pažengusi KS remodeliacija, todėl minėti rodikliai gali būti naudojami kaip ankstyvieji KS pažeidimo biožymenys.

4. TTR širdies amiloidozė gali būti diagnozuota AS sergantiems pacientams. Ji susijusi su pažengusia KS remodeliacija ir blogesnėmis klinikinėmis baigtimis.

2. TYRIMO METODAI

2.1 Metaanalizė

Metaanalizė atlikta vadovaujantis sisteminių apžvalgų ir metaanalizių atlikimo (PRISMA) gairėmis [72]. Pirmiausia, atlikta sisteminė mokslinių straipsnių paieška *PubMed* ir *EMBASE* elektroninėse duomenų bazėse. Kuriant paieškos strategiją vartoti terminai „aortos stenozė" (angl. *aortic stenosis*), „vėlyvas gadolinio kaupimas" (angl. *late gadolinium enhancement*) arba „uždelstas gadolinio kaupimas" (angl. *delayed gadolinium enhancement*), arba „*LGE*" (angl. *late gadolinium enhancement*, *LGE*), taip pat „širdies ir kraujagyslių magnetinis rezonansas" (angl. *cardiovascular magnetic resonance*). Įgyvendinta tik anglų kalba paskelbtų tyrimų ir tik tyrimų, atliktų su žmonėmis, paieška. Siekiant identifikuoti aktualias publikacijas, kurios nebuvo įtrauktos į pradinę paiešką, peržiūrėti atrinktų mokslinių straipsnių literatūros sąrašai.

Į metaanalizę įtraukti perspektyviniai stebėsenos tyrimai, analizuojantys ŠMRT ir VKMK metodu nustatytos židininės miokardo fibrozės ypatumus pacientams, sergantiems AS. Visi tyrimai suskirstyti į dvi grupes: 1) tyrimai, teikiantys duomenų apie židininę miokardo fibrozę, 2) tyrimai, teikiantys duomenų apie nepageidaujamų reiškinių dažnį tarp tiriamųjų grupių su nustatyta ar nenustatyta židinine miokardo fibroze.

Mirtingumas nuo įvairių priežasčių ir kardiovaskulinis mirtingumas – pagrindiniai šios metaanalizės rodikliai. Vertinant židininę fibrozę, atsižvelgta į bet kokį jos tipą – tiek infarktinį, tiek neinfarktinį. Jei toje pačioje populiacijoje buvo atlikti keli tyrimai, į metaanalizę įtraukti tyrimų, kuriuose dalyvavo didžiausias pacientų skaičius, rezultatai. Surinkti duomenys apie židininės fibrozės paplitimą, tipą ir išplitimą miokarde. Duomenys apie pacientus, kuriems pasireiškė arba nepasireiškė nepageidaujami reiškiniai, priklausomai nuo to, ar jiems nustatyta židininė fibrozė ar nenustatyta, imti iš publikuotų duomenų arba apskaičiuoti atsižvelgiant į bendrąjį pacientų skaičių ir mirčių skaičių skirtingose grupėse. Publikacijų atrankos procesas pavaizduotas 4 pav.
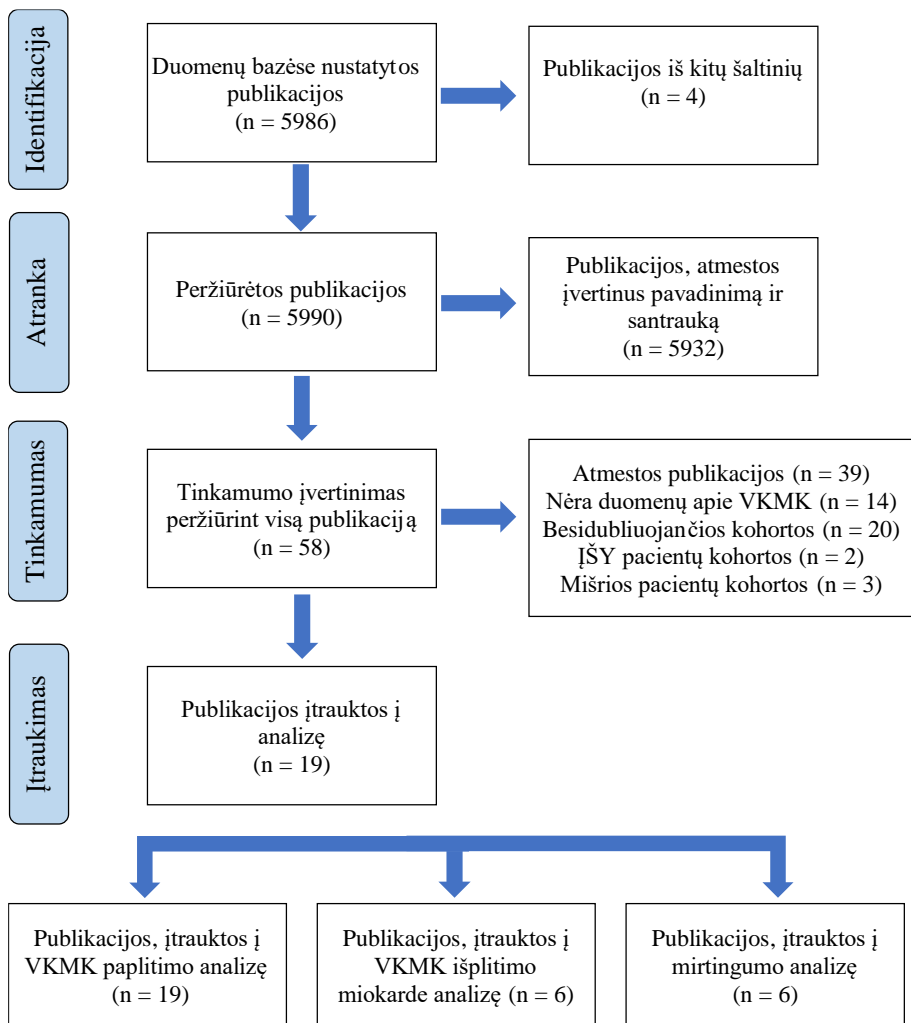
IŠY - įgimtos širdies ydos, VKMK - vėlyvas kontrastinės medžiagos kaupimas (LGE)

4 pav. PRISMA srauto diagrama

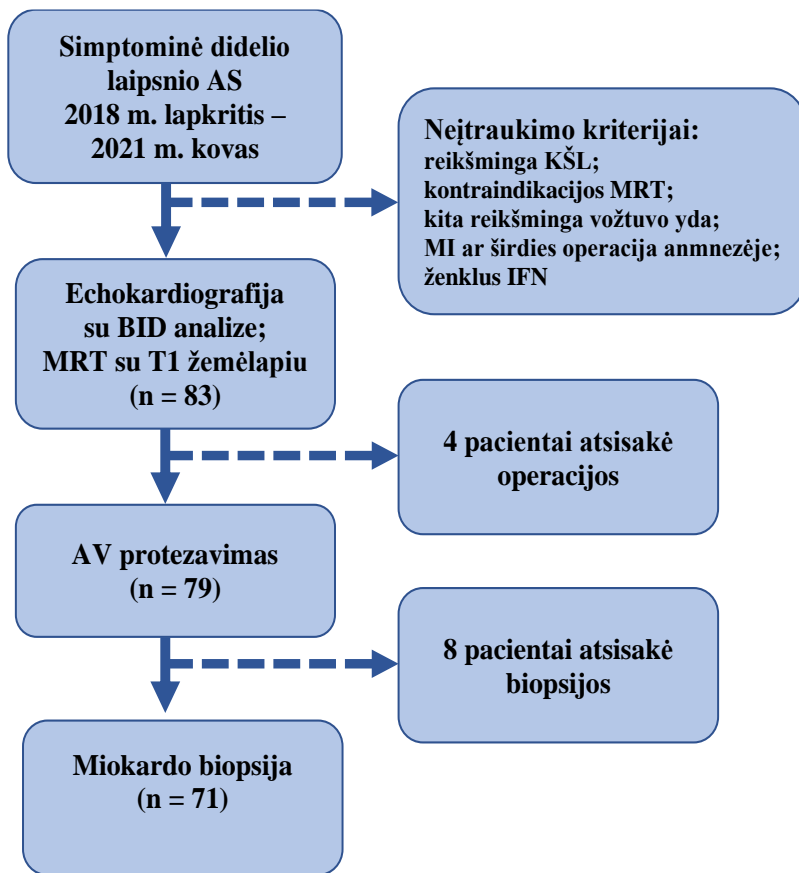## 2.2 FIB-AS tyrimas

2.2.1 Tyrimo planas

Pristatomam perspektyviniam stebėsenos tyrimui atlikti VUL Santaros klinikose nuo 2018 m. lapkričio mėn. iki 2021 m. kovo mėn. atrinkti pacientai, sergantys didelio laipsnio simptomine AS, kuriems, remiantis dabartinėmis gydymo rekomendacijomis, indikuotas chirurginis aortos vožtuvo protezavimas [4]. Tyrimas patvirtintas Vilniaus regiono biomedicininių

tyrimų etikos komiteto (patvirtinimo nr. 158200-18/9-1014-558) ir atliktas kaip FIB-AS tyrimo (NCT03585933) dalis. Šis tyrimas atitiko Helsinkio deklaracijos principus, visi tiriamieji pateikė raštišką sutikimą dalyvauti tyrime.

Pacientai atrinkti priešoperacinio įvertinimo metu. Rinkti šie pacientų duomenys: ligos istorijos, Minesotos gyvenimo, sergant širdies nepakankamumu, klausimyno (angl. *Minnesota Living with Heart Failure questionnaire*, MLHFQ), 6MĖT, kraujo tyrimų (hematokrito, inkstų funkcijos, smegenų natriuretinio peptido (BNP) ir didelio jautrumo troponino I (Hs-Tn-I) rodiklių), transtorakalinės echokardiografijos ir ŠMRT rodikliai. Pacientų įtraukimo kriterijai: indikuotinas AV protezavimas dėl didelio laipsnio AS (ultragarsu nustatytas aortos vožtuvo angos plotas (AVA) ≤1 cm^2 arba AVA indeksas ≤0,6 cm^2/m^2), amžius – >18 metų, galimybė atlikti ŠMRT, paciento sutikimas su tyrimo protokolu. Kriterijai, pagal kuriuos pacientai nebuvo įtraukti į klinikinį tyrimą: reikšminga KŠL (>50 % pažeidimas epikardinėse vainikinėse arterijose), anamnezėje nurodytas diagnozuotas miokardo infarktas, kitos didelio laipsnio vožtuvų ydos, eGFR <30 mL/min/1,73 m^2, su ŠMRT nesuderinami implantuoti prietaisai, persistuojanti prieširdžių tachiaritmija, anamnezėje nurodyta patirta širdies operacija (5 pav.). Chirurginis AVP atliktas taikant standartinę chirurginę metodiką per vidurinę sternotomiją arba J ministernotomiją, esant dirbtinei kraujo apykaitai ir lengvai hipotermijai. Skirtingo dydžio „St. Jude Medical Trifecta" aortos bioprotezai („St. Jude Medical, Inc.", San Paulas, Minesota, JAV) arba mechaniniai „CarboMedics" standartiniai aortos vožtuvų („CarboMedics, Inc.", Ostinas, Teksaso valstija, JAV) protezai buvo naudojami atsižvelgiant į chirurgų komandos poreikius ir pacientų prioritetus. Pacientai buvo reguliariai stebimi ir gydomi vadovaujantis galiojančiomis gairėmis [4]. Tyrimo duomenys buvo renkami ir saugomi tam skirtoje internetinėje duomenų bazėje *REDCap* (angl. *Research Electronic Data Capture*) [73].

Simptominė didelio laipsnio AS
2018 m. lapkritis – 2021 m. kovas

Neįtraukimo kriterijai:
reikšminga KŠL;
kontraindikacijos MRT;
kita reikšminga vožtuvo yda;
MI ar širdies operacija anmnezėje;
ženklus IFN

Echokardiografija su BID analize;
MRT su T1 žemėlapiu (n = 83)

4 pacientai atsisakė operacijos

AV protezavimas (n = 79)

8 pacientai atsisakė biopsijos

Miokardo biopsija (n = 71)

LIL – lėtinė inkstų liga (angl. *chronic kidney disease*, CKD), MI – miokardo infarktas.

5 pav. FIB-AS tyrimo schema

2.2.2 Tyrimai

2.2.2.1 Echokardiografija ir 2D deformacijos analizė

Transtorakalinė 2D echokardiografija atlikta naudojant „Vivid" ultragarso sistemą (S70, E9 arba E95) („GE Healthcare", Hortenas, Norvegija). Gauti rezultatai buvo saugomi duomenų bazėje tolesnei duomenų analizei. AS sunkumo laipsnis ir KS sistolinė bei diastolinė funkcijos įvertintos vadovaujantis echokardiografijos rekomendacijomis [74, 75]. AVA apskaičiuota naudojant tėkmės tolygumo lygtį.

BID analizei išsaugoti 2, 3 ir 4 kamerų viršūniniai vaizdai, o duomenys apdoroti naudojant „EchoPac 112.0.1"programinę įrangą („GE

Medical Systems", Hortenas, Norvegija) [76]. Kadrų dažnis – nuo 50 iki 80 kadrų per sekundę. Sistolės pabaigos laikui nustatyti naudotas Doplerinės tėkmės KS išvarymo trakte laikas. Apskaičiavus vidurkį iš visų tinkamos kokybės segmentų vidutinių verčių, buvo gaunamas BID įvertis (17 segmentų modelis 2D STE). Segmentai su prastos kokybės signalais (nepaisant koregavimo rankiniu būdu) į analizę nebuvo įtraukti. Santykinai išsaugotos viršūnės deformacijos (SIVD) tipas apibrėžtas naudojant lygtį: (vidutinė viršūninių segmentų išilginė deformacija / (vidutinė bazinių segmentų išilginė deformacija + vidutinė vidurinių segmentų išilginė deformacija). Dėl trūkstamų duomenų arba prastos vaizdo kokybės STE tyrimas atliktas 77 iš 83 pacientų.

2.2.2.2 ŠMRT ir T1 žemėlapio analizė

ŠMRT vaizdai gauti naudojant standartinius „1.5 T Siemens Aera" skenavimo įrangos su paviršinėmis ritėmis ir retrospektyviąja elektrokardiografija (EKG) protokolus. KS tūriai, masė ir išstūmimo frakcija išmatuoti taikant komerciškai prieinamą programinę įrangą „suiteHEART®", naudojant 8 mm trumposios ašies pjūvius (0–2 mm tarpas) nuo atrioventrikulinio žiedo iki viršūnės. Matavimai indeksuoti kūno paviršiaus plotui m² (naudojant DuBois formulę).

VKMK vaizdai buvo gaunami praėjus 10–15 min. po gadobutrolio (0,2 mmol/kg) suleidimo į veną („Gadovist", „Bayer AG", Vokietija), sekos parametrai: pjūvio storis – 8 mm, atstumo faktorius – 0 % trumposios ir ilgosios ašies KS plokštumose. Miokardo fibrozės sritis apibrėžta kaip pikselių, kurių signalo intensyvumas viršija 5 standartinius nuokrypius nuo normalaus tolimojo miokardo. VKMK kokybiškai vertino du nepriklausomi tyrėjai, kurie neturėjo informacijos apie klinikinius pacientų duomenis.

Difuzinė miokardo fibrozė vertinta naudojant natyvinį ir pokontrastinį T1 žemėlapį skilvelio vidurinėje dalyje, trumposios ašies vaizduose, taikant modifikuotą „Look-Locker" inversijos atkūrimo („MOLLI") seką, esant judesio korekcijai (standartinis protokolas 3–3–5), prieš procedūrą ir praėjus 15 min. po kontrastinės medžiagos suleidimo [77]. Gauti T1 parametriniai žemėlapiai apdoroti naudojant komerciškai prieinamą programinę įrangą („NeoSoft suiteHEART"). Dominanti sritis (angl. ROI) rankiniu būdu pažymėta trumposios ašies vaizduose, natyvinio ir pokontrastinio T1 žemėlapiuose, pertvaros vidurinėje dalyje. Siekiant išvengti dalinio tūrio efektų, visi T1 matavimai atlikti viduriniame miokardo trečdalyje. Segmentai, kuriuose buvo nustatyta židinė fibrozė, nebuvo įtraukti į T1 žemėlapio analizę

[38]. Norint išmatuoti kraujo T1 vertę, KS ertmėje atidėtos apskritos dominančios sritys, vengiant papiliarinių raumenų. Tada apskaičiuotos natyvinio T1, ET% ir indeksuotos ET vertės. ET apskaičiuotas pagal formulę:

ET% = (ΔR1m/ΔR1b) × (1 – hematokritas) × 100,

kur R1 – 1/T1, R1m – R1 miokarde, R1b – R1 kraujyje, ΔR1 – pokytis atsipalaidavimo metu [78].

Hematokrito koncentracija buvo nustatoma ŠMRT atlikimo dieną. Dėl nepilnų duomenų rinkinių T1 žemėlapio parametrai išmatuoti 67 iš 83 pacientų.

2.2.2.3 Histologinė analizė

Chirurginio AVP metu biopsijos mėginiai buvo paimti iš bazinės priekinės pertvaros dalies, naudojant chirurginį skalpelį. Iš 71 paciento paimta po vieną intraoperacinį miokardo biopsijos mėginį (vidutinis plotas – 22,5±12 mm^2). Visi miokardo audinių mėginiai užfiksuoti naudojant 10 % neutralų buferinį formaliną ir įterpti į parafiną. Mėginių pjūviai (3 μm storio) supjaustyti naudojant mikrotomą „Leica RM2145" ir nudažyti hematoksilinu ir eozinu, Masono trichromu ir Kongo raudonuoju. Skaitmeniniai vaizdai užfiksuoti „Aperio Scan-Scope XT Slide Scanner" („Aperio Technologies", „Vista", Kalifornija, JAV), 20 kartų padidinti (skiriamoji geba – 0,5 μm). Mėginius analizavo histologai, neturintys duomenų apie klinikinių tyrimų ir ŠMRT rezultatus.

Miokardo dalis, kurią sudarė kolageno audinys (kolageno tūrio frakcija, KTF), nustatyta kiekybinės morfometrijos metodu, naudojant automatinės vaizdo analizės sistemą („HALOTM"). Miokardo fibrozės plotas apskaičiuotas naudojant „HALOTM Area Quantification v2.1.1" 1 algoritmą („IndicaLabs", Naujoji Meksika, JAV) [79]. Subendokardinis sluoksnis apibrėžtas kaip 1 mm nuo endokardo paviršiaus esantis sluoksnis, o likusi mėginio dalis apibrėžta kaip vidurinis miokardo sluoksnis.

2.3 Statistinė analizė

2.3.1 Metaanalizė

Statistinė analizė atlikta naudojant R programavimo kalbą ir statistinio skaičiavimo aplinką (3.5.1 versija) [80]. Taip pat naudotas „Metaphor" paketas (2.1-0 versija) [81]. Apskaičiuojant jungtinius įverčius, taikytas atsitiktinių efektų modelis su ribotos tikimybės įverčiu [82]. Siekiant pateikti bendrus analizės rezultatus, nubrėžtos blobogramos (angl. *forest plots*).

Poveikio heterogeniškumas vertintas naudojant I^2 vertę, atitinkamą testą ir piltuvo pavidalo grafikus (angl. *funnel plots*). Publikacijų šališkumo įtaka vertinta taikant linijinį Eggerio testą (statistiškai reikšminga, kai $p < 0,10$) [83]. Be to, atlikta 1 tyrimo pašalinimo analizė, siekiant identifikuoti potencialiai svarbius tyrimus, ir kaupiamoji metaanalizė, skirta tyrimų dinamikai suvokti. Skirtumai buvo laikomi statistiškai reikšmingi, kai dvipusė p reikšmė buvo < 0,05.

2.3.2 FIB-AS tyrimas

Kintamieji pateikti kaip vidurkis±standartinis nuokrypis arba mediana ir tarpkvartilio intervalai. Kategoriniai kintamieji išreikšti dažniais ir procentais, jie lyginti naudojant v2 testą. Dviem nuolatinių kintamųjų grupėms palyginti naudotas neporinis Stjudento t-testas bei Manno ir Whitney U testas. Siekiant įvertinti tolydžių kintamųjų ryšius, apskaičiuoti Pirsono (Pearson) ir Spirmeno (Spearman) koreliacijos koeficientai. Skirtumai tarp to paties stebėtojo kartotinių matavimų ir skirtingų stebėtojų matavimų analizuoti naudojant Blando ir Altmano metodą bei apskaičiuojant koreliacijos koeficientą. Statistinė analizė atlikta naudojant R programavimo kalbą (4.1.2 versija) [84]. Skirtumai buvo laikomi statistiškai reikšmingi, kai dvipusė p reikšmė buvo <0,05.

3. REZULTATAI

3.1 Metaanalizės rezultatai

Iš viso į metaanalizę įtraukta 19 tyrimų, kuriuose dalyvavo 2 032 pacientai [10, 11, 43, 45, 46, 52, 55, 85–96]. Daug tyrimų (n = 20) neįtraukta į analizę dėl galimo duomenų dubliavimosi. Šeši tyrimai [10, 11, 43, 45, 85, 86], kuriuose dalyvavo 1 300 pacientų, buvo įtraukti į mirtingumo nuo įvairių priežasčių galimybių santykio (ŠS) skaičiavimus. Viename iš tyrimų nebuvo duomenų apie kardiovaskulinį mirtingumą [85], todėl naudoti penkių tyrimų, kuriuose dalyvavo 1 246 pacientai, rezultatai. Galiausiai, šeši tyrimai (1 044 pacientai) įtraukti vertinant kiekybinį židininės miokardo fibrozės išplitimą KS miokarde [43, 45, 55, 85, 88, 90]. Visi 19 tyrimų analizuoti, siekiant įvertinti židininės fibrozės paplitimą.

Atrinkti tyrimai buvo perspektyviniai kohortiniai. Dauguma jų buvo vieno centro kohortiniai tyrimai, išskyrus du daugiacentrinius tyrimus [45, 96]. Vidutinė stebėjimo trukmė siekė 2,8 metų. Daugelyje tyrimų pacientams, sergantiems didelio laipsnio AS, buvo atliktas chirurginis AVP. Šešiuose tyrimuose analizuoti pacientų, kuriems taikytas TAVI, duomenys [43, 45, 52, 89, 90, 92].

Pacientų amžius svyravo nuo 47 iki 83 metų (vidurkis – 69,8), didžiąją tiriamųjų dalį sudarė vyrai. Dažniausiai diagnozuota gretutinė liga – hipertenzija (nustatyta 61,4 proc. pacientų). 39,8 proc. visų pacientų buvo diagnozuota reikšminga KŠL, į septynis tyrimus pacientai, kuriems nustatyta reikšminga KŠL, nebuvo įtraukti [46, 55, 85, 87, 93–95]. Dauguma pacientų turėjo išsaugotą KSIF (vidutiniškai 57 %), visuose tyrimuose dominavo aukšto gradiento AS (vidutinis AV slėgio gradientas – 46 mmHg).

Dauguma tyrėjų židininę fibrozę vertino pagal skirtingus signalo intensyvumo slenksčius [43, 55, 85–90, 94]. Trijuose tyrimuose taikytas pusės maksimumo viso pločio nustatymo metodas (angl. FWHM) [11, 45, 95], tik nedaugelyje tyrimų naudotas vizualinis vertinimas. AS sergančių pacientų kohortose židininės fibrozės paplitimas varijavo 27–90 proc. Iš viso židininė fibrozė nustatyta 944 pacientams (49,6 %). Devyniuose tyrimuose detalizuotas židininės fibrozės tipas [10, 11, 43, 45, 46, 55, 86, 87, 89]. Minėtina, kad daugiau negu pusei pacientų, sergančių AS, būdinga neinfarktinio tipo židininė fibrozė (63,6 %).

Atsižvelgiant į sergamumą KŠL, atlikta papildoma židininės fibrozės tipo ir paplitimo analizė. Palyginti su pacientais, kurių vainikinės arterijos nepažeistos, pacientams, sergantiems KŠL, nustatytas didesnis židininės
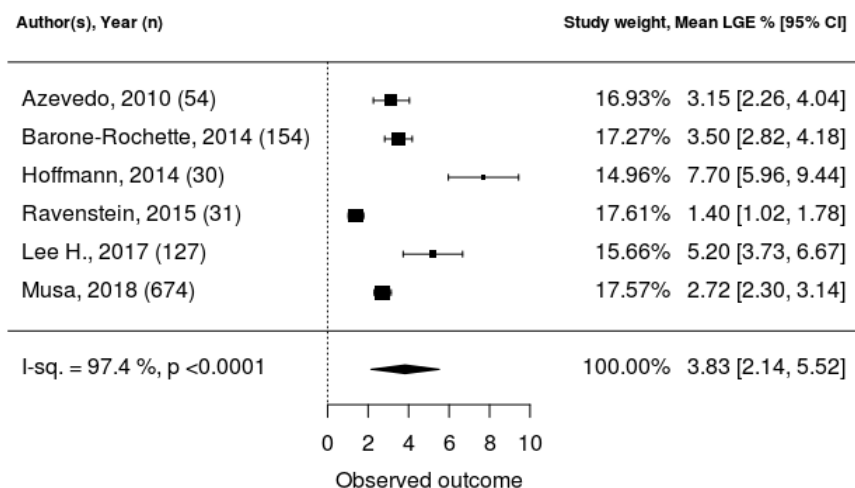
fibrozės paplitimas (atitinkamai 44,0 proc. ir 62,8 proc. tiriamųjų). Daugumai pacientų, nesergančių KŠL, diagnozuota neinfarktinio tipo židininė fibrozė (nustatyta 93,6 proc. tiriamųjų). Infarktinio tipo židininė fibrozė dominavo tarp pacientų, kuriems patvirtinta KŠL (nustatyta 54,6 proc. tiriamųjų) (žr. 1 lentelę).

1 lentelė. Židininės fibrozės paplitimas, atsižvelgiant į vainikinių arterijų ligą ir fibrozės tipą

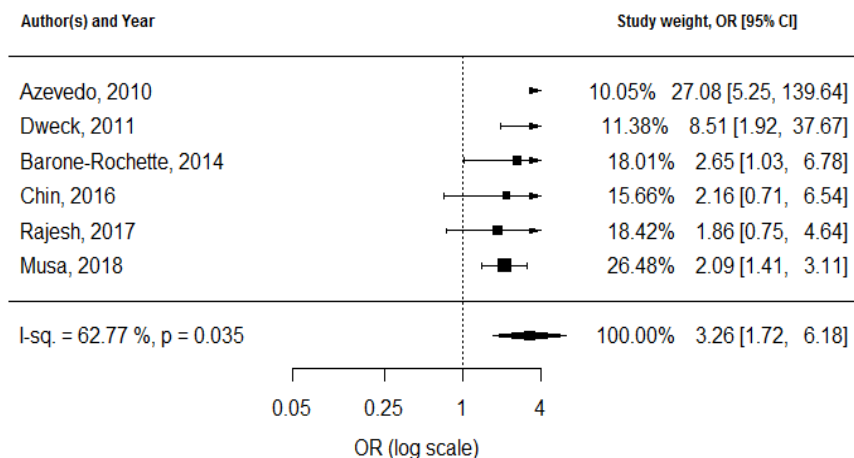| KŠL	Pacientų skaičius	VKMK (+), sk. (%)	Neinfarktinis VKMK, %
KŠL (–)	976	430 (44)	93,6 [$]
KŠL (+)[&]	400	251 (62,8)	45,4

Reikšmės yra n (%). ([&]) žymimi 5 tyrimų, kuriuose pateikti duomenys apie židininę fibrozę, atsižvelgiant į sergamumą KŠL, rezultatai. ([$]) žymimi 4 tyrimų, kuriuose pateikti duomenys apie pacientų, nesergančių KŠL, židininės fibrozės tipą, rezultatai. KŠL – koronarinė širdies liga, VKMK – vėlyvas kontrastinės medžiagos kaupimas.

Židininė fibrozė dažniau nustatoma vyrams, ypač tiems, kuriems pasireiškia sistolinė KS disfunkcija ir kurių funkcinė būklė (pgl. NYHA f.kl.) yra prastesnė. Be to, židininė fibrozė dažniau nustatoma pacientams, turintiems didesnę indeksuotą KS masę, kuriems būdingi didesni indeksuoti KS galiniai sistoliniai ir diastoliniai tūriai. 12 tyrimų duomenys atskleidė židininės fibrozės apimtį procentais, atsižvelgiant į KS masę, ji svyravo nuo 1,4 proc. iki 18,3 proc. [11, 43, 45, 52, 55, 85, 88–90, 94–96]. Suminis židininės fibrozės išplitimas miokarde siekė apie 4 proc. visos KS masės – 3,83 ([95 % PI], [2,14, 5,52]) (žr. 6 pav.).
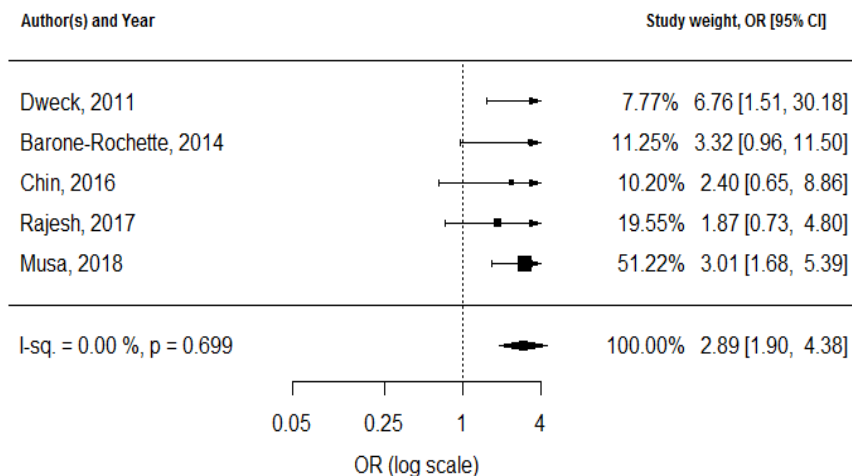
Author(s), Year (n)		Study weight, Mean LGE % [95% CI]
Azevedo, 2010 (54)		16.93% 3.15 [2.26, 4.04]
Barone-Rochette, 2014 (154)		17.27% 3.50 [2.82, 4.18]
Hoffmann, 2014 (30)		14.96% 7.70 [5.96, 9.44]
Ravenstein, 2015 (31)		17.61% 1.40 [1.02, 1.78]
Lee H., 2017 (127)		15.66% 5.20 [3.73, 6.67]
Musa, 2018 (674)		17.57% 2.72 [2.30, 3.14]
I-sq. = 97.4 %, p <0.0001		100.00% 3.83 [2.14, 5.52]

Observed outcome

6 pav. Kiekybiškai įvertintos židininės fibrozės išplitimas miokarde, išreikštas procentais nuo KS masės (židininės fibrozės apimtis – 3,83 proc. nuo visos KS masės)

Minėtina, kad dėl įvairių priežasčių mirė 247 pacientai (19 %). 169 iš jų buvo nustatyta židininė fibrozė (28 proc. pacientų, kuriems nustatyta židininė fibrozė). Židininė fibrozė buvo susijusi su statistiškai reikšmingai didesniu mirtingumu dėl įvairių priežasčių (bendras GS [95 % PI] = 3,26 [1,72, 6,18], p = 0,0003) (7 pav.).

Author(s) and Year		Study weight, OR [95% CI]
Azevedo, 2010		10.05% 27.08 [5.25, 139.64]
Dweck, 2011		11.38% 8.51 [1.92, 37.67]
Barone-Rochette, 2014		18.01% 2.65 [1.03, 6.78]
Chin, 2016		15.66% 2.16 [0.71, 6.54]
Rajesh, 2017		18.42% 1.86 [0.75, 4.64]
Musa, 2018		26.48% 2.09 [1.41, 3.11]
I-sq. = 62.77 %, p = 0.035		100.00% 3.26 [1.72, 6.18]

OR (log scale)

7 pav. Blobograma (angl. *forest plot*) ir mirtingumo nuo visų priežasčių galimybių santykis (GS) (apskaičiuotas bendras GS = 3,26)

136 pacientai mirė dėl kardiovaskulinių priežasčių (10,9 %). 99 iš jų nustatyta židininė fibrozė (7,9 proc. visų pacientų, kuriems nustatyta židininė fibrozė). Židininė fibrozė buvo susijusi su statistiškai reikšmingai didesniu mirtingumu dėl kardiovaskulinių priežasčių (bendras GS [95 % PI] = 2,89 [1,90, 4,38], p < 0,0001) (8 pav.).

Author(s) and Year		Study weight, OR [95% CI]
Dweck, 2011		7.77% 6.76 [1.51, 30.18]
Barone-Rochette, 2014		11.25% 3.32 [0.96, 11.50]
Chin, 2016		10.20% 2.40 [0.65, 8.86]
Rajesh, 2017		19.55% 1.87 [0.73, 4.80]
Musa, 2018		51.22% 3.01 [1.68, 5.39]
I-sq. = 0.00 %, p = 0.699		100.00% 2.89 [1.90, 4.38]

OR (log scale)
0.05   0.25   1   4

8 pav. Blobograma (angl. *forest plot*) ir mirtingumo nuo kardiovaskulinių priežasčių galimybių santykis (GS) (apskaičiuotas bendras GS = 2,89).

Dviejuose tyrimuose analizuota kiekybiškai įvertintos židininės fibrozės įtaka prognozei [11, 45]. Dweckas ir bendraautoriai [11] nustatė, kad, židininės fibrozės kiekiui padidėjus 1 %, mirtingumo rizika išauga 5 % (HR 1,05; 95 % PI: 1,01–1,09; p = 0,005). Panašūs rezultatai pateikiami ir Musos ir kt. tyrime [45] – nustatyta, kad židininės fibrozės padidėjimas 1 % sąlygoja 11 % didesnę mirtingumo nuo visų priežasčių (HR 1,11; 95 % PI: 1,05–1,17; p < 0,001) ir 8 % didesnę kardiovaskulinio mirtingumo (HR 1,08; 95 % PI: 1,01–1,17; p < 0,001) riziką.

Taip pat buvo surinkti duomenys apie mirtingumo nuo įvairių priežasčių prognostinius rodiklius. Tyrimų metu identifikuoti šie nepriklausomi veiksniai, susiję su mirtingumu nuo įvairių priežasčių: amžius, KSIF, NYHA funkcinė klasė ir VKMK (tiek infarktinio, tiek neinfarktinio tipo). Trijų tyrimų rezultatai patvirtino reikšmingą prastos pacientų funkcinės būklės (NYHA f.kl.) ir mirtingumo nuo įvairių priežasčių ryšį [43, 45, 86].

Taigi metaanalizė atskleidė, kad židininė miokardo fibrozė buvo nustatyta beveik pusei pacientų, sergančių AS (49,7 %). Taip pat nustatytas

reikšmingas židininės fibrozės ryšys su klinikinėmis baigtimis – pacientų, kuriems nustatyta židininė fibrozė, mirtingumas nuo įvairių priežasčių ir kardiovaskulinis mirtingumas padidėjo tris kartus (bendras GS atitinkamai: 3,26 ir 2,89).

3.2 Parametrinio vaizdinimo norminių reikšmių nustatymas

2019–2021 m. VUL Santaros klinikose atlikta 30 MRT tyrimų sveikiems, širdies ir kraujagyslių ligomis nesergantiems asmenims (43 proc. vyrų, amžiaus vidurkis – 35±10 metų). Mūsų centro norminių natyvinio T1 ir ET reikšmių intervalai pateikti 2 lentelėje. Minėtina, kad VUL Santaros klinikose nustatytų parametrinio ŠMRT žemėlapio norminių reikšmių intervalai artimi T1 ir ET reikšmėms, kurios gautos kituose centruose, ištyrus mažiausiai 30 sveikų asmenų grupę, naudojant 1,5 T magnetinio rezonanso įrangą. Metodines ŠMRT parametrinio vaizdinimo rekomendacijas, kuriose pateikiami ŠMRT parametrinio vaizdinimo fizikiniai principai, indikacijos ir klinikinis pritaikymas, taip pat mūsų centro pradinė klinikinė patirtis, naudojant šį metodą, 2020 m. pristatė prof. S. Glaveckaitės vadovaujama komanda.

2 lentelė. Norminės miokardo natyvinio T1 ir ET reikšmės (vidurkis±standartinis nuokrypis)

Kintamieji	Visi tiriamieji (n = 30)	Moterys (n = 17)	Vyrai (n = 13)
Natyvinis T1, ms	956±59	931±38	978±67
Ekstraląstelinis tūris, %	24±3	22±1	26±3

3.3 FIB-AS tyrimo rezultatai

3.3.1 Matavimų atkartojamumo analizė

Dvidešimčiai atsitiktinai atrinktų pacientų buvo atlikta BID ir ŠMRT T1 žemėlapio rodiklių matavimų atkartojamumo analizė. Tiek BID, tiek ŠMRT T1 žemėlapio matavimai parodė puikų atkartojamumą tiek tarp to paties tyrėjo kartotinių matavimų, tiek tarp skirtingų tyrėjų matavimų. Atkartojamumo analizės rezultatai pateikiami **3** lentelėje.

3 lentelė. Atkartojamumo analizės rezultatai.

	Koreliacijos koeficientas	95 % PI	Paklaida
Matavimų atkartojamumas tarp skirtingų tyrėjų			
Natyvinis T1	0,958	0,91–0,98	9,1±15,1
Pokontrastinis T1	0,973	0,94–0,99	0,8±9,2
T2	0,968	0,93–0,99	0,2±1,3
BID	0,981	0,96–0,99	1,5±1
Vieno tyrėjo matavimų atkartojamumas			
Natyvinis T1	0,945	0,88–0,97	3,3±11,0
Pokontrastinis T1	0,987	0,9–0,99	0,95±7,53
T2	0,983	0,96–0,99	0,59±0,84
BID	0,969	0,93–0,98	0,51±1,3

BID – bendra išilginė deformacija, PI – pasikliautinasis intervalas.

3.3.2 Pacientų kohortos aprašymas

Iš viso tyrime dalyvavo 83 pacientai (66,4±8,3 m. amžiaus, 58 proc. moterų, AVA indeksas – 0,44±0,1 cm^2/m^2, maksimalus greitis per AV – 4,8±0,6 m/s, vidutinis AV gradientas – 57,8±16 mmHg). Pagrindinės priežastys, dėl kurių pacientai nebuvo įtraukti į tyrimą: reikšminga KŠL, inkstų funkcijos nepakankamumas ir kitos reikšmingos vožtuvų ydos. Vidutinis nustatytas KSIF – 66,8±13 %, 10 proc. pacientų diagnozuota sumažėjusi KSIF (<50 %). Daugumai pacientų nustatyta maža chirurginė rizika, nes Krūtinės ląstos chirurgų draugijos operacinės rizikos vertinimo skaičiuoklės (STS-PROM) ir II Europos širdies operacinės rizikos vertinimo skaičiuoklės (EuroSCORE II) rezultatai buvo <2 proc. (atitinkamai 1,9 proc. ir 1,5 proc.). Pacientai, sergantys įgimta AS, dažniau buvo jaunesni (p < 0,001), jiems nustatyta mažesnė chirurginės intervencijos rizika (p = 0,004), taip pat jų inkstų funkcija buvo geresnė (p = 0,002). Iš 83 į tyrimą įtrauktų pacientų 79 pacientams atliktas chirurginis AVP. Keturi pacientai operacijos atsisakė. Be AVP, 4 proc. pacientų atlikta krūtininės aortos operacija. Pacientų klinikiniai ir širdies vaizdinimo tyrimų rezultatai apibendrinami 4 ir 5 lentelėse.

4 lentelė. Visos tyrime dalyvaujančios grupės ir pacientų, kuriems nustatyta židininė fibrozė ir židininė fibrozė nenustatyta, klinikinių duomenų ir kraujo tyrimų rezultatų palyginimas

Parametrai	Visi pacientai (n = 83)	Pacientai, kuriems nustatyta židininė MRT fibrozė (n = 61)	Pacientai, kuriems nenustatyta židininė MRT fibrozė (n = 22)	p reikšmė
Amžius, m	66,4±8,3	65,8±8,3	68,3±8,3	0,235
Vyriškoji lytis	35 (42 %)	29 (48 %)	6 (27 %)	0,162
KMI, kg/m^2	30±5,8	30,4±5,6	28,7±6	0,245
KPP m^2	1,9±0,2	2,0±0,2	1,8±0,2	**0,011**
Sistolinis AKS, mmHg	150±25	148±25	156±23	0,223
Diastolinis AKS, mmHg	85±11	84±12	85±11	0,842
Gretutinės ligos				
Hipertenzija	73 (88 %)	55 (90 %)	19 (86 %)	0,732
Dislipidemija	66 (80 %)	48 (79 %)	19 (86 %)	0,640
Neobstrukcinė KŠL	39 (47 %)	30 (49 %)	9 (41 %)	0,677
Cukrinis diabetas	14 (17 %)	10 (16 %)	5 (22 %)	0,735
Prieširdžių virpėjimas	6 (7 %)	5 (8 %)	1 (5 %)	0,931
PKI anamnezėje	1 (1 %)	1 (2 %)	–	1,000
Simptomai ir funkcinė būklė				
Dusulys	61 (74 %)	46 (75 %)	15 (68 %)	0,706
Krūtinės angina	41 (49 %)	30 (49 %)	11 (50 %)	1,000
Sinkopė	9 (11 %)	9 (15 %)	–	0,131
NYHA f. kl.				0,591[*]
I	16 (19 %)	11 (18 %)	5 (23 %)	
II	24 (29 %)	19 (31 %)	5 (23 %)	
III	40 (48 %)	28 (46 %)	12 (54 %)	
IV	3 (4 %)	3 (5 %)	–	
6 MĖT, m	357,6±105,6	352±108	372±101	0,459
MLHFQ skalė	35±20,4	36±20	31±22	0,277
Vaistų vartojimas				
AKFI/ARB	61 (74 %)	43 (71 %)	18 (82 %)	0,453
Betablokatoriai	57 (69 %)	42 (69 %)	15 (68 %)	1,000
Statinai	54 (65 %)	40 (66 %)	14 (64 %)	1,000

Kilpiniai diuretikai	15 (18 %)	11 (18 %)	4 (18 %)	1,000
Spironolaktonas	22 (27 %)	14 (23 %)	8 (36 %)	0,347
Rizikos skalės				
STS-PROM, %	1,9 (1,2–2,3)	1,6 (1–2,2)	1,75 (1,4–2,4)	0,415
EuroSCORE II, %	1,5 (0,7–1,6)	1 (0,7–1,7)	1,2 (0,8–1,5)	0,415
AV protezavimas (n = 79)				
Biologinis protezas	70 (89 %)	55 (90 %)	15 (83 %)	**0,037**
Mechaninis protezas	9 (11 %)	6 (10 %)	3 (17 %)	0,927
Aortos chirurgija	3 (4 %)	1 (2 %)	2 (11 %)	0,348
Vožtuvo morfologija				
Triburis	54 (65 %)	41 (67 %)	13 (59 %)	0,671
Dviburis	28 (34 %)	19 (31 %)	9 (41 %)	0,429
Vienburis	1 (1%)	1 (2 %)	–	1,000
Kraujo tyrimai				
Kreatininas, μmol/l	76,2±16,3	77±17	73,9±16	0,447
eGFG, ml/min/1,73 m^2	78,6 (69–90)	85 (69–90)	86 (69–90)	0,996
Tn-I, pg/l	10 (5–19)	13,5 (6–29)	5,3 (5–9)	**0,003**
BNP, pg/l	122 (65–340)	167 (77–511)	74 (43–145)	**0,004**
EKG rodikliai				
ŠSD, k/min	77±12,4	78±12	76±13	0,519
S-L indeksas (mm)	30,8±10	31,7±10	28,4±10	0,189
QRS, ms	96,8 (88–102)	94 (88–102)	92 (85–101)	0,449

Tolydūs kintamieji pateikti nurodant vidurkius ± SD arba medianas (interkvartilinį skirtumą). Diskretūs kintamieji išreikšti n (%). Paryškintos statistiškai reikšmingus skirtumus žyminčios p reikšmės.

AKFI – angiotenziną konvertuojančio fermento inhibitoriai, ARB – angiotenzino receptorių blokatoriai, AKS – arterinis kraujospūdis, AV – aortos vožtuvas, BNP – smegenų natriuretinis peptidas, EKG – elektrokardiograma, eGFG – apskaičiuotas glomerulų filtracijos greitis, KMI – kūno masės indeksas, KPP – kūno paviršiaus plotas, KŠL – koronarinė širdies liga, 6MĖT – 6 min. ėjimo testas, MLHFQ – Minesotos gyvenimo, sergant širdies nepakankamumu, klausimynas, NYHA – Niujorko širdies asociacija, MRT – magnetinio rezonanso tomografija, PKI – perkutaninė koronarinė intervencija, S-L – Sokolovo ir Lyono indeksas, ŠSD – širdies susitraukimų dažnis, Tn-I – troponinas I.

* – NYHA I ir II *vs.* III ir IV funkcinės klasės palyginimo reikšmė.

5 lentelė. Visos tyrime dalyvaujančios grupės ir pacientų, kuriems nustatyta židininė fibrozė ir židininė fibrozė nenustatyta, širdies vaizdinimo ir histologinių duomenų rezultatų palyginimas

	Visi pacientai (n = 83)	Pacientai, kuriems nustatyta židininė fibrozė (n = 61)	Pacientai, kuriems nenustatyta židininė fibrozė (n = 22)	p reikšmė
Echokardiografijos duomenys				
Greitis per AV, m/s	4,8±0,6	4,9±0,6	4,6±0,5	0,074
Vidutinis gradientas per AV, mmHg	57,8±16	59,8±17	52,4±14	0,071
Sumažinto gradiento AS	10 (12 %)	6 (10 %)	4 (18 %)	0,422
AVA, cm^2	0,84±0,2	0,83±0,2	0,88±0,2	0,364
AVA indeksas, cm^2/m^2	0,44±0,1	0,43±0,1	0,49±0,1	**0,018**
TSPd, mm	12,7±1,7	13,1±1,5	11,5±1,5	**<0,001**
KSUSd, mm	11,5±1,4	11,9±1,3	10,3±1,2	**<0,001**
KSdd, mm	51,4±5,4	52,1±5,4	49,3±4,9	**0,034**
KSsd, mm	32,7±5,9	33,1±6,1	31,7±5,6	0,362
E/A	1,1±0,5	1,1±0,5	1,2±0,3	0,615
E bangos deceleracijos laikas, ms	259±70	257±69	262±74	0,813
E/e' septalinis	17,6±7	17,9±6,3	16,8±9,5	0,619
E/e' lateralinis	14,5±6	15±6,5	13,2±5,8	0,276
E/e' vidutinis	15,6±6	16±5,9	14,3±5,7	0,254
KP tūrio indeksas, ml/m^2	47,9±12	49,2±12	44,7±12	0,129
PA sistolinis slėgis, mmHg	38±15	40,5±15	33,6±12	0,175
DS S', cm/s	11,6±3	11,4±3	12±2	0,377
TAPSE, mm	21,7±3	21,7±4	21,8±3	0,924
BID, %*	−18±5	−17,5±4,8	−19,4±5,3	0,147
MRT duomenys				
TSPd, mm	13,3±2	13,6±2	12,6±2	0,062
KSdd, mm	50,6±6	51±6	49,3±6	0,264
KSsd, mm	33,8±8	34,2±8	33±9	0,561
KSGD tūris, ml	144,3±44	149,7±44	130±44	0,079
KSGS tūris, ml	51 (28–61)	46 (31–69)	29 (24–45)	0,106

KS smūginio tūrio indeksas, ml/m^2	48±11	48,3±10	48,4±11	0,982
KSIF, %	66,8±13	65,3±13	70,8±12	0,088
KSIF <50 %	9 (11 %)	8 (13 %)	1 (5 %)	0,427
KS masės indeksas, g/m^2	97,6±32	103,4±32	82,6±29	**0,009**
DSGD tūris, ml	125,3±31	129,5±31	114,2±31	0,052
DSGS tūris, ml	49,3±18	49,7±19	48,3±17	0,747
DSIF, %	60,8±10	61,9±10	58±8	0,111
Natyvinis T1, ms[#]	959,7±34	961,8±31	952,5±43	0,359
Pokontrastinis T1, ms[#]	351 (326–362)	361 (325–376)	350 (326–358)	0,415
Ekstraląstelinis tūris, %[#]	22,7±3,6	23,4±3,7	22,2±3,5	0,541
Ekstraląstelinio tūrio indeksas, %/m^2	11,8±2	12,3±2	11,3±2	0,271
Histologijos duomenys (n = 71)				
KTF, %[&]	15,1 (9–21)	15,9 (9–19)	12,4 (9–24)	0,887
KTF subendokardinė, %[&]	21,1 (12–29)	28,7 % (19–33)	20,7 % (15–30)	**0,040**

Tolydūs kintamieji pateikti nurodant vidurkius ± SD arba medianas (interkvartilinį skirtumą). Diskretūs kintamieji išreikšti n (%). Paryškintos statistiškai reikšmingus skirtumus žyminčios p reikšmės.

AKS – arterinis kraujospūdis, AS – aortos stenozė, AV – aortos vožtuvas, AVA – aortos vožtuvo anga, BID – bendra išilginė deformacija, DSIF – dešiniojo skilvelio išstūmimo frakcija, DSGD – dešiniojo skilvelio galinis diastolinis, DSGS – dešiniojo skilvelio galinis sistolinis, DS S' – dešiniojo skilvelio sistolinės bangos greitis, EKG – elektrokardiograma, 6MĖT – 6 min. ėjimo testas, KP – kairysis prieširdis, KS – kairysis skilvelis, KSdd – kairiojo skilvelio diastolinis diametras, KSIF – kairiojo skilvelio išstūmimo frakcija, KSGD – kairiojo skilvelio galinis diastolinis, KSGS – kairiojo skilvelio galinis sistolinis, KSsd – kairiojo skilvelio sistolinis diametras, KŠL – koronarinė širdies liga, KTF – kolageno tūrio frakcija, KSUSd – kairiojo skilvelio užpakalinė sienelė diastolėje, MLHFQ – Minesotos gyvenimo, sergant širdies nepakankamumu, klausimynas, MRT – magnetinio rezonanso tomografija, NYHA – Niujorko širdies asociacija, PA – plaučių arterija, S-L – Sokolovo ir Lyono voltažo kriterijus, ŠSD – širdies susitraukimų dažnis, TAPSE – triburio vožtuvo žiedo amplitudė sistolėje, TSPd – tarpskilvelinė pertvara diastolėje.

* – reikšmė, išmatuota 77 pacientams; # – reikšmė, išmatuota 67 pacientams; & – reikšmė, išmatuota 71 pacientui.

3.3.3 Histologinės analizės rezultatai

Iš viso paimta 71 miokardo biopsija. Vienos pacientės duomenys neįtraukti į analizę dėl atsitiktinai nustatyto toksoplazminio miokardito. KTF svyravo nuo 2,06 proc. iki 41,30 proc., KTF mediana – 15,1 proc. (8,6–21). Pacientai, kuriems nustatytas didesnis KTF rodiklis, dažniau sirgo hipertenzija (p = 0,024) ir dislipidemija (p = 0,036). Pacientams, kuriems, atliekant ŠMRT, nustatyta židininė fibrozė, nustatytos ir didesnės KTF reikšmės negu pacientams, kuriems židininė fibrozė nenustatyta: atitinkamai 28,7 proc. (19–33) ir 20,7 proc. (15–30) (p = 0,040). Reikšmingų KTF medianos skirtumų tarp pacientų, sergančių neobstrukcine KŠL ir šia liga nesergančių, nenustatyta (atitinkamai 17,2 % (10–23) ir 13,4 % (9–19); p = 0,094]. Segmentinė miokardo biopsijų analizė parodė, kad subendokardinis miokardo sluoksnis yra labiau pažeistas fibrozės negu vidurinis miokardo sluoksnis (21,1 % (12–29) ir 8 % (5–12); p < 0,001).

Apibendrinant rezultatus galima teigti, kad fibrozės kiekis miokardo mėginiuose svyravo labai plačiai – nuo 2 proc. iki 41 proc. (vidutiniškai apėmė 15 proc. bioptato). Reikšmingai didesnis fibrozės kiekis aptiktas subendokardiniame sluoksnyje, palyginti su gilesniais miokardo sluoksniais, taip pat daugiau fibrozės nustatyta tiems pacientams, kuriems atliekant ŠMRT nustatyta ir židininė fibrozė.

3.3.4 ŠMRT metodu nustatyta miokardo fibrozė

Vidutinis laiko intervalas tarp ŠMRT ir operacijos buvo 53,3 dienos (17–78). Vidutinė natyvinio T1 reikšmė – 959,7±34 ms (intervalas – 897–1044 ms), vidutinė ET reikšmė – 22,7±3,6 % (intervalas – 15,7–34,4 %). Vidutinių natyvinio T1 ir ET reikšmių reikšmingo skirtumo tarp vyrų ir moterų nepastebėta (atitinkamai 962±29 ms ir 957±37 ms (p = 0,391), 22,9±3 % ir 22,6±4 % (p = 0,821).

Norint palyginti natyvines T1 reikšmes su klinikiniais ir struktūriniais KS parametrais, kintamieji suskirstyti į esančius virš medianos ir žemiau jos – 957 ms (6 lentelė). Minėtina, kad pacientams, kuriems nustatytas padidėjęs natyvinis T1, nustatytas mažesnis sistolinis kraujospūdis (p = 0,006), didesnis QRS voltažas (p = 0,036), didesni sistoliniai (p = 0,009) ir diastoliniai KS matmenys (p = 0,049), didesnis KS masės indeksas (p = 0,021). Didesnei daliai pacientų, kuriems nustatytas padidėjęs natyvinis T1, nustatyta ir sumažėjusi BID (atitinkamai 18 % ir 6 %; p = 0,049).

6 lentelė. Pacientų klinikiniai duomenys, širdies vaizdinių tyrimų, histologinės analizės ir kraujo tyrimų rezultatai, suskirstyti pagal BID ir natyvinio T1 medianas

Parametrai	BID ≥ –18,5 % (n = 40)	BID < –18,5 % (n = 37)	p reikšmė	Natyvinis T1 ≥957 ms (n = 34)	Natyvinis T1 <957 ms (n = 33)	p reikšmė
Amžius, m	66±8	68±8	0,256	65,8±9	66±9	0,917
Vyriškoji lytis	18 (45%)	14 (38%)	0,548	15 (44%)	11 (33%)	0,446
KPP, m^2	1,98±0,2	1,86±0,2	**0,004**	1,96±0,16	1,93±0,19	0,607
Sistolinis AKS, mmHg	143±23	158±23	**0,005**	139±21	156±26	**0,006**
Diastolinis AKS, mmHg	83±11	85±11	0,485	82±10	86±13	0,203
Neobstrukcinė KŠL	20 (50 %)	18 (49 %)	1,0	20 (59 %)	14 (42 %)	0,893
Hipertenzija	36 (90 %)	33 (89 %)	0,447	27 (79 %)	33 (100 %)	0,109
Cukrinis diabetas	8 (20 %)	4 (11 %)	0,768	6 (18 %)	7 (21 %)	1,0
NYHA f. kl. ≥3	26 (65 %)	14 (38 %)	0,085	16 (47 %)	15 (46 %)	0,749
MLHFQ skalė	37±20	32±20	0,257	37±21	36±20	0,839
6MĖT, m	351±105	358±104	0,767	367±106	352±94	0,558
EKG						
ŠSD, k/min	80±14	75±11	0,100	78±4	77±12	0,742
QRS, ms	95 (90–102)	90 (86–98)	0,105	94 (89–102)	90 (84–101)	0,313
S-L indeksas, mm	34±11	28±8,5	**0,011**	34±10	29±9	**0,036**
Echokardiografijos duomenys						
AVA indeksas, cm^2/m^2	0,42±0,1	0,47±0,08	**0,018**	0,4±0,1	0,45±0,1	0,075
Greitis per AV, m/s	5,0±0,7	4,7±0,5	0,055	5,0±0,6	4,8±0,6	0,105

Vidutinis gradientas per AV, mmHg	63±17,7	53±13,2	**0,004**	64±16	57±15	0,052
TSPd, mm	13,3±1,8	12,2±1,4	**0,009**	13±1,9	12,6±1,6	0,368
KSdd, mm	53,7±12	48,8±4,7	**0,002**	53±5	50±5	**0,049**
KSsd, mm	35,4±6	29,6±4	**<0,001**	35±6	32±6	0,057
E bangos deceleracijos laikas, ms	254±76	264±67	0,542	252±68	266±75	0,759
E/e' septalinis	17,1 (14–22)	14 (11,7–18)	**0,011**	16,5 (12,8–18)	16 (12–20)	0,845
E/e' vidutinis	17,4±6,9	14,2±4,4	**0,021**	15±5	16±7	0,909
KP tūrio indeksas, ml/m^2	53±12	44±11	**0,002**	48±9	48±15	0,473
PA sistolinis slėgis, mmHg	43,5±18	32,9±7	**0,031**	41±17	37±12	0,947
BID, %	14,3±3,9	21,7±2,7	**<0,001**	16,7±5,6	18,2±4	0,120
BID >–15 %	16 (40 %)	–	**<0,001**	10 (29 %)	4 (12 %)	**0,049**
MRT duomenys						
TSPd, mm	14±2	12,6±2	**0,005**	14±1,6	13±2,3	0,364
KSdd, mm	53±7	48,3±5	**<0,001**	52±6	50±5	0,074
KSsd, mm	37±9	30,6±6	**<0,001**	36,5±7	32±6	**0,009**
KSGD tūris, ml	160,7±48	126±35	**<0,001**	153±40	143±44	0,201
KSGS tūris, ml	56,9 (41–77)	29 (24–41)	**<0,001**	52 (37–72)	41 (28–53)	0,083
KSIF, %	59±14	74±7	**<0,001**	62,4±14	68±12	0,053
KSIF <50 %	8 (20 %)	0	**0,009**	6 (18 %)	2 (6 %)	0,541
KS masės indeksas, g/m^2	113±33	80,6±24	**<0,001**	109±31	91±30	**0,021**
VKMK dažnis	34 (85 %)	23 (62 %)	0,058	27 (79 %)	25 (76 %)	0,802

Natyvinis T1, ms	967±31	950±37	0,066	987±26	936±18	**<0,001**
Pokontrastinis T1, ms	349 (326–354)	355 (332–366)	0,201	352 (328–362)	348 (318–362)	0,445
Ekstraląstelinis tūris, %	22,3±4	22,9±2,4	0,456	23±3,2	22±3,9	0,243
Histologijos duomenys						
KTF, %	17,2 (10–22)	13,5 (8–20)	0,279	18,1 (8–24)	13,4 (10–21)	0,564
KTF subendokardinė,%	23,4 (13–33)	18,4 (11–27)	0,199	22,3 (9–28)	18,8 (12–26)	0,855
Serumo žymenys						
BNP, pg/l	252 (98–813)	79 (59–173)	**0,001**	163 (73–581)	120 (62–260)	0,413
Tn-I, pg/l	15 (7,5–29)	6,9 (5–12,9)	**0,002**	14 (7–27)	7,5 (5–16)	0,089

Tolydūs kintamieji pateikti nurodant vidurkius ± SD arba medianas (interkvartilinį skirtumą). Diskretūs kintamieji išreikšti n (%). Paryškintos statistiškai reikšmingus skirtumus žyminčios p reikšmės. Sutrumpinimus žr. 4 ir 5 lentelėse.

Kaip matyti iš ŠMRT rezultatų, židininė fibrozė buvo aptinkama pakankamai dažnai – ji nustatyta net 74 proc. visų tirtų pacientų (83 proc. vyrų ir 67 proc. moterų). Nors židininė fibrozė buvo dažnas radinys, jos išplitimas miokarde dažniausiai buvo apribotas iki 1 arba 2 KS segmentų, vidutiniškai – 2,5 segmento vienam pacientui.

92 proc. atvejų židininė fibrozė buvo neinfarktinio tipo (89 proc. – vidurio miokardo, 3 proc. – subepikardinio sluoksnio). Nors į tyrimą įtraukti pacientai nesirgo obstrukcine KŠL, 8 proc. jų buvo nustatyta infarktinio tipo židininė fibrozė. Dažniausiai židininė fibrozė buvo nustatoma dešiniojo ir kairiojo skilvelių jungties taškuose (68 %). Židininė fibrozė taip pat buvo aptinkama šoninėje (11 %), pertvarinėje (8 %), užpakalinėje (6 %) ir apatinėje (6 %) sienelėse, rečiausiai – KS viršūnėje (1 %). Reikšmingo židininės fibrozės paplitimo skirtumo tarp pacientų, sergančių neobstrukcine KŠL ir šia liga nesergančių, tyrimo metu nenustatyta (atitinkamai 77 % ir 70 %; p = 0,67).

Pacientai, kuriems nustatyta židininė fibrozė, sirgo labiau pažengusia AS, t. y. jiems apskaičiuotas mažesnis AVA indeksas (p = 0,018). Šiems pacientams taip pat nustatyta labiau išreikšta KS remodeliacija: didesnis KS sienelės storis (p < 0,001), didesnis KS diastolinis skersmuo (p = 0,034) ir didesnis KS masės indeksas (p = 0,009). Pacientams, kuriems buvo aptikta židininė fibrozė, taip pat nustatytos didesnės BNP (p = 0,004) ir Dj-trop I (p = 0,003) koncentracijos.

Taigi gauti rezultatai rodo, kad neinfarktinio tipo židininė fibrozė yra labai paplitusi tarp pacientų, sergančių didelio laipsnio AS. Pacientams, kuriems nustatyta židininė ir difuzinė fibrozė, būdinga labiau išreikšta KS remodeliacija, KS diastolinės ir sistolinės disfunkcijos požymiai ir didesnės serumo širdies nepakankamumo ir miokardo pažeidimo biožymenų koncentracijos. Pacientų, kuriems nustatyta židininė fibrozė ir kuriems židininė fibrozė nenustatyta, klinikinių ir širdies vaizdinimo tyrimų rezultatai apibendrinti 4 ir 5 lentelėse.

3.3.5 BID analizė

Vidutinė BID buvo –18±5 % (intervalas – nuo –3 % iki –31 %). BID sumažėjimas >–20 % nustatytas 61 proc. pacientų. Siekiant analizuoti BID, atsižvelgiant į klinikinius duomenis ir struktūrinius KS parametrus, kintamieji suskirstyti į grupes (aukščiau ir žemiau BID medianos: –18,5 %; žr. 6 lentelę). Pacientai, kuriems nustatyta sumažėjusi BID, sirgo labiau išreikšta AS; tai

spręstina iš šiems pacientams nustatyto mažesnio AVA indekso (p = 0,018) ir
didesnio vidutinio AV gradiento (p = 0,004). Minėtiems pacientams taip pat
nustatytas mažesnis sistolinis kraujospūdis (p = 0,005) ir didesnis QRS
voltažas (p = 0,011). Pacientams, kuriems nustatyta sumažėjusi BID, taip pat
būdingos storesnės KS sienelės (p = 0,009), didesni KS tūriai (p < 0,001),
didesnis KS masės indeksas (p < 0,001), mažesnė KSIF (p < 0,001). Šios
tiriamosios grupės pacientams nustatyti ir padidėjusio KS prisipildymo slėgio
požymiai: apskaičiuotas didesnis E/e' santykis (p = 0,011), didesnis kairiojo
prieširdžio (KP) tūrio indeksas (p = 0,002), menamas sistolinis slėgis plaučių
arterijoje (p = 0,031). Minėtina, kad šiems pacientams nustatytos didesnės
BNP (p = 0,001) ir Dj-trop I (p = 0,002) koncentracijos.

Tirta galimybė pagal BID vertę nustatyti padidėjusią histologinę
miokardo fibrozę. Šiam tikslui realizuoti atlikta gavėjų veiklos charakteristikų
kreivių (angl. *Receiver operating characteristic*, ROC) analizė. BID > –14 %
(jautrumas – 33 proc., specifiškumas – 94 proc.) gali padėti nustatyti didesnę
negu vidutinę miokardo fibrozę: plotas po kreive – 0,65, 95 % PI [0,51–0,78],
p = 0,034.
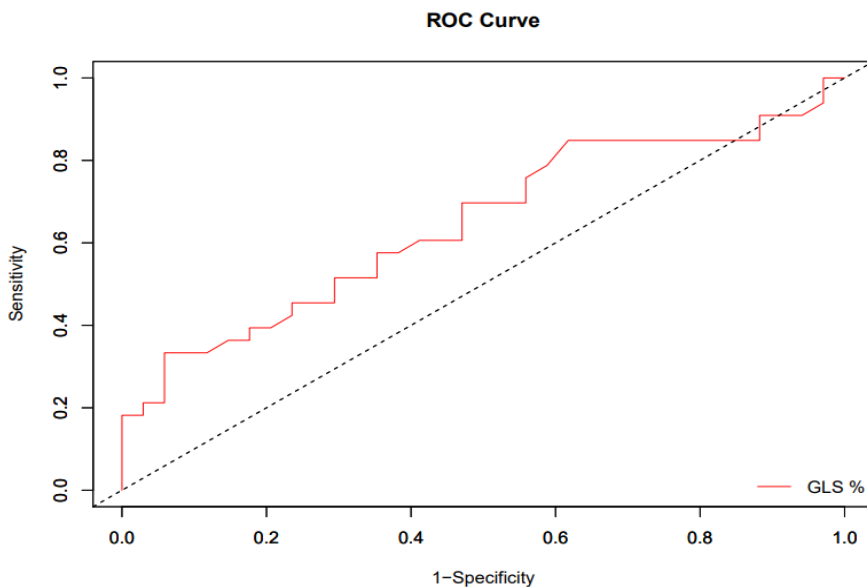
9 pav. ROC kreivė rodo bendrosios išilginės deformacijos (BID) gebėjimą
prognozuoti padidėjusią miokardo fibrozę, nustatomą histologinės analizės
metu (kolageno tūrio frakcijos padidėjimas virš medianos)

Be to, papildomai buvo palyginti širdies vaizdinimo tyrimų rodikliai tarp
pacientų, kuriems nustatyta santykinai išsaugota viršūnės deformacija (SIVD)

ir kuriems šis deformacijos tipas nenustatytas. Pacientams, kuriems būdingas SIVD tipas, nustatytas didesnis AV greitis (p = 0,005), didesnis vidutinis AV gradientas (p = 0,013) ir labiau pažengusi KS remodeliacija: storesnės KS sienelės (p < 0,001), didesnis KS diastolinis skersmuo (p = 0,006), didesnis KS masės indeksas (p = 0,001). Pacientams, kuriems nustatytas SIVD tipas, diagnozuota KS sistolinė disfunkcija, nes jų BID (p = 0,006) ir KSIF (p = 0,040) reikšmės buvo sumažintos. Pacientai, kuriems pasireiškia SIVD tipas, nustatyti miokardo pažeidimo ir širdies nepakankamumo požymiai, nes jų serume rastos padidėjusios BNP (p = 0,032) ir Dj-trop I (p = 0,026) koncentracijos (8 lentelė). Taigi SIVD tipas buvo susijęs su labiau išreikšta AS, nepalankia KS remodeliacija ir širdies nepakankamumu.

8 lentelė. Pacientų širdies vaizdinimo tyrimų rodiklių, histologinės analizės ir serumo žymenų rezultatų palyginimas tarp pacientų, kuriems nustatyta santykinai išsaugotos viršūnės deformacija (SIVD) ir kuriems šis deformacijos tipas nenustatytas

Parametrai	SIVD (+) (n = 14)	SIVD (–) (n = 63)	p reikšmė
Echokardiografijos duomenys			
AV angos indeksas, cm^2/m^2	0,4±0,1	0,5±0,1	0,163
Maksimalus AV greitis, m/s	5,3±0,7	4,8±0,6	**0,005**
Vidutinis AV gradientas, mmHg	70±20	56±14	**0,013**
TSPd, mm	14,6±1,1	12,4±1,5	**<0,001**
KSdd, mm	51,8±4,4	51,2±5,6	0,384
KSsd, mm	34,5±6	32±6	0,124
E/e' septalinis	17,1 (16–18)	16 (13–20)	0,238
E/e' vidutinis	16±7	16±6	0,717
KP tūrio indeksas, ml/m^2	52±14	48±12	0,253
PA sistolinis slėgis, mmHg	39±18	38±14	0,826
BID, %	14,9±3	18,7±5	**0,002**
BID >–15 %	7 (50 %)	9 (14 %)	**0,006**
MRT duomenys			
TSPd, mm	14,8±1	12,9±2	**0,004**
KSdd, mm	54±4	50±6	**0,006**
KSsd, mm	37±7	33±8	0,140
KSGD tūris, ml	149±30	143±348	0,265
KSGS tūris, ml	56 (46–73)	36 (26–56)	0,062
KSIF, %	62±12	68±13	**0,040**
KSIF <50%	1 (7 %)	7 (11 %)	1,0
KS masės indeksas, g/m^2	125±28	91±32	**0,001**

LGE paplitimas	13 (93 %)	44 (70 %)	0,175
Nativinis T1, ms	973±36	955±33	0,094
Pokontrastinis T1, ms	351 (329–363)	352 (327–362)	0,739
Ekstraląstelinis tūris, %	23,4±3	22,3±3	0,292
Histologijos duomenys			
KTF, %	22 (18–25)	22 (15–28)	0,729
KTF subendokardinė, %	30 (23–32)	33 (22–40)	0,168
Serumo žymenys			
BNP, pg/l	409 (161–961)	119 (66–245)	**0,032**
Tn-I, pg/l	15 (13–29)	9 (5–18)	**0,026**

Tolydūs kintamieji pateikti nurodant vidurkius ± SD arba medianas (interkvartilinį skirtumą). Diskretūs kintamieji išreikšti n (%). Paryškintos statistiškai reikšmingus skirtumus žyminčios p reikšmės. Sutrumpinimus žr. 4 ir 5 lentelėse.

3.3.6 Asociacijų analizė

KTF koreliavo su KS galiniu diastoliniu skersmeniu ($r = 0,242$, $p = 0,043$), KS galiniu sistoliniu tūriu ($r = 0,265$, $p = 0,028$), KSIF ($r = -0,246$, $p = 0,04$) ir KP tūrio indeksu ($r = 0,314$, $p = 0,009$). Kai subendokardas buvo pašalintas iš analizės, KTF koreliavo su KS mase ($r = 0,247$, $p = 0,041$), KSIF ($r = -0,354$, $p = 0,003$), BID ($r = -0,03$, $p = 0,013$) ir BNP ($r = 0,242$, $p = 0,045$).

Stipriausios koreliacijos aptiktos tarp BID ir KS struktūrą ir funkciją apibūdinančių rodiklių: BID koreliavo su KS galiniu diastoliniu tūriu ($r = -0,485$, $p < 0,001$), KS galiniu sistoliniu tūriu ($r = -0,636$, $p < 0,001$), KS masės indeksu ($r = -0,615$, $p < 0,001$) ir KSIF ($r = 0,7$, $p < 0,01$).

BID taip pat buvo susijęs su parametrais, kurie nurodo padidėjusį KS prisipildymo slėgį: vidutiniu E/e' ($r = -0,4$, $p = 0,002$), KP tūrio indeksu ($r = -0,405$, $p < 0,001$) ir menamu sistoliniu slėgiu plaučių arterijoje ($r = -0,376$, $p < 0,05$). Natyvinis T1 koreliavo su KS galiniu sistoliniu tūriu ($r = 0,349$, $p = 0,003$), KS galiniu diastoliniu tūriu ($r = 0,269$, $p = 0,03$), KS masės indeksu ($r = 0,414$, $p < 0,001$) ir KSIF ($r = -0,317$, $p < 0,05$). Tyrimo metu nustatyta, kad BID ir natyvinis T1 koreliavo su AS sunkumo laipsnį atspindinčiais rodikliais: AV vidutiniu gradientu (atitinkamai $r = -0,387$, $p < 0,001$ ir $r = 0,408$, $p < 0,001$) ir AVA (atitinkamai $r = 0,30$, $p < 0,05$ ir $r = -0,3$, $p = 0,02$).

Tiriant serumo biožymenis, nustatyta, kad BID ir natyvinis T1 koreliavo su BNP (atitinkamai $r = -0,653$, $p < 0,001$ ir $r = 0,371$, $p < 0,05$) ir Dj-trop I

(atitinkamai r = –0,486, p < 0,001 ir r = 0,333, p < 0,05). Šie rodikliai koreliavo ir tarpusavyje (r = –0,321, p < 0,05).

Taigi gauti rezultatai rodo, kad invaziniais ir neinvaziniais tyrimo metodais nustatyta miokardo fibrozė yra susijusi su nepalankia širdies remodeliacija ir širdies nepakankamumo žymenimis. BID geriausiai išskyrė pacientus, kuriems pasireiškia nepageidaujama KS remodeliacija. BID taip pat gali būti laikomas pakaitiniu miokardo fibrozės žymeniu, nes koreliavo tiek su invaziniu, tiek su neinvaziniu būdu nustatyta miokardo fibroze. Gauti duomenys taip pat rodo, kad SIVD tipas tarp AS sergančių pacientų gali būti nepalankios KS remodeliacijos požymis.

3.3.7 ATTR širdies amiloidozė

Iš 79 pacientų, kuriems buvo atliktas chirurginis AVP, 71 pacientui buvo paimtas miokardo biopsijos mėginys iš bazinio priekinės pertvaros segmento. Histologinės analizės metu nė vienoje iš miokardo biopsijų širdies amiloidozės požymių nenustatyta.

IŠVADOS

1. Remiantis atliktos metaanalizės duomenimis, galima daryti išvadą, kad židininė fibrozė nustatoma beveik pusei tirtų AS pacientų (49,6 %) ir vidutiniškai apima iki 4 proc. KS masės. Dažniausia neinfarktinio tipo židininė fibrozė, nustatoma 63,6 proc. AS sergančių pacientų. Klinikinių baigčių metaanalizė atskleidė, kad AS sergantiems pacientams židininė fibrozė tris kartus padidino mirtingumo nuo įvairių priežasčių (bendras GS [95 % PI] = 3,26 [1,72, 6,18], p = 0,0003) ir kardiovaskulinio mirtingumo (bendras GS [95 % PI]) = 2,89 [1,90, 4,38], p < 0,0001) riziką.

2. FIB-AS tyrimas atskleidė, kad židininė neinfarktinio tipo ir difuzinė miokardo fibrozė dažnai aptinkama didelio laipsnio AS sergantiems pacientams, kuriems atliktas chirurginis AVP. Židininė fibrozė susijusi su nepalankia KS remodeliacija. Histologiškai išmatuota miokardo fibrozė labiau pakenkia subendokardinį sluoksnį ir yra susijusi su širdies vaizdinimo ir serumo širdies nepakankamumo biožymenimis bei kairiųjų širdies ertmių padidėjimu.

3. Sumažėjusi BID ir padidėjęs natyvinis T1 susiję su labiau pažengusia KS remodeliacija, todėl gali būti naudojami kaip ankstyvieji KS pažeidimo žymenys. BID gali būti naudojama kaip pakaitinis miokardo fibrozės žymuo, nes ji susijusi tiek su invaziniu, tiek su neinvaziniu būdu miokardo fibrozei nustatyti. BID slenkstinė vertė >–14 % prognozuoja padidėjusią miokardo fibrozę.

4. Dėl mažo ligos paplitimo chirurginėse AS kohortose TTR širdies amiloidozės požymių nei atliekant ŠMRT, nei histologinės analizės metu nenustatyta.

5. PRAKTINĖS REKOMENDACIJOS

5.1 Miokardo fibrozė, sergant aortos stenoze

Labai svarbu į priešintervencinio tyrimo protokolus įtraukti išplėstinį AS poveikio KS miokardui vertinimą. KSIF skaičiavimas yra įprastas KS sistolinės funkcijos įvertinimo metodas ir išlieka svarbus klinikinis parametras, tačiau jam trūksta jautrumo, ypač tiriant pacientus, kuriems nustatyta koncentrinė KS hipertrofija. Reikėtų siekti nustatyti ankstyvą, subklinikinį KS miokardo pažeidimą, kai įprasti sistolinės disfunkcijos žymenys išlieka nepakitę. Gauti duomenys rodo, kad BID, įvertintas STE metodu, ir natyvinis T1, įvertintas ŠMRT tyrimo metu, gali būti naudojami kaip ankstyvieji nepalankios KS remodeliacijos biožymenys didelio laipsnio AS sergantiems pacientams ir gali būti naudingi šių pacientų rizikai stratifikuoti. BID taip pat gali būti naudojama kaip pakaitinis difuzinės miokardo fibrozės žymuo (taikytina –14 % ribinė vertė). BID vertinimas sąlygiškai pigus ir plačiai prieinamas metodas, todėl jis gali būti taikomas pirmiausia. Ir tik tam tikrai pacientų grupei, kuomet klinikiniai simptomai yra sunkiai interpretuojami ar kyla abejonių dėl AS išreikštumo ir sprendžiama dėl indikacijų intervenciniam gydymui, gali būti atliekamas ŠMRT tyrimas. Ankstyvas KS struktūrinių ir funkcinių pakitimų nustatymas leistų anksčiau suplanuoti AV intervenciją ir padėtų apsaugoti KS miokardą nuo negrįžtamų pokyčių bei pagerinti pacientų prognozę.

5.2 TTR-ŠA, sergant aortos stenoze

Atsižvelgiant į reikšmingą TTR-ŠA paplitimą vyresnio amžiaus pacientų, kuriems taikoma TAVI dėl didelio laipsnio AS, grupėje, būtina skirti daugiau dėmesio šių pacientų sistemingai priežiūrai. Pirmiausia, svarbu atpažinti ligos įtarimą didinančius klinikinių ir širdies vaizdinimo tyrimų požymius (angl. *red flags*). Minėtina, kad SIVD tipas aptinkamas iki 17–30 proc. pacientų, sergančių izoliuota AS, todėl jis negali būti naudojamas kaip specifinis širdies amiloidozės požymis šioje pacientų populiacijose. Pacientams, kuriems patvirtinta tiek TTR-ŠA, tiek didelio laipsnio AS, turėtų būti taikomas AV intervencinis gydymas, pirmenybę teikiant TAVI – ši procedūra siejama su geresniais rezultatais negu chirurginis AVP. Galiausiai, turėtų būti skiriamas specifinis TTR-ŠA gydymas, nepaisant AS sunkumo laipsnio ar sprendimo atlikti AV intervenciją. Dėl mažo TTR-ŠA paplitimo santykinai jaunesnių ir mažos chirurginės rizikos sergančiųjų AS grupėse, rutininė patikra dėl širdies amiloidozės chirurginėse kohortose nerekomenduojama.

PADĖKA

Noriu širdingai padėkoti visiems įvairių sričių specialistams už indėlį į šį mokslinį darbą. Ypač dėkoju prof. dr. S. Glaveckaitei už vadovavimą viso projekto įgyvendinimo metu: rengiant projektą, bendradarbiaujant su tarptautiniais partneriais, koordinuojant pacientų atranką ir priežiūrą, taip pat kritiškai peržiūrint visus publikuotus mokslinius straipsnius ir disertaciją.

Dėkoju prof. dr. N. Valevičienei už pasidalijimą savo žiniomis ir patirtimi ŠMRT srityje ir vertingą indėlį rengiant tyrimo protokolą ir jį įgyvendinant, taip pat už galimybę dalintis tyrimų rezultatais Lietuvos ir tarptautinėje kardiologų bendruomenėje, dalyvaujant Baltijos širdies magnetinio rezonanso konferencijose. Ypatingą padėką skiriu dr. D. Palioniui už itin kvalifikuotą ir laiku atliktą ŠMRT vaizdų analizę, pagalbą rengiant publikacijas ir ruošiant vaizdus moksliniams straipsniams ir pranešimams. Taip pat dėkoju ŠMRT kabineto techniniam personalui už atliktus tyrimus. Esu dėkinga kardiochirurgų komandai – prof. K. Ručinskui, doc. V. Janušauskui, dr. A. Zorinui, G. Turkevičiui, A. Podkopajevui – už produktyvų bendradarbiavimą, sėkmingą visų mūsų pacientų chirurginį gydymą ir didelį paimtų miokardo biopsijos mėginių skaičių. Ačiū patologams – doc. E. Žurauskui ir dr. J. Besuspariui – už histologinę analizę, doc. V. Skorniakovui už statistinę analizę, E. Čiburienei už atkartojamumo analizę, prof. D. Zakarkaitei, G. Bieliauskienei ir E. Dvineliui už pagalbą atliekant echokardiografinius tyrimus, Kardiologijos ambulatorinio skyriaus slaugytojai M. Filipovai už pacientų priežiūrą ir atliktą 6MĖT tyrimą.

Norėčiau padėkoti visiems savanoriams, dalyvavusiems ŠMRT tyrimuose, siekiant nustatyti normines rodiklių reikšmes, visiems pacientams, kurie mumis pasitikėjo ir sutiko dalyvauti šiame projekte.

Galiausiai, nuoširdžiai dėkoju savo šeimai: tėvams Irenai ir Henrikui, vyrui Aleksejui ir vaikams Motiejui bei Barborai už besąlygišką meilę, nuolatinį palaikymą ir už tai, kad esate šalia, kad ir kas benutiktų.

TYRIMO TĘSTINUMAS

Dėl nepalankios COVID-19 epidemiologinės situacijos pacientai kiek vėliau, negu planuota, buvo įtraukti į tyrimą, jie vėliau ištirti prieš operaciją ir hospitalizuoti operacijai. Siekiant į tyrimą įtraukti pakankamą skaičių pacientų, reikėjo pratęsti pacientų įtraukimo į tyrimą laikotarpį iki 2021 m. kovo mėn., todėl pooperacinis stebėjimo laikotarpis buvo pernelyg trumpas, kad iki doktorantūros studijų pabaigos būtų galima ištirti miokardo fibrozės poveikį pacientų klinikinėms baigtims. Šiuo metu surinkti pacientų 12 mėn. stebėjimo vizitų duomenys, renkami klinikinių baigčių duomenys. Juos išanalizavus bus siekiama įvertinti pooperacinę grįžtamąją KS remodeliaciją ir KS miokardo fibrozės įtaką pacientų prognozei.

Minėtina, kad FIB-AS tyrimas atliekamas bendradarbiaujant su Olborgo universitetinės ligoninės kardiologijos centru (Danija). Kolegos iš Danijos taip pat renka didelio laipsnio AS sergančių pacientų, kuriems atliekama TAVI, klinikinius ir širdies vaizdinimo tyrimų duomenis, kuriuos ateityje planuojama palyginti su VUL Santaros klinikose gautais duomenimis.

REFERENCE LIST

1. Lithuanian Institute of Hygiene. https://stat.hi.lt. Accessed on 26/Oct/2021.

2. Généreux P, Pibarot P, Redfors B, Mack MJ, Makkar RR, Jaber WA et al. Staging classification of aortic stenosis based on the extent of cardiac damage. Eur Heart J. 2017 Dec 1;38(45):3351-3358. doi: 10.1093/eurheartj/ehx381.

3. Schewel J, Kuck KH, Frerker C, Schmidt T, Schewel D. Outcome of aortic stenosis according to invasive cardiac damage staging after transcatheter aortic valve replacement. Clin Res Cardiol. 2021 May;110(5):699-710. doi: 10.1007/s00392-021-01835-w.

4. Vahanian A, Beyersdorf F, Praz F, Milojevic M, Baldus S, Bauersachs J et al. ESC/EACTS Scientific Document Group, 2021 ESC/EACTS Guidelines for the management of valvular heart disease: Developed by the Task Force for the management of valvular heart disease of the European Society of Cardiology (ESC) and the European Association for Cardio-Thoracic Surgery (EACTS). *Eur Heart J*, 2021; ehab395. https://doi.org/10.1093/eurheartj/ehab395

5. Hein S, Arnon E, Kostin S, Schonburg M, Elsasser A, Polyakova V et al. Progression from compensated hypertrophy to failure in the pressure-overloaded human heart: structural deterioration and compensatory mechanisms. Circulation. 2003;107:984–91.

6. Unverferth DV, Baker PB, Swift SE, Chaffee R, Fetters JK, Uretsky BF et al. Extent of myocardial fibrosis and cellular hypertrophy in dilated cardiomyopathy. Am J Cardiol. 1986 Apr 1;57(10):816-20. doi: 10.1016/0002-9149(86)90620-x.

7. Lehrke S, Lossnitzer D, Schöb M, Steen H, Merten C, Kemmling H et al. Use of cardiovascular magnetic resonance for risk stratification in chronic heart failure: prognostic value of late gadolinium enhancement in patients with non-ischaemic dilated cardiomyopathy. Heart. 2011; May; 97(9):727-32.

8. Green JJ, Berger JS, Kramer CM, Salerno M. Prognostic Value of Late Gadolinium Enhancement in Clinical Outcomes for Hypertrophic Cardiomyopathy. JACC Cardiovasc Imaging. 2012; Apr; 5(4):370-7.

9. Schelbert EB, Fridman Y, Wong TC , Abu Daya H, Piehler KM, Kadakkal A et al. Temporal relation between myocardial fibrosis and heart failure with preserved ejection fraction: association with baseline disease severity and

subsequent outcome. *JAMA Cardiol.* 2017;2:995–1006. doi: 10.1001/jamacardio.2017.2511.

10. Chin CW, Everett RJ, Kwiecinski J, Vesey AT, Yeung E, Esson G et al. Myocardial Fibrosis and Cardiac Decompensation in Aortic Stenosis. JACC Cardiovasc Imaging. 2017; 10(11):1320-1333.

11. Dweck MR, Joshi S, Murigu T, Alpendurada F, Jabbour A, Melina G et al. Midwall fibrosis is an independent predictor of mortality in patients with aortic stenosis. J Am Coll Cardiol. 2011; 58(12):1271-9.

12. Ng ACT, Prihadi EA, Antoni ML, Bertini M, Ewe SH, Ajmone Marsan N et al. Left ventricular global longitudinal strain is predictive of all-cause mortality independent of aortic stenosis severity and ejection fraction. Eur Heart J Cardiovasc Imaging. 2018; 19:859–67.

13. Kusunose K, Goodman A, Parikh R et al. Incremental prognostic value of left ventricular global longitudinal strain in patients with aortic stenosis and preserved ejection fraction. Circ Cardiovasc Imaging. 2014; 7:938–45.

14. Dungu JN, Anderson LJ, Whelan CJ, Hawkins PN. Cardiac transthyretin amyloidosis. Heart. 2012 Nov;98(21):1546-54.

15. Martinez-Naharro A, Kotecha T, Norrington K, Boldrini M, Rezk T, Quarta C et al. Native T1 and Extracellular Volume in Transthyretin Amyloidosis. JACC Cardiovasc Imaging. 2019, 12.5: 810-819.

16. Perugini E, Guidalotti PL, Salvi F, Cooke RM, Pettinato C, Riva L et al. Noninvasive etiologic diagnosis of cardiac amyloidosis using 99mTc-3, 3-diphosphono-1, 2-propanodicarboxylic acid scintigraphy. J Am Coll Cardiol 2005;46: 1076–1084.

17. Rapezzi C, Quarta CC, Guidalotti PL, Longhi S, Pettinato C, Leone O et al. Usefulness and limitations of 99mTc-3, 3-diphosphono-1, 2-propanodicarboxylic acid scintigraphy in the aetiological diagnosis of amyloidotic cardiomyopathy. Eur J Nucl Med Mol Imaging. 2011;38: 470–478.

18. Dumesnil JG, Pibarot P, Carabello B. Paradoxical low flow and/or low gradient severe aortic stenosis despite preserved left ventricular ejection fraction: implications for diagnosis and treatment. Eur Heart J. 2010;31:281–289.

19. Treibel TA, Fontana M, Gilbertson JA, Castelletti S, White SK, Scully PR et al. Occult Transthyretin Cardiac Amyloid in Severe Calcific Aortic

Stenosis: Prevalence and Prognosis in Patients Undergoing Surgical Aortic Valve Replacement. Circ Cardiovasc Imaging. 2016, 9.8: e005066.

20. Damy T, Judge DP, Kristen AV, Berthet K, Li H, Aarts J. Cardiac findings and events observed in an open-label clinical trial of tafamidis in patients with non-Val30Met and non-Val122Ile hereditary transthyretin amyloidosis. J Cardiovasc Transl Res. 2015 Mar;8(2):117-27.

21. Galat A, Guellich A, Bodez D, Slama M, Dijos M, Zeitoun DM et al. Aortic stenosis and transthyretin cardiac amyloidosis: the chicken or the egg? Eur Heart J. 2016 Dec 14;37(47):3525-3531.

22. Sperry BW, Jones BM, Vranian MN, Hanna M, Jaber WA. Recognizing Transthyretin Cardiac Amyloidosis in Patients With Aortic Stenosis: Impact on Prognosis. JACC Cardiovasc Imaging. 2016 Jul;9(7):904-906.

23. Cavalcante JL, Rijal S, Abdelkarim I, Althouse AD, Sharbaugh MS, Fridman Y et al. Cardiac amyloidosis is prevalent in older patients with aortic stenosis and carries worse prognosis. J Cardiovasc Magn Reson. 2017 Dec 7;19(1):98.

24. Nitsche C, Scully PR, Patel KP, Kammerlander AA, Koschutnik M, Dona C et al. Prevalence and outcomes of concomitant aortic stenosis and cardiac amyloidosis. J Am Coll Cardiol 2021; 77:128–139.

25. Rosenblum H, Masri A, Narotsky DL, Goldsmith J, Hamid N, Hahn RT et al. Unveiling outcomes in coexisting severe aortic stenosis and transthyretin cardiac amyloidosis. Eur J Heart Fail 2021;23:250–258.

26. Lorenz CH, Walker ES, Morgan VL, Klein SS, Graham TP. Normal human right and left ventricular mass, systolic function, and gender differences by cine magnetic resonance imaging. J. Cardiovasc. Magn. Reson. 1999; 1.1: 7-21.

27. Patel AR, Antkowiak PF, Nandalur KR, West AM, Salerno M, Arora V et al. Assessment of advanced coronary artery disease: advantages of quantitative cardiac magnetic resonance perfusion analysis. J. Am. Coll. Cardiol. 2010;56:561–569.

28. Jerosch-Herold M, Sheridan DC, Kushner JD, Nauman D, Burgess D, Dutton et al. Cardiac magnetic resonance imaging of myocardial contrast uptake and blood flow in patients affected with idiopathic or familial dilated cardiomyopathy. Am. J. Physiol. Heart Circ. Physiol. 2008;295:H1234–H1242.

29. Assomull RG, Prasad SK, Lyne J, Smith G, Burman ED, Khan M et al. Cardiovascular magnetic resonance, fibrosis, and prognosis in dilated cardiomyopathy. J. Am. Coll. Cardiol. 2006; 48:1977–1985.

30. Salerno M, Kramer CM. Advances in parametric mapping with CMR imaging. JACC Cardiovasc. Imaging 2013; 6:806–822.

31. Čelutkienė J, Plymen CM, Flachskampf FA, de Boer RA, Grapsa J, Manka R et al. Innovative imaging methods in heart failure: a shifting paradigm in cardiac assessment. Position statement on behalf of the Heart Failure Association of the European Society of Cardiology. Eur J Heart Fail 2018; 20:1615-33.

32. Iles L, Pfluger H, Phrommintikul A, Cherayath J, Aksit P, Gupta SN et al. Evaluation of diffuse myocardial fibrosis in heart failure with cardiac magnetic resonance contrast-enhanced T1 mapping. J. Am. Coll. Cardiol. 2008; 52:1574–1580.

33. Broberg CS, Chugh SS, Conklin C, Sahn DJ, Jerosch-Herold M. Quantification of diffuse myocardial fibrosis and its association with myocardial dysfunction in congenital heart disease. Circ. Cardiovasc. Imaging 2010; 3:727–734.

34. https://pubmed.ncbi.nlm.nih.gov. Accessed on March/2022.

35. Schelbert EB, Testa SM, Meier CG, Ceyrolles WJ, Levenson JE, Blair AJ et al. Myocardial extravascular extracellular volume fraction measurement by gadolinium cardiovascular magnetic resonance in humans: slow infusion versus bolus. J. Cardiovasc. Magn. Reson. Off. J. Soc. Cardiovasc. Magn. Reson. 2011; 13:16.

36. Foussier C, Barral PA, Jerosh-Herold M, Gariboldi V, Rapacchi S, Gallon A et al. Quantification of diffuse myocardial fibrosis using CMR extracellular volume fraction and serum biomarkers of collagen turnover with histologic quantification as standard of reference. Diagn Interv Imaging. 2021 Mar;102(3):163-169. doi: 10.1016/j.diii.2020.07.005.

37. Lee S-P, Lee W, Lee JM, Park E-A, Kim H-K, Kim Y-J et al. Assessment of diffuse myocardial fibrosis by using MR imaging in asymptomatic patients with aortic stenosis. Radiology. 2015; 274:359–69.

38. Messroghli DR, Moon JC, Ferreira VM, Grosse-Wortmann L, He T, Kellman P et al. Clinical recommendations for cardiovascular magnetic resonance mapping of T1, T2, T2* and extracellular volume: A consensus

statement by the Society for Cardiovascular Magnetic Resonance (SCMR) endorsed by the European Association for Cardiovascular Imaging (EACVI). Journal of Cardiovascular Magnetic Resonance 2017; 19:75.

39. Dweck MR, Boon NA, Newby DE. Calcific aortic stenosis: a disease of the valve and the myocardium. J Am Coll Cardiol. 2012; 60:1854-1863.

40. Carabello BA, Paulus WJ. Aortic stenosis. Lancet 2009; 373:956-966.

41. Anderson KR, Sutton MG, Lie JT. Histopathological types of cardiac fibrosis in myocardial disease. J Pathol. 1979; 128(2):79-85. https://doi: 10.1002/path.1711280205.

42. Villari B, Campbell SE, Hess OM, Mall G, Vassalli G, Weber KT et al. Influence of collagen network on left ventricular systolic and diastolic function in aortic valve disease. J Am Coll Cardiol. 1993; 22:1477–1484.

43. Barone-Rochette G, Pierard S, De Meester de Ravenstein C, Seldrum S, Melchior J, Maes F et al. Prognostic significance of LGE by CMR in aortic stenosis patients undergoing valve replacement. J Am Coll Cardiol. 2014; 64:144–154.

44. Chin CW, Semple S, Malley T, White AC, Mirsadraee S, Weale PJ et al. Optimization and comparison of myocardial T1 techniques at 3T in patients with aortic stenosis. Eur Heart J Cardiovasc Imaging. 2014; 15:556–65.

45. Musa TA, Treibel TA, Vassiliou VS et al. Myocardial Scar and Mortality in Severe Aortic Stenosis. Circulation. 2018; Oct 30;138(18):1935-1947. https://doi.org/10.1161/CIRCULATIONAHA.117.032839

46. Nassenstein K, Bruder O, Breuckmann F, Erbel R, Barkhausen J, Schlosser T. Prevalence, pattern, and functional impact of late gadolinium enhancement in left ventricular hypertrophy due to aortic valve stenosis. Rofo. 2009; May;181(5):472-6.

47. Dweck MR, Joshi S, Murigu T, Gulati A, Alpendurada F, Jabbour A et al. Left ventricular remodeling and hypertrophy in patients with aortic stenosis: insights from cardiovascular magnetic resonance. J Cardiovasc Magn Reson. 2012; Jul 28; 14:50.

48. Treibel TA, López B, González A, Menacho K, Schofield RS, Ravassa S et al. Reappraising myocardial fibrosis in severe aortic stenosis: An invasive and non-invasive study in 133 patients. Eur Heart J. 2018; Feb 21;39(8):699-709.

49. Kuribayashi T, Roberts WC. Myocardial disarray at junction of ventricular septum and left and right ventricular free walls in hypertrophic cardiomyopathy. Am J Cardiol 1992; 70:1333–40.

50. Chan RH, Maron BJ, Olivotto I, Assenza GE, Haas TS, Lesser JR et al. Significance of late gadolinium enhancement at right ventricular attachment to ventricular septum in patients with hypertrophic cardiomyopathy. Am J Cardiol. 2015; 116:436–41.

51. Everett RJ, Tastet L, Clavel MA, Chin CW, Capoulade R, Vassiliou VS et al. Progression of Hypertrophy and Myocardial Fibrosis in Aortic Stenosis: A Multicenter Cardiac Magnetic Resonance Study. Circ Cardiovasc Imaging. 2018; Jun; 11(6): e007451.

52. Kim WK, Rolf A, Liebetrau C, Van Linden A, Blumenstein J, Kempfert J, et al. Detection of myocardial injury by CMR after transcatheter aortic valve replacement. J Am Coll Cardiol. 2014; Jul 29; 64(4): 349-57.

53. Carter-Storch R, Møller JE, Christensen NL, Irmukhadenov A, Rasmussen LM, Pecini R, et al. Postoperative Reverse Remodeling and Symptomatic Improvement in Normal-Flow Low-Gradient Aortic Stenosis After Aortic Valve Replacement. Circ Cardiovasc Imaging. 2017; Dec;10(12). pii: e006580.

54. Dobson LE, Musa TA, Uddin A, Fairbairn TA, Swoboda PP, Ripley DP, Garg P, Evans B, Malkin CJ, Blackman DJ, Plein S, Greenwood JP. Post-procedural myocardial infarction following surgical aortic valve replacement and transcatheter aortic valve implantation. EuroIntervention. 2017; Jun 2;13(2): e153-e160.

55. de Meester de Ravenstein C, Bouzin C, Lazam S, Boulif J, Amzulescu M, Melchior J et al. Histological Validation of measurement of diffuse interstitial myocardial fibrosis by myocardial extravascular volume fraction from Modified Look-Locker imaging (MOLLI) T1 mapping at 3 T. J Cardiovasc Magn Reson. 2015 Jun 11;17(1):48. doi: 10.1186/s12968-015-0150-0.

56. Park SJ, Cho SW, Kim SM, Ahn J, Carriere K, Jeong DS et al. Assessment of Myocardial Fibrosis Using Multimodality Imaging in Severe Aortic Stenosis: Comparison With Histologic Fibrosis. JACC Cardiovasc Imaging. 2019 12(1): 109-119. https://doi: 10.1016/j.jcmg.2018.05.028.

57. Everett RJ, Treibel TA, Fukui M, Lee H, Rigolli M, Singh A et al. Extracellular myocardial volume in patients with aortic stenosis. J Am Coll Cardiol 2020; 75:304–316.

58. Kwak S, Everett RJ, Treibel TA, Yang S, Hwang D, Ko T et al. Markers of Myocardial Damage Predict Mortality in Patients With Aortic Stenosis. J Am Coll Cardiol. 2021 Aug 10;78(6):545-558. doi: 10.1016/j.jacc.2021.05.047.

59. Hwang I-C, Kim H-K, Park J-B, Park E-A, Lee W, Lee S-P et al. Aortic valve replacement-induced changes in native T1 are related to prognosis in severe aortic stenosis: T1 mapping cardiac magnetic resonance imaging study. Eur Heart J Cardiovasc Imaging 2020; 21:653–663.

60. Rapezzi C, Merlini G, Quarta CC, Riva L, Longhi S, Leone O et al. S. Systemic cardiac amyloidoses: disease profiles and clinical courses of the 3 main types. Circulation. 2009 Sep 29;120(13):1203-12.

61. Ueda M, Horibata Y, Shono M, Misumi Y, Oshima T, Su Y et al. Clinicopathological features of senile systemic amyloidosis: an ante- and post-mortem study. Mod Pathol 2011; 24:1533–44.

62. Nietlispach F, Webb JG, Ye J, Cheung A, Lichtenstein SV, Carere RG et al. Pathology of transcatheter valve therapy. JACC Cardiovasc Interv 2012; 5:582–590.

63. Scully PR, Treibel TA, Fontana M, Lloyd G, Mullen M, Pugliese F et al. Prevalence of Cardiac Amyloidosis in Patients Referred for Transcatheter Aortic Valve Replacement. J Am Coll Cardiol. 2018 Jan 30;71(4):463-464.

64. Castaño A, Narotsky DL, Hamid N, Khalique OK, Morgenstern R, DeLuca A et al. Unveiling transthyretin cardiac amyloidosis and its predictors among elderly patients with severe aortic stenosis undergoing transcatheter aortic valve replacement. Eur Heart J. 2017 Oct 7;38(38):2879-2887.

65. Balciunaite G, Rimkus A, Zurauskas E, Zaremba T, Palionis D, Valeviciene N et al. Transthyretin cardiac amyloidosis in aortic stenosis: Prevalence, diagnostic challenges, and clinical implications. Hellenic J Cardiol. 2019 Nov 15. pii: S1109-9666(19)30278-7. doi: 10.1016/j.hjc.2019.10.004.

66. Scully PR, Patel KP, Treibel TA, Thornton GD, Hughes RK, Chadalavada S et al. Prevalence and outcome of dual aortic stenosis and cardiac amyloid pathology in patients referred for transcatheter aortic valve

implantation, *European Heart Journal*, Volume 41, Issue 29, 1 August 2020, Pages 2759–2767.

67. Gillmore JD, Damy T, Fontana M, Hutchinson M, Lachmann HJ, Martinez-Naharro A et al. A new staging system for cardiac transthyretin amyloidosis. Eur Heart J 2018; 39:2799–806.

68. Maurer MS, Schwartz JH, Gundapaneni B, Elliott PM, Merlini G, Waddington-Cruz M et al. Tafamidis treatment for patients with transthyretin amyloid cardiomyopathy. N Eng J Med. 2018; 379(11), 1007-1016.

69. Elliott P, Drachman BM, Gottlieb SS, Hoffman JE, Hummel SL, Lenihan DJ et al. Long-Term Survival With Tafamidis in Patients With Transthyretin Amyloid Cardiomyopathy. Circ Heart Fail. 2022 Jan;15(1): e008193. doi: 10.1161/CIRCHEARTFAILURE.120.008193.

70. Benson MD, Waddington-Cruz M, Berk JL, Polydefkis M, Dyck PJ, Wang AK et al. Inotersen treatment for patients with hereditary transthyretin amyloidosis. N Engl J Med 2018; 379:22–31.

71. Judge DP, Heitner SB, Falk RH, Maurer MS, Shah SJ, Witteles RM et al. Transthyretin stabilization by AG10 in symptomatic transthyretin amyloid cardiomyopathy. J Am Coll Cardiol 2019; 74:285–95.

72. Moher D, Liberati A, Tetzlaff J, Altman DG, for the PRISMA Group. Preferred Reporting Items for Systematic Reviews and Meta-Analyses: the PRISMA statement. BMJ. 2009; 339: b2535.

73. Harris PA, Taylor R, Thielke R, Payne J, Gonzalez N, Conde JG. Research electronic data capture (REDCap) -a metadata-driven methodology and workflow process for providing translational research informatics support. *J Biomed Inform*. 2009;42(2):377–381. doi:10.1016/j.jbi.2008.08.010.

74. Lang RM, Badano LP, Mor-Avi V, Afilalo J, Armstrong A, Ernande L et al. Recommendations for cardiac chamber quantification by echocardiography in adults: an update from the American Society of Echocardiography and the European Association of Cardiovascular Imaging. J Am Soc Echocardiogr 2015; 28:1–39.

75. Baumgartner H, Hung J, Bermejo J, Chambers JB, Edvardsen T, Goldstein S et al. Recommendations on the echocardiographic assessment of aortic valve stenosis: a focused update from the European Association of Cardiovascular Imaging and the American Society of Echocardiography. Eur Heart J Cardiovasc Imaging 2017; 18:254–75.

76. Voigt JU, Pedrizzetti G, Lysyansky P, Marwick TH, Houle H, Baumann R et al. Definitions for a common standard for 2D speckle tracking echocardiography: consensus document of the EACVI/ASE/Industry Task Force to standardize deformation imaging. Eur Heart J Cardiovasc Imaging 2015; 16:1–11.

77. Taylor AJ, Salerno M, Dharmakumar R, Jerosch-Herold M. T1 mapping: basic techniques and clinical applications. JACC Cardiovasc Imaging 2016; 9:67–81. https://doi.org/10.1016/j.jcmg.2015.11.005.

78. Ugander M, Oki AJ, Hsu LY, Kellman P, Greiser A, Aletras AH et al. Extracellular volume imaging by magnetic resonance imaging provides insights into overt and sub-clinical myocardial pathology. Eur Heart J. 2012; 33:1268–78.

79. Horai Y, Mizukawa M, Nishina H, Nishikawa S, Ono Y, Takemoto K et al. Quantification of histopathological findings using a novel image analysis platform. *J Toxicol Pathol*. 2019;32(4):319-327. doi:10.1293/tox.2019-0022.

80. R Core Team. R: A language and environment for statistical computing. R Foundation for Statistical Computing, Vienna, Austria. 2018. https://www.R-project.org/. Accessed 12/Sep/2018.

81. Viechtbauer W. Conducting meta-analyses in R with the metafor package. Journal of Statistical Software. 2010; *36*(3), 1-48. http://www.jstatsoft.org/v36/i03/. Accessed 12/Sep/2018.

82. Veroniki AA, Jackson D, Viechtbauer W, Bender R, Bowden J, Knapp G et al. Methods to estimate the between-study variance and its uncertainty in meta-analysis. Res Synth Methods. 2016; 7(1):55-79.

83. Sterne JA, Egger M, Regression Methods to Detect Publication and Other Bias in Meta-Analysis. Publication Bias in Meta-Analysis. 2006; doi:10.1002/0470870168.ch6.

84. R Core Team. R: A language and environment for statistical computing (2021) R Foundation for Statistical Computing, Vienna, Austria. R version 4.1.2 (2021-11-01) -- "Bird Hippie" https://www.R-project.org/

85. Azevedo CF, Nigri M, Higuchi ML, Pomerantzeff PM, Spina GS, Sampaio RO et al. Prognostic significance of myocardial fibrosis quantification by histopathology and magnetic resonance imaging in patients with severe aortic valve disease. J Am Coll Cardiol. 2010; 56(4):278-87.

86. Rajesh GN, Thottian JJ, Subramaniam G, Desabandhu V, Sajeev CG, Krishnan MN. Prevalence and prognostic significance of left ventricular myocardial late gadolinium enhancement in severe aortic stenosis. Indian Heart J. 2017 Nov - Dec; 69(6):742-750.

87. Park J, Chang HJ, Choi JH, Yang PS, Lee SE, Heo R et al. Late gadolinium enhancement in cardiac MRI in patients with severe aortic stenosis and preserved left ventricular systolic function is related to attenuated improvement of left ventricular geometry and filling pressure after aortic valve replacement. Korean Circ J. 2014; Sep; 44(5): 312-9.

88. Hoffmann R, Altiok E, Friedman Z, Becker M, Frick M et al. Myocardial deformation imaging by two-dimensional speckle-tracking echocardiography in comparison to late gadolinium enhancement cardiac magnetic resonance for analysis of myocardial fibrosis in severe aortic stenosis. Am J Cardiol. 2014; Oct 1; 114 (7):1083-8.

89. Nucifora G, Tantiongco JP, Crouch G, Bennetts J, Sinhal A, Tully PJ et al. Changes of left ventricular mechanics after trans-catheter aortic valve implantation and surgical aortic valve replacement for severe aortic stenosis: A tissue-tracking cardiac magnetic resonance study. Int J Cardiol. 2017; Feb 1; 228:184-190.

90. Lee H, Park JB, Yoon YE, Park EA, Kim HK, Lee W et al. Noncontrast Myocardial T1 Mapping by Cardiac Magnetic Resonance Predicts Outcome in Patients With Aortic Stenosis. JACC Cardiovasc Imaging. 2018; Jul; 11(7):974-983.

91. Carter-Storch R, Møller JE, Christensen NL, Irmukhadenov A, Rasmussen LM, Pecini R, et al. Postoperative Reverse Remodeling and Symptomatic Improvement in Normal-Flow Low-Gradient Aortic Stenosis After Aortic Valve Replacement. Circ Cardiovasc Imaging. 2017; Dec;10(12). pii: e006580.

92. Buckert D, Cieslik M, Tibi R, Radermacher M, Rasche V, Bernhardt P et al. Longitudinal strain assessed by cardiac magnetic resonance correlates to hemodynamic findings in patients with severe aortic stenosis and predicts positive remodeling after transcatheter aortic valve replacement. Clin Res Cardiol. 2018; Jan; 107(1):20-29.

93. Weidemann F, Herrmann S, Störk S, Niemann M, Frantz S, Lange V et al. Impact of myocardial fibrosis in patients with symptomatic severe aortic stenosis. Circulation. 2009; Aug 18; 120(7):577-84.

94. Debl K, Djavidani B, Buchner S, et al. Delayed hyperenhancement in magnetic resonance imaging of left ventricular hypertrophy caused by aortic stenosis and hypertrophic cardiomyopathy: visualisation of focal fibrosis. Heart. 2006 Oct;92(10):1447-51.

95. Mahmod M, Piechnik SK, Levelt E, et al. Adenosine stress native T1 mapping in severe aortic stenosis: evidence for a role of the intravascular compartment on myocardial T1 values. J Cardiovasc Magn Reson. 2014 Nov 20;16:92.

96. Singh A, Greenwood JP, Berry C, et al. Comparison of exercise testing and CMR measured myocardial perfusion reserve for predicting outcome in asymptomatic aortic stenosis: the PRognostic Importance of MIcrovascular Dysfunction in Aortic Stenosis (PRIMID AS) Study. Eur Heart J. 2017 Apr 21;38(16):1222-1229.

97. Chen H, Zeng J, Liu D, Yang Q. Prognostic value of late gadolinium enhancement on CMR in patients with severe aortic valve disease: a systematic review and meta-analysis. Clin Radiol. 2018; Aug 4. pii: S0009-9260(18)30365-9.

98. Papanastasiou CA, Kokkinidis DG, Kampaktsis PN, Bikakis I, Cunha DK, Oikonomou EK et al. The Prognostic Role of Late Gadolinium Enhancement in Aortic Stenosis: A Systematic Review and Meta-Analysis. JACC Cardiovasc Imaging. 2020 Feb;13(2 Pt 1):385-392. doi: 10.1016/j.jcmg.2019.03.029.

99. Flett AS, Hasleton J, Cook C, Hausenloy D, Quarta G, Ariti C et al. Evaluation of techniques for the quantification of myocardial scar of differing etiology using cardiac magnetic resonance. JACC Cardiovasc Imaging. 2011; Feb;4 (2):150-6.

100. Tanaka M, Fujiwara H, Onodera T, Wu DJ, Hamashima Y, Kawai C. Quantitative analysis of myocardial fibrosis in normals, hypertensive hearts, and hypertrophic cardiomyopathy. Br Heart J. 1986 Jun;55(6):575-81. doi: 10.1136/hrt.55.6.575.

101. Galiuto L, Lotrionte M, Crea F, Anselmi A, Biondi-Zoccai GG, De Giorgio F et al. Impaired coronary and myocardial flow in severe aortic stenosis is associated with increased apoptosis: a transthoracic Doppler and myocardial contrast echocardiography study. *Heart*. 2006;92(2):208-212. doi:10.1136/hrt.2005.062422.

102. Magne J, Cosyns B, Popescu BA, Carstensen HG, Dahl J, Desai MY et al. Distribution and Prognostic Significance of Left Ventricular Global Longitudinal Strain in Asymptomatic Significant Aortic Stenosis: An Individual Participant Data Meta-Analysis. JACC Cardiovasc Imaging. 2019 Jan;12(1):84-92. doi: 10.1016/j.jcmg.2018.11.005.

103. Vo HQ, Marwick TH, Negishi K. Pooled summary of native T1 value and extracellular volume with MOLLI variant sequences in normal subjects and patients with cardiovascular disease. Int J Cardiovasc Imaging. 2020 Feb;36(2):325-336. doi: 10.1007/s10554-019-01717-3.

104. Kawel, N, Nacif, M, Zavodni A, Jones J, Liu S, Cibley CT et al. T1 mapping of the myocardium: intra-individual assessment of the effect of field strength, cardiac cycle and variation by myocardial region. J Cardiovasc Magn Reson. 2012 May 1;14(1):27. doi: 10.1186/1532-429X-14-27.

105. Dabir D, Child N, Kalra A, Rogers T, Gebker R, Jabbour A et al. Reference values for healthy human myocardium using a T1 mapping methodology: results from the International T1 Multicenter cardiovascular magnetic resonance study. J Cardiovasc Magn Reson. 2014 Oct 21;16(1):69. doi: 10.1186/s12968-014-0069-x.

106. Puls M, Beuthner BE, Topci R, Vogelgesang A, Bleckmann A, Sitte M et al. Impact of myocardial fibrosis on left ventricular remodelling, recovery, and outcome after transcatheter aortic valve implantation in different haemodynamic subtypes of severe aortic stenosis. Eur Heart J. 2020 May 21;41(20):1903-1914. doi: 10.1093/eurheartj/ehaa033.

107. Koyama J, Ray-Sequin PA, Falk RH. Longitudinal myocardial function assessed by tissue velocity, strain, and strain rate tissue Doppler echocardiography in patients with AL (primary) cardiac amyloidosis. Circulation. 2003;107: 2446e2452.

108. Abecasis J, Mendes G, Ferreira A, Andrade MJ, Ribeiras R, Ramos S et al. Relative apical sparing in patients with severe aortic stenosis: prevalence and significance, *European Heart Journal*, Volume 41, Issue Supplement_2, November 2020, ehaa946.1987.

109. Henderson BC, Tyagi, N, Ovechkin A, Kartha GK, Moshal KS, Tyagi SC. Oxidative remodeling in pressure overload induced chronic heart failure. Eur. J. Heart Fail. 2007, 9, 450–457.

110. Kristen AV, Schnabel PA, Winter B, Helmke BM, Longerich T, Hardt S et al. High prevalence of amyloid in 150 surgically removed heart valves–a

comparison of histological and clinical data reveals a correlation to athero-inflammatory conditions. Cardiovasc. Pathol. Off. J. Soc. Cardiovasc. Pathol. 2010, 19, 228–235.

111. Bing R, Everett RJ, Tuck C, Semple S, Lewis S, Harkess R et al. Rationale and design of the randomized, controlled Early Valve Replacement Guided by Biomarkers of Left Ventricular Decompensation in Asymptomatic Patients with Severe Aortic Stenosis (EVOLVED) trial. American Heart Journal, Volume 212, 2019, DOI: 10.1016/j.ahj.2019.02.018

ACKNOWLEDGEMENTS

LIST OF PRESENTATIONS

No.	International oral presentations	Date	Location
1.	6th meeting of the Baltic Society of CMR. "Myocardial fibrosis in aortic stenosis: emerging results of FIB-AS study".	10/Sep/2021	Vilnius, Lithuania
2.	Essential questions in cardiology and cardiac surgery. "Diagnostic challenges in TTR cardiac amyloidosis"	30/Oct/2020	Kijev, Ukraine
3.	5th meeting of the Baltic Society of CMR. "Multimodality imaging in TTR cardiac amyloidosis".	18/Sep/2020	Dubingiai, Lithuania
4.	Functional diagnostics of cardiovascular diseases. "Aortic stenosis- more than a disease of a valve".	03/Jun/2020	Kijev, Ukraine
5.	4th meeting of the Baltic Society of CMR. "Focal and diffuse myocardial fibrosis in aortic stenosis – an update".	13/Sep/2019	Klaipėda, Lithuania
6.	3rd meeting of the Baltic Society of CMR. "The role of CMR in severe aortic stenosis".	07/Sep/2018	Riga, Latvija

COPIES OF PUBLICATIONS

1st publication/1 publikacija

Prevalence and prognostic value of late gadolinium enhancement on CMR in aortic stenosis: meta-analysis.

Balciunaite G, Skorniakov V, Rimkus A, Zaremba T, Palionis D, Valeviciene N, Aidietis A, Serpytis P, Rucinskas K, Sogaard P, Glaveckaite S.

CARDIAC

Prevalence and prognostic value of late gadolinium enhancement on CMR in aortic stenosis: meta-analysis

Giedre Balciunaite[1] · Viktor Skorniakov[2] · Arnas Rimkus[1] · Tomas Zaremba[1,3] · Darius Palionis[4] · Nomeda Valeviciene[4] · Audrius Aidietis[1] · Pranas Serpytis[1] · Kestutis Rucinskas[1] · Peter Sogaard[1,3] · Sigita Glaveckaite[1]

Abstract

Objectives The aim of this study was to investigate the prevalence and prognostic value of late gadolinium enhancement (LGE), as assessed by cardiovascular magnetic resonance (CMR) imaging, in patients with aortic stenosis.

Methods and results A systematic search of PubMed and EMBASE was performed, and observational cohort studies that analysed the prevalence of LGE and its relation to clinical outcomes in patients with aortic stenosis were included. Odds ratios were used to measure an effect of the presence of LGE on both all-cause and cardiovascular mortality. Nineteen studies were retrieved, accounting for 2032 patients (mean age 69.8 years, mean follow-up 2.8 years). We found that LGE is highly prevalent in aortic stenosis, affecting half of all patients (49.6%), with a non-infarct pattern being the most frequent type (63.6%). The estimated extent of focal fibrosis, expressed in % of LV mass, was equal to 3.83 (95% CI [2.14, 5.52], $p < 0.0001$). The meta-analysis showed that the presence of LGE was associated with increased all-cause (pooled OR [95% CI] = 3.26 [1.72, 6.18], $p = 0.0003$) and cardiovascular mortality (pooled OR [95% CI] = 2.89 [1.90, 4.38], $p < 0.0001$).

Conclusions LGE by CMR is highly prevalent in aortic stenosis patients and exhibits a substantial value in all-cause and cardiovascular mortality prediction. These results suggest a potential role of LGE in aortic stenosis patient risk stratification.

Key Points
• *Up to the half of aortic stenosis patients are affected by myocardial focal fibrosis.*
• *Sixty-four percent of focal fibrosis detected by LGE-CMR is non-infarct type.*
• *The presence of focal fibrosis triples all-cause and cardiovascular mortality.*

Abbreviations

AS	Aortic stenosis
CAD	Coronary artery disease
CMR	Cardiovascular magnetic resonance
FWHM	Full width half maximum
LGE	Late gadolinium enhancement
LV	Left ventricular
LVEF	Left ventricular ejection fraction

✉ Giedre Balciunaite
   dr.giedre.balciunaite@gmail.com

[1] Clinic of Cardiovascular Diseases, Institute of Clinical Medicine, Vilnius University Faculty of Medicine, Santariskiu st. 2, 08661 Vilnius, Lithuania

[2] Faculty of Mathematics and Informatics, Institute of Applied Mathematics, Vilnius University, Naugarduko str. 24, LT-03225 Vilnius, Lithuania

[3] Aalborg University Hospital, Clinical Institute of Aalborg University, Hobrovej 18-22, 9100 Aalborg, Denmark

[4] Department of Radiology, Nuclear Medicine and Medical Physics, Institute of Biomedical Sciences, Vilnius University Faculty of Medicine, Santariskiu st. 2, 08661 Vilnius, Lithuania

⛤ Springer

NYHA   New York Heart Association
SAVR   Surgical aortic valve replacement
TAVI   Transcatheter aortic valve implantation

Introduction

Degenerative aortic stenosis (AS) is one of the most common valvular heart diseases, characterised by progressive narrowing of the aortic valve and by compensatory hypertrophic remodelling of the left ventricular (LV) myocardium [1]. Whilst LV hypertrophy maintains wall stress and cardiac output, it eventually decompensates, with cell death and myocardial fibrosis identified as key processes [2, 3]. LV ejection fraction (LVEF) remains one of the markers of cardiac decompensation by the current guidelines [4]. However, reduction in LVEF is a late and non-specific feature in AS, leading to interest in alternative methods for detecting LV decompensation [5]. Cardiovascular magnetic resonance (CMR) imaging allows non-invasive visualisation and quantification of scarring using late gadolinium enhancement (LGE) and can offer new insights into the pathophysiological processes within the myocardium [6]. Replacement fibrosis by LGE has been found to represent a marker of adverse prognosis in a variety of cardiomyopathies [7–9]. Risk stratification among patients with AS remains inadequate, causing an ongoing discussion and clinical challenges in the appropriate identification of high-risk patients who would benefit from aortic valve intervention before LV decompensation develops. With the most recent data from a large longitudinal multicentre study, we aimed to summarise the available evidence and evaluate the prevalence and prognostic significance of LGE, as assessed by CMR, in AS patients.

Methods

The meta-analysis was performed in accordance with the Preferred Reporting Items for Systematic Reviews and Meta-Analyses (PRISMA) statement [10].

A systematic search of PubMed and EMBASE was performed by 2 investigators (G.B. and A.R.) from inception to October 2018. Indexing terms 'aortic stenosis' and 'late gadolinium enhancement', or 'delayed gadolinium enhancement', or 'LGE', or 'cardiovascular magnetic resonance' were used to design the search strategy. Prospective observational studies describing myocardial fibrosis detected by LGE-CMR in adult patients with AS were included in the meta-analysis. All-cause mortality and cardiovascular mortality represent the main outcomes of this meta-analysis. Any pattern of LGE was accounted for to define the presence or absence of LGE. If several studies were performed in the same population, the studies with the largest number of patients were included.

Data on presence, pattern and extent of LGE were obtained. Data concerning the numbers of patients with and without adverse events, stratified by the presence or absence of LGE, were extracted from the original reports or estimated from the total number of patients and number of deaths in different groups.

Quality assessment The risk for bias within individual studies investigating adverse clinical events was evaluated according to the established methods of the Cochrane collaboration [11] and the Newcastle-Ottawa Quality Assessment Scale for Cohort Studies [12]. Quality assessment was performed only in studies included in the quantitative mortality meta-analysis (Table 1). Five of 6 studies were rated as high quality with a median of 8 points (range 6–9) by the Newcastle Ottawa Quality Assessment Scale (Supplementary Files Table S1).

Statistical analysis

Statistical analysis was performed by making use of R language and environment for statistical computing (version 3.5.1) [19], in particular, metafor package (version 2.1–0) [20]. To compute pooled estimators, random effects model with restricted-likelihood estimator was applied [21]. In order to present results of the pooled analysis, forest plots were used. Effects' heterogeneity was assessed by I^2 value, corresponding test and funnel plots. Publication bias was assessed by linear Egger's test and was treated as significant at $p < 0.10$. [22]. Additionally, we have performed a 1-study removal analysis to look for potentially influential studies and a cumulative meta-analysis to gain insight into the research dynamics in time. Differences were considered statistically significant at a 2-sided p value < 0.05.

Results

Search results and eligible studies Nineteen studies, accounting for 2032 patients, were finally included in the meta-analysis [13–18, 23–35]. The review process is depicted in Fig. 1. Six studies [13–18], combining 1300 patients, were included for the calculations of the pooled ORs of all-cause mortality. The data for cardiovascular mortality were not available in one study [13]. Therefore, it was based on five studies comprising 1246 patients [13–16, 24]. The characteristics of these studies and number of events stratified by the presence or absence of LGE are listed in Table 2. Finally, 6 studies (1044 patients) were included for the calculations of the pooled ORs of quantitative LGE by % of LV mass [13, 15, 18, 29, 30, 32]. All 19 studies were analysed for prevalence of LGE.

Table 1 Quality assessment using Cochrane method

First author, study year (ref. no.)	Selection bias	Performance bias	Attrition bias	Detection bias	Reporting bias
Azevedo et al 2009 [13]	Yes	No	Yes	No	No
Dweck et al 2010 [14]	Yes	No	No	No	No
Barone-Rochette et al 2014 [15]	Yes	No	No	No	No
Chin et al 2016 [16]	Yes	No	Unclear	No	No
Rajesh et al 2017 [17]	Yes	Yes	Unclear	No	No
Musa et al 2018 [18]	Yes	No	Unclear	No	No

No—low risk of bias, yes—high risk of bias

Study characteristics All studies were prospective cohort studies, and the majority was single centre, except for 2 studies, which were multicentre [18, 34]. Mean follow-up duration was 2.8 years. In the majority of studies, patients with severe AS underwent surgical aortic valve replacement (SAVR), and 6 studies also investigated patients undergoing transcatheter aortic valve implantation (TAVI) [15, 18, 27, 31, 32, 35].

Patient characteristics The age of patients ranged from 47 to 83 years (mean 69.8) and male patients dominated in all of the studies. Hypertension was the most common co-morbidity

(61.4%). Also, 39.8% of all patients had coronary artery disease (CAD), and 7 studies excluded patients with CAD [13, 23–26, 28, 30]. The majority of patients had preserved LVEF (mean 57%), and high-gradient aortic stenosis (mean gradient 46 mmHg). Patients' clinical characteristics are listed in Table 3.

Prevalence and extent of LGE The majority of investigators evaluated focal fibrosis by different signal intensity thresholds above remote myocardium [13, 14, 23, 24, 26–30], 3 studies used full width half maximum (FWHM) technique [13, 16,

Fig. 1 PRISMA flow chart of study selection. CMR, cardiovascular magnetic resonance; HD, heart disease; LGE, late gadolinium enhancement
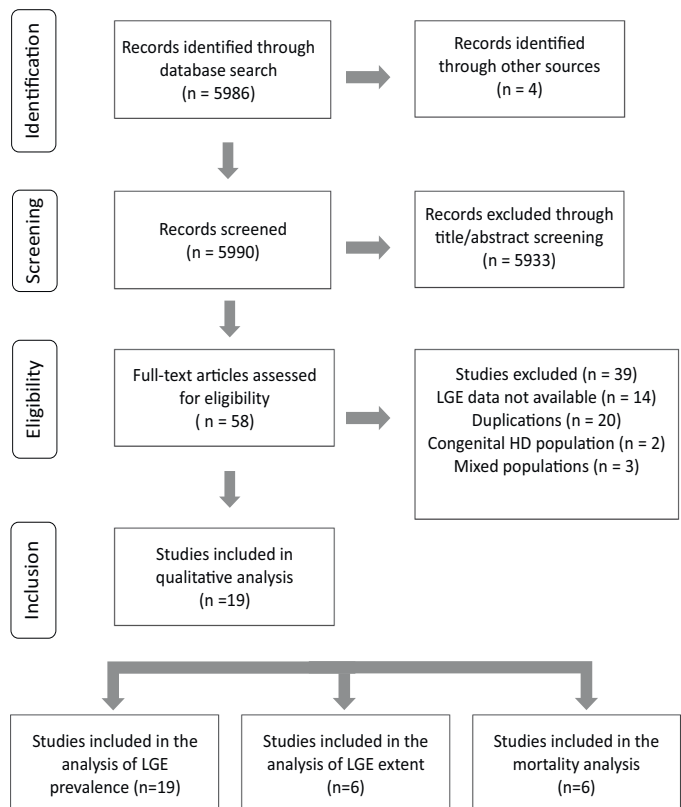
Table 2 Description of studies included in meta-analysis of clinical outcomes and number of outcomes by LGE status

First author, study year, (ref. no.)	Study design	Number of patients	Population	Valve intervention, n	Mean follow-up duration, years	All-cause mortality, n		CV mortality, n	
						LGE (−)	LGE (+)	LGE (−)	LGE (+)
Azevedo et al 2010 [13]	Prospective longitudinal, single centre	54	Severe AS (28), severe AR (26)	SAVR (54)	4.3 ± 1.4	3	13	NR	NR
Dweck et al 2011 [14]	Prospective longitudinal, single centre	143	Moderate AS (57), severe AS (86)	SAVR (72)	2 ± 1.4	2	25	2	21
Barone-Rochette et al 2014 [15]	Prospective longitudinal, single centre	154	Severe AS	SAVR (114), TAVI (40)	2.9	11	10	5	6
Chin et al 2016 [16]	Prospective longitudinal, single centre	166	Mild AS (34), moderate AS (45), severe AS (87)	SAVR (37)	2.9 ± 0.8	6	8	4	6
Rajesh et al 2017 [17]	Prospective longitudinal, single centre	109	Severe AS	SAVR (38)	0.96 ± 0.46	11	13	10	12
Musa et al 2018 [18]	Prospective longitudinal, multicentre	674	Severe AS	SAVR (399), TAVI (275)	3.6	45	100	16	54
Pooled, mean		1300			2.8	78	169	37	99

Values are presented as mean ± SD or n. *AS* aortic stenosis, *AR* aortic regurgitation, *CV* cardiovascular, *LGE* (+) late gadolinium enhancement positive, *LGE* (−) late gadolinium enhancement negative, *NR* not reported, *SAVR* surgical aortic valve replacement, *TAVI* transcatheter aortic valve implantation

Table 3 Patients clinical characteristics

First author, study year (ref. no.)	No. of patients	Mean age, years	Male gender, %	CAD, %	HTN, %	DM, %	AF, %	NYHA I/II/III/IV, %	LVEF, %	AV mean gradient, mm Hg
Debl et al 2006 [23]	22	64	73	Excluded	NR	NR	NR	NR	52.7	>30
Azevedo et al 2010 [13]	28	47.2±13.5	64	Excluded	0	0	NR	4/43/53/0	53±9	63±20
Dweck et al 2011 [14]	143	68±14	67	57	54	25	19	NR	57.9	NR
Barone-Rochette et al 2014 [15]	154	74±9	62	29	62	23	9	27 (III–IV)	60±15	49±17
Mahmod et al 2014 [24]	26	67.8±9.73	73	excluded	38	15	NR	NR	74.5±5.8	NR
Chin et al 2016 [16]	166	69	69	37	67	15	2	45/34/19/2	67 (63–71)	35±19
Rajesh et al 2017 [17]	109	57.3±12.5	57.8	34.8	50.4	10	NR	83.5 (I–II), 16.5 (III–IV)	56.5±12.4	44.7±13.6
Musa et al 2018 [18]	674	74.6	63	29.2	53.1	21.7	12.5	13.3/42.3/40.7/3.6	61±16.7	46±18
Weidemann et al 2009 [25]	46	69	60	Excluded	88	28	22	0/13/66/20	54.6	50.3
Nassenstein et al 2009 [26]	40	76	57.5	Excluded	NR	NR	NR	NR	64.8±13.3	NR
Kim et al 2014 [27]	61	81.9±5.3	52.5	68.9	95.1	27.9	36.1	NR	53.5±13.8	43.4±17.3
Park et al 2014 [28]	41	63.1±8.7	58.5	Excluded	36.6	7.3	NR	57.9 (III–IV)	68±8.2	55.6±20.4
Hoffmann et al 2014 [29]	30	78±7	57	NR	NR	NR	excluded	3/3/73/20	55±10	53±21
Ravenstein et al 2015 [30]	31	70±12	83	Excluded	75	17	33	48/52/0/0	NR	NR
Nucifora et al 2016 [31]	43	83	51	17	89	40	27	NR	71	NR
Lee et al 2017 [32]	127	68.8±9.2	49.6	13.4	66.1	26.8	11.8	NR	61.8±14.1	48±19.3
Carter-Storch et al. 2017 [33]	87	70	62	32	59	18	NR	NR	62±9	45.5
Singh et al 2017 [34]	174	66.2±13.34	76	NR	53.4	14.4	Excluded	NR	57	35.4
Buckert et al 2018 [35]	30	78.8±5.9	50	80	96.7	36.7	43.3	NR	56.7±18.4	34±14.6
Pooled, mean	2032	69.8	62.6	39.8	61.4	20.4	21.6		57.2	46.3

Values are mean ± SD, n (%), or median (interquartile range). *AV* aortic valve, *AF* atrial fibrillation, *AV* aortic valve, *CAD* coronary artery disease, *DM* diabetes mellitus, *LVEF* left ventricular ejection fraction, *No.* number, *NR* not reported, *NYHA* New York Heart Association

Table 4 Studies included in analysis of the prevalence and extent of LGE

First author, study year (ref. no.)	Population	No. of patients	CMR field, T	Method for evaluation of LGE	LGE (+), n (%)	LGE non-infarct pattern, n (%)	LGE % of LV mass
Debl et al 2006 [23]	Severe symptomatic AS	22	1.5	SI > 2 SDs of remote myocardium	6 (27)	NR	4.3
Azevedo et al 2010 [13] $	Severe AS (28), severe AR (26)	28	1.5	Mean SI of total myocardium ±2 SDs of mean SI of remote area+ 2 SDs of mean of air	17 (61)$	NR	3.15 ±1.87$
Dweck et al 2011 [14]	Moderate AS (57), severe AS (86)	143	1.5	FWHM	94 (66)	54 (38)	6.25
Barone-Rochette et al 2014 [15]	Severe AS	154	1.5	SI >2,4 SDs of remote myocardium	44 (29)	30 (19)	3.5 ±2.3
Mahmod et al 2014 [24]	Severe AS	26	3	FWHM	21 (81)	NR	18.3 ±9.4
Chin et al 2016 [16]	Mild AS (34), moderate AS (45), severe AS (87)	166	3	Semiautomatic	44 (27)	44 (100)	NR
Rajesh et al 2017 [17]	Severe AS	109	1.5	SI >2.4 SDs of remote myocardium	46 (42)	33 (30)	NR
Musa et al 2018 [18]	Severe AS	674	1.5 and 3	FWHM	341 (50.6)	222 (65)	2.72 13.95
Weidemann et al 2009 [25]	Severe AS	46	1.5	Visual	28 (60.8)	NR	NR
Nassenstein et al 2009 [26]	Moderate AS (14), severe AS (26) with LVH ≥15 mm	40	1.5	Visual	13 (32.5)	13 (100)	NR
Kim et al 2014 [27]	Severe AS	61	1.5	Semiautomatic	42 (68.8)	NR	7.4
Park et al 2014 [28]	Severe AS, preserved LVEF	41	1.5	Mean SI of total myocardium ±2 SDs of mean SI of remote area + 2 SDs of mean of air	12 (29.3)	12 (100)	NR
Hoffmann et al 2014 [29]	Severe AS	30	1.5	SI > 6 SDs of remote myocardium	27 (90)	NR	7.7 ±4.6
Ravenstein et al 2015 [30] $	Severe AS (12), severe AR (9), severe MR (10)	31	3	SI >2.4 SDs of remote myocardium	17 (54.8)	17 (100)	1.4 ±0.8$
Nucifora et al 2016 [31]	Severe AS	43	1.5	SI > 5 SDs of remote myocardium	29 (67.4)	NR	5.8
Lee et al 2017 [32]	Moderate AS, severe AS	127	3	SI > 5 SDs of remote myocardium	41 (32.3)	NR	5.2 ±4.8
Carter-Storch et al 2017 [33]	Severe AS	87	1.5	Visual	26 (30)	18 (20.6)	NR
Singh et al 2017 [34]	Asymptomatic moderate-severe AS	174	3	NR	82 (47)	NR	4.3
Buckert et al 2018 [35]	Severe AS	30	1.5	Visual	14 (46.7)	NR	NR
Pooled, mean		2032			944 (49.6)	443 (63.6)	5.8

Values are mean ± SD or n (%). *CMR* cardiovascular magnetic resonance, *FWHM* full width half maximum, *LVH* left ventricular hypertrophy, *MR* mitral regurgitation, *SI* signal intensity. Other abbreviations as in Tables 2 and 3

$ Only the data of severe AS patients extracted

Table 5 LGE prevalence by the presence of coronary artery disease

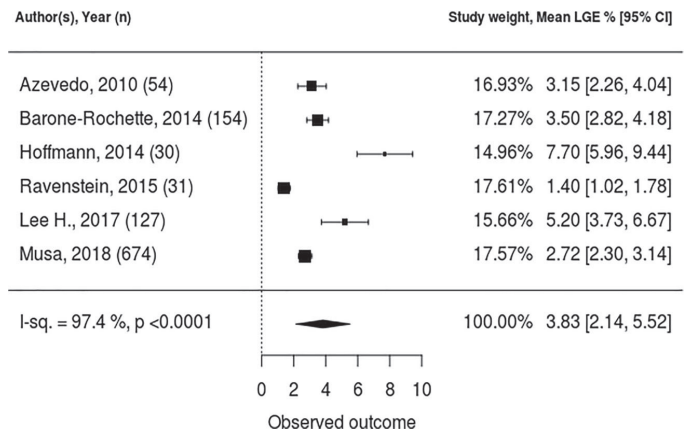| Patients by CAD status	No. of patients	LGE (+), n (%)	LGE non-infarct pattern, %
CAD (−)	976	430 (44.0)	93.6[$]
CAD (+)[&]	400	251 (62.8)	45.4

Values are n (%). Abbreviations as in Tables 2 and 3

[$] Data from 4 studies reporting LGE pattern in CAD-free patients

[&] Data from 5 studies reporting presence of LGE by CAD status

24] and the minority used visual assessment. The prevalence and extent of LGE are depicted in Table 4. LGE was present in a variable proportion of patients with AS (27% to 90%), and overall, 944 patients (49.6%) had LGE. Nine studies have reported the type of LGE [14–18, 26, 28, 30, 33], and two thirds of AS patients (63.6%) exhibited a non-infarct LGE pattern. An additional analysis of the type and prevalence of LGE depending on the CAD status was performed. Patients with concomitant coronary artery disease, compared to those with unobstructed coronary arteries, had higher prevalence of LGE (62.8% vs. 44%, respectively). The vast majority of CAD-free patients exhibited non-infarct LGE pattern (93.6%), whilst infarct pattern LGE dominated in patients with coexistent CAD (54.6%) (Table 5). LGE was reported to be more prevalent in males and in those with LV systolic dysfunction and worse functional status. LGE was more frequently found in patients with higher indexed LV mass and higher indexed LV end-systolic and LV end-diastolic volumes. The clinical characteristics of patients with and without LGE, when available, are presented in Supplementary Files Table S2.

In addition, 12 studies reported the extent of LGE by % of LV mass, which ranged from 1.4 to 18.3% [13–15, 18, 23, 24, 27, 29–32, 34]. The pooled extent of focal fibrosis as measured in % of LV mass was around 4% with precise point estimate and (95% CI) being equal to 3.83 and (2.14, 5.52), respectively (Fig. 2).

LGE and prognosis The all-cause mortality occurred in 247 patients (19%), 169 of them with LGE (28% of LGE-positive patients) and 78 without LGE (11.2% of LGE-negative patients). The presence of LGE was associated with significantly higher all-cause mortality (pooled OR [95% CI] = 3.26 [1.72, 6.18], $p = 0.0003$) (Fig. 3). The cardiovascular mortality occurred in 136 patients (10.9%), 99 of them with LGE (7.9% of LGE-positive patients) and 37 without LGE (3% of LGE-negative patients). The presence of LGE was associated with significantly higher cardiovascular mortality (pooled OR [95% CI] = 2.89 [1.90, 4.38], $p < 0.0001$) (Fig. 4).

Sensitivity analysis and cumulative meta-analysis We have performed 1-study removal analysis to see whether removal of any of the studies changes the meta-analysis results substantially.

Sensitivity analysis for all-cause mortality Heterogeneity was absent after removal of studies by Azevedo et al [13] or Dweck et al [14] (p values for heterogeneity were 0.480 and 0.056, respectively). No change was detected after removing of any of the remaining four studies: heterogeneity was present, pooled OR was substantially higher and it did not fall below 3.52 (Supplementary Files Table S3). These findings fully agree with simple and cumulative all-cause mortality forest plots given in Fig. 3 and Fig. 5, respectively.

Fig. 2 Forest plot for quantitative LGE, expressed in % of LV mass

Author(s), Year (n)		Study weight, Mean LGE % [95% CI]
Azevedo, 2010 (54)		16.93% 3.15 [2.26, 4.04]
Barone-Rochette, 2014 (154)		17.27% 3.50 [2.82, 4.18]
Hoffmann, 2014 (30)		14.96% 7.70 [5.96, 9.44]
Ravenstein, 2015 (31)		17.61% 1.40 [1.02, 1.78]
Lee H., 2017 (127)		15.66% 5.20 [3.73, 6.67]
Musa, 2018 (674)		17.57% 2.72 [2.30, 3.14]
I-sq. = 97.4 %, p <0.0001		100.00% 3.83 [2.14, 5.52]

Fig. 3 Forest plot and pooled odds ratio for all-cause mortality

Author(s) and Year	Study weight, OR [95% CI]
Azevedo, 2010	10.05% 27.08 [5.25, 139.64]
Dweck, 2011	11.38% 8.51 [1.92, 37.67]
Barone-Rochette, 2014	18.01% 2.65 [1.03, 6.78]
Chin, 2016	15.66% 2.16 [0.71, 6.54]
Rajesh, 2017	18.42% 1.86 [0.75, 4.64]
Musa, 2018	26.48% 2.09 [1.41, 3.11]
I-sq. = 62.77 %, p = 0.035	100.00% 3.26 [1.72, 6.18]
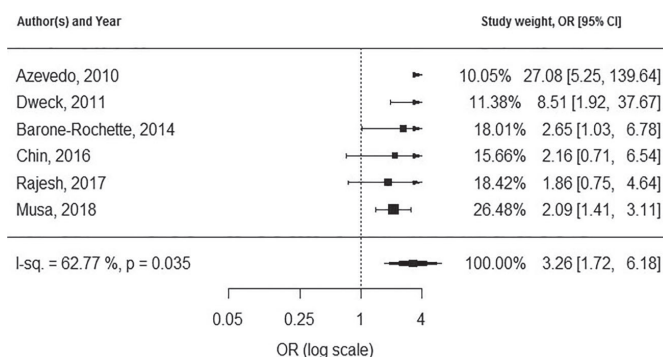
Sensitivity analysis for CV mortality The results did not change substantially after removal any of the studies (Supplementary Files Table S4) (Fig.6).

Compared to the other studies, 2 studies [13, 14] reported very high odds ratios for adverse events. Dweck et al [14] studied 143 patients with moderate and severe AS and reported 8- and 6-fold higher rates of all-cause mortality in patients with non-ischemic and ischemic LGE, respectively, compared with those without LGE. However, in that study, patients with LGE were significantly older (70 vs. 64 years, respectively, $p = 0.031$) and had a higher burden of CAD (98% vs. 42% vs. 37%, respectively, $p < 0,001$). Azevedo et al [13], in a mixed cohort of patients (28 with AS and 24 with aortic regurgitation), demonstrated that LGE was associated with higher all-cause mortality late after surgical AVR. In that study, more than half of all patients were in poor functional status (53% NYHA functional class III). The mortality rate (6.8%/year) was high, which may reflect the more heterogeneous patient population with higher baseline risk in the earlier study.

Publication bias

We have performed two types of tests for publication bias measured by asymmetry of funnel plot: the tests having standard error as independent variable and the tests having sample size as an independent variable. Egger's test suggested the absence of publication bias (Supplementary Files Table S5). Visual inspection of Begg's funnel plot for cardiovascular mortality revealed that the studies were equally distributed around the overall estimate (Supplementary Files Fig. 1). In the plot of all-cause mortality, several points did not fall within the confidence region (Supplementary Files Fig. 2). This resulted in the presence of heterogeneity ($I^2 = 62.77\%$, $p = 0.0035$; see forest plot for all-cause mortality given in Fig. 3).

Discussion

This meta-analysis is the first large-scale analysis consolidating the data from single-centre and multicentre studies on the prevalence and prognostic value of LGE in aortic stenosis. From the data of 19 studies with 2032 patients, we have demonstrated that LGE was present in a considerable proportion of patients with AS (49.6%) and had a strong and significant association with the clinical outcomes. This association was consistently observed across all studies and was independent of potential confounders on multivariable analysis. LGE remained an independent risk factor after adjusting for age, NYHA functional class, LV ejection fraction and other variables.

Fig. 4 Forest plot and pooled odds ratio for cardiovascular mortality
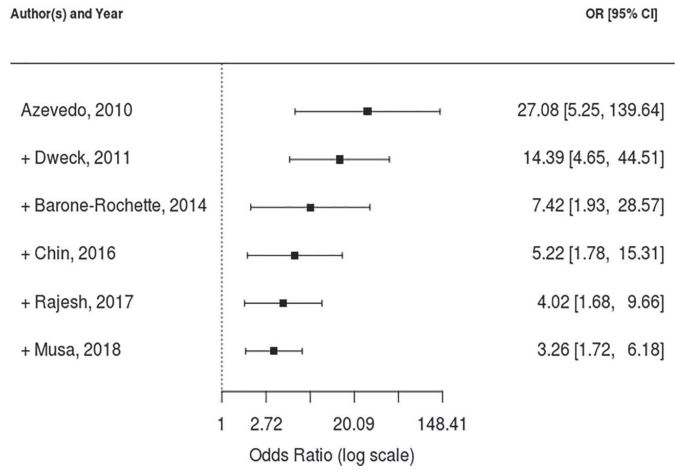

Author(s) and Year	Study weight, OR [95% CI]
Dweck, 2011	7.77% 6.76 [1.51, 30.18]
Barone-Rochette, 2014	11.25% 3.32 [0.96, 11.50]
Chin, 2016	10.20% 2.40 [0.65, 8.86]
Rajesh, 2017	19.55% 1.87 [0.73, 4.80]
Musa, 2018	51.22% 3.01 [1.68, 5.39]
I-sq. = 0.00 %, p = 0.699	100.00% 2.89 [1.90, 4.38]

Springer
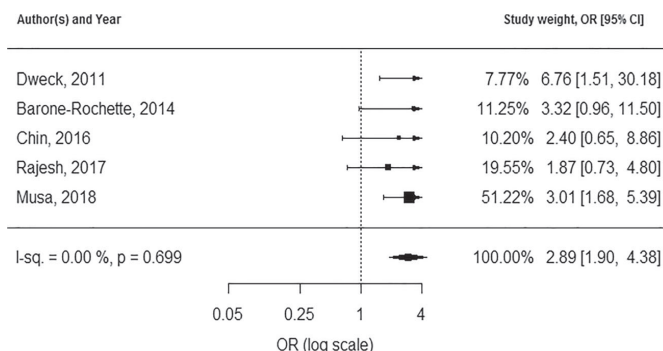
Fig. 5 Cumulative analysis for all-cause mortality

Author(s) and Year		OR [95% CI]
Azevedo, 2010		27.08 [5.25, 139.64]
+ Dweck, 2011		14.39 [4.65, 44.51]
+ Barone-Rochette, 2014		7.42 [1.93, 28.57]
+ Chin, 2016		5.22 [1.78, 15.31]
+ Rajesh, 2017		4.02 [1.68, 9.66]
+ Musa, 2018		3.26 [1.72, 6.18]

1   2.72   20.09   148.41

Odds Ratio (log scale)

In the present meta-analysis, including 6 studies with 1300 patients over a mean follow-up of 2.8 years, we have demonstrated that LGE tripled all-cause and cardiovascular mortality (pooled ORs, 3.26 and 2.89, respectively). Focal fibrosis was associated with increased mortality irrespective of scar aetiology [14, 18]. Two studies [15, 18], incorporating 315 patients with severe AS patients undergoing TAVI, have demonstrated that the prognostic value of LGE also applies to this population. This is of great importance, because TAVI candidates represent a much higher risk population in whom the indications and the timing of intervention are still being defined.

Our study is consistent and extends the results of previous reports. Chen et al [36] performed a meta-analysis evaluating 626 patients over a mean follow-up of 2.5 years, and significant associations between LGE and mortality were found. Since that meta-analysis, a large multicentre study was published [18], allowing to increase the number of studied patients and to improve the validity and precision of the final result. Additionally, the present meta-analysis also includes an analysis of the prevalence and type of LGE, as well as a pooled meta-analysis of the burden of LGE in the AS population. For that reason, we considered that the present work was appropriate and necessary.

The most frequent type of LGE described was non-infarct, found in 63.6% of all LGE-positive patients. The large variability in the prevalence of LGE between the studies can be explained by inconsistent characteristics of study populations—patients differing by the aortic stenosis severity, symptom status and other variables. The role of CAD in the development of LGE deserves further consideration, as it was present in about 40% of patients. As anticipated, patients with concomitant CAD had higher prevalence of LGE, which was predominantly infarct type. On the

Fig. 6 Cumulative analysis for cardiovascular mortality

Author(s) and Year		OR [95% CI]
Dweck, 2011		6.76 [1.51, 30.18]
+ Barone-Rochette, 2014		4.44 [1.70, 11.54]
+ Chin, 2016		3.58 [1.66, 7.74]
+ Rajesh, 2017		2.76 [1.52, 5.01]
+ Musa, 2018		2.89 [1.90, 4.38]

1   2.72   7.39   20.09   54.6

Odds Ratio (log scale)
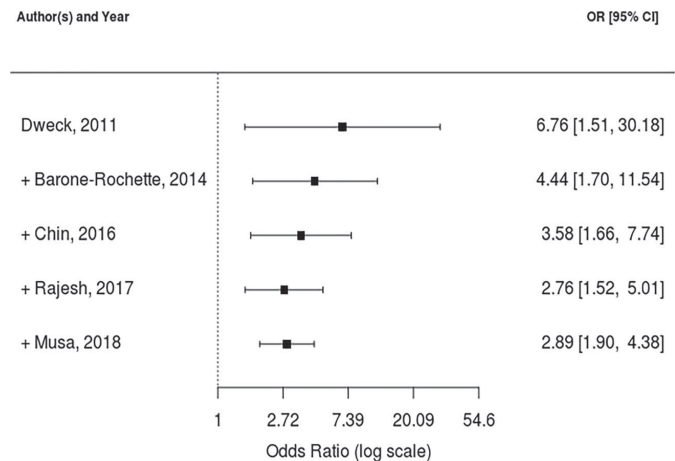
contrary, CAD-free patients mostly exhibited non-infarct or AS-related focal fibrosis. A dual LGE pattern of both myocardial infarction and mid-wall fibrosis was observed in some patients. Although it is important to make a distinction between the different LGE patterns, it appears that all myocardial scars, regardless of their aetiology, are predictive of adverse outcomes. In a study by Musa et al [18], outcomes of severe AS patients with different types of LGE were compared. Investigators showed that either type of focal fibrosis (infarct and non-infarct) significantly reduced long-term survival, when compared to patients with no LGE. Moreover, in a study by Dweck et al [14], non-infarct LGE pattern was associated with the worst prognosis. Authors showed that patients with mid-wall or infarct pattern of enhancement, compared to patients with no LGE, experienced an 8- and 6-fold increase in mortality, respectively.

The LV sites of myocardial involvement were highly variable, with a predominant location of myocardial fibrosis in the basal part of the LV [17, 25, 26, 37]. One possible explanation for that is the magnitude of hypertrophy at the base of the LV, with the highest involvement of the basal septum [38]. Treibel et al [39], investigating 133 patients with severe AS undergoing SAVR, found that up to 60% of the LGE was located at the right ventricular insertion point. Although it is generally presumed that LGE equates myocardial fibrosis, this may not always be the case. LGE, when isolated to the right ventricular insertion point, frequently observed in AS patients, may represent expanded extracellular volume, rather than replacement fibrosis [40]. It has been shown that in patients with hypertrophic cardiomyopathy, LGE that is isolated to right ventricular insertion points was not associated with increased risk [41]. However, none of the studies included in the present meta-analysis investigated the association between location of the LGE and the risk for adverse events.

Although the presence of LGE clearly portends a higher risk for adverse events, it should not be used as a binary tool, as half of all patients with AS have some degree of LGE on CMR. Across the included studies, reported extent of LGE was variable, and the pooled extent of focal fibrosis as measured by % of LV mass was around 4%. These differences probably are due not only to the heterogeneity of included populations but also to the different methods used for myocardial fibrosis quantification. As there is no consensus for how to quantify LGE, different methods have been used. The majority of investigators used different signal intensity thresholds above remote myocardium, and the FWHM method was used by a few. In AS, LGE is frequently less well defined than in infarction, and delineation of myocardium with normal signal might be challenging. Previous reports have shown that the FWHM technique was the most reproducible for LGE quantification across the spectrum of cardiac diseases [42]. Two studies have analysed the risk ratios expressed by quantitative LGE by % of LV mass [14, 18]. Dweck et al [14] reported that with every 1% increase in the LGE mass, the risk of mortality increased by 5% (HR, 1.05; 95%

CI, 1.01 to 1.09; $p = 0.005$). Similarly, in a study by Musa et al [18], a 1% increase in LV myocardial scar burden was associated with an 11% higher all-cause mortality hazard (HR 1.11; 95% CI, 1.05–1.17; $p < 0.001$) and an 8% higher cardiovascular mortality hazard (HR 1.08; 95% CI, 1.01–1.17; $p < 0.001$). In addition to the traditional LGE-CMR image analysis, novel markers of myocardial texture analysis have been investigated in patients with cardiomyopathies, providing further insights into the myocardial structural arrangement. By using a range of quantitative parameters, including energy, skewness, uniformity and cluster tendency, it characterises the heterogeneity of fibrotic lesions. Preliminary data show that texture features linked to LGE heterogeneity were strongly associated with adverse events in hypertrophic cardiomyopathy patients [43] and with malignant arrhythmias in patients with previous myocardial infarction [44]. Therefore, LGE texture analysis could be further tested in aortic stenosis patients, possibly providing new information and aiding in patient risk stratification.

Everett et al [45], in a cohort of 61 asymptomatic moderate and severe AS patients over a median follow-up of 2.1 years, demonstrated the rapid progression of mid-wall fibrosis (78% increase in LGE mass per year). None of the patients with LGE showed resolution of established fibrosis post-AVR. In agreement, no change in LGE following aortic valve replacement was reported in 5 other studies [13, 14, 25, 31, 39]. It appears that once established, focal fibrosis is not reversible after the valve intervention, leaving these patients with residual risk for adverse events. These findings suggest that current management strategies do not completely identify high-risk patients with severe AS and that the scar that patients develop whilst waiting for intervention contributes to their poorer long-term prognosis. A key goal of decision-making is to reliably identify those who are 'pre-symptomatic', so that intervention can be offered before the LV dysfunctions develops and operative morbidity increases. Therefore, randomised clinical trials investigating structural LV remodelling and optimal timing for aortic valve intervention in asymptomatic severe AS patients are needed. Currently, this hypothesis is being tested in EVOLVED (Early Valve Replacement guided by Biomarkers of Left Ventricular Decompensation in Asymptomatic Patients with Severe Aortic Stenosis) randomised controlled trial (NCT03094143), which hopefully will give as answers whether patients with signs of LV decompensation will benefit from early AVR.

Study limitations

As in many cardiac centres CMR is not a routine workup test before aortic valve intervention, some patients may have been referred for investigation on clinical grounds, which may have introduced a referral bias. This could have led to overestimation of the LGE prevalence and limit the applicability of the results to the broad population of patients with aortic stenosis. The

🖄 Springer

meta-analysis was also limited to inconsistent characteristics of the study populations and variability in the degree of aortic valve disease severity included. A significant number of single-centre studies (20) was excluded from the analysis due to the risk of data overlap. Without access to individual patient data, we had to use estimated event rates in several studies that could have had an impact on the final result of the pooled analysis. Limited data and inability to use raw datasets precluded subgroup analysis.

Conclusion

The present report significantly strengthens and clarifies the evidence available to date about the association between LGE detected by CMR and mortality in patients with AS. Our results suggest that LGE is highly prevalent in aortic stenosis patients, likely representing irreversible LV damage and predicting poor outcomes. Further refinement of risk stratification is required in asymptomatic AS patients.

Compliance with ethical standards

Guarantor The scientific guarantor of this publication is Prof. Peter Sogaard, MD, PhD.

Conflict of interest The authors state that they have no conflict of interest.

Statistics and biometry One of the authors has significant statistical expertise—Assoc. Prof. Viktor Skorniakov, PhD.

Informed consent Written informed consent was not required for this study because only published data were used.

Ethical approval Institutional Review Board approval was not required for this study because only published data were used.

Study subjects or cohorts overlap Studies with possibly overlapping data were excluded from the analysis.

Methodology
• Meta-analysis

References

1. Dweck MR, Boon NA, Newby DE (2012) Calcific aortic stenosis: a disease of the valve and the myocardium. J Am Coll Cardiol 60: 1854–1863
2. Carabello BA, Paulus WJ (2009) Aortic stenosis. Lancet 373:956–966
3. Hein S, Arnon E, Kostin S et al (2003) Progression from compensated hypertrophy to failure in the pressure-overloaded human

heart: structural deterioration and compensatory mechanisms. Circulation. 107:984–991
4. Baumgartner H, Falk V, Bax JJ, Group ESCSD et al (2017) 2017 ESC/EACTS Guidelines for the management of valvular heart disease. Eur Heart J 38:2739–2791
5. Kusunose K, Goodman A, Parikh R et al (2014) Incremental prognostic value of left ventricular global longitudinal strain in patients with aortic stenosis and preserved ejection fraction. Circ Cardiovasc Imaging 7:938–945
6. Iles LM, Ellims AH, Llewellyn H et al (2015) Histological validation of cardiac magnetic resonance analysis of regional and diffuse interstitial myocardial fibrosis. Eur Heart J Cardiovasc Imaging 16: 14–22
7. Lehrke S, Lossnitzer D, Schöb M et al (2011) Use of cardiovascular magnetic resonance for risk stratification in chronic heart failure: prognostic value of late gadolinium enhancement in patients with non-ischaemic dilated cardiomyopathy. Heart 97(9):727–732
8. Green JJ, Berger JS, Kramer CM, Salerno M (2012) Prognostic value of late gadolinium enhancement in clinical outcomes for hypertrophic cardiomyopathy. JACC Cardiovasc Imaging 5(4):370–377
9. Avanesov M, Münch J, Weinrich J et al (2017) Prediction of the estimated 5-year risk of sudden cardiac death and syncope or nonsustained ventricular tachycardia in patients with hypertrophic cardiomyopathy using late gadolinium enhancement and extracellular volume CMR. Eur Radiol 27(12):5136–5145
10. Moher D, Liberati A, Tetzlaff J, Altman DG, PRISMA Group (2009) Preferred reporting items for systematic reviews and meta-analyses: the PRISMA statement. BMJ 339:b2535
11. Higgins JPT, Altman DG (2008) Chapter 8: assessing risk of bias in included studies. In: Higgins JPT, Green S (eds) Cochrane handbook for systematic reviews of interventions. Cochrane Collaboration, Copenhagen
12. Wells GA, Shea B, O'Conell D, et al The Newcastle-Ottawa Scale (NOS) for assessing the quality of nonrandomized studies in meta-analysis. http://www.ohri.ca/programs/clinical_ epidemiology/oxford.asp
13. Azevedo CF, Nigri M, Higuchi ML et al (2010) Prognostic significance of myocardial fibrosis quantification by histopathology and magnetic resonance imaging in patients with severe aortic valve disease. J Am Coll Cardiol 56(4):278–287
14. Dweck MR, Joshi S, Murigu T et al (2011) Midwall fibrosis is an independent predictor of mortality in patients with aortic stenosis. J Am Coll Cardiol 58(12):1271–1279
15. Barone-Rochette G, Piérard S, De Meester de Ravenstein C et al (2014) Prognostic significance of LGE by CMR in aortic stenosis patients undergoing valve replacement. J Am Coll Cardiol 64(2): 144–154
16. Chin CW, Everett RJ, Kwiecinski J et al (2017) Myocardial fibrosis and cardiac decompensation in aortic stenosis. JACC Cardiovasc Imaging 10(11):1320–1333
17. Rajesh GN, Thottian JJ, Subramaniam G, Desabandhu V, Sajeev CG, Krishnan MN (2017) Prevalence and prognostic significance of left ventricular myocardial late gadolinium enhancement in severe aortic stenosis. Indian Heart J 69(6):742–750
18. Musa TA, Treibel TA, Vassiliou VS et al (2018) Myocardial scar and mortality in severe aortic stenosis. Circulation 138(18):1935–1947
19. R Core Team. R: a language and environment for statistical computing. R Foundation for Statistical Computing, Vienna, Austria. 2018. https://www.R-project.org/
20. Viechtbauer W (2010) Conducting meta-analyses in R with the metafor package. J Stat Softw 36(3):1–48 http://www.jstatsoft.org/v36/i03/

21. Veroniki AA, Jackson D, Viechtbauer W et al (2016) Methods to estimate the between-study variance and its uncertainty in meta-analysis. Res Synth Methods 7(1):55–79

22. Sterne JA, Egger M. Regression methods to detect publication and other bias in meta-analysis. Publication Bias in Meta-Analysis 2006; https://doi.org/10.1002/0470870168.ch6

23. Debl K, Djavidani B, Buchner S et al (2006) Delayed hyperenhancement in magnetic resonance imaging of left ventricular hypertrophy caused by aortic stenosis and hypertrophic cardiomyopathy: visualisation of focal fibrosis. Heart. 92(10):1447–1451

24. Mahmod M, Piechnik SK, Levelt E et al (2014) Adenosine stress native T1 mapping in severe aortic stenosis: evidence for a role of the intravascular compartment on myocardial T1 values. J Cardiovasc Magn Reson 16:92

25. Weidemann F, Herrmann S, Störk S et al (2009) Impact of myocardial fibrosis in patients with symptomatic severe aortic stenosis. Circulation 120(7):577–584

26. Nassenstein K, Bruder O, Breuckmann F, Erbel R, Barkhausen J, Schlosser T (2009) Prevalence, pattern, and functional impact of late gadolinium enhancement in left ventricular hypertrophy due to aortic valve stenosis. Rofo 181(5):472–476

27. Kim WK, Rolf A, Liebetrau C et al (2014) Detection of myocardial injury by CMR after transcatheter aortic valve replacement. J Am Coll Cardiol 64(4):349–357

28. Park J, Chang HJ, Choi JH et al (2014) Late gadolinium enhancement in cardiac MRI in patients with severe aortic stenosis and preserved left ventricular systolic function is related to attenuated improvement of left ventricular geometry and filling pressure after aortic valve replacement. Korean Circ J 44(5):312–319

29. Hoffmann R, Altiok E, Friedman Z, Becker M, Frick M (2014) Myocardial deformation imaging by two-dimensional speckle-tracking echocardiography in comparison to late gadolinium enhancement cardiac magnetic resonance for analysis of myocardial fibrosis in severe aortic stenosis. Am J Cardiol 114(7):1083–1088

30. de Meester de Ravenstein C, Bouzin C, Lazam S et al (2015) Histological validation of measurement of diffuse interstitial myocardial fibrosis by myocardial extravascular volume fraction from Modified Look-Locker imaging (MOLLI) T1 mapping at 3 T. J Cardiovasc Magn Reson 17:48

31. Nucifora G, Tantiongco JP, Crouch G et al (2017) Changes of left ventricular mechanics after trans-catheter aortic valve implantation and surgical aortic valve replacement for severe aortic stenosis: A tissue-tracking cardiac magnetic resonance study. Int J Cardiol 228:184–190

32. Lee H, Park JB, Yoon YE et al (2018) Noncontrast myocardial T1 mapping by cardiac magnetic resonance predicts outcome in patients with aortic stenosis. JACC Cardiovasc Imaging 11(7):974–983

33. Carter-Storch R, Møller JE, Christensen NL et al (2017) Postoperative reverse remodeling and symptomatic improvement in normal-flow low-gradient aortic stenosis after aortic valve replacement. Circ Cardiovasc Imaging 10(12):e006580

34. Singh A, Greenwood JP, Berry C et al (2017) Comparison of exercise testing and CMR measured myocardial perfusion reserve for predicting outcome in asymptomatic aortic stenosis: the PRognostic Importance of MIcrovascular Dysfunction in Aortic Stenosis (PRIMID AS) Study. Eur Heart J 38(16):1222–1229

35. Buckert D, Cieslik M, Tibi R et al (2018) Longitudinal strain assessed by cardiac magnetic resonance correlates to hemodynamic findings in patients with severe aortic stenosis and predicts positive remodeling after transcatheter aortic valve replacement. Clin Res Cardiol 107(1):20–29

36. Chen H, Zeng J, Liu D, Yang Q (2018) Prognostic value of late gadolinium enhancement on CMR in patients with severe aortic valve disease: a systematic review and meta-analysis. Clin Radiol S0009–9260(18)30365–9

37. Fairbairn TA, Steadman CD, Mather AN et al (2013) Assessment of valve haemodynamics, reverse ventricular remodelling and myocardial fibrosis following transcatheter aortic valve implantation compared to surgical aortic valve replacement: a cardiovascular magnetic resonance study. Heart. 99(16):1185–1191

38. Dweck MR, Joshi S, Murigu T et al (2012) Left ventricular remodeling and hypertrophy in patients with aortic stenosis: insights from cardiovascular magnetic resonance. J Cardiovasc Magn Reson 14:50

39. Treibel TA, López B, González A et al (2018) Reappraising myocardial fibrosis in severe aortic stenosis: an invasive and noninvasive study in 133 patients. Eur Heart J 39(8):699–709

40. Kuribayashi T, Roberts WC (1992) Myocardial disarray at junction of ventricular septum and left and right ventricular free walls in hypertrophic cardiomyopathy. Am J Cardiol 70:1333–1340

41. Chan RH, Maron BJ, Olivotto I et al (2015) Significance of late gadolinium enhancement at right ventricular attachment to ventricular septum in patients with hypertrophic cardiomyopathy. Am J Cardiol 116:436–441

42. Flett AS, Hasleton J, Cook C et al (2011) Evaluation of techniques for the quantification of myocardial scar of differing etiology using cardiac magnetic resonance. JACC Cardiovasc Imaging 4(2):150–156

43. Cheng S, Fang M, Cui C et al (2018) LGE-CMR-derived texture features reflect poor prognosis in hypertrophic cardiomyopathy patients with systolic dysfunction: preliminary results. Eur Radiol 28(11):4615–4624

44. Gibbs T, Villa ADM, Sammut E et al (2018) Quantitative assessment of myocardial scar heterogeneity using cardiovascular magnetic resonance texture analysis to risk stratify patients post-myocardial infarction. Clin Radiol 73(12):1059.e17–1059.e26

45. Everett RJ, Tastet L, Clavel MA et al (2018) Progression of hypertrophy and myocardial fibrosis in aortic stenosis: a multicenter cardiac magnetic resonance study. Circ Cardiovasc Imaging 11(6):e007451

2nd publication/2 publikacija

Transthyretin cardiac amyloidosis in aortic stenosis: Prevalence, diagnostic challenges, and clinical implications.

Balciunaite G, Rimkus A, Zurauskas E, Zaremba T, Palionis D, Valeviciene N, Aidietis A, Serpytis P, Rucinskas K, Sogaard P, Glaveckaite S, Zorinas A, Janusauskas V.

Review Article

Transthyretin cardiac amyloidosis in aortic stenosis: Prevalence, diagnostic challenges, and clinical implications

Giedre Balciunaite [1,*], Arnas Rimkus [1], Edvardas Zurauskas [2], Tomas Zaremba [1,3], Darius Palionis [4], Nomeda Valeviciene [4], Audrius Aidietis [1], Pranas Serpytis [1], Kestutis Rucinskas [1], Peter Sogaard [1,3], Sigita Glaveckaite [1], Aleksejus Zorinas [1], Vilius Janusauskas [1]

[1] Clinic of Cardiovascular Diseases, Institute of Clinical Medicine, Vilnius University Faculty of Medicine, Santariskiu st. 2, 08661, Vilnius, Lithuania
[2] National Center of Pathology, Vilnius University Hospital Santaros Klinikos, P. Baublio str. 5, 08406, Vilnius, Lithuania
[3] Aalborg University Hospital, Clinical Institute of Aalborg University, Hobrovej 18-22, 9100, Aalborg, Denmark
[4] Department of Radiology, Nuclear Medicine and Medical Physics, Institute of Biomedical Sciences, Vilnius University Faculty of Medicine, Santariskiu st. 2, 08661, Vilnius, Lithuania

ABSTRACT

Transthyretin cardiac amyloidosis (ATTR-CA) is a challenging and underdiagnosed cause of heart failure. Advances in cardiac imaging have enabled noninvasive diagnosis of ATTR-CA, causing the recent upsurge in disease awareness and detection. ATTR-CA has been increasingly recognized in patients with degenerative aortic stenosis (AS). With the growing number of elderly patients undergoing aortic valve intervention, the identification of ATTR-CA in this group of patients is of high clinical importance. Timely and correct diagnosis is essential for amyloid-directed therapies, as well as deciding on the AS treatment strategy. This review provides a comprehensive overview of the recent studies investigating coexistence of these two entities. We present the data on the prevalence of ATTR-CA in AS and their prognostic associations. As the diagnosis of ATTR-CA may be challenging, special attention is paid to the diagnostic utility of different imaging modalities, namely, echocardiography, cardiovascular magnetic resonance, nuclear imaging, and distinctive imaging features, in patients with dual pathology. We also present a flowchart summarizing integrated imaging in patients with suspected ATTR-CA.
© 2019 Hellenic Society of Cardiology. Publishing services by Elsevier B.V. This is an open access article under the CC BY-NC-ND license (http://creativecommons.org/licenses/by-nc-nd/4.0/).

1. Introduction

Transthyretin cardiac amyloidosis (ATTR-CA) is described as a progressive infiltrative cardiomyopathy with ventricular wall thickening and, predominantly, diastolic heart failure.[1] ATTR-CA can be either hereditary, resulting from >120 mutations in the transport protein transthyretin, or acquired, wild-type ATTR-CA.[2,3] Until recently, ATTR-CA was considered a rare type of infiltrative cardiomyopathy, and traditional gold standard for diagnosis was positive endomyocardial biopsy in the context of characteristic clinical and imaging features. Advances in diagnostic imaging, including contrast-enhanced cardiovascular magnetic resonance (CMR) with T1 mapping,[4] and nuclear imaging with technetium-labeled bone-seeking tracers,[5,6] permit noninvasive, non-histological diagnosis of ATTR-CA that substantially increased disease awareness and recognition in the last decade.[7] Degenerative aortic stenosis (AS) is the most common valvular heart disease in developed countries.[8] Excessive remodeling of the left ventricular (LV) myocardium and restrictive physiology with preserved LV ejection fraction are both features of ATTR-CA and AS.[3,9] The prevalence of both ATTR-CA and AS increases with age, and a growing number of studies have investigated their coexistence.[10–16] As both diseases share similar clinical and

echocardiographic characteristics, recognition of superimposed ATTR-CA in patients with AS can be very challenging. However, accurate diagnosis is critical for the management of both pathologies, guiding amyloid-directed therapies and deciding on the AS treatment strategy. In this review, we aimed to summarize the available evidence on prevalence, diagnostic implications, and prognostic associations of ATTR-CA in patients with AS.

2. Prevalence of ATTR-CA in aortic stenosis

Data from postmortem studies in unselected subjects indicate a prevalence of cardiac amyloidosis of 22% to 25% in subjects older than 80 years of age.[17] In an autopsy series of patients who had undergone transcatheter aortic valve replacement (TAVR), varying degrees of ventricular myocardium amyloid infiltration was found in approximately one-third of cases.[18] In a recent series, the proportion of patients with AS identified with ATTR-CA varied greatly and was between 4% and 16%.[10,14,15,16] The large variability in the prevalence of ATTR-CA in patients with AS could be explained by different study inclusion criteria and diverse study populations investigated (Table 1). The higher prevalence of ATTR-CA was found in TAVR cohorts. Scully et al[16] reported 13.9% prevalence of ATTR-CA in patients with severe AS referred for TAVR. In a study by Castano et al,[15] occult ATTR-CA was identified in 16% of patients after TAVR. The lower prevalence of ATTR-CA was described in a cohort of patients with severe AS undergoing surgical AVR (SAVR). Amyloid deposition was identified in endomyocardial biopsies of 6 out of 146 (4%) patients at the time of SAVR.[10] The prevalence increased to 5.6% if only patients with calcific AS >65 years of age were considered. On average, patients in that study were younger and had preserved LV ejection fraction, representing a lower risk population and explaining lower prevalence of ATTR-CA. In a retrospective study by Cavalcante et al,[14] among 113 patients with severe and moderate AS, 9 had cardiac amyloidosis confirmed by CMR with Late gadolinium enhancement (LGE). It appears that approximately 1 in 7 patients currently undergoing TAVR have occult cardiac amyloidosis—a higher prevalence than that in surgical AVR

cohorts. Furthermore, ATTR-CA typically affects males more than females, and the prevalence increases progressively with age. It has important clinical implications, as with aging population, the number of patients with coexistent ATTR-CA and severe AS will likely increase.

3. Diagnosing ATTR-CA in aortic stenosis

Recognition of ATTR-CA is complex owing to variability in disease clinical presentation, absence of disease specific symptoms, and ambiguous findings using common diagnostic tools. Diagnosis of ATTR-CA in AS is even more difficult, as their clinical and imaging features can overlap. Comorbidities such as coronary heart disease and hypertension frequently present in the older population, which creates a diverse clinical picture and adds to diagnostic challenges.

3.1. Electrocardiography

Patients with ATTR-CA rarely have normal electrocardiography (ECG). The most commonly observed electrocardiographic abnormality is a pseudoinfarct pattern (mainly in anterior leads), observed in approximately 60% of patients with ATTR-CA.[19–21] The association between low voltage and cardiac amyloidosis has long been considered pathognomonic; however, the prevalence in a contemporary series of ATTR-CA was as low as 20% to 30%.[19,21,22] On the contrary, up to a fifth (7-10%) of patients with ATTR-CA may show LV hypertrophy on ECG.[19,20] Direct involvement of the sino-atrial node, atrioventricular node and bundle branches can manifest as various degrees of conduction abnormalities.[19,23] As myocardial amyloid deposition is a continuum from minimal to transmural, all the above-mentioned ECG abnormalities tend to become more frequent with increasing disease severity. In a cohort of 425 patients with ATTR-CA, presence of low ECG voltage, pathologic Q waves and duration of PR, QRS, and QT intervals progressively increased with increasing thickness of interventricular septum and were most common in patients with the thickest hearts.[22] Patients with concomitant ATTR-CA and AS tend to exhibit

Table 1
Studies investigating ATTR cardiac amyloidosis in aortic stenosis

First author, study year (Ref No.)	Study design	No. of patients	Patients ATTR(+), n (%)	Population	Confirmation of diagnosis	Management of AS	Follow-up duration	No. of deaths
Treibel, 2016[10]	Prospective longitudinal, single center	146	6 (4%, 5.6% in calcific AS)	Severe AS undergoing SAVR	EMB (6), scintigraphy (DPD) (4)	SAVR (146)	2.3 (0.02-4.7) yrs	11 3 — ATTR(+) 8 — ATTR(−)
Galat, 2016[11]	Retrospective longitudinal, multicenter	16	16	Patients with concomitant ATTR and AS (severe AS 14, moderate AS 2)	EMB (6), scintigraphy (HMDP/DPD) (13)	SAVR (10), TAVR (2), conservative (4)	33 mos	7
Sperry, 2016[12]	Retrospective, longitudinal, single center	171	171	Group 1: patients with ATTR (144), Group 2: patients with ATTR + AS (27)	EMB or scintigraphy (PYP)	SAVR (11)	6 yrs	2 yrs mortality rate group 1: 37%; group 2: 33%
Longhi, 2016[13]	Cross-sectional, single center	43	5 (11.9%)	Severe AS + ≥1 of echocardiographic red flag for cardiac amyloidosis	EMB and scintigraphy (DPD) (5)	AV balloon angioplasty (5)	–	–
Cavalcante, 2017[14]	Retrospective longitudinal, single center	113	9 (8%)	Severe and moderate AS scheduled for CMR	CMR-LGE	SAVR (42), TAVR (17)	18 (11-30) mos	40 (35%)
Castano, 2017[15]	Cross-sectional, single center	151	24 (16%)	Severe AS undergoing TAVR	Scintigraphy (PYP)	TAVR	2 yrs	–
Scully, 2018[16]	Prospective longitudinal, multicenter	101	14 (13.9%)	Severe AS undergoing TAVR	Scintigraphy (DPD)	TAVR	Data pending	Data pending

Values are represented as median or n (%). AS = aortic stenosis; ATTR = transthyretin cardiac amyloidosis; CMR = cardiovascular magnetic resonance; DPD = Tc-99m-3,3-diphosphono-1,2-propanodicarboxylic acid; EMB = endomyocardial biopsy; HMDP=Tc-99m-hydroxymethylene diphosphonate; LGE = late gadolinium enhancement; PYP=Tc-99m-pyrophosphate; SAVR = surgical aortic valve replacement; TAVR = transcatheter aortic valve replacement.

more pronounced ECG abnormalities than patients with solely AS. In a study by Castano et al,[15] patients with AS diagnosed with ATTR-CA compared to those with isolated AS had longer QRS duration (127 ms vs. 110 ms, p = 0.017) and higher prevalence of right bundle branch block (37.5% vs. 15.8%, p = 0.023). The most common arrhythmia in a reported series was atrial fibrillation, present in 41.7-67% of patients with concomitant AS and ATTR-CA [11,12,14,15] (Table 2). Although atrial fibrillation is a frequent comorbidity of the AS population, in patients with dual pathology, the prevalence of atrial arrhythmias was significantly higher: 67% in the ATTR-CA group vs. 20.2% in the isolated AS group, p = 0.006.[14] In summary, multiple ECG findings may suggest ATTR-CA but are nonspecific in isolation. Pseudoinfarct pattern, low ECG voltage, conduction abnormalities, and presence of atrial arrhythmias in a context of other compatible clinical signs should alert physicians to suspect cardiac amyloidosis.

3.2. Echocardiography

Echocardiography is the initial test in a pathway leading to the diagnosis of ATTR-CA. However, classical echocardiographic features such as left and right ventricular wall thickening, biatrial dilatation, mild pericardial effusion, thickening of atrioventricular valves and atrial septum, and restrictive filling pattern[1] may be absent at an early stage of the disease. Moreover, the absence of increased ventricular wall thickness does not exclude the disorder, as up to one-third of cases can present with normal LV wall size.[24] Increased myocardial echogenicity, termed "granular sparking," strongly suggests cardiac amyloid, but it also becomes apparent at the late phase of the disease. It was traditionally believed that a concentric hypertrophic pattern is a classical feature of infiltrative cardiomyopathies, including cardiac amyloidosis. However, the data from the most recent echocardiographic and CMR studies[19,25] show that an asymmetric pattern does not exclude amyloid deposition, as asymmetric septal hypertrophy was the most common morphologic phenotype, found in 79% of patients with ATTR-CA.[25]

LV wall thickening, impaired diastolic filling, and/or LV systolic dysfunction is frequently present in both pathologies. Nevertheless, these alterations appear to be expressed to a higher degree in patients with coexisting ATTR-CA. Patients with coexisting ATTR-CA and AS, in comparison to those with isolated AS, manifest greater LV wall thickness and higher LV mass index — mean wall thickness 18 mm ± 0.5 vs. 13 mm ± 0.3, mean LV mass index 105 g/m² ± 21 vs. 73 g/m² ± 21.[14] Diastolic dysfunction is another common finding in

both of these entities, which progresses from a delayed relaxation pattern in the early stage through a pseudonormal pattern to a restrictive filling pattern in the late stage of the disease.[26,27] Patients with coexisting AS and ATTR-CA, compared to those with solely AS, exhibited more advanced grade of diastolic dysfunction — E/A ratio 2.3 vs. 0.9, p = 0.001; E wave deceleration time 176 ms vs. 257 ms, p < 0.0001).[15]

Low-flow low-gradient AS physiology should raise a suspicion for cardiac amyloidosis, as it was frequently observed in reported series. Four studies have demonstrated that patients with AS and concomitant ATTR-CA, compared to those with isolated AS, had significantly lower LV ejection fraction, lower stroke volume index, and lower trans-aortic gradient.[11,13,14,15] In a study by Cavalcante et al,[14] out of 9 patients with AS diagnosed with ATTR-CA, 7 (78%) exhibited a low-flow low gradient pattern. Similarly, Galat et al[11] have found low-flow low-gradient AS physiology in 12 (86%) out of 14 patients with ATTR-CA. The observation of a low–flow low-gradient hemodynamic profile can serve as a red flag for cardiac amyloidosis and prompt search for other echocardiographic or clinical markers of the disease.

3.3. Deformation imaging

The analysis of myocardial deformation by tissue Doppler and speckle-tracking echocardiography plays an important role in the recognition of cardiac amyloidosis.[28] Reduction in LV longitudinal deformation is an early marker of cardiac amyloid deposition and may be detected even before LV wall thickening of heart failure occurs.[29–31] In a recent series, patients with concomitant ATTR-CA and AS exhibited significantly reduced LV longitudinal deformation measured by tissue Doppler or 2D speckle tracking.[10,11,15] In a study by Castano et al[15] patients with dual pathology compared to those with isolated AS had more impaired LV longitudinal deformation — global longitudinal strain −12% vs. −16%, respectively, p = 0.007; mitral annular tissue Doppler S′ 4.0 cm/s vs. 6.6 cm/s, respectively, p < 0.0001.[15] Furthermore, average mitral annular S′ was the best predictor of ATTR-CA in a multivariable logistic regression analysis, and a cut-off value of S′ < 6 cm/s conferred 100% sensitivity to predict a positive 99mTc-PYP (99mTc-labeled pyrophosphate) amyloid scan. However, the relative apical sparing, with lower longitudinal deformation in basal segments with regard to apical ones, was not depicted in patients with ATTR-CA in that study. It has been speculated that the observed reduction in apical longitudinal strain in the ATTR group could be due to elevated wall stress and

Table 2
Clinical and imaging characteristics of patients with concomitant aortic stenosis and ATTR cardiac amyloidosis

First author, study year (Ref No.)	Age, years	Male, (%)	AF (%)	NYHA I/II/III/IV, (%)	IVST, mm	LVEF (%)	Mean AV gradient (mmHg)	LV SV index, ml/m²	Low-flow low-gradient AS, %	GLS (%)	LV mass index, g/m²	LGE (+) n (%)
Treibel, 2016[10]	77	67	—	—	16.7	67	—	—	—	12.6	121.7	2 (30%)
Galat, 2016[11]	79 ± 6	81	56	60 (III–IV)	18 ± 4	50 ± 13	33 ± 23	27 ± 7	86	7 ± 0.7	—	12 (100%)
Sperry, 2016[12]	79.4 ± 6.6	70.8	58.3	66.6 (III–IV)	18.6 ± 4.4	50 ± 13.9	21.8 ± 13	—	40.7	—	173.8 ± 55.3	—
Longhi, 2016[13]	84 (79–90)	80	—	100 (III–IV)	18 (16–21)	Reduced in 40%	—	—	80	—	—	—
Cavalcante, 2017[14]	88 ± 6	89	67	78 (III–IV)	18 ± 5	43 ± 17	30 ± 14	33 ± 10	78	—	105 ± 21	9 (100%)
Castano, 2017[15]	86.3 ± 5.7	91.7	41.7	0/25/75/0	13 ± 0.3	47.6 ± 17.6	35.2 ± 13.9	29.9 ± 10.5	37.5	12.4 ± 5.2	129.8 ± 43.6	—
Scully, 2018[16]	88 ± 6	50	—	—	—	—	37 ± 12	32 ± 7	—	—	—	—
Mean	83	75.6	55.8		17	51.5	31	30.5	64	10.7	136	

Values are represented as mean ± SD or n (%). AF = atrial fibrillation; AS = aortic stenosis; AV = aortic valve; GLS = global longitudinal strain; IVST = interventricular septal thickness; LGE(+) = late gadolinium enhancement positive; LVEF = left ventricular ejection fraction; LVSV = left ventricular stroke volume; NYHA= New York Heart Association.

increased afterload induced by AS that masks reduced apical deposition of amyloid in comparison to other segments. Therefore, the discriminatory value of 2D speckle-tracking in patients with dual pathology requires further investigation, as a classical apical-sparing pattern may be concealed by the presence of AS.

3.4. Cardiovascular magnetic resonance

CMR imaging has a high diagnostic value in cardiac amyloidosis and provides additive information through myocardial tissue characterization. LGE on CMR is very common in cardiac amyloidosis and represents interstitial expansion from amyloid deposition. The most frequent prototypical pattern is subendocardial and global transmural LGE, which is associated with the greatest interstitial amyloid deposition on myocardial histology.[25,32,33] Regional differences in LGE distribution have been described in patients with ATTR-CA, with higher involvement of basal segments and decreasing involvement extending to mid-cavity and apical levels.[33–35] CMR also enables more detailed evaluation of amyloid deposition in other parts of the heart. Right ventricular LGE is also extremely common and found in 37% to 97% of patients with ATTR-CA, depending on the stage of the disease.[36] Increased left atrial wall thickness and left atrial wall LGE were found in 70% and 90% of patients with ATTR, respectively.[37] (Fig. 1). There may be absence of late enhancement in cardiac amyloidosis, which should be taken into account, as amyloid deposition is a continuum from no LGE to subendocardial to transmural.[38] It appears that patients with biopsy-proven cardiac amyloidosis, but negative or minor LGE, have less advanced stage of the disease,[32] and restricting CMR protocols to LGE imaging carries the risk of missing early stages of cardiac amyloidosis.

Nonischemic patchy or mid-wall LGE is also found in approximately one-third of patients with severe AS and associated with impaired cardiac function and adverse clinical outcomes.[39] Therefore, patients with dual pathology may present with various combinations of CMR-LGE, creating difficulties in ATTR identification.

3.5. T1 mapping

Amyloid infiltration results in expansion of the extracellular space, which can be measured with T1 mapping, providing a novel tool to detect and quantify amyloid load. Elevated native myocardial T1 and extracellular volume (ECV) in cardiac ATTR was shown to be more sensitive than LGE imaging and had high diagnostic accuracy.[4,7,25] ECV was found to be elevated in patients with an early-stage disease when conventional clinical testing and LGE were normal.[4] Native T1 and ECV values become abnormal sequentially with increasing cardiac amyloid burden, being normal or mildly abnormal at an early stage and attaining the highest values at the advanced stage of the disease.[36,38] To date, only one study investigated native T1 and ECV values in patients with concomitant ATTR-CA and AS. The authors reported that, compared to patients with isolated AS, patients with concomitant ATTR-CA exhibited higher native T1 and ECV values: mean ECV 41.2% ± 16.7 vs. 27.9% ± 4.1, p < 0.001; mean native T1 1125 ms ± 49 vs. 1035 ms ± 60, p = 0.002.[14]

3.6. Nuclear imaging

Recent advances in nuclear imaging revolutionized ATTR-CA detection methodology. A new diagnostic algorithm was proposed and validated in 2016 that enabled noninvasive, nonhistological diagnosis of ATTR amyloid deposition, diminishing the need for an endomyocardial biopsy. Three technetium-labeled radiotracers have been evaluated clinically for ATTR-CA identification: Tc-99m-pyrophosphate (PYP), Tc-99m-3,3-diphosphono-1,2-propanodicarboxylic acid (DPD), and Tc-99m_hydroxymethylene diphosphonate (HMDP). It has been shown that grade 2 or 3 uptake on scintigraphy and the absence of a monoclonal protein have specificity and a positive predictive value of 100% for ATTR-CA.[40] Radionuclide bone scintigraphy has high sensitivity and may identify cardiac ATTR amyloid deposits early in the course of the disease, sometimes before the development of abnormalities on echocardiography or CMR.[41] Diagnosis of cardiac ATTR amyloidosis should be followed by TTR genotyping in all patients to differentiate between wild-type and mutant ATTR-CA. In the mutant ATTR-CA, the pathogenic mutation results in destabilization and misfolding of the transthyretin protein, whereas in the wild-type ATTR-CA, the genetic sequence of transthyretin is normal and the aging process is believed to be responsible for
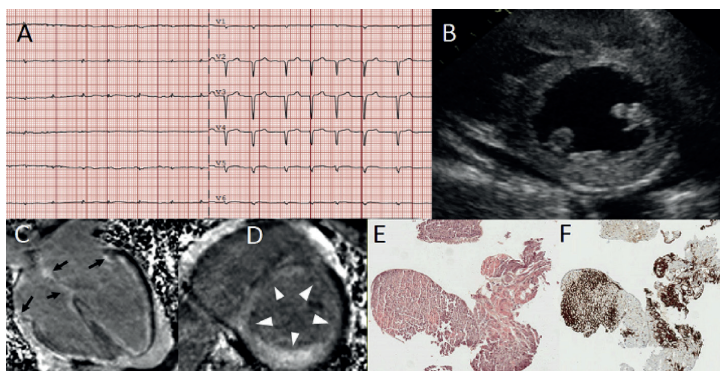

Figure 1. Multimodality imaging of a patient with advanced ATTR cardiac amyloidosis. (A) ECG showing atrial fibrillation, with a low-voltage, and pseudoinfarct pattern in precordial leads. (B) Echocardiographic parasternal short-axis view showing increased left ventricular wall thickness and mild pericardial effusion. Cardiac magnetic resonance imaging with global subendocardial circumferential enhancement of left ventricular walls in four-chamber (C) and short-axis views (arrowheads) (D). Note the diffuse enhancement of interatrial septum, both atria (arrows) and right ventricular wall. Endomyocardial biopsy with ATTR-related amyloid infiltration: (E) Congo red staining, (F) immunohistochemistry with anti-TTR antibodies.

protein instability and altered aggregation. Histological confirmation and typing of amyloid may still be required in patients undergoing a positive radionuclide scan and with the presence of a monoclonal protein.

3.7. Diagnostic workup of ATTR-CA in as

Given the high prevalence of calcific AS in the general population and the increasing frequency of TAVR in elderly patients, it is prudent to screen those in whom there is a suspicion of concomitant ATTR-CA. Echocardiography with deformation analysis may be the initial diagnostic steps, followed by contrast-enhanced CMR with T1 mapping. While endomyocardial biopsy with histological staining and tissue typing remain the gold standard for the diagnosis of ATTR-CA, it may not be appropriate in frail elderly patients. Nuclear imaging with technetium-labeled bone-seeking tracers, coupled with serum and urine electrophoresis for exclusion of monoclonal protein, may be a more suitable approach in this population (Fig. 2). However, owing to disease heterogeneity and the wide spectrum of clinical presentation, the optimal diagnostic algorithm for cardiac amyloidosis screening in patients with AS is still unclear and needs to be sorted out by further investigation.

4. Prognosis of patients with ATTR-CA and AS

The ATTR-CA is characterized by years of relative stability and slow disease progression. The reported median survival from diagnosis in untreated patients is approximately 3.6 years; however, a major determinant of outcomes is the extent of cardiac involvement.[42] In a recent meta-analysis of 23 studies, the predictors of death in patients with cardiac amyloidosis (AL and ATTR — wild and mutant types) were investigated.[43] Multivariate predictors of mortality were NYHA functional class, mean LV wall thickness, LV ejection fraction, and echocardiographic parameters of diastolic dysfunction (restrictive filling pattern, E/E' ratio, and E wave deceleration time). Right ventricular involvement, manifesting as increased right ventricular wall thickness and systolic dysfunction, is another independent predictor of poor prognosis in cardiac amyloidosis. It has been shown that right ventricular longitudinal systolic dysfunction, as assessed by depressed right ventricular longitudinal strain, is a negative prognostic marker in cardiac amyloidosis.[44]

To date, 3 longitudinal studies have investigated outcomes of patients with concomitant ATTR-CA and AS[10,13,14] (Table 1). In all of these studies, presence of ATTR-CA was associated with worse outcomes. In a study by Treibel et al,[10] 146 patients with severe AS
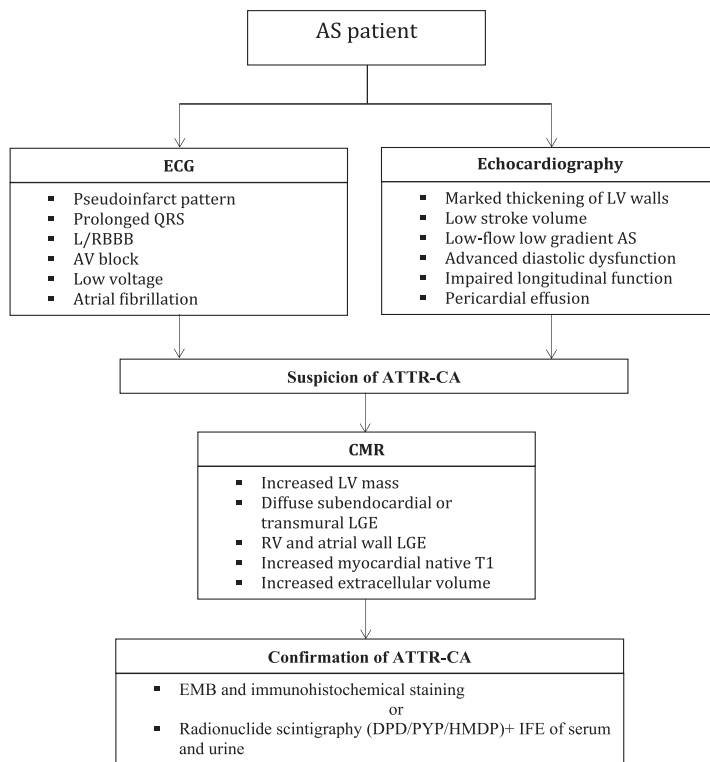

Figure 2. Flowchart of integrated imaging for the diagnosis of ATTR cardiac amyloidosis in aortic stenosis. AS = aortic stenosis; ATTR-CA = Transthyretin cardiac amyloidosis; CMR = cardiovascular magnetic resonance; DPD = Tc-99m-3,3-diphosphono-1,2-propanodicarboxylic acid; EMB = endomyocardial biopsy; HMDP=Tc-99m-hydroxymethylene diphosphonate; IFE = immunofixation electrophoresis; LGE = late gadolinium enhancement; LV = left ventricular; PYP=Tc-99m-pyrophosphate; RV = right ventricular.

who underwent surgical AVR were followed up for a median of 2.3 years. Three out of 6 (50%) patients with AS who had ATTR-CA died, while 8 out of 106 (7.5%) deaths were observed in patients with isolated severe AS. Of all variables assessed, the presence of ATTR-CA had the highest hazard ratio for all-cause mortality (HR = 9.5, 95% CI 2.5-35.8, p = 0.001). In a retrospective study by Cavalcante et al,[14] patients with coexisting ATTR-CA had a higher 1-year all-cause mortality than patients with isolated AS (56% vs. 20%, p < 0.0001). Furthermore, patients with combined disease had higher all-cause mortality rate even after adjustment of possible confounders, including AVR, LV ejection fraction, and functional class. Sperry et al[12] in a retrospective study compared outcomes of ATTR-CA patients with and without AS. Study revealed no significant difference in the 2-year mortality rate between the two groups: 37% in the ATTR-CA with AS group and 33% in the isolated ATTR-CA group (HR = 1.22, 95% CI: 0.62-2.42, p = 0.566). These results suggest that the mortality in patients with combined disease may be driven by the presence of ATTR-CA, as patients with AS died at the same rate as those without AS despite some having undergone AVR. There is a need to further evaluate whether amyloidosis affects mortality synergistically with severe AS or whether it is the primary driver of poor outcomes in patients.

5. Management of patients with ATTR-CA and AS

Recognition of ATTR-CA is important before aortic valve intervention for better risk stratification and management choices, as unrecognized ATTR-CA in symptomatic patients with severe AS may be a cause of periprocedural complications in patients undergoing aortic valve intervention.[45] There are reports of perioperative mortality in ATTR-CA patients due to fatal arrhythmias, progressive heart failure, and myocardial infarction with mechanical complications.[46,47] On the other hand, TAVR, which is indicated for older and higher risk patients, is not without a risk as well. There are reports of LV rupture and complete atrioventricular block leading to death during or after the TAVR procedure in patients with cardiac amyloidosis.[48,49] Early diagnosis of ATTR-CA is also critical to gain the best efficacy of amyloid-directed therapies. Contemporary treatment strategies that stabilize transthyretin have recently reported to improve survival in patients with ATTR-CA.[50] Tafamidis treatment, compared to placebo, resulted in lower all-cause mortality, a 32% relative risk reduction in cardiovascular hospitalizations, and a lower rate of decline in the 6-minute walk test. The drug is currently under review by the U.S. Food and Drug Administration for ATTR-CA. The question regarding its use in patients with AS remains unanswered and will require dedicated prospective trials. There are no recommendations on the management of patients with concomitant AS and ATTR-CA, which makes the treatment of the coexisting diseases challenging for clinicians. Currently, management choices are left to the discretion of the treating heart team and should be discussed with each patient individually. The decision to operate should depend on the type of amyloidosis, the severity of the cardiac involvement, and the overall patient prognosis. Cardiac biomarkers can be used to risk stratify ATTR-CA patients. Two staging systems have been proposed. Thresholds of troponin T (0.05 ng/ml) and NT-proBNP (3.000 pg/ml) were used by The Mayo Clinic staging system.[42] The respective 4-year survival estimates were 57%, 42%, and 18% for stage I (both values below cutoff), stage II (one above), and stage III (both above), respectively. The staging system from the U.K. National Amyloidosis Center is applicable for both wild-type and mutant ATTR-CA and discriminates patients into three prognostic categories depending on their NT-proBNP levels and estimated glomerular filtration rate.[51] The risk and benefit of aortic valve intervention should be carefully reconsidered in patients at stage III

cardiac amyloidosis. Keeping in mind the higher risk of periprocedural complications and reduced overall survival in patients with ATTR-CA, a more conservative approach may be adapted in this population. Medical management with repeated aortic valve balloon valvuloplasties could be preferred over valve replacement strategies. However, at present, there are no studies comparing different treatment strategies in patients with coexisting ATTR-CA and AS. Prospective multicenter studies in larger cohorts of patients with AS are needed before the conclusions could be drawn regarding the best management strategy. There is also lack of data whether aortic valve replacement will improve long-term survival in these patients. Outcome data are pending, but early results suggest higher medium-term mortality in patients referred for TAVR with severe AS (ATTRact-AS Study, NCT03029026). Our prospective multicenter study (NCT03585933) also aims at determining the prevalence, phenotype, and outcomes of ATTR-CA in patients with severe AS undergoing surgical and transcatheter AVR.

6. Conclusion

ATTR cardiac amyloidosis appears to be prevalent in AS, particularly among octogenarian males undergoing TAVR. Identification of cardiac amyloid deposition in the context of AS may be challenging because of overlapping clinical and imaging features. However, the presence of ATTR-CA is associated with a more severe AS phenotype, especially low-flow low-gradient AS. Preliminary data show that coexistence of ATTR-CA and AS is associated with worse outcomes, irrespective of the AS treatment received. Further work is pending to determine the optimal screening algorithm, AS management strategy, and to refine our understanding of the role of ATTR cardiac amyloidosis in these patients.

Competing interests

The authors declare that they have no competing interests.

References

1. Dungu JN, Anderson LJ, Whelan CJ, Hawkins PN. Cardiac transthyretin amyloidosis. *Heart.* 2012 Nov;98(21):1546−1554.
2. Rapezzi C, Merlini G, Quarta CC, et al. Systemic cardiac amyloidoses: disease profiles and clinical courses of the 3 main types. *Circulation.* 2009 Sep 29;120(13):1203−1212.
3. Damy T, Judge DP, Kristen AV, Berthet K, Li H, Aarts J. Cardiac findings and events observed in an open-label clinical trial of tafamidis in patients with non-Val30Met and non-Val122Ile hereditary transthyretin amyloidosis. *J Cardiovasc Transl Res.* 2015 Mar;8(2):117−127.
4. Fontana M, Banypersad SM, Treibel TA, et al. Native T1 mapping in transthyretin amyloidosis. *JACC Cardiovasc Imaging.* 2014;7:157−165.
5. Perugini E, Guidalotti PL, Salvi F, et al. Noninvasive etiologic diagnosis of cardiac amyloidosis using 99mTc-3, 3-diphosphono-1, 2-propanodicarboxylic acid scintigraphy. *J Am Coll Cardiol.* 2005;46:1076−1084.
6. Rapezzi C, Quarta CC, Guidalotti PL, et al. Usefulness and limitations of 99mTc-3, 3- diphosphono-1, 2-propanodicarboxylic acid scintigraphy in the aetiological diagnosis of amyloidotic cardiomyopathy. *Eur J Nucl Med Mol Imaging.* 2011;38:470−478.
7. Martinez-Naharro A, Kotecha T, Norrington K, et al. Native T1 and Extracellular Volume in Transthyretin Amyloidosis. *JACC Cardiovasc Imaging.* 2019 May;12(5):810−819. https://doi.org/10.1016/j.jcmg.2018.02.006.

8. Nkomo VT, Gardin JM, Skelton TN, Gottdiener JS, Scott CG, Enriquez-Sarano M. Burden of valvular heart diseases: a population-based study. *Lancet.* 2006;368: 1005—1011.

9. Dumesnil JG, Pibarot P, Carabello B. Paradoxical low flow and/or low gradient severe aortic stenosis despite preserved left ventricular ejection fraction: implications for diagnosis and treatment. *Eur Heart J.* 2010;31:281—289.

10. Treibel TA, Fontana M, Gilbertson JA, et al. Occult Transthyretin Cardiac Amyloid in Severe Calcific Aortic Stenosis: Prevalence and Prognosis in Patients Undergoing Surgical Aortic Valve Replacement. *Circ Cardiovasc Imaging.* 2016 Aug;9(8).

11. Galat A, Guellich A, Bodez D, et al. Aortic stenosis and transthyretin cardiac amyloidosis: the chicken or the egg? *Eur Heart J.* 2016 Dec 14;37(47): 3525—3531.

12. Sperry BW, Jones BM, Vranian MN, Hanna M, Jaber WA. Recognizing Transthyretin Cardiac Amyloidosis in Patients With Aortic Stenosis: Impact on Prognosis. *JACC Cardiovasc Imaging.* 2016 Jul;9(7):904—906.

13. Longhi S, Lorenzini M, Gagliardi C, et al. Coexistence of Degenerative Aortic Stenosis and Wild-Type Transthyretin-Related Cardiac Amyloidosis. *JACC Cardiovasc Imaging.* 2016;9:325—327.

14. Cavalcante JL, Rijal S, Abdelkarim I, et al. Cardiac amyloidosis is prevalent in older patients with aortic stenosis and carries worse prognosis. *J Cardiovasc Magn Reson.* 2017 Dec 7;19(1):98.

15. Castaño A, Narotsky DL, Hamid N, et al. Unveiling transthyretin cardiac amyloidosis and its predictors among elderly patients with severe aortic stenosis undergoing transcatheter aortic valve replacement. *Eur Heart J.* 2017 Oct 7;38(38):2879—2887.

16. Scully PR, Treibel TA, Fontana M, et al. Prevalence of Cardiac Amyloidosis in Patients Referred for Transcatheter Aortic Valve Replacement. *J Am Coll Cardiol.* 2018 Jan 30;71(4):463—464.

17. Ueda M, Horibata Y, Shono M, et al. Clinicopathological features of senile systemic amyloidosis: an ante- and post-mortem study. *Mod Pathol.* 2011;24: 1533—1544.

18. Nietlispach F, Webb JG, Ye J, et al. Pathology of transcatheter valve therapy. *JACC Cardiovasc Interv.* 2012;5:582—590.

19. González-López E, Gagliardi C, Domínguez F, et al. Clinical characteristics of wild-type transthyretin cardiac amyloidosis: disproving myths. *Eur Heart J.* 2017 Jun 21;38(24):1895—1904.

20. Rapezzi C, Lorenzini M, Longhi S, et al. Cardiac amyloidosis: the great pretender. *Heart Fail Rev.* 2015;20:117—124.

21. Maurer MS, Elliott P, Comenzo R, Semigran M, Rapezzi C. Addressing common questions encountered in the diagnosis and management of cardiac amyloidosis. *Circulation.* 2017;135:1357—1377.

22. Damy T, Maurer MS, Rapezzi C, et al. Clinical, ECG and echocardiographic clues to the diagnosis of TTR-related cardiomyopathy. *Open Heart.* 2016 Feb 8;3(1), e000289.

23. Falk RH, Skinner M. The systemic amyloidoses an overview. *Adv Intern Med.* 2000;45:107—137.

24. Lee GY, Kim K, Choi JO, et al. Cardiac amyloidosis without increased left ventricular wall thickness. *Mayo Clin Proc.* 2014;89(6):781—789.

25. Martinez-Naharro A, Treibel TA, Abdel-Gadir A, et al. Magnetic Resonance in Transthyretin Cardiac Amyloidosis. *J Am Coll Cardiol.* 2017 Jul 25;70(4): 466—477.

26. Koyama J, Davidoff R, Falk RH. Longitudinal myocardial velocity gradient derived from pulsed Doppler tissue imaging in AL amyloidosis: a sensitive indicator of systolic and diastolic dysfunction. *J Am Soc Echocardiogr.* 2004;17: 36—44.

27. Klein AL, Hatle LK, Taliercio CP, et al. Prognostic significance of Doppler measures of diastolic function in cardiac amyloidosis. A Doppler echocardiography study. *Circulation.* 1991;83:808—816.

28. Yingchoncharoen T, Agarwal S, Popović ZB, Marwick TH. Normal ranges of left ventricular strain: a meta-analysis. *J Am Soc Echocardiogr.* 2013;26:185—191.

29. Porciani MC, Lilli A, Perfetto F, et al. Tissue Doppler and strain imaging: a new tool for early detection of cardiac amyloidosis. *Amyloid.* 2009;16:63—70.

30. Lindqvist P, Olofsson BO, Backman C, Suhr O, Waldenström A. Pulsed tissue Doppler and strain imaging discloses early signs of infiltrative cardiac disease: a study on patients with familial amyloidotic polyneuropathy. *Eur J Echocardiogr.* 2006;7:22—30.

31. Koyama J, Ray-Sequin PA, Falk RH. Longitudinal myocardial function assessed by tissue velocity, strain, and strain rate tissue Doppler echocardiography in patients with AL (primary) cardiac amyloidosis. *Circulation.* 2003;107: 2446—2452.

32. Syed IS, Glockner JF, Feng D, et al. Role of cardiac magnetic resonance imaging in the detection of cardiac amyloidosis. *JACC Cardiovasc Imaging.* 2010;3(2): 155—164.

33. Dungu JN, Valencia O, Pinney JH, et al. CMR-based differentiation of AL and ATTR cardiac amyloidosis. *JACC Cardiovasc Imaging.* 2014;7(2):133—142.

34. Williams LK, Forero JF, Popovic ZB, et al. Patterns of CMR measured longitudinal strain and its association with late gadolinium enhancement in patients with cardiac amyloidosis. *J Cardiovasc Magn Reson.* 2017 Aug 7;19(1):61. https://doi.org/10.1186/s12968-017-0376-0.

35. Ternacle J, Bodez D, Guellich A, et al. Causes and Consequences of Longitudinal LV Dysfunction Assessed by 2D Strain Echocardiography in Cardiac Amyloidosis. *JACC Cardiovasc Imaging.* 2016 Feb;9(2):126—138.

36. Knight DS, Zumbo G, Barcella W, et al. Cardiac Structural and Functional Consequences of Amyloid Deposition by Cardiac Magnetic Resonance and Echocardiography and Their Prognostic Roles. *JACC Cardiovasc Imaging.* 2018 Apr 13.

37. de Gregorio C, Dattilo G, Casale M, Terrizzi A, Donato R, Di Bella G. Left Atrial Morphology, Size and Function in Patients With Transthyretin Cardiac Amyloidosis and Primary Hypertrophic Cardiomyopathy - Comparative Strain Imaging Study. *Circ J.* 2016 Jul 25;80(8):1830—1837.

38. Fontana M, Pica S, Reant P, et al. Prognostic value of late gadolinium enhancement cardiovascular magnetic resonance in cardiac amyloidosis. *Circulation.* 2015;132:1570—1579.

39. Musa TA, Treibel TA, Vassiliou VS, et al. Myocardial Scar and Mortality in Severe Aortic Stenosis: Data from the BSCMR Valve Consortium. *Circulation.* 2018 Oct 30;138(18):1935—1947.

40. Gillmore JD, Maurer MS, Falk RH, et al. Nonbiopsy diagnosis of cardiac transthyretin amyloidosis. *Circulation.* 2016;133:2404—2412.

41. Glaudemans AW, van Rheenen RW, van den Berg MP, et al. Bone scintigraphy with (99m)technetium-hydroxymethylene diphosphonate allows early diagnosis of cardiac involvement in patients with transthyretin-derived systemic amyloidosis. *Amyloid.* 2014;21:35—44.

42. Grogan M, Scott CG, Kyle RA, et al. Natural history of wild-type transthyretin cardiac amyloidosis and risk stratification using a novel staging system. *J Am Coll Cardiol.* 2016;68:1014—1020.

43. Xin Y, Hu W, Chen X, Hu J, Sun Y, Zhao Y. Prognostic impact of light-chain and transthyretin-related categories in cardiac amyloidosis: A systematic review and meta-analysis. *Hellenic J Cardiol.* 2019 Feb 8. pii: S1109-9666(18)30543-30548.

44. Cappelli F, Porciani MC, Bergesio F, et al. Right ventricular function in AL amyloidosis: characteristics and prognostic implication. *Eur Heart J Cardiovasc Imaging.* 2012;13:416—422.

45. Castaño A, Bokhari S, Maurer MS. Could late enhancement and need for permanent pacemaker implantation in patients undergoing TAVR be explained by undiagnosed transthyretin cardiac amyloidosis? *J Am Coll Cardiol.* 2015;65: 311—312.

46. Fitzmaurice GJ, Wishart V, Graham AN. An unexpected mortality following cardiac surgery: a post-mortem diagnosis of cardiac amyloidosis. *Gen Thorac Cardiovasc Surg.* 2013;61:417—421.

47. Kotani N, Hashimoto H, Muraoka M, Kabara S, Okawa H, Matsuki A. Fatal perioperative myocardial infarction in four patients with cardiac amyloidosis. *Anesthesiology.* 2000;92:873—875.

48. Monticelli FC, Kunz SN, Keller T, Bleiziffer S. Cardiac amyloidosis as a potential risk factor for transapical transcatheter aortic valve implantation. *J Card Surg.* 2014;29:623—624.

49. Moreno R, Dobarro D, Lopez de Sa E, et al. Cause of complete atrioventricular block after percutaneous aortic valve implantation: insights from a necropsy study. *Circulation.* 2009;120:e29—e30.

50. Maurer MS, Schwartz JH, Gundapaneni B, et al. Tafamidis Treatment for Patients with Transthyretin Amyloid Cardiomyopathy. *N Engl J Med.* 2018 Sep 13;379(11):1007—1016.

51. Gillmore JD, Damy T, Fontana M, et al. A new staging system for cardiac transthyretin amyloidosis. *Eur Heart J.* 2018;39:2799—2806.

3rd publication/3 publikacija

Prognostic value of myocardial fibrosis in severe aortic stenosis: study protocol for a prospective observational multi-center study (FIB-AS).

Balčiūnaitė G, Palionis D, Žurauskas E, Skorniakov V, Janušauskas V, Zorinas A, Zaremba T, Valevičienė N, Aidietis A, Šerpytis P, Ručinskas K, Sogaard P, Glaveckaitė S.

BMC Cardiovascular Disorders

Prognostic value of myocardial fibrosis in severe aortic stenosis: study protocol for a prospective observational multi-center study (FIB-AS)

Giedrė Balčiūnaitė[1*] ⓓ, Darius Palionis[2], Edvardas Žurauskas[3], Viktor Skorniakov[4], Vilius Janušauskas[1], Aleksejus Zorinas[1], Tomas Zaremba[1,5], Nomeda Valevičienė[2], Audrius Aidietis[1], Pranas Šerpytis[1], Kęstutis Ručinskas[1], Peter Sogaard[1,5] and Sigita Glaveckaitė[1]

Abstract

Background: Adverse cardiac remodeling with a myocardial fibrosis as a key pathophysiologic component may be associated to worse survival in aortic stenosis (AS) patients. Therefore, with the application of advanced cardiac imaging we aim to investigate left ventricular myocardial fibrosis in severe AS patients undergoing aortic valve replacement (AVR) and determine its impact with post-intervention clinical outcomes.

Methods: In a prospective, observational, cohort study patients with severe AS scheduled either for surgical or transcatheter AVR will be recruited from two tertiary heart centers in Denmark and Lithuania. All patients will receive standard of care in accordance with the current guidelines and will undergo additional imaging testing before and after AVR: echocardiography with deformation analysis and cardiovascular magnetic resonance (CMR) with T1 parametric mapping. Those undergoing surgical AVR will also have a myocardial biopsy sampled at the time of a surgery for histological validation. Patients will be recruited over a 2-year period and followed up to 2 years to ascertain clinical outcomes. Follow-up CMR will be performed 12 months following AVR, and echocardiography with deformation analysis will be performed 3, 12, and 24 months following AVR. The study primary outcome is a composite of all-cause mortality and major adverse cardiovascular events.

Discussion: Despite continuous effort of research community there is still a lack of early predictors of left ventricular decompensation in AS, which could improve patient risk stratification and guide the optimal timing for aortic valve intervention, before irreversible left ventricular damage occurs. Advanced cardiac imaging and CMR derived markers of diffuse myocardial fibrosis could be utilized for this purpose. FIB-AS study is intended to invasively and non-invasively assess diffuse myocardial fibrosis in AS patients and investigate its prognostic significance in post-interventional outcomes. The results of the study will expand the current knowledge of cardiac remodeling in AS and will bring additional data on myocardial fibrosis and its clinical implications following AVR.

(Continued on next page)

* Correspondence: dr.giedre.balciunaite@gmail.com
[1]Clinic of Cardiac and Vascular Diseases, Institute of Clinical Medicine, Vilnius University Faculty of Medicine, Santariškių str. 2, LT-08661 Vilnius, Lithuania
Full list of author information is available at the end of the article

(Continued from previous page)

Ethics/dissemination: The study has full ethical approval and is actively recruiting patients. The results will be disseminated through scientific journals and conference presentations.

Trial registration: ClinicalTrials.gov NCT03585933. Registered on 02 July 2018.

Keywords: Magnetic resonance imaging, Aortic valve stenosis, Myocardial fibrosis, Aortic valve replacement, Prognosis

Background

Since increased afterload is the main pathophysiology of aortic stenosis (AS) leading to the progressive development of left ventricular (LV) structural and functional alterations, AS is regarded a disease of the aortic valve, as well as of the myocardium [1]. The increasing wall stress triggers cardiac fibroblasts to upregulate fibronectin synthesis, with subsequent alteration in collagen architecture and myocardial fibrosis, compromising systolic and diastolic LV function [2]. Two distinct types of myocardial fibrosis have been described: (i) diffuse myocardial fibrosis and (ii) focal replacement fibrosis [3]. Focal replacement fibrosis can be detected by cardiovascular magnetic resonance (CMR) with late gadolinium enhancement (LGE) and is observed in up to half of aortic stenosis patients with non-infarct type being the most prevalent [4]. Multicenter trials and meta-analyses have shown that the presence and extent of LGE are associated with higher long-term all-cause and cardiovascular mortality after aortic valve replacement (AVR), indicating more advanced myocardial injury [4, 5]. Focal myocardial fibrosis has been demonstrated to be irreversible following AVR [6, 7], resulting in incomplete LV recovery and worse clinical outcomes, suggesting suboptimal timing of aortic valve intervention in some patients. On the contrary, diffuse interstitial fibrosis has been reported to be reversible with afterload relief and could be utilized as a potential marker of early LV dysfunction [8, 9]. However, the most recent study showed that regression of diffuse fibrosis may be incomplete in certain patients, leading to persistent LV systolic dysfunction and worse survival [10]. Application of T1 mapping techniques, which measures native and postcontrast T1 relaxation time or extracellular volume fraction (ECV), facilitates non-invasive detection and quantification of interstitial fibrosis with high spatial resolution [11–14]. Several studies in AS patients have reported that native T1 and ECV values correlate with the degree of diffuse myocardial fibrosis and predict cardiovascular events and mortality [9, 10, 15]. Thus, myocardial fibrosis detection by CMR is potentially useful for improving patient risk stratification and perhaps can justify earlier aortic valve intervention, before extensive fibrosis and irreversible myocardial damage develop.

Furthermore, because the subendocardial layer is the first to be affected in AS, the longitudinal alignment of myocardial fibers in this layer causes decreased longitudinal contraction, an early sign of LV dysfunction. There are data showing, that global longitudinal strain (GLS) correlate with LV myocardial fibrosis and is a predictor of adverse events in patients with severe AS [16, 17].

Novel diagnostic strategies and more accurate evaluation of the disease severity and consequences of AS are needed in the assessment of subclinical myocardial dysfunction and the detection of myocardial fibrosis to challenge current recommendations for the timing of AVR. To date there are limited data on simultaneous assessment of diffuse myocardial fibrosis by noninvasive multimodality imaging and histological confirmation in severe AS. Optimal T1 mapping application also remains unclear, and data assessing its prognostic value in severe AS are still lacking. Our multicenter prospective trial aims to: (i) non-invasively assess myocardial fibrosis and validate it against histological data in patients undergoing surgical AVR and (ii) assess the impact of myocardial fibrosis on clinical outcomes following AVR in both surgical and TAVR cohorts.

Hypothesis

Primary hypothesis: diffuse and focal myocardial fibrosis in patients with severe AS is associated with worse immediate (in-hospital) and long-term clinical outcomes, all-cause mortality, and major adverse cardiovascular events (MACEs).

Secondary hypotheses:

- The presence and extent of myocardial fibrosis are associated with markers of LV decompensation.
- The presence and extent of myocardial fibrosis have a negative effect on LV reverse remodeling and patient functional recovery following AVR.

Study objectives

Primary objective:

- To evaluate the prognostic significance of myocardial fibrosis in patients with severe AS undergoing AVR.

Secondary objectives:

- To identify parameters of multimodality imaging [two-dimensional (2D) echocardiography with an extended myocardial deformation analysis, 1.5 T contrast-enhanced CMR with T1 parametric mapping] predictive of LV decompensation.
- To quantify LV reverse remodeling 12 months following AVR through CMR and echocardiographic measurements.

Methods

Study design

FIB-AS is a prospective, observational, cohort study with clinical endpoints, conducted in two participating sites (in Lithuania and Denmark) from tertiary care hospitals. A total of 110 patients with severe AS undergoing AVR will be recruited from both institutions, and their data will be collected in a dedicated online database, REDCap (Research Electronic Data Capture) [18]. The choice of aortic valve intervention, either surgical or transcatheter, will be based on the heart team's decision in accordance to current guidelines [19]. Standard work-up examinations for surgical AVR or TAVR will be conducted, consisting of coronary angiography, echocardiography, computed tomography, electrocardiography, and blood tests. Once consent is confirmed, and prior to the AVR procedure (window of 0–30 days), a contrast-enhanced CMR scan with T1 mapping will be performed, in addition to the standard-of-care. A follow-up CMR scan will be performed 1 year following AVR. Those undergoing surgical AVR will also have a myocardial biopsy sampled at the time of a surgery, which will be sent for histological evaluation. Outcome assessments will continue for a total of 2 years post-intervention. The study flow diagram is presented in Fig. 1. Both sites have received approval from local ethics committees (Approval Numbers: for Vilnius University Hospital (VUH): 158200–18/9–1014-558; for Aalborg University Hospital (AAUH): N-20180081. All patients will give written informed consent.

Study population

We will recruit patients with severe AS requiring AVR according to current treatment recommendations [19]. We will exclude patients with obstructive coronary artery disease requiring revascularization or other significant valvular pathology. The inclusion and exclusion criteria are set in Table 1. The recruitment period will be 24 months, from May 2019 to May 2021. We expect
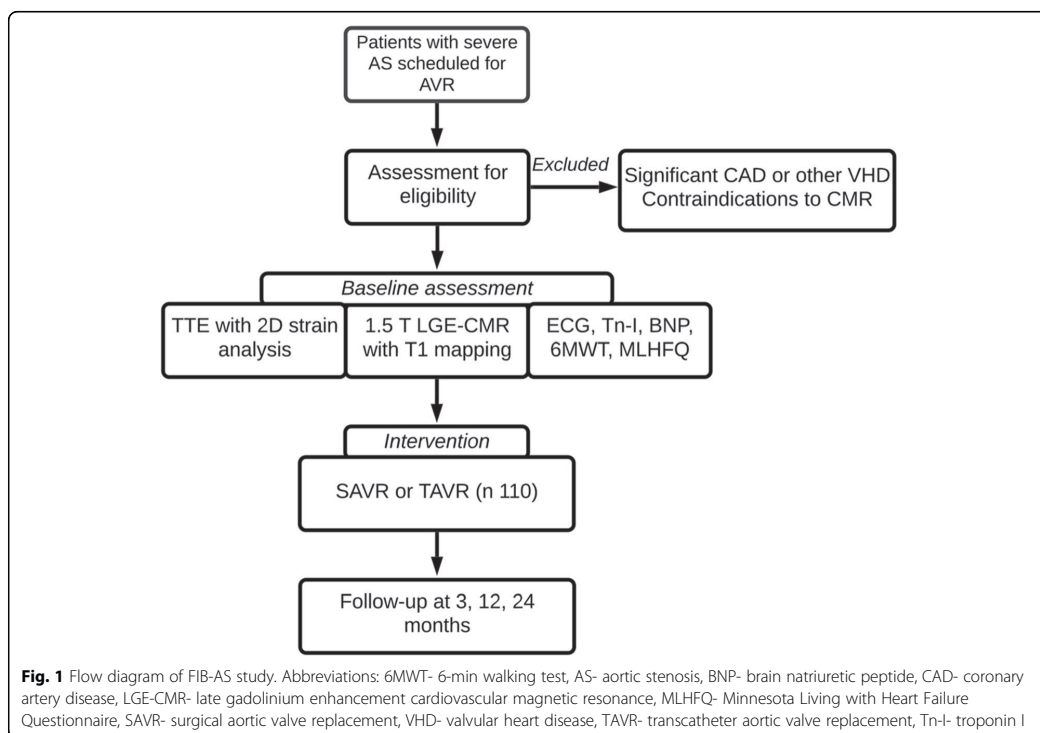

Fig. 1 Flow diagram of FIB-AS study. Abbreviations: 6MWT- 6-min walking test, AS- aortic stenosis, BNP- brain natriuretic peptide, CAD- coronary artery disease, LGE-CMR- late gadolinium enhancement cardiovascular magnetic resonance, MLHFQ- Minnesota Living with Heart Failure Questionnaire, SAVR- surgical aortic valve replacement, VHD- valvular heart disease, TAVR- transcatheter aortic valve replacement, Tn-I- troponin I

Table 1 Inclusion and exclusion criteria

Inclusion Criteria:

• Severe AS (defined as AVA ≤1 cm^2 or AVA index (iAVA) ≤0.6 cm^2/m^2 as determined by ultrasound examination)

• Males and females of any ethnic group ≥18 years of age

• Signed an informed patient consent form

Exclusion Criteria:

• Unable to provide informed consent

• Severe valvular heart disease other than AS

• Coronary artery disease requiring revascularization

• History of myocardial infarction

• Prior cardiac surgery

• Severe renal impairment - eGFR < 30 ml/min/1.73 m^2

• Any absolute contraindication to CMR

• Permanent atrial fibrillation

• Patient with implanted cardiac devices (pacemaker, ICD)

• Inherited or acquired cardiomyopathy

• Other medical conditions that limit life expectancy or preclude AVR

• Pregnant or nursing women

• Mental condition rendering the patient unable to understand the nature, scope, and possible consequences of the study or to follow the protocol

Abbreviations: AS- aortic stenosis, AVA- aortic valve area, iAVA- aortic valve area index, AVR- aortic valve replacement, CMR- cardiovascular magnetic resonance, eGFR- estimated glomerular filtration rate, ICD- implantable cardioverter defibrillator

to enroll a total of 110 patients: 60 patients undergoing surgical AVR and 50 patients undergoing TAVR.

Aortic valve replacement

Surgical AVR will be performed by standard midline sternotomy or J mini sternotomy with cardiopulmonary bypass and mild hypothermia. The St. Jude Medical Trifecta aortic bioprosthesis (St. Jude Medical, Inc., St. Paul, MN, USA) or mechanical CarboMedics Standard Aortic Valve (CarboMedics, Inc.; Austin, Tex) prostheses of varying sizes will be used according to the surgical team's or patient's preference. TAVR will be performed under conscious sedation. A balloon-expandable Edwards Sapien-3 Ultra Valve system, size 23, 26, or 29 mm (Edwards Lifesciences Inc., Irvine, CA, USA), will be deployed. Preferably a transfemoral route of access will be used, when vascular access will be judged suitable.

Data collection

The risk of interventional mortality will be assessed by calculating European System for Cardiac Operative Risk Evaluation II (EuroSCORE II) risk scores and Society of Thoracic Surgeons (STS) risk scores using the online calculators available at http://www.euroscore.org/calc.html [20] and at http://riskcalc.sts.org/stswebriskcalc [21]. Although not designed for TAVR, the STS score has been

validated and proved as a sensitive predictor of 30-day mortality and may be used in both SAVR and TAVR groups [22]. New York Heart Association (NYHA) functional class and 6-min walking test (6MWT) will be applied to assess patients' functional capacity and performed using standard method [23]. The Minnesota Living with Heart Failure Questionnaire (MLHFQ) [24] will be used to assess health-related quality of life from the patient's perspective, as it has been specifically validated in patients with aortic valve disease [25].

Blood testing

Blood samples will be collected and levels of cardiac biomarkers (B-type natriuretic peptide and troponin I) will be tested at baseline and at each follow-up visit. In addition, blood samples will be taken on the day of CMR scanning to determine hematocrit and creatinine concentration.

Echocardiography

Comprehensive transthoracic 2D echocardiography will be performed using a commercially available Vivid ultrasound (S70, E9 or E95) systems (GE Healthcare, Horten, Norway) and stored on a dedicated workstation for subsequent off-line analysis. AS severity, LV systolic and diastolic functions will be evaluated in accordance with the echocardiographic guidelines [26–28]. Simpson's biplane method will be used to calculate LV ejection fraction. The aortic valve area at the pre-interventional assessment and the effective prosthetic orifice area in the post-interventional assessment will be calculated using the continuity eq.

2D speckle tracking echocardiography (STE)

From the 2D grey-scale images of the apical two-, three-, and four-chamber views, left ventricular global longitudinal strain (GLS) will be measured and processed off-line using commercially available software (EchoPac 112.0.1, GE Medical Systems; Horten, Norway) [29]. The frame rate will be adjusted to 50 to 80 frames/s. The end-systole will be defined by detecting the closure click on the spectral tracing of the pulsed-wave Doppler of aortic valve flow. During analysis, the endocardial border will be traced manually at an end-systolic frame, and the software will automatically trace a region of interest that includes the entire myocardium. The change in length versus the initial length of the speckle pattern over the cardiac cycle will be used to calculate longitudinal strain, with myocardial lengthening or stretching represented as positive strain and myocardial shortening defined as negative strain. GLS will be acquired by the average regional strain curves (16-segment model for 2D STE). 2D STE analysis will be performed only in patients from VUH by an accredited investigator (G.B.). Segments with

poor quality tracking or aberrant curves despite manual adjustment will be removed from analysis.

CMR protocol
Basic description
For each patient, baseline and 1-year post-interventional CMR scans will be performed using standard protocols on a 1.5 T Siemens Aera scanner (at VUH) or a 1.5 T GE Discovery MR 450 scanner (at AAUH) with surface coils and prospective ECG triggering [3, 9]. Both sites will use corresponding CMR protocols. LV end-systolic and end-diastolic diameters, as well as maximal (end-diastolic) wall thickness, will be traced and recorded from the short-axis and long-axis views of the standard ECG-gated steady state-free precession cine sequence (8-mm slice thickness). LV volumes, mass, and ejection fraction will be measured using commercially available software (suiteHEART®, Neo-Soft, USA or cmr42, Circle Cardiovascular Imaging Inc., Canada) from a stack of sequential 8-mm short axis slices (0–2-mm gap) from the atrio-ventricular ring to the apex. Measurements will be indexed to body surface area in m^2 (using the DuBois and DuBois formula).

LGE imaging
For detection of delayed hyperenhancement, images will be acquired 10–15 min after intravenous administration of Gadobutrol (0.2 mmol/kg) (Gadovist; Bayer AG, Germany) or Gadoteridol (0.2 mmol/kg) (Prohance; Bracco Imaging, Sweden) using a breath-hold segmented inversion recovery fast gradient echo sequence in the short-axis and long-axis planes of the LV, with an 8-mm slice thickness and 20% distance factor. The image parameters (VUH) are: repetition time of 700 ms, echo time 1.42 ms, flip angle 45°, matrix 256 × 184, and field of view 360 mm. For AAUH, the typical imaging parameters are as follows: repetition time 5.79 ms, echo time 2.72 ms, flip angle 15°, matrix 256 × 256, and field of view 380 mm. The optimal inversion time will be optimized for each patient to null normal myocardial signal, ranging from 220 to 320 ms (usually around 240 ms). The region of myocardial fibrosis will be defined as the sum of pixels with signal intensity above 5 standard deviations of the normal remote myocardium in each short-axis slice. The presence of myocardial fibrosis will be qualitatively determined by two independent readers, blinded to clinical data (2 radiologists with > 10 years of experience at VUH- N.V. and D.P., and 2 cardiologists with 8–10 years of experience at AAUH- P.S. and T.Z.).

T1 mapping
The present study describes image acquisition parameters by focusing on T1 mapping images, which will be acquired in four-chamber long-axis and short-axis (at the basal and midventricular levels) images before and at 15 min after contrast administration. All T1 mapping images have been acquired using modified Look-Locker inversion-recovery (MOLLI) [30, 31] using the Motion Correction technique (on the Siemens scanner). The following readout parameters will be used: slice thickness: 8 mm; flip angle: 35; field of view: 384 × 327; effective TI: 193 ms; voxel size: 1.5 × 1.5 × 8 mm; TR/TE: 312.64/1.33 ms; partial Fourier: 7/8; and parallel imaging factor: 2 (VUH) and slice thickness 8 mm, flip angle 35, matrix size 256 × 256, inversion time 130 ms, and FOV 380 mm (AAUH).

Measurement of the ECV and native T1 values
The T1 maps will be generated from the CMR workstation after in-line motion correction just after image acquisition (Siemens scanner) or in post-processing software (GE scanner). Two blinded reviewers will independently review all T1 mapping sequences. Regions of interest will be drawn manually in the blood and septum at the midventricular level on the short-axis image, excluding the myocardium with LGE for T1 measurements [13, 32]. Regions of interest in the septum are chosen for myocardial T1, because this area corresponds to the site of myocardial biopsy. The regions of interest will be drawn on the compact myocardium, and the border of the myocardium will not be included. To measure the T1 value of blood, circular regions of interest will be positioned in the LV cavity, avoiding papillary muscle (Fig. 2).

The ECV of the myocardium will be calculated as follows: ECV% = (ΔR1m/ΔR1b) x (1 - hematocrit level) × 100, where R1 is 1/T1, R1m is R1 in the myocardium, R1b is R1 in the blood, and ΔR1 is the change in relaxivity. The change in relaxivity (ΔR1) was determined using the following equation: ΔR1 = R1post - R1pre, where R1post and R1pre are the R1 after and before gadolinium chelate administration, respectively [33]. Blood samples will be taken on the day of CMR scanning to determine hematocrit and creatinine concentration. Interobserver agreement between 2 different experienced observers will be assessed on different days for 10 randomly selected patients. Figure 3 summarizes the CMR sequences used in this study.

Histological analysis
In patients undergoing surgical AVR biopsy specimens will be obtained under direct vision by the surgical team using a surgical scalpel from the basal anteroseptum just after removal of the diseased aortic valve. All myocardium tissue samples will be fixed in 10% neutral buffered formalin and embedded in paraffin. Sections of 3-μm thickness will be made on a Leica RM2145 microtome and stained by hematoxylin and eosin, Masson's trichrome, and Congo red methods. Digital images will be captured by using the Aperio Scan-Scope XT Slide Scanner (Aperio Technologies, Vista, CA, USA) under 20× objective magnification
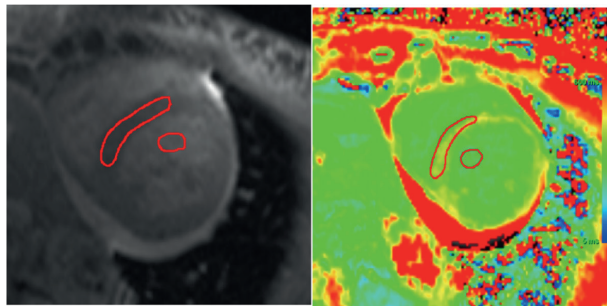
Fig. 2 CMR T1 assessment. To measure the T1 value, regions of interest will be drawn manually in the blood and septum at the midventricular level on the short-axis, avoiding papillary muscle

(0.5-µm resolution). Histological slides (typically measuring 20–30 sq./mm) will be processed for evaluation of myocardial fibrosis. An experienced (> 25 years of experience) histologist (E.Ž.) blinded to the clinical and CMR data will investigate all biopsy specimens. The fraction of myocardial volume occupied by collagen tissue (collagen volume fraction) will be determined by quantitative morphometry with an automated image analysis system (HALO™) in sections stained with Masson's trichrome. Quantification of the myocardial fibrosis area will be performed using HALO™ Classifier Module and HALO™ Area Quantification v1.0 algorithms (IndicaLabs, NM, USA) within manually selected regions of interest enclosing the tissue section and excluding endocardium from the analysis. All study assessments are summarized in Table 2.

Outcome measures

Primary outcome measure: a composite of all-cause mortality and MACEs (time frame: from 30 days up to 24 months following AVR).

Secondary outcomes measures:

- In-hospital and 30-day all-cause mortality (time frame: 30 days)
- Length of hospital stay
- Time to the event (death or MACE) (time frame: 24 months)
- Cardiovascular mortality (from 30 days up to 24 months following AVR)

Primary outcome endpoints will be defined according to current guidelines: Valve Academic Research Consortium-2 (VARC-2) definitions [34] and guidelines for reporting mortality and morbidity after cardiac valve interventions [35]. Cardiovascular mortality defined as: (1) death due to proximate cardiac cause (e.g., myocardial infarction, cardiac tamponade, worsening heart failure, and low cardiac output syndrome); (2) death caused by non-coronary vascular conditions (e.g., pulmonary embolism, stroke, aortic rupture, or vascular dissection); (3) all procedure-related deaths; (4) all valve-related deaths; and (5) sudden or unwitnessed death [35]. All-cause mortality defined as the sum of cardiovascular and non-cardiovascular deaths, with the latter defined as any
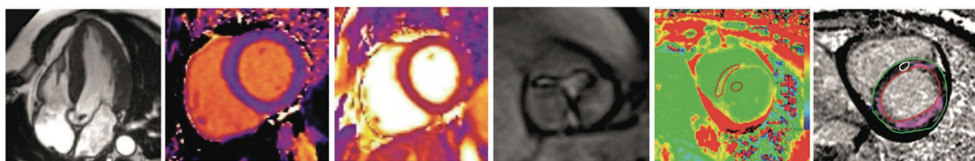
Localisers and cine imaging	T1 mapping (pre contrast)	T2 mapping	Aortic diameters and flow / cine / LVOT	T1 mapping (post contrast)	LGE
0	10	12	15	25	

Gadovist 0,2 mmol/kg

Fig. 3 CMR protocol for FIB-AS study

Balčiūnaitė *et al. BMC Cardiovascular Disorders*   (2020) 20:275

Page 7 of 10

Table 2 Study assessments

Demographic data and comorbidities
STS risk score
EuroSCORE II
Serum biomarkers:
‣ Brain natriuretic peptide
‣ Troponin I
Cardiovascular imaging biomarkers:
‣ Transthoracic 2D echocardiogram with strain analysis (GLS)
‣ 1.5 T contrast-enhanced CMR with T1 mapping (Native T1, ECV)
Myocardial histological analysis:
‣Quantitative myocardial fibrosis assessment (CVF)
Functional status and quality of life assessment:
‣New York Heart Association functional class
‣Minnesota Living with Heart Failure Questionnaire
‣6-min walking test

Abbreviations: 2D- two-dimensional, ECV- extracellular volume, EuroSCORE-
European System for Cardiac Operative Risk Evaluation, CMR- cardiovascular
magnetic resonance, CVF- collagen volume fraction, GLS- global longitudinal
strain, STS- Society of Thoracic Surgeons

death in which the primary cause is clearly related to other than cardiovascular condition. 30-day mortality defined as death occurring within 30 days or during index procedure hospitalization, if the postoperative length of stay is longer than 30 days.

Clinical follow-up

Patients will be routinely followed and managed according to available guidelines. Clinical outcome data will be collected from patient clinical visits at 3, 12, and 24 months following AVR. Serum biomarker analysis and 2D echocardiography with STE analysis will be performed at each follow-up visit. A second CMR scan will be performed 1 year after AVR. The 6MWT will be performed, and the MLHF questionnaire will be administered at the 12-month follow-up visit. FIB-AS study follows the standard protocol items: recommendation for interventional trials (SPIRIT) guidelines [36]. The study timeline is presented in Fig. 4**.**

Statistical analysis

- Linear regression analysis to model the relationship between the extent of myocardial fibrosis and patient outcomes.
- Univariate and multivariate regression analysis of CMR-derived predictors of adverse clinical events.
- Comparison of clinical, serum, and imaging (CMR and echocardiography) biomarker data between patients with different extents of fibrosis.

The statistical analysis will be performed under the supervision of V.S. at the Institute of Applied Mathematics, Vilnius University Faculty of Mathematics and Informatics. Descriptive statistics will be used to summarize the demographic, clinical, and imaging data characteristics of each patient. Categorical variables will be presented as the frequency and percentage, and continuous variables will be expressed as the mean and standard deviation or median and interquartile range. The 95% confidence interval will be reported for primary outcomes. Patients will be grouped, depending on the presence and extent of histologically measured myocardial fibrosis, and their clinical and imaging data will be compared for significant differences. Bivariate correlation analysis of the native T1, ECV, and GLS values with the degree of histologically measured myocardial fibrosis will be performed. Pearson or Spearman correlation coefficient will be used as the measure of correlation. To identify independent predictors of the degree of myocardial fibrosis, multivariate stepwise regression analysis will be performed separately for native T1, ECV, and GLS values, along with demographic and clinical data. The composite event will be assessed from a simple Cox model for survival analysis using ECV, native T1, and GLS, and their c-indexes will be compared for how well each marker predicts the clinical outcome. In addition, the Kaplan–Meier method will be used for the cumulative survival analysis with log-rank test to assess statistical differences between the curves of patients with different degree of myocardial fibrosis. A two-tailed p-value of < 0.05 will be considered statistically significant. The statistical analysis will be performed using the R language and environment for statistical computing (version 3.5.1) [37].

Sample size justification

A sample size calculation was performed for the primary outcome: a composite of all-cause mortality and MACEs following AVR. To estimate the sample size required for the detection of a hazard ratio for ECV% of 1.32, R package powerSurvEpi was used [38]. Calculations were made assuming that the Cox proportional hazards regression model applies and taking into consideration a correlation of ECV% with other possible confounding covariates. On the basis of previous studies [15, 17] and assuming that the power of the test should be at least 0.8, a sample size of 100 patients is required. After an adjustment for 10% patient loss or withdrawal, a total sample size of 110 patients was selected. The selected sample size is comparable to other studies testing the association of myocardial fibrosis with adverse clinical outcomes.

Study timetable

The ethics application was approved in March 2018. Study enrollment started in May 2019, and recruitment is expected to be completed in May 2021, with a further

	STUDY PERIOD							
	Enrolment	Allocation	Post-allocation					Close-out
TIMEPOINT	*0*	*0*	*Pre-AVR*	*AVR*	*3m*	*12m*	*24m*	*24m*
ENROLMENT:								
Eligibility screen	X							
Informed consent	X							
Allocation		X						
INTERVENTIONS:								
CMR			X			X		
Endomyocardial biopsy				X*				
2D Echo with strain analysis			X		X	X	X	
Serum biomarkers			X		X	X	X	
6MWT			X			X	X	
MLHFQ			X			X	X	
ASSESSMENTS:								
Baseline demographics and comorbidities	X	X	X					
All-cause mortality					●————————————————————●			
MACE					●————————————————————●			

Fig. 4 Standard protocol items: recommendation for interventional trials (SPIRIT) figure of participant timeline. Abbreviations: 2D- two-dimensional, 6MWT- 6-min walking test, CMR- cardiovascular magnetic resonance, MACEs- major adverse cardiovascular events, m- months, MLHFQ- Minnesota Living with Heart Failure Questionnaire. *Endomyocardial biopsy will be performed only in patients undergoing surgical AVR

24 months for follow-up, post-processing, and close-out of the study. The main study paper will be submitted within 6 months of the study close-out.

Dissemination of results
The study results will be presented to the participating physicians and the general medical community. Following the complete data collection, the manuscript(s) based on the trial results will be submitted to peer-reviewed journals. Authorship criteria as defined by the International Committee of Medical Journal Editors will be followed.

Discussion
FIB-AS is a study intended to investigate the role of multimodality imaging in the assessment of myocardial fibrosis in severe aortic stenosis patients and its prognostic significance in post-interventional outcomes. We sought to assess diffuse myocardial fibrosis by measuring the ECV and native T1 values obtained from CMR with T1 mapping and GLS from STE and to validate these results against the degree of myocardial fibrosis found from the histological examination. In addition, we will explore LV reverse remodeling following aortic valve intervention and its associations with patient clinical recovery. The results of the study will expand the current knowledge of cardiac remodeling in AS and will bring additional data on myocardial fibrosis and its clinical implications following AVR.

Strengths

- The present prospective multicenter study is designed to explore associations between left ventricular myocardial fibrosis and clinical outcomes in severe AS patients undergoing AVR. It has clearly established aims, inclusion and exclusion criteria, as well as defined methods and endpoints.

- The non-invasive measurement of myocardial fibrosis by CMR with T1 mapping is validated against invasive histological assessment.
- The trial is restricted to isolated AS, excluding cardiac pathologies which could possibly contribute to myocardial fibrosis burden, such as obstructive coronary heart disease and other significant valvular heart diseases.
- Inclusion of both surgical and TAVR cohorts will allow the investigation of patients with different risk profiles.

Limitations

- The selected sample size may be inadequate to allow a subgroup analysis.
- Limitations of CMR to establish diffuse and focal fibrosis: no reference regions of normal myocardium due to diffuse fibrosis, arbitrary selection of threshold of signal intensity, overlap of T1 values between normal and diseased myocardium.
- The FIB-AS study excludes patients with comorbidities, such as obstructive coronary artery disease, a history of myocardial infarction, renal failure, and persistent atrial arrhythmias; therefore, our results should not be overgeneralized to a broader AS patient population.

Abbreviations
2D STE: Two-dimensional speckle tracking echocardiography; 6MWT: 6-min walking test; AAUH: Aalborg University hospital; AS: Aortic stenosis; AVR: Aortic valve replacement; CAD: Coronary artery disease; CMR: Cardiovascular magnetic resonance; ECV: Extracellular volume; GLS: Global longitudinal strain; LGE: Late gadolinium enhancement; MOLLI: Modified look-locker inversion-recovery; NYHA: New York heart association; TAVR: Transcatheter aortic valve replacement; VUH: Vilnius University hospital

Author details
[1]Clinic of Cardiac and Vascular Diseases, Institute of Clinical Medicine, Vilnius University Faculty of Medicine, Santariškių str. 2, LT-08661 Vilnius, Lithuania. [2]Department of Radiology, Nuclear Medicine and Medical Physics, Institute of Biomedical Sciences, Vilnius University Faculty of Medicine, Santariškių str. 2, LT-08661 Vilnius, Lithuania. [3]Department of Pathology, Forensic Medicine and Pharmacology, Institute of Biomedical Sciences, Vilnius University Faculty of Medicine, P. Baublio str. 5, LT-08406 Vilnius, Lithuania. [4]Institute of Applied Mathematics, Vilnius University Faculty of Mathematics and Informatics, Naugarduko str. 24, LT-03225 Vilnius, Lithuania. [5]Aalborg University Hospital, Clinical Institute of Aalborg University, Hobrovej 18-22, 9100 Aalborg, Denmark.

References
1. Chin CWL, Everett RJ, Kwiecinski J, Vesey AT, Yeung E, Esson G, et al. Myocardial fibrosis and cardiac decompensation in aortic stenosis. JACC Cardiovasc Imaging. 2017;10:1320–33.
2. Fielitz J, Hein S, Mitrovic V, Pregla R, Zurbrügg HR, Warnecke C, et al. Activation of the cardiac renin-angiotensin system and increased myocardial collagen expression in human aortic valve disease. J Am Coll Cardiol. 2001;37:1443–9.
3. Lee SP, Lee W, Lee JM, Park EA, Kim HK, Kim YJ, et al. Assessment of diffuse myocardial fibrosis by using MR imaging in asymptomatic patients with aortic stenosis. Radiology. 2015;274:359–69.
4. Balciunaite G, Skorniakov V, Rimkus A, Zaremba T, Palionis D, Valeviciene N, et al. Prevalence and prognostic value of late gadolinium enhancement on CMR in aortic stenosis: meta-analysis. Eur Radiol. 2020 Jan;30(1):640–51. https://doi.org/10.1007/s00330-019-06386-3.
5. Musa TA, Treibel TA, Vassiliou VS, Captur G, Singh A, Chin C, et al. Myocardial scar and mortality in severe aortic stenosis. Circulation. 2018 Oct 30;138(18):1935–47.
6. Treibel TA, Kozor R, Schofield R, Benedetti G, Fontana M, Bhuva AN, et al. Reverse myocardial remodeling following valve replacement in patients with aortic stenosis. J Am Coll Cardiol. 2018;71:860–71.
7. Everett RJ, Tastet L, Clavel MA, Chin CWL, Capoulade R, Vassiliou VS, et al. Progression of hypertrophy and myocardial fibrosis in aortic stenosis: a multicenter cardiac magnetic resonance study. Circ Cardiovasc Imaging. 2018;11:e007451.
8. Chin CW, Pawade TA, Newby DE, Dweck MR. Risk stratification in patients with aortic stenosis using novel imaging approaches. Circ Cardiovasc Imaging. 2015;8:e003421.
9. Lee H, Park JB, Yoon YE, Park EA, Kim HK, Lee W, et al. Noncontrast myocardial T1 mapping by cardiac magnetic resonance predicts outcome in patients with aortic stenosis. JACC Cardiovasc Imaging. 2018;11:974–83.
10. Hwang IC, Kim HK, Park JB, Park EA, Lee W, Lee SP, et al. Aortic valve replacement-induced changes in native T1 are related to prognosis in severe aortic stenosis: T1 mapping cardiac magnetic resonance imaging study. Eur Heart J Cardiovasc Imaging. 2019 Aug 4. pii: jez201. doi: https://doi.org/10.1093/ehjci/jez201.
11. Singh A, Horsfield MA, Bekele S, Khan JN, Greiser A, McCann GP. Myocardial T1 and extracellular volume fraction measurement in asymptomatic patients with aortic stenosis: reproducibility and comparison with age-matched controls. Eur Heart J Cardiovasc Imaging. 2015;16:763–70.

12. Chin CW, Semple S, Malley T, White AC, Mirsadraee S, Weale PJ, et al. Optimization and comparison of myocardial T1 techniques at 3T in patients with aortic stenosis. Eur Heart J Cardiovasc Imaging. 2014;15:556–65.
13. Kockova R, Kacer P, Pirk J, Maly J, Sukupova L, Sikula V, et al. Native T1 relaxation time and extracellular volume fraction as accurate markers of diffuse myocardial fibrosis in heart valve disease- comparison with targeted left ventricular myocardial biopsy. Circ J. 2016;80:1202–9.
14. Child N, Suna G, Dabir D, Yap ML, Rogers T, Kathirgamanathan M, et al. Comparison of MOLLI, shMOLLLI, and SASHA in discrimination between health and disease and relationship with histologically derived collagen volume fraction. Eur Heart J Cardiovasc Imaging. 2018;19:768–76.
15. Everett RJ, Treibel TA, Fukui M, Lee H, Rigolli M, Singh A, et al. Extracellular myocardial volume in patients with aortic stenosis. J Am Coll Cardiol. 2020 Jan 28;75(3):304–16. https://doi.org/10.1016/j.jacc.2019.11.032.
16. Nagata Y, Takeuchi M, Wu VC, Izumo M, Suzuki K, Sato K, et al. Prognostic value of LV deformation parameters using 2D and 3D speckle-tracking echocardiography in asymptomatic patients with severe aortic stenosis and preserved LV ejection fraction. J Am Coll Cardiol Img. 2015;8:235–45.
17. Park SJ, Cho SW, Kim SM, Ahn J, Carriere K, Jeong DS, et al. Assessment of myocardial fibrosis using multimodality imaging in severe aortic stenosis: comparison with histologic fibrosis. JACC Cardiovasc Imaging. 2019 Jan; 12(1):109–19. https://doi.org/10.1016/j.jcmg.2018.05.028.
18. Harris PA, Taylor R, Thielke R, Payne J, Gonzalez N, Conde JG. Research electronic data capture (REDCap)-a metadata-driven methodology and workflow process for providing translational research informatics support. J Biomed Inform. 2009;42(2):377–81. https://doi.org/10.1016/j.jbi.2008.08.010.
19. Baumgartner H, Falk V, Bax JJ, De Bonis M, Hamm C, Holm PJ, et al. ESC scientific document group. 2017 ESC/EACTS guidelines for the management of valvular heart disease. Eur Heart J. 2017 Sep 21;38(36):2739–91. https://doi.org/10.1093/eurheartj/ehx391.
20. Nashef SA, Roques F, Sharples LD, Nilsson J, Smith C, Goldstone AR, et al. EuroSCORE II. Eur J Cardiothorac Surg. 2012;41:734–45.
21. Shih T, Paone G, Theurer PF, McDonald D, Shahian DM, Prager RL. The society of thoracic surgeons adult cardiac surgery database version 2.73: more is better. Ann Thorac Surg. 2015;100:516–21.
22. Balan P, Zhao Y, Johnson S, Arain S, Dhoble A, Estrera A, et al. The Society of Thoracic Surgery Risk Score as a predictor of 30-day mortality in Transcatheter vs surgical aortic valve replacement: A single-center experience and its implications for the development of a TAVR risk-prediction model. J Invasive Cardiol. 2017 Mar;29(3):109–14.
23. de Arenaza DP, Pepper J, Lees B, Rubinstein F, Nugara F, Roughton M, et al. Preoperative 6-minute walk test adds prognostic information to Euroscore in patients undergoing aortic valve replacement. Heart. 2010;96:113–7.
24. Rector TS, Cohn JN. Assessment of patient outcome with the Minnesota living with heart failure questionnaire: reliability and validity during a randomized, double-blind, placebo-controlled trial of pimobendan. Pimobendan multicenter research group. Am Heart J. 1992;124:1017–25.
25. Supino PG, Borer JS, Franciosa JA, Preibisz JJ, Hochreiter C, Isom OW, et al. Acceptability and psychometric properties of the Minnesota living with heart failure questionnaire among patients undergoing heart valve surgery: validation and comparison with SF-36. J Card Fail. 2009;15:267–77.
26. Lang RM, Badano LP, Mor-Avi V, Afilalo J, Armstrong A, Ernande L, et al. Recommendations for cardiac chamber quantification by echocardiography in adults: an update from the American Society of Echocardiography and the European Association of Cardiovascular Imaging. J Am Soc Echocardiogr. 2015;28:1–39.
27. Baumgartner H, Hung J, Bermejo J, Chambers JB, Edvardsen T, Goldstein S, et al. Recommendations on the echocardiographic assessment of aortic valve stenosis: a focused update from the European Association of Cardiovascular Imaging and the American Society of Echocardiography. Eur Heart J Cardiovasc Imaging. 2017;18:254–75.
28. Nagueh SF, Smiseth OA, Appleton CP, Byrd BF 3rd, Dokainish H, Edvardsen T, et al. Recommendations for the evaluation of left ventricular diastolic function by echocardiography: an update from the American Society of Echocardiography and the European Association of Cardiovascular Imaging. Eur Heart J Cardiovasc Imaging. 2016;17:1321–60.
29. Voigt JU, Pedrizzetti G, Lysyansky P, Marwick TH, Houle H, Baumann R, et al. Definitions for a common standard for 2D speckle tracking echocardiography: consensus document of the EACVI/ASE/industry task force to standardize deformation imaging. Eur Heart J Cardiovasc Imaging. 2015;16:1–11.
30. Taylor AJ, Salerno M, Dharmakumar R, Jerosch-Herold M. T1 mapping: basic techniques and clinical applications. JACC Cardiovasc Imaging. 2016;9:67–81.
31. de Meester de Ravenstein C, Bouzin C, Lazam S, Boulif J, Amzulescu M, Melchior J, et al. Histological validation of measurement of diffuse interstitial myocardial fibrosis by myocardial extravascular volume fraction from modified look-locker imaging (MOLLI) T1 mapping at 3 T. J Cardiovasc Magn Reson. 2015;17:48.
32. Puntmann VO, Voigt T, Chen Z, Mayr M, Karim R, Rhode K, et al. Native T1 mapping in differentiation of normal myocardium from diffuse disease in hypertrophic and dilated cardiomyopathy. J Am Coll Cardiol Img. 2013;6: 475–84.
33. Ugander M, Oki AJ, Hsu LY, Kellman P, Greiser A, Aletras AH, et al. Extracellular volume imaging by magnetic resonance imaging provides insights into overt and sub-clinical myocardial pathology. Eur Heart J. 2012; 33:1268–78.
34. Kappetein AP, Head SJ, Généreux P, Piazza N, van Mieghem NM, Blackstone EH, et al. Updated standardized endpoint definitions for transcatheter aortic valve implantation: the valve academic research Consortium-2 consensus document (VARC-2). Eur J Cardiothorac Surg. 2012;42:S45–60.
35. Akins CW, Miller DC, Turina MI, Kouchoukos NT, Blackstone EH, Grunkemeier GL, et al. Guidelines for reporting mortality and morbidity after cardiac valve interventions. J Thorac Cardiovasc Surg. 2008;135:732–8.
36. Chan AW, Tetzlaff JM, Altman DG, Laupacis A, Gøtzsche PC, Krle A-Jerić K, et al. SPIRIT 2013 statement: defining standard protocol items for clinical trials. Rev Panam Salud Publica. 2015 Dec;38(6):506–14.
37. R Core Team. R: A language and environment for statistical computing. R Foundation for Statistical Computing, Vienna, Austria. 2018. https://www.R-project.org/.
38. Qiu W, Chavarro J, Lazarus R. Rosner B. PowerSurvEpi: Ma J. R package for power and sample size calculation for survival analysis of epidemiological studies; 2018. https://cran.r-project.org/web/packages/powerSurvEpi/index.html).

Publisher's Note

4th publication/4 publikacija

Exploring myocardial fibrosis in severe aortic stenosis: echo, CMR and histology data from FIB-AS study.

Balčiūnaitė G, Besusparis J, Palionis D, Žurauskas E, Skorniakov V, Janušauskas V, Zorinas A, Zaremba T, Valevičienė N, Šerpytis P, Aidietis A, Ručinskas K, Sogaard P, Glaveckaitė S.

ORIGINAL PAPER

Exploring myocardial fibrosis in severe aortic stenosis: echo, CMR and histology data from FIB-AS study

Giedrė Balčiūnaitė[1] · Justinas Besusparis[1] · Darius Palionis[1] · Edvardas Žurauskas[1] · Viktor Skorniakov[1] ·
Vilius Janušauskas[1] · Aleksejus Zorinas[1] · Tomas Zaremba[1,2] · Nomeda Valevičienė[1] · Pranas Šerpytis[1] ·
Audrius Aidietis[1] · Kęstutis Ručinskas[1] · Peter Sogaard[1,2] · Sigita Glaveckaitė[1]

Abstract

Myocardial fibrosis in aortic stenosis is associated with worse survival following aortic valve replacement. We assessed myocardial fibrosis in severe AS patients, integrating echocardiographic, cardiovascular magnetic resonance (CMR) and histological data. A total of 83 severe AS patients (age 66.4 ± 8.3, 42% male) who were scheduled for surgical AVR underwent CMR with late gadolinium enhancement and T1 mapping and global longitudinal strain analysis. Collagen volume fraction was measured in myocardial biopsies (71) that were sampled at the time of AVR. Results. CVF correlated with imaging and serum biomarkers of LV systolic dysfunction and left side chamber enlargement and was higher in the sub-endocardium compared with midmyocardium ($p<0.001$). CVF median values were higher in LGE-positive versus LGE-negative patients [28.7% (19–33) vs 20.7% (15–30), respectively, $p=0.040$]. GLS was associated with invasively (CVF; r=−0.303, $p=0.013$) and non-invasively (native T1; r=−0.321, $p<0.05$) measured myocardial fibrosis. GLS and native T1 correlated with parameters of adverse LV remodelling, systolic and diastolic dysfunction and serum biomarkers of heart failure and myocardial injury. Conclusion. Our data highlight the role of myocardial fibrosis in adverse cardiac remodelling in AS. GLS has potential as a surrogate marker of myocardial fibrosis, and high native T1 and low GLS values differentiated patients with more advanced cardiac remodelling.

Keywords Aortic stenosis · Myocardial fibrosis · Cardiovascular magnetic resonance · T1 mapping · Global longitudinal strain

Abbreviations

6MWT	6-Minute walking test
AS	Aortic stenosis
AV	Aortic valve
AVR	Aortic valve replacement
BNP	Brain natriuretic peptide
CAD	Coronary artery disease
CMR	Cardiovascular magnetic resonance
ECG	Electrocardiography
ECV	Extracellular volume
GLS	Global longitudinal strain
Hs-Tn-I	High-sensitivity troponin I
LA	Left atrium
LGE	Late gadolinium enhancement
LV	Left ventricle
LVEF	Left ventricular ejection fraction
MLHFQ	Minnesota Living With Heart Failure Questionnaire
NYHA	New York Heart Association
STE	Speckle tracking echocardiography

✉ Giedrė Balčiūnaitė
dr.giedre.balciunaite@gmail.com

1 Present Address: Vilnius University: Vilniaus Universitetas, Vilnius, Lithuania

2 Aalborg University Hospital, Clinical Institute of Aalborg University, Hobrovej 18-22, 9100 Aalborg, Denmark

Introduction

Myocardial fibrosis is fundamental in the pathogenesis of heart failure in the spectrum of cardiovascular diseases [1]. It is associated with the disruption of normal myocardial structure by excessive deposition of the extracellular matrix and creates a mechanistic base for adverse cardiac remodelling [2]. Myocardial fibrosis in aortic stenosis (AS) patients

Springer

has been linked to impaired left ventricular (LV) function and adverse clinical outcomes [3].

Changes in cellular and extracellular matrix architecture, triggered by the greater afterload and wall stress in AS, increases tissue stiffness and impairs contraction [4, 5]. This complex interplay between components of cardiac remodelling can be evaluated by histological analysis of myocardial biopsy samples or the use of advanced imaging techniques with ability of tissue characterization.

Cardiovascular magnetic resonance (CMR), strengthened by the development of T1 mapping, provides a non-invasive and global estimation of myocardial fibrosis. Two distinct types of myocardial fibrosis can be depicted by CMR: the late gadolinium enhancement (LGE) technique quantifies focal fibrosis [6, 7], and diffuse interstitial expansion can be measured by T1 mapping [8]. Multicentre trials and meta-analyses have shown that the presence and extent of LGE are predictors of worse survival following aortic valve replacement (AVR), indicating advanced myocardial injury [9, 10]. Focal myocardial fibrosis is also irreversible following AVR [11, 12], effecting incomplete recovery of LV function and worse post-operative clinical outcomes, suggesting delayed timing of aortic valve intervention in some patients.

Several studies in AS patients have reported that native T1 and extracellular volume (ECV) values correlate with the degree of diffuse myocardial fibrosis, predict cardiovascular events and mortality [13–15] and are reversible with afterload relief [16], demonstrating potential as an early marker of adverse remodelling.

As a possible surrogate marker of myocardial fibrosis, LV myocardial global longitudinal strain (GLS), as assessed by speckle tracking echocardiography (STE), has been shown to be an independent predictor of adverse events in patients with severe AS, both with preserved and impaired LV systolic function [17].

Thus, novel diagnostic strategies and more accurate evaluations of the disease severity and consequences of AS are needed in assessing subclinical myocardial dysfunction to further risk-stratify severe AS patients. There are limited studies on myocardial fibrosis that have integrated multimodality imaging and sufficient histological analyses in severe AS. The optimal T1 image analysis strategy remains debated, requiring further validation. Our prospective study aims to: (i) non-invasively assess markers of myocardial fibrosis and validate them against histological data in patients who are undergoing surgical AVR and (ii) identify early imaging biomarkers of adverse LV remodelling in severe AS patients.
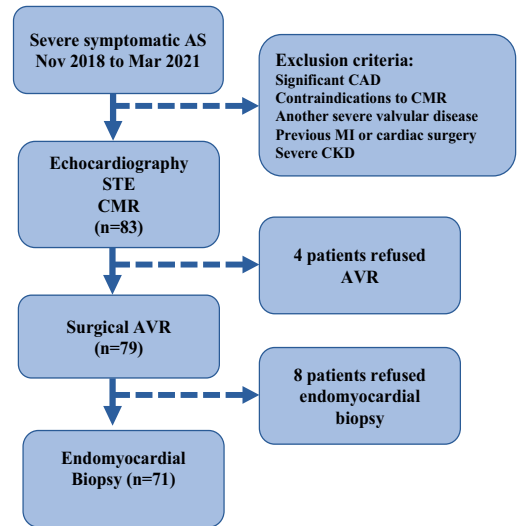

Fig. 1 FIB-AS study flow chart

Methods

Study population and protocol

In this prospective observational study at Vilnius University Hospital between November 2018 and December 2020, patients with severe symptomatic AS that were scheduled for AVR according to current treatment recommendations [18] were recruited. The study was approved by the Biomedical Research Ethics Committee of the Vilnius Region (Approval Number: 158200-18/9-1014-558) and was performed as part of the FIB-AS study (NCT03585933). This study conformed to the principles of the Helsinki Declaration, and all subjects gave written consent to participate.

Patients were recruited prior to a pre-operative assessment and underwent a clinical assessment, comprising a clinical history, the Minnesota Living with Heart Failure Questionnaire (MLHFQ), the 6-min walking test (6MWT), blood sampling [for haematocrit, renal function, brain natriuretic peptide (BNP) and high sensitivity troponin I (Hs-Tn-I)], a transthoracic echocardiogram, and CMR. The inclusion criteria were patients who were undergoing AVR for severe AS [defined as aortic valve area (AVA) ≤ 1 cm^2 or AVA index ≤ 0.6 cm^2/m^2, as determined by ultrasonography], age > 18 years, ability to undergo a CMR scan, and consent to the study protocol. The exclusion criteria were

significant coronary artery disease (CAD) (> 50% lesion), history of myocardial infarction, severe valve disease other than AS, estimated glomerular filtration rate < 30 mL/min/1.73 m^2, CMR-incompatible devices, persistent atrial tachyarrhythmias, and previous cardiac surgery (Fig. 1). The study data were collected and stored in a dedicated online database, REDCap (Research Electronic Data Capture) [19].

Cardiac imaging

Echocardiography

Transthoracic 2D echocardiography was performed using a commercially available Vivid ultrasound system (S70, E9 or E95) (GE Healthcare, Horten, Norway), and the data were stored on a dedicated workstation for subsequent off-line analysis. AS severity and LV systolic and diastolic function were evaluated per the echocardiographic guidelines [20, 21]. AVA was calculated using the continuity equation.

The 2D speckle tracking echocardiography (STE)

From the 2D grey-scale images of the apical 2-, 3- and 4-chamber views, LV global longitudinal strain (GLS) was measured and processed off-line using commercially available software (EchoPac 112.0.1, GE Medical Systems, Horten, Norway) [22]. The frame rate was adjusted to 50 to 80 frames/s. End-systole was defined, based on the closure click on the spectral tracing of the pulsed-wave Doppler of AV flow. GLS was acquired using the average regional strain curves (17-segment model for 2D STE). Segments with poor quality tracking or aberrant curves (despite manual adjustment) were removed from analysis. Due to missing data or poor image quality, STE analysis was completed for 77 of 83 patients.

CMR Protocol

CMR scans were obtained using standard protocols on a 1.5 T Siemens Aera scanner with surface coils and retrospective electrocardiography (ECG) triggering. LV end-systolic and end-diastolic diameters and maximum wall thickness were traced and recorded from the short-axis and long-axis views of the standard ECG-gated steady-state-free precession cine sequence. LV volumes, mass and ejection fraction were measured using commercial software (suiteHEART®) from a stack of sequential 8-mm short-axis slices (0–2-mm gap) from the atrio-ventricular ring to the apex. Measurements were indexed to body surface area in m^2 (using the DuBois formula).

LGE Imaging

To detect late gadolinium enhancement, images were acquired 10–15 min after intravenous administration of gadobutrol (0.2 mmol/kg) (Gadovist, Bayer AG, Germany) using a breath-hold segmented inversion recovery fast-gradient echo sequence in the short-axis and long-axis planes of the LV, with an 8-mm slice thickness and 0% distance factor. The region of myocardial fibrosis was defined as the sum of pixels with a signal intensity above 5 standard deviations of the normal remote myocardium in each short-axis slice. The presence of LGE was determined qualitatively by two independent readers who were blinded to the clinical data.

T1 Mapping

Myocardial fibrosis was assessed using native and post contrast T1 mapping at a mid-ventricular short-axis section, acquired using a modified Look-Locker inversion-recovery (MOLLI) sequence with motion correction (the '3–3–5'standard protocol) before and 15 min after contrast administration [23]. Scanner generated T1 maps were processed off-line using commercially available software (suiteHEART by NeoSoft). The region of interest was manually traced on short-axis, native and post-contrast T1 maps in the septum at the mid-ventricular level. All T1-related measures were traced in the middle third of myocardium to avoid partial volume effects. Segments containing LGE were excluded from the T1 mapping analysis [24]. To measure the T1 value

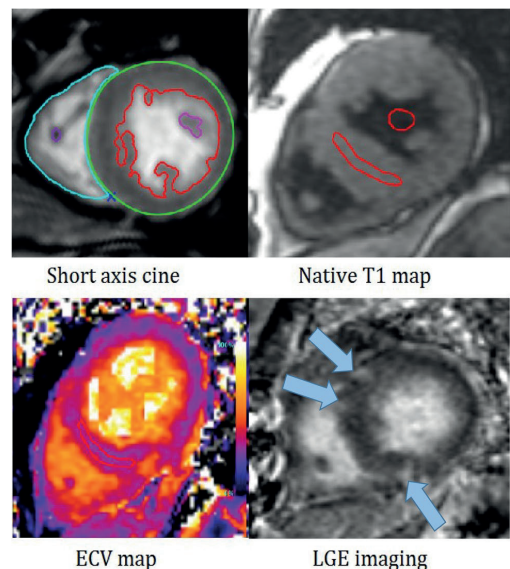| Short axis cine | Native T1 map |
| ECV map | LGE imaging |

Fig. 2 Multiparametric CMR assessment protocol

of blood, circular regions of interest were positioned in the LV cavity, avoiding papillary muscle (Fig. 2). Native T1, ECV%, and indexed ECV values were then calculated. The ECV of the myocardium was calculated as follows: ECV% = ($\Delta R1m/\Delta R1b$) × (1—haematocrit level) × 100, where R1 is 1/T1, R1m is R1 in the myocardium, R1b is R1 in the blood and $\Delta R1$ is the change in relaxation [25]. Hematocrit was drawn on the day of CMR scanning. Due to incomplete datasets, T1 mapping parameters were measured in 67 of 83 patients.

Histological analysis

At the time of surgical AVR, biopsy specimens were obtained under direct vision by the surgical team using a surgical scalpel from the basal anteroseptum just after removal of the diseased AV. One intraoperative myocardial biopsy sample (mean area 22.5 ± 12 mm^2) was taken from each patient. All myocardial tissue samples were fixed in 10% neutral buffered formalin and embedded in paraffin. Sections (3-μm-thick) were sliced on a Leica RM2145 microtome and stained with haematoxylin and eosin and Masson 's trichrome. Digital images were captured by on an Aperio Scan-Scope XT Slide Scanner (Aperio Technologies, Vista, CA, USA) under 20 × objective magnification (0.5 μm resolution). Histologists who were blinded to the clinical and CMR data examined all biopsy specimens.

The fraction of myocardial volume that was occupied by collagen tissue (collagen volume fraction, CVF) was determined by quantitative morphometry on an automated image analysis system (HALO™). The area of myocardial fibrosis was calculated using the HALO™ Area Quantification v2.1.11 algorithm (IndicaLabs, NM, USA) [26]. The subendocardial layer was defined as 1 mm from the endocardial surface, whereas the rest of the tissue sample was defined as the midmyocardial layer.

Statistical analysis

Variables were presented as mean ± standard deviation or median and interquartile ranges. Categorical variables were expressed as frequencies and percentages and were compared by v2 test. Unpaired student's t-test and Mann–Whitney U test were used to compare two groups of continuous variables. Pearson's and Spearman's correlation coefficients were calculated to assess the relationships between continuous variables.

Intra- and inter-observer variation was analysed by Bland–Altman method and calculation of the correlation coefficient. The statistical analysis was performed in R (version 4.1.2). Differences were considered statistically significant provided a 2-sided p value < 0.05 [27].

Results

A total of 83 patients were included (age 66.4 ± 8.3 years, 58% female, AVA index 0.44 ± 0.1 cm^2/m^2, peak AV velocity 4.8 ± 0.6 m/s, mean gradient 57.8 ± 16 mm Hg). The main reasons for non-eligibility were significant CAD, renal dysfunction and other valvular abnormalities. The mean LV ejection fraction (LVEF) was $66.8 \pm 13\%$, with 11% of patients having reduced LVEF (< 50%). Overall, patients had low surgical risk, with STS-PROM and EuroScore < 4% (1.9% and 1.5%, respectively). Patients with congenital AS were more likely to be younger ($p < 0.001$), were at lower surgical risk ($p = 0.004$), and had better renal function ($p = 0.002$). Of the 83 enrolees, 79 underwent surgical AVR and 4 postponed surgery due to Covid-19. The patients' clinical and imaging characteristics are summarised in Tables 1 and 2.

Myocardial fibrosis by histology

Of 71 myocardial biopsies, 2 were epicardial. The data of one patient was excluded from the analysis due to an incidental finding of toxoplasmic myocarditis. The median CVF was 15.1% (8.6–21). Patients with higher CVF had a greater prevalence of hypertension ($p = 0.024$) and dyslipidaemia ($p = 0.036$). Higher values of CVF were observed in LGE-positive versus LGE-negative patients—28.7% (19–33) vs 20.7% (15–30), respectively ($p = 0.040$). No significant differences in median CVF value were noted between patients with and without CAD [17.2% (10–23) vs 13.4% (9–19), respectively; $p = 0.094$]. Segmental analysis of myocardial biopsies revealed more fibrosis in the subendocardial layer compared with a midmyocardial layer [21.1% (12–29) vs 8% (5–12); $p < 0.001$; Fig. 3].

Myocardial fibrosis by CMR

The median delay between CMR and surgery was 53.3 days (17–78). Mean native T1 was 959.7 ± 34 ms (range: 897–1044 ms), and the mean ECV was $22.7 \pm 3.6\%$ (range: 15.7–34.4%). No significant difference in mean native T1 and ECV values was observed between men and women (962 ± 29 ms vs 957 ± 37 ms, $p = 0.391$ and $22.9 \pm 3\%$ vs. $22.6 \pm 4\%$, $p = 0.821$, respectively).

To compare native T1 with clinical and structural parameters, we divided variables (above and below the median: 957 ms, Table 3). Patients with elevated native T1 had lower systolic blood pressure ($p = 0.006$), higher QRS voltage on the ECG ($p = 0.036$), greater systolic ($p = 0.009$) and diastolic LV dimensions ($p = 0.049$) and higher LV mass index ($p = 0.021$). Among those with elevated native T1, a higher

Table 1 Clinical characteristics of the study population stratified by the presence of focal fibrosis

Variable	All patients ($n=83$)	LGE (+) patients ($n=61$)	LGE (-) patients ($n=22$)	P- value
Age, yrs	66.4 ± 8.3	65.8 ± 8.3	68.3 ± 8.3	0.235
Male gender	35 (42%)	29 (48%)	6 (27%)	0.162
BMI, kg/ m^2	30 ± 5.8	30.4 ± 5.6	28.7 ± 6	0.245
BSA, m^2	1.9 ± 0.2	2.0 ± 0.2	1.8 ± 0.2	**0.011**
Systolic BP, mmHg	150 ± 25	148 ± 25	156 ± 23	0.223
Diastolic BP, mmHg	85 ± 11	84 ± 12	85 ± 11	0.842
Comorbidities				
Hypertension	73 (88%)	55 (90%)	19 (86%)	0.732
Dyslipidemia	66 (80%)	48 (79%)	19 (86%)	0.640
Unobstructive CAD	39 (47%)	30 (49%)	9 (41%)	0.677
Diabetes mellitus	14 (17%)	10 (16%)	5 (22%)	0.735
Atrial fibrillation	6 (7%)	5 (8%)	1 (5%)	0.931
History of PCI	1 (1%)	1 (2%)	-	1.000
Symptoms and functional status				
Dyspnea	61 (74%)	46 (75%)	15 (68%)	0.706
Chest pain	41 (49%)	30 (49%)	11 (50%)	1.000
Syncope	9 (11%)	9 (15%)	-	0.131
NYHA functional class				0.591[*]
I	16 (19%)	11 (18%)	5 (23%)	
II	24 (29%)	19 (31%)	5 (23%)	
III	40 (48%)	28 (46%)	12 (54%)	
IV	3 (4%)	3 (5%)	-	
6 MWT, m	357.6 ± 105.6	352 ± 108	372 ± 101	0.459
MLHFQ score	35 ± 20.4	36 ± 20	31 ± 22	0.277
Drug history				
ACE-I/ARB	61 (74%)	43 (71%)	18 (82%)	0.453
Betablocker	57 (69%)	42 (69%)	15 (68%)	1.000
Statin	54 (65%)	40 (66%)	14 (64%)	1.000
Loop diuretic	15 (18%)	11 (18%)	4 (18%)	1.000
Spironolactone	22 (27%)	14 (23%)	8 (36%)	0.347
Risk scores				
STS-PROM, %	1.9 (1.2–2.3)	1.6 (1–2.2)	1.75 (1.4–2.4)	0.415
EuroSCORE II, %	1.5 (0.7–1.6)	1 (0.7–1.7)	1.2 (0.8–1.5)	0.415
Surgery (n = 79)				
Tissue valve	70 (89%)	55 (90%)	15 (83%)	**0.037**
Mechanical valve	9 (11%)	6 (10%)	3 (17%)	0.927
Aortic intervention	3 (4%)	1 (2%)	2 (11%)	0.348
Valve morphology				
Tricuspid	54 (65%)	41 (67%)	13 (59%)	0.671
Bicuspid	28 (34%)	19 (31%)	9 (41%)	0.429
Unicuspid	1 (1%)	1 (2%)	–	1.000
Blood tests				
Creatinine μmol/l	76.2 ± 16.3	77 ± 17	73.9 ± 16	0.447
eGFR, ml/min/1.73 m^2	78.6 (69–90)	85 (69–90)	86 (69–90)	0.996
Hs-Tn-I, pg/l	10 (5–19)	13.5 (6–29)	5.3 (5–9)	**0.003**
BNP, pg/l	122 (65–340)	167 (77–511)	74 (43–145)	**0.004**
ECG parameters				
Heart rate, beats/min	77 ± 12.4	78 ± 12	76 ± 13	0.519
S-L criteria (mm)	30.8 ± 10	31.7 ± 10	28.4 ± 10	0.189

Table 1 (continued)

Variable	All patients (n=83)	LGE (+) patients (n=61)	LGE (-) patients (n=22)	P- value
QRS duration, ms	96.8 (88–102)	94 (88–102)	92 (85–101)	0.449

The boldface values indicate statistical significance

Continuous variables are presented as mean ± SD or median [interquartile range]. Categorical variables are expressed as n (%)

6 MWT 6 min walking test, *BMI* Body mass index, *BNP* Brain natriuretic peptide, *BP* Blood pressure, *BSA* Body surface area, *CAD* Coronary artery disease, *ECG* Electrocardiography, *LGE* Late gadolinium enhancement, *MLHFQ* Minnesota living with heart failure questionnaire, *NYHA* New York Heart Association, *PCI* Percutaneous coronary intervention, *S-L* Sokolow Lyon voltage criterion, *STS* Society of Thoracic Surgeons' risk model score, *EuroScoreII* European System for Cardiac Operative Risk Evaluation II score, *ACE-I* Angiotensin-converting-enzyme inhibitor, *ARB* Angiotensin-receptor blocker, *hs-Tn-I* High sensitivity troponin I, *eGFR* Estimated glomerular filtration rate

-P-value for comparison among NYHA I and II vs. III and IV

proportion of patients had reduced GLS (18% vs 6%, respectively; $p = 0.049$).

Focal fibrosis, measured by LGE, was common, affecting 74% of all patients (83% of men and 67% of women). Further, 92% of focal fibrosis was the non-infarct type (89% mid-myocardial, 3% subepicardial). Despite having unobstructed coronary arteries 8% of patients had infarct-type focal fibrosis. The most common location of LGE was the right ventricular insertion point (68%). LGE was also detected in the anterolateral (11%), septal (8%), posterolateral (6%), inferior (6%) and apical (1%) segments. We found no significant difference in the prevalence of LGE between patients with and without CAD (77% and 70%, respectively; $p = 0.67$). Compared with patients without focal fibrosis, LGE-positive subjects had more severe AS, as evidenced by smaller AVA index ($p = 0.018$), thicker LV walls ($p < 0.001$) and higher LV mass index ($p = 0.009$). Patients with LGE also had higher levels of BNP ($p = 0.004$) and Hs-Tn-I ($p = 0.003$). The patients' clinical and imaging characteristics stratified by the presence of LGE are summarised in Tables 1 and 2.

Longitudinal deformation analysis

The mean GLS was $-18 \pm 5\%$ (range: -3% to -31%), and a reduction in GLS $> -20\%$ was observed in 61% of patients.

To analyse GLS with regard to clinical and structural parameters, we dichotomised the variables (above and below median: -18.5; Table 3). Patients with lower GLS had more severe AS, based on smaller AVA index ($p = 0.018$), higher mean transvalvular gradient ($p = 0.004$), lower systolic blood pressure ($p = 0.005$) and greater QRS voltage on the ECG ($p = 0.011$). The low-GLS group also had thicker LV walls ($p = 0.009$), higher LV volumes ($p < 0.001$), greater LV mass index ($p < 0.001$) and lower LVEF ($p < 0.001$). This group showed signs of elevated LV filling pressures, as evident by higher E/e' ratios ($p = 0.011$), with consequently higher LA volume index ($p = 0.002$) and pulmonary artery systolic pressure (p = 0.031). Higher levels of BNP ($p = 0.001$) and Hs-Tn-I ($p = 0.002$) were detected in these patients. Representative images of patients with various degrees of LV remodelling by echocardiography, CMR and histology are shown in Fig. 4.

Analysis of associations

CVF correlated with LV end-diastolic diameter (r = 0.242, $p = 0.043$), LV end-systolic volume (r = 0.265, $p = 0.028$), LVEF (r = −0.246, $p = 0.04$) and LA volume index (r = 0.314, $p = 0.009$). When subendocardium was excluded from the analysis, CVF correlated with LV mass (r = 0.247, $p = 0.041$), LVEF (r = −0.354, $p = 0.003$), GLS (r = −0.303, $p = 0.013$) and BNP (r = 0.242, $p = 0.045$) (Fig. 5). Native T1, ECV and indexed ECV did not associate with CVF.

With regards to LV structure and function, GLS correlated with LV end-diastolic volume (r = −0.485, $p < 0.001$), LV end-systolic volume (r = −0.636, $p < 0.001$), LV mass index (r = −0.615, $p < 0.001$) and LVEF (r = 0.7, $p < 001$). GLS was also linked to parameters that were associated with elevated LV filling pressures: mean E/e' (r = −0.4, $p = 0.002$), LA volume index (r = −0.405, $p < 0.001$) and estimated pulmonary artery systolic pressure (r = −0.376, $p < 0.05$). Native T1 correlated with LV end-systolic volume (r = 0.349, $p = 0.003$), LV end-diastolic volume (r = 0.269, $p = 0.03$), LV mass index (r = 0.414, $p < 0.001$) and LVEF (r = 0.317, $p < 0.05$). GLS and native T1 were associated with the degree of AS severity: AV mean gradient (r = −0.387, $p < 0.001$ and r = 0.408, $p < 0.001$, respectively) and AVA (r = 0.30, $p < 0.05$ and r = 0.3, $p = 0.02$, respectively).

With regard to serum biomarkers, GLS and native T1 correlated with BNP (r = −0.653, $p < 0.001$ and r = 0.371, $p < 0.05$, respectively) and hs-Tn-I (r = −0.486, $p < 0.001$

Table 2 Cardiovascular imaging and histology data of study cohort, stratified by the presence of focal fibrosis

Echocardiography data ($n=83$)	All patients ($n=83$)	LGE (+) patients ($n=61$)	LGE (-) patients ($n=22$)	P-value
Peak AV velocity, m/s	4.8 ± 0.6	4.9 ± 0.6	4.6 ± 0.5	0.074
Mean AV gradient, mm Hg	57.8 ± 16	59.8 ± 17	52.4 ± 14	0.071
Low gradient AS	10 (12%)	6 (10%)	4 (18%)	0.422
AVA, cm^2	0.84 ± 0.2	0.83 ± 0.2	0.88 ± 0.2	0.364
AVA index, cm^2/ m^2	0.44 ± 0.1	0.43 ± 0.1	0.49 ± 0.1	**0.018**
IVSd, mm	12.7 ± 1.7	13.1 ± 1.5	11.5 ± 1.5	**< 0.001**
Posterior wall diameter, mm	11.5 ± 1.4	11.9 ± 1.3	10.3 ± 1.2	**< 0.001**
LVdd, mm	51.4 ± 5.4	52.1 ± 5.4	49.3 ± 4.9	**0.034**
LVsd, mm	32.7 ± 5.9	33.1 ± 6.1	31.7 ± 5.6	0.362
E/A	1.1 ± 0.5	1.1 ± 0.5	1.2 ± 0.3	0.615
E deceleration time, ms	259 ± 70	257 ± 69	262 ± 74	0.813
E/e' septal	17.6 ± 7	17.9 ± 6.3	16.8 ± 9.5	0.619
E/e' lateral	14.5 ± 6	15 ± 6.5	13.2 ± 5.8	0.276
E/e' mean	15.6 ± 6	16 ± 5.9	14.3 ± 5.7	0.254
LA volume index, ml/ m^2	47.9 ± 12	49.2 ± 12	44.7 ± 12	0.129
PASP, mm Hg	38 ± 15	40.5 ± 15	33.6 ± 12	0.175
RV S', cm/s	11.6 ± 3	11.4 ± 3	12 ± 2	0.377
TAPSE	21.7 ± 3	21.7 ± 4	21.8 ± 3	0.924
GLS, %*	-18 ± 5	-17.5 ± 4.8	-19.4 ± 5.3	0.147
CMR data ($n=83$)				
IVSd, mm	13.3 ± 2	13.6 ± 2	12.6 ± 2	0.062
LVdd, mm	50.6 ± 6	51 ± 6	49.3 ± 6	0.264
LVsd, mm	33.8 ± 8	34.2 ± 8	33 ± 9	0.561
LVEDV, ml	144.3 ± 44	149.7 ± 44	130 ± 44	0.079
LVESV, ml	51 (28- 61)	46 (31–69)	29 (24–45)	0.106
LV stroke volume index, ml/m^2	48 ± 11	48.3 ± 10	48.4 ± 11	0.982
LVEF, %	66.8 ± 13	65.3 ± 13	70.8 ± 12	0.088
LVEF < 50%	9 (11%)	8 (13%)	1 (5%)	0.427
LV mass index, g/m^2	97.6 ± 32	103.4 ± 32	82.6 ± 29	**0.009**
RVEDV, ml	125.3 ± 31	129.5 ± 31	114.2 ± 31	0.052
RVESV, ml	49.3 ± 18	49.7 ± 19	48.3 ± 17	0.747
RVEF, %	60.8 ± 10	61.9 ± 10	58 ± 8	0.111
Native T1, ms[#]	959.7 ± 34	961.8 ± 31	952.5 ± 43	0.359
Post-contrast T1, ms[#]	351 (326- 362)	361 (325–376)	350 (326–358)	0.415
ECV, %[#]	22.7 ± 3.6	23.4 ± 3.7	22.2 ± 3.5	0.541
ECV index, %/m^2	11.8 ± 2	12.3 ± 2	11.3 ± 2	0.271
Histology data ($n=71$)				
CVF, %[&]	15.1 (9–21)	15.9 (9–19)	12.4 (9–24)	0.887
CVF subendocardial, %[&]	21.1 (12–29)	28.7% (19–33)	20.7% (15–30)	**0.040**

The boldface values indicate statistical significance

Continuous variables are presented as mean ± SD or median [interquartile range]. Categorical variables are expressed as *n* (%)

AV Aortic valve, *AVA* Aortic valve area, *E* Peak early velocity of the transmitral flow, *CMR* Cardiovascular magnetic resonance, *CVF* Collagen volume fraction, *e'* Peak early diastolic velocity of the mitral annulus displacement, *GLS* Global longitudinal strain, *ECV* Extracellular volume, *IVSd* Interventricular septum diastolic diameter, *LVEDV* Left ventricular end-diastolic volume, *LVESV* Left ventricular end-systolic volume, *LVEF* Left ventricular ejection fraction, *LA* Left atrium, *LGE* Late gadolinium enhancement, *LGE(+)* Patients with late gadolinium enhancement, *LGE(-)* Patients without late gadolinium enhancement, *PASP* Pulmonary artery systolic pressure measured by echocardiography, *RVEDV* Right ventricular end-diastolic volume, *RVEF* Right ventricular ejection fraction, *RVESV* Right ventricular end-systolic volume, *RV S'* Peak systolic velocity of the tricuspid annulus displacement, *TAPSE* Tricuspid annulus plane systolic excursion, *- value based on the data analysis in 77 patients; #- values based on the data analysis in 67 patients; &- values based on the data analysis in 71 patient
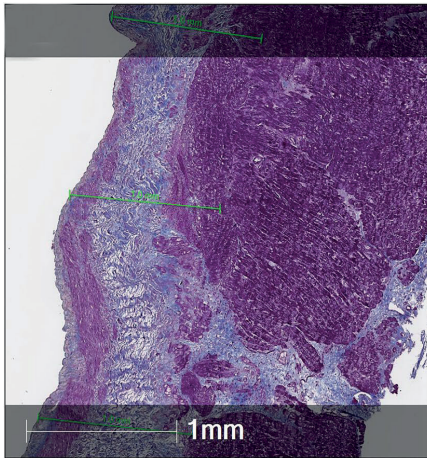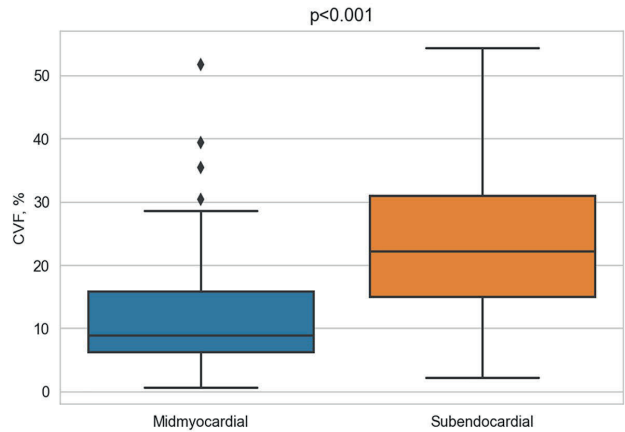
Fig. 3 Image on the left shows myocardial biopsy sample stained with Masson 's trichrome. Graph on the right shows comparison of collagen volume fraction (CVF) in different layers of myocardium. Higher proportion of collagen detected in subendocardium compared to midmyocardium

and r = 0.333, $p < 0.05$, respectively) and with each other (r = −0.321, $p < 0.05$) (Fig. 6).

Reproducibility of measurements

The intraclass correlation coefficients for native T1 were 0.945 (95% CI 0.88–0.97, bias 3.3 ± 11.0 ms) for intra-observer variation and 0.958 (95% CI 0.91–0.98, bias 9.1 ± 15.1 ms) for inter-observer variation. The GLS measurements also demonstrated excellent reproducibility: 0.969 (95% CI 0.93–0.98, bias 0.51 ± 1.3) for intra-observer variation and 0.981 (95% CI 0.96–0.99, bias 1.5 ± 1) for inter-observer variation.

Discussion

This prospective study presents a comprehensive assessment of the consequences of AS on LV myocardium by integrating CMR and STE data with a large number of myocardial biopsies.

The main study findings are as follows:

(1) The non-infarct type of focal fibrosis is highly prevalent in severe low-risk AS patients and determines more advanced LV remodeling.

(2) Histologically measured myocardial fibrosis is associated with imaging and serum biomarkers of LV systolic dysfunction and left side chamber enlargement.

(3) The subendocardium is affected by myocardial fibrosis to a greater extent and determines longitudinal dysfunction.

(4) GLS is associated with invasively and non-invasively measured myocardial fibrosis; low GLS and elevated native T1 differentiated patients with more advanced LV remodelling.

Compared with previous studies in severe AS patients, our cohort was younger and free from significant CAD, thus representing low-risk isolated AS patients. Although 90% of our study population had preserved LVEF, a more detailed assessment of myocardial structure and function through cardiac imaging and histological analysis revealed evidence of varying degrees of myocardial injury.

The amount of fibrosis in the myocardial biopsies varied substantially, from 2% to 41%. Diffuse fibrosis, which is present in healthy myocardium, constituted less than 2%, based on the autopsy results of subjects who died of non-cardiovascular causes [28, 29]. If the amount of myocardial fibrosis increases with age is less clear. We found that histological myocardial fibrosis was associated with LV and LA enlargement and worse systolic function, underscoring the role of myocardial fibrosis in the pathophysiological progression to cardiac decompensation in AS, in terms morphology and function. Consistent with earlier studies, we found that the subendocardial layer contained more fibrosis compared with a midmyocardium. Gradients of myocardial fibrosis in the LV wall have been described in patients with severe AS and those with hypertrophic cardiomyopathy and hypertensive heart disease—conditions that are both

Table 3 Patients clinical and imaging characteristics stratified by median GLS and native T1 values

	GLS ≥ -18.5% (n=40)	GLS < -18.5% (n=37)	P-value	Native T1 ≥ 957 ms (n=34)	Native T1 < 957 ms (n=33)	P-value
Age, yrs	66±8	68±8	0.256	65.8±9	66±9	0.917
Male gender	18 (45%)	14 (38%)	0.548	15 (44%)	11 (33%)	0.446
BSA, m²	1.98±0.2	1.86±0.2	**0.004**	1.96±0.16	1.93±0.19	0.607
Systolic BP, mmHg	143±23	158±23	**0.005**	139±21	156±26	**0.006**
Diastolic BP, mmHg	83±11	85±11	0.485	82±10	86±13	0.203
Unobstructive CAD	20 (50%)	18 (49%)	1.0	20 (59%)	14 (42%)	0.893
Hypertension	36 (90%)	33 (89%)	0.447	27 (79%)	33 (100%)	0.109
Diabetes mellitus	8 (20%)	4 (11%)	0.768	6 (18%)	7 (21%)	1.0
NYHA f.cl. ≥ 3	26 (65%)	14 (38%)	0.085	16 (47%)	15 (46%)	0.749
MLHFQ score	37±20	32±20	0.257	37±21	36±20	0.839
6 MWT, m	351±105	358±104	0.767	367±106	352±94	0.558
ECG						
HR, b/min	80±14	75±11	0.100	78±4	77±12	0.742
QRS, ms	95 (90–102)	90 (86–98)	0.105	94 (89–102)	90 (84–101)	0.313
S-L, mm	34±11	28±8.5	**0.011**	34±10	29±9	**0.036**
Echo data						
AVA index, cm²/m²	0.42±0.1	0.47±0.08	**0.018**	0.4±0.1	0.45±0.1	0.075
Peak AV velocity, m/s	5.0±0.7	4.7±0.5	0.055	5.0±0.6	4.8±0.6	0.105
Mean gradient, mmHg	63±17.7	53±13.2	**0.004**	64±16	57±15	0.052
IVSd, mm	13.3±1.8	12.2±1.4	**0.009**	13±1.9	12.6±1.6	0.368
LVdd, mm	53.7±12	48.8±4.7	**0.002**	53±5	50±5	**0.049**
LVsd, mm	35.4±6	29.6±4	**<0.001**	35±6	32±6	0.057
E deceleration time, ms	254±76	264±67	0.542	252±68	266±75	0.759
E/e' septal	17.1 (14–22)	14 (11.7–18)	**0.011**	16.5 (12.8–18)	16 (12–20)	0.845
E/e' mean	17.4±6.9	14.2±4.4	**0.021**	15±5	16±7	0.909
LA volume index, ml/m²	53±12	44±11	**0.002**	48±9	48±15	0.473
PASP, mmHg	43.5±18	32.9±7	**0.031**	41±17	37±12	0.947
GLS,%	14.3±3.9	21.7±2.7	**<0.001**	16.7±5.6	18.2±4	0.120
GLS > -15%	16 (40%)	-	**<0.001**	10 (29%)	4 (12%)	**0.049**
CMR and histology data						
IVSd, mm	14±2	12.6±2	**0.005**	14±1.6	13±2.3	0.364
LVdd, mm	53±7	48.3±5	**<0.001**	52±6	50±5	0.074
LVsd, mm	37±9	30.6±6	**<0.001**	36.5±7	32±6	**0.009**
LVEDV, ml	160.7±48	126±35	**<0.001**	153±40	143±44	0.201
LVESV, ml	56.9 (41–77)	29 (24–41)	**<0.001**	52 (37–72)	41 (28–53)	0.083
LVEF, %	59±14	74±7	**<0.001**	62.4±14	68±12	0.053
LVEF < 50%	8 (20%)	0	**0.009**	6 (18%)	2 (6%)	0.541
LV mass index, g/m²	113±33	80.6±24	**<0.001**	109±31	91±30	**0.021**
LGE prevalence	34 (85%)	23 (62%)	0.058	27 (79%)	25 (76%)	0.802
Native T1, ms	967±31	950±37	0.066	987±26	936±18	**<0.001**
Post-contrast T1, ms	349 (326–354)	355 (332–366)	0.201	352 (328–362)	348 (318–362)	0.445
ECV, %	22.3±4	22.9±2.4	0.456	23±3.2	22±3.9	0.243
T2, ms	43 (41–45)	42 (40–44)	0.196	43.3(41–45)	42(40–44)	0.291
BNP, pg/l	252 (98–813)	79 (59–173)	**0.001**	163 (73–581)	120 (62–260)	0.413
Hs-Tn-I, pg/l	15 (7.5–29)	6.9 (5–12.9)	**0.002**	14 (7–27)	7.5 (5–16)	0.089
CVF, %	17.2 (10–22)	13.5 (8–20)	0.279	18.1 (8–24)	13.4 (10–21)	0.564
CVF subendocardial,%	23.4 (13–33)	18.4 (11–27)	0.199	22.3 (9–28)	18.8 (12–26)	0.855

Continuous variables are presented as mean±SD or median [interquartile range]. Categorical variables are expressed as n (%). The boldface values indicate statistical significance. Abbreviations as in Tables 1 and 2
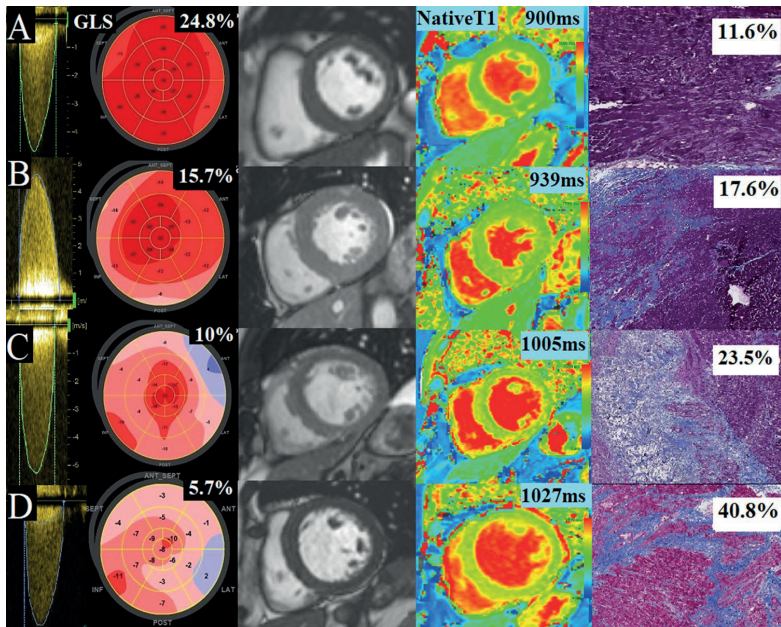
Fig. 4 Four exemplar patients showing progressive cardiac remodeling: continuous-wave Doppler (maximum velocities > 4 m/s; Column 1), global longitudinal strain (GLS; Column 2), short axis cine stills demonstrating degrees of left ventricular (LV) remodeling (Column 3), matching native T1 (Column 4) and collagen volume fraction (CVF) in myocardial biopsies stained with Masson 's trichrome (Column 5). Patient A has preserved GLS, minimal LV hypertrophy, low native T1 and CVF of 11.6%. Patient B has reduced GLS, concentric LV hypertrophy, higher native T1 and moderate histological fibrosis (CVF-17.6%). Patient C has low GLS, evidence of LV hypertrophy, high native T1 and significant histological fibrosis (CVF-23.5%). Patient D, with decompensated heart failure, has low GLS, LV cavity dilatation, high native T1 and extensive histological fibrosis (CVF-40.8%)

associated with chronic pressure overload and an increase in LV mass [28, 29]. These findings can be explained by a transmural gradient of wall stress and ischemia in the subendocardial layer due to the relative decrease in capillary density, with subsequent cell loss and reparative fibrosis [30].

GLS and native T1 median values differentiated patients with more advanced LV remodelling, wherein patients with lower GLS and higher native T1 had evidence of altered LV structure, diastolic and systolic impairments and higher levels of serum biomarkers, indicative of heart failure and myocardial injury. Notably, patients with reduced GLS and elevated native T1 still had preserved LVEF, and only 20% of patients with adverse structural and functional cardiac remodelling had LVEF below 50%. Thus, only 1 in 5 patients with advanced cardiac remodelling can be detected if only this echocardiographic criterion of cardiac decompensation is used, overlooking a substantial number of patients who would benefit from early AV intervention. Our results are consistent with previous studies, showing that fibrotic changes that are induced by AS begin in the subendocardium and initially affect longitudinal function, which is not well represented by LVEF, because it can be compensated by global radial function [7, 31].

Notably, patient groups did not differ by symptom status, functional capacity or quality of life assessment. This finding suggests that symptom assessments can be challenging and misleading and do not always reflect true cardiac condition, indicating that the decision to intervene should be supported by objective markers of cardiac injury, rather than based on subjective assessment of symptom status.

Imaging biomarkers, or the integration of several parameters, might be particularly useful in patients with no or minimal symptoms or when ascertaining valve-related symptoms is challenging. Our data implicate GLS and native T1 as early markers of cardiac decompensation. GLS can also be used as a surrogate marker of myocardial fibrosis, as it was associated with both, invasively and non-invasively measured myocardial fibrosis.

Seventy-four percent of our patients had areas of focal fibrosis, 98% of which were the non-infarct type and which were independent of the presence of nonobstructive CAD. Although only 1 or 2 segments were affected by LGE in most patients, data from a recent large multicentre study show that > 2% of
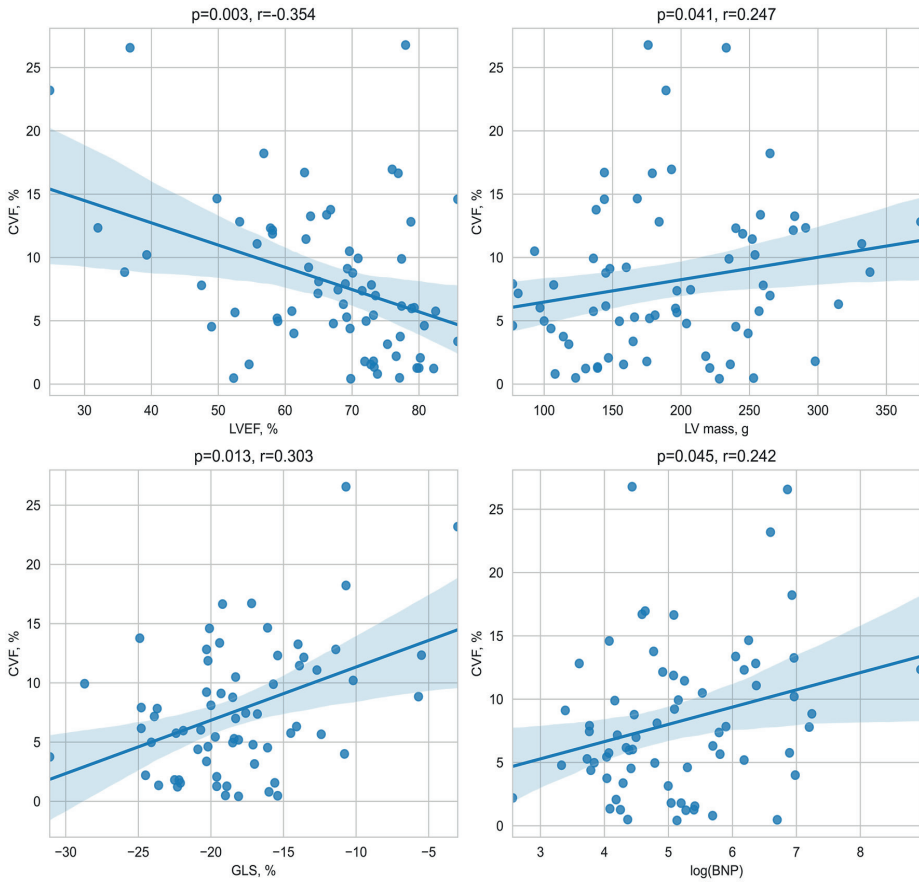
Fig. 5 Correlations between histological myocardial fibrosis (CVF) and LV ejection fraction (**a**), LV mass (**b**), GLS (**c**) and brain natriuretic peptide (BNP) (**d**) are shown. Abbrevations are as in Fig. 4
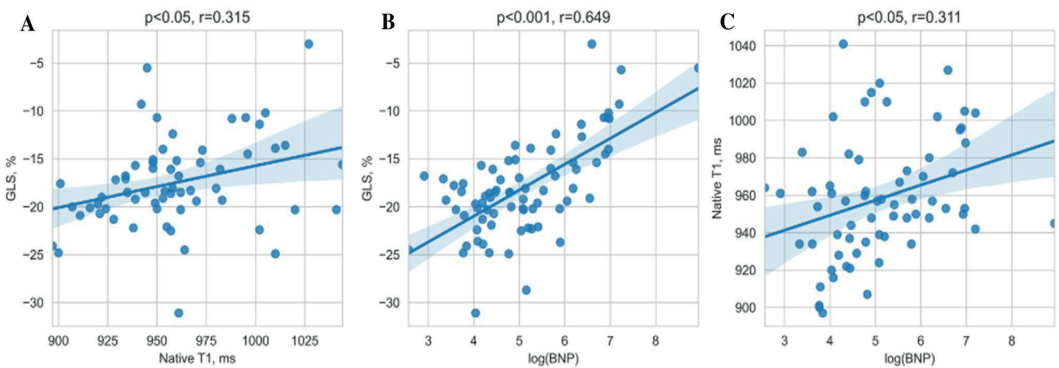

Fig. 6 Correlations between GLS and native T1 (**a**), GLS and BNP (**b**), native T1 and BNP (**c**) are shown. Abbrevations are as in Figs. 4 and 5

LGE in patients with severe AS who undergo AVR is associated with worse postoperative survival [32]. We found, that the myocardium of patients who have progressed to more advanced myocardial injury and have developed areas of irreversible replacement fibrosis on CMR also contains higher degree of diffuse fibrosis measured histologically. Unexpectedly, we found no associations between CVF and CMR markers of diffuse fibrosis, for which there are several explanations. There was a possible sampling error, because only 1 biopsy sample per patient was analysed. Further, the histological and T1 mapping analyses were performed at different levels and layers of the interventricular septum. The myocardial biopsies were endocardial and taken from the basal anteroseptum, possibly containing higher amounts of fibrotic tissue, and the region of interest for the T1 mapping measurements was drawn in the middle of the septum at the midventricular level, avoiding endo and epicardial borders. The data in this field are inconsistent, with some studies reporting significant associations between invasively and non-invasively measured myocardial fibrosis in AS cohorts [15, 33] and others failing to demonstrate this association [24, 29].

Although our patients presented with increased LV mass and myocardial fibrosis in the histological analysis, ECV values were not elevated in our cohort compared with our local reference range. This finding can be explained by the greater increase in cellular mass (adaptive hypertrophy), as opposed to the expansion of extracellular space, because ECV per se represents the percentage of space that is occupied by the extracellular compartment of the total LV mass. The average native T1 and ECV values in our cohort were lower in comparison to AS populations in other studies [13, 15]. A large T1 mapping data variability across different centers have been previously reported, influenced by differences in field strength, vendor-specific set-up and variations in sequences [34, 35]. Disparities in ECV values can also be expected with the non-uniformity of contrast agents and their doses [36]. Another explanation for such variability relates to differences in the study cohorts. When interpreting our results, we should consider that we examined relatively young, low-risk patients who were free from significant CAD, whereas other studies, especially those that included transcatheter treatment cohorts, enrolled patients who were in their 80 s and had a higher rate of comorbidities [37].

Study limitations

The study was composed of a small number of AS patients, however it included substantial number of myocardial biopsies. Due to the Covid-19 pandemic, delays in patient examinations and surgeries were experienced, causing uneven time frames between the preoperative patient assessment (echocardiographic and CMR) and surgery with myocardial sampling, potentially affecting the final result. Proportion of histologically measured myocardial fibrosis could have been affected by the size and depth of biopsy samples, as more superficially sampled and smaller biopsies may contain higher proportion of fibrotic tissue in comparison to larger biopsy samples. Although measuring T1 values only in the septum is a validated and common method, it might not represent the entire myocardium. Because we excluded patients with comorbidities, such as obstructive CAD, a history of myocardial infarction, renal failure and persistent atrial arrhythmias, our results should not be overgeneralized to the broader AS patient population. Another limitation of our study is that the increase in type I error across the statistical analyses was not controlled.

Conclusion

A comprehensive assessment of LV response to AS by integrating histology, CMR and STE reveals varying degrees of myocardial injury that are not apparent with traditional measures of LV systolic function. Histological myocardial fibrosis was associated with imaging and serum biomarkers of LV systolic dysfunction and left side chamber enlargement. We found that native T1 by CMR and GLS by STE differentiated patients with advanced cardiac remodelling, constituting a marker of subclinical cardiac damage. Of all imaging parameters, only GLS was associated with invasively and non-invasively measured myocardial fibrosis, demonstrating its potential as a surrogate marker of myocardial fibrosis.

Declarations

References

1. Unverferth DV, Baker PB, Swift SE, Chaffee R, Fetters JK, Uretsky BF et al (1986) Extent of myocardial fibrosis and cellular hypertrophy in dilated cardiomyopathy. Am J of Cardiol 57(10):816–820. https://doi.org/10.1016/0002-9149(86)90620-x

2. Anderson KR, Sutton MG, Lie JT (1979) Histopathological types of cardiac fibrosis in myocardial disease. J Pathol 128(2):79–85. https://doi.org/10.1002/path.1711280205

3. Chin CWL, Everett RJ, Kwiecinski J, Vesey AT, Yeung E, Esson G et al (2017) Myocardial fibrosis and cardiac decompensation in aortic stenosis. JACC Cardiovasc Imaging 10:1320–1333

4. Dweck MR, Joshi S, Murigu T, Alpendurada F, Jabbour A, Melina G et al (2011) Midwall fibrosis is an independent predictor of mortality in patients with aortic stenosis. J Am Coll Cardiol 58:1271–1279

5. Villari B, Campbell SE, Hess OM, Mall G, Vassalli G, Weber KT et al (1993) Influence of collagen network on left ventricular systolic and diastolic function in aortic valve disease. J Am Coll Cardiol 22:1477–1484

6. Barone-Rochette G, Pierard S, Meester De, de Ravenstein C, Seldrum S, Melchior J, Maes F et al (2014) Prognostic significance of LGE by CMR in aortic stenosis patients undergoing valve replacement. J Am Coll Cardiol 64:144–154

7. Weidemann F, Herrmann S, Stork S, Niemann M, Frantz S, Lange V et al (2009) Impact of myocardial fibrosis in patients with symptomatic severe aortic stenosis. Circulation 120:577–584

8. Chin CW, Semple S, Malley T, White AC, Mirsadraee S, Weale PJ et al (2014) Optimization and comparison of myocardial T1 techniques at 3T in patients with aortic stenosis. Eur Heart J Cardiovasc Imaging 15:556–565

9. Balciunaite G, Skorniakov V, Rimkus A, Zaremba T, Palionis D, Valeviciene N et al (2020) Prevalence and prognostic value of late gadolinium enhancement on CMR in aortic stenosis: meta-analysis. Eur Radiol 30(1):640–651

10. Musa TA, Treibel TA, Vassiliou VS, Captur G, Singh A, Chin C et al (2018) Myocardial scar and mortality in severe aortic stenosis. Circulation 138(18):1935–1947. https://doi.org/10.1161/CIRCULATIONAHA.117.032839

11. Treibel TA, Kozor R, Schofield R, Benedetti G, Fontana M, Bhuva AN et al (2018) Reverse myocardial remodeling following valve replacement in patients with aortic stenosis. J Am Coll Cardiol 71:860–871

12. Everett RJ, Tastet L, Clavel MA, Chin CWL, Capoulade R, Vassiliou VS et al (2018) Progression of hypertrophy and myocardial fibrosis in aortic stenosis: a multicenter cardiac magnetic resonance study. Circ Cardiovasc Imaging 11:e007451

13. Everett RJ, Treibel TA, Fukui M, Lee H, Rigolli M, Singh A et al (2020) Extracellular myocardial volume in patients with aortic stenosis. J Am Coll Cardiol 75(3):304–316. https://doi.org/10.1016/j.jacc.2019.11.032

14. Chin CW, Pawade TA, Newby DE, Dweck MR (2015) Risk stratification in patients with aortic stenosis using novel imaging approaches. Circ Cardiovasc Imaging 8(8):e003421. https://doi.org/10.1161/CIRCIMAGING.115.003421

15. Park SJ, Cho SW, Kim SM, Ahn J, Carriere K, Jeong DS et al (2019) Assessment of myocardial fibrosis using multimodality imaging in severe aortic stenosis: comparison with histologic fibrosis. JACC Cardiovasc Imaging 12(1):109–119. https://doi.org/10.1016/j.jcmg.2018.05.028

16. Hwang IC, Kim HK, Park JB, Park EA, Lee W, Lee SP et al (2020) Aortic valve replacement-induced changes in native T1 are related to prognosis in severe aortic stenosis: T1 mapping cardiac magnetic resonance imaging study. Eur Heart J Cardiovasc Imaging 21(6):653–663. https://doi.org/10.1093/ehjci/jez201

17. Ng ACT, Prihadi EA, Antoni ML, Bertini M, Ewe SH, Ajmone Marsan N et al (2018) Left ventricular global longitudinal strain is predictive of all-cause mortality independent of aortic stenosis severity and ejection fraction. Eur Heart J Cardiovasc Imaging 19:859–867

18. Vahanian A, Beyersdorf F, Praz F, Milojevic M, Baldus S, Bauersachs J et al (2021) ESC/EACTS Scientific Document Group, 2021 ESC/EACTS Guidelines for the management of valvular heart disease: Developed by the Task Force for the management of valvular heart disease of the European Society of Cardiology (ESC) and the European Association for Cardio-Thoracic Surgery (EACTS). Eur Heart J. https://doi.org/10.1093/eurheartj/ehab395

19. Harris PA, Taylor R, Thielke R, Payne J, Gonzalez N, Conde JG (2009) Research electronic data capture (REDCap)-a metadata-driven methodology and workflow process for providing translational research informatics support. J Biomed Inform 42(2):377–381. https://doi.org/10.1016/j.jbi.2008.08.010

20. Lang RM, Badano LP, Mor-Avi V, Afilalo J, Armstrong A, Ernande L et al (2015) Recommendations for cardiac chamber quantification by echocardiography in adults: an update from the American Society of Echocardiography and the European Association of Cardiovascular Imaging. J Am Soc Echocardiogr 28:1–39

21. Baumgartner H, Hung J, Bermejo J, Chambers JB, Edvardsen T, Goldstein S et al (2017) Recommendations on the echocardiographic assessment of aortic valve stenosis: a focused update from the European Association of Cardiovascular Imaging and the American Society of Echocardiography. Eur Heart J Cardiovasc Imaging 8:254–275

22. Voigt JU, Pedrizzetti G, Lysyansky P, Marwick TH, Houle H, Baumann R et al (2015) Definitions for a common standard for 2D speckle tracking echocardiography: consensus document of the EACVI/ASE/Industry Task Force to standardize deformation imaging. Eur Heart J Cardiovasc Imaging 16:1–11

23. Taylor AJ, Salerno M, Dharmakumar R, Jerosch-Herold M (2016) T1 mapping: basic techniques and clinical applications. JACC Cardiovasc Imaging 9:67–81. https://doi.org/10.1016/j.jcmg.2015.11.005

24. Messroghli DR, Moon JC, Ferreira VM, Grosse-Wortmann L, He T et al (2017) Clinical recommendations for cardiovascular magnetic resonance mapping of T1, T2, T2* and extracellular volume: A consensus statement by the Society for Cardiovascular Magnetic Resonance (SCMR) endorsed by the European Association for Cardiovascular Imaging (EACVI). J Cardiovasc Magn Reson 19:75. https://doi.org/10.1186/s12968-017-0389-8

25. Ugander M, Oki AJ, Hsu LY, Kellman P, Greiser A, Aletras AH et al (2012) Extracellular volume imaging by magnetic resonance imaging provides insights into overt and sub-clinical myocardial pathology. Eur Heart J 33:1268–1278

26. Horai Y, Mizukawa M, Nishina H, Nishikawa S, Ono Y, Takemoto K et al (2019) Quantification of histopathological findings using a novel image analysis platform. J Toxicol Pathol 32(4):319–327. https://doi.org/10.1293/tox.2019-0022

27. R Core Team. R: A language and environment for statistical computing (2021) R Foundation for Statistical Computing, Vienna, Austria. R version 4.1.2 (2021–11–01) – "Bird Hippie". https://www.R-project.org/

28. Tanaka M, Fujiwara H, Onodera T, Wu DJ, Hamashima Y, Kawai C (1986) Quantitative analysis of myocardial fibrosis in normals, hypertensive hearts, and hypertrophic cardiomyopathy. Br Heart J 55(6):575–81. https://doi.org/10.1136/hrt.55.6.575

29. Treibel TA, López B, González A, Menacho K, Schofield RS, Ravassa S et al (2018) Reappraising myocardial fibrosis in severe aortic stenosis: an invasive and non-invasive study in 133 patients. Eur Heart J 39(8):699–709. https://doi.org/10.1093/eurheartj/ehx353

30. Galiuto L, Lotrionte M, Crea F, Anselmi A, Biondi-Zoccai GG, De Giorgio F et al (2006) Impaired coronary and myocardial flow in severe aortic stenosis is associated with increased apoptosis: a transthoracic Doppler and myocardial contrast echocardiography study. Heart 92(2):208–12. https://doi.org/10.1136/hrt.2005.062422

31. Hein S, Arnon E, Kostin S, Schon̈burg M, Elsässer A, Polyakova V et al (2003) Progression from compensated hypertrophy to failure in the pressure-overloaded human heart: structural deterioration and compensatory mechanisms. Circulation 107(7):984–91

32. Kwak S, Everett RJ, Treibel TA, Yang S, Hwang D, Ko T et al (2021) Markers of myocardial damage predict mortality in patients with aortic stenosis. J Am Coll Cardiol 78:545–558. https://doi.org/10.1016/j.jacc.2021.05.047

33. Bull S, White SK, Piechnik SK, Flett AS, Ferreira VM, Loudon M et al (2013) Human non-contrast T1 values and correlation with histology in diffuse fibrosis. Heart 99(13):932–7. https://doi.org/10.1136/heartjnl-2012-303052

34. Vo HQ, Marwick TH, Negishi K (2020) Pooled summary of native T1 value and extracellular volume with MOLLI variant sequences in normal subjects and patients with cardiovascular disease. Int J Cardiovasc Imaging 36:325–336. https://doi.org/10.1007/s10554-019-01717-3

35. Kawel N, Nacif M, Zavodni A, Jones J, Liu S, Cibley CT et al (2012) T1 mapping of the myocardium: Intra-individual assessment of the effect of field strength, cardiac cycle and variation by myocardial region. J Cardiovasc Magn Reson 14(1):27. https://doi.org/10.1186/1532-429X-14-27

36. Dabir D, Child N, Kalra A, Rogers T, Gebker R, Jabbour A et al (2014) Reference values for healthy human myocardium using a T1 mapping methodology: results from the International T1 Multicenter cardiovascular magnetic resonance study. J Cardiovasc Magn Reson 16(1):69. https://doi.org/10.1186/s12968-014-0069-x

37. Puls M, Beuthner BE, Topci R, Vogelgesang A, Bleckmann A, Sitte M et al (2020) Impact of myocardial fibrosis on left ventricular remodelling, recovery, and outcome after transcatheter aortic valve implantation in different haemodynamic subtypes of severe aortic stenosis. Eur Heart J 41(20):1903–1914. https://doi.org/10.1093/eurheartj/ehaa033